Modelling Wildfire Occurrences and their Present and Future Patterns of Variability over the Contiguous United States

DOCTOR OF PHILOSOPHY
School of Archaeology, Geography and Environmental Science

University of Reading

Theodore R. Keeping

Main supervisor: Sandy P. Harrison
Co-supervisors: I. Colin Prentice, Theodore G. Shepherd

July 2025

Declaration

I confirm that this is my own work and the use of all material from other sources has been properly and fully acknowledged.

Theodore R. Keeping

Acknowledgements

Firstly, my great thanks to Sandy Harrison for her continuous guidance, without which I would not have developed half as much as a scientist as I have in these almost four years. I count myself very lucky to have had such an engaged supervisor so willing to share her expertise. I hope I have gleaned a fraction of Sandy's instinct for good science. My sincere thanks also to Ted Shepherd for the good advice, many valuable conversations and for his moral support. Many thanks to Colin Prentice for his incisive questions and expertise.

I acknowledge funding from the SCENARIO NERC Doctoral Training Programme and Schmidt Sciences, LLC.

I am thankful to colleagues from the Leverhulme Centre for Wildfires and the SPECIAL group for their friendship, perspectives and feedback.

I thank my parents, Ilona and Miles Keeping, for always supporting and believing in me. I also thank Walker Harmer, a great friend and without whom I would not have become interested in wildfire. Finally, I thank Sophia Rosenthal, my wife and best friend, who facilitated this thesis with wonderful patience. I am beyond grateful for her uplifting companionship.

Thesis Overview

This thesis consists of two peer-reviewed published papers and one paper that is in press. Author contributions and references are detailed below:

Chapter 2: Modelling the daily probability of wildfire occurrence in the contiguous United States

Keeping TR, Harrison SP, Prentice IC, 2024. Modelling the daily probability of wildfire occurrence in the contiguous United States. *Environ. Res. Lett.* 19(2):024036, https://doi.org/10.1088/1748-9326/ad21b0.

> *Concepts, methodology and interpretation were developed by TRK, SPH and ICP jointly. TRK was responsible for data curation, processing and analysis, and produced the graphics and tables. TRK wrote the original draft, and all authors contributed to the final version. ICP and SPH supervised the research.*

Chapter 3: Present and future interannual variability in wildfire occurrence: a large ensemble application to the United States

Keeping TR, Zhou B, Cai W, Shepherd TG, Prentice IC, Van Der Wiel K, Harrison SP, 2025. Present and future interannual variability in wildfire occurrence: a large ensemble application to the United States. *Front. For. Glob. Change* 8:1519836, https://doi.org/10.3389/ffgc.2025.1519836.

> *Concepts and interpretation were developed by TRK, TGS, ICP and SPH jointly. Bias correction methodology was developed by TRK, TGS and SPH jointly. The plant productivity methodology was developed by BZ, WC, ICP and SPH jointly. KW provided the climate ensemble data. TRK was responsible for data curation, processing and analysis, and produced the graphics and tables. TRK wrote the original draft, and all authors contributed to the final version. TGS, ICP and SPH supervised the research.*

Chapter 4: Influence of global climate modes on wildfire occurrence in the contiguous United States under recent and future climates

Keeping TR, Shepherd TG, Prentice IC, Van Der Wiel K, Harrison SP, 2025. Influence of global climate modes on wildfire occurrence in the contiguous United States under recent and future climates. *Clim. Dyn.* [in press].

> *Concepts, methodology and interpretation were developed by TRK, TGS and SPH jointly. KW provided the climate ensemble data. TRK was responsible for data curation, processing and analysis, and produced the graphics and tables. TRK wrote the original draft, and all authors contributed to the final version. TGS, ICP and SPH supervised the research.*

The thesis also led to the publication of an additional paper, included in the appendix. This followed from work presented in Chapter 2.

Appendix: The Global Drivers of Wildfire

Haas O, Keeping TR, Gomez-Dans J, Prentice IC, Harrison SP, 2024. The Global Drivers of Wildfire. *Front. Environ. Sci.* 12:438262. https://doi.org/10.3389/fenvs.2024.1438262

> *Concepts, investigation, writing, review and editing were developed by TRK, OH, JGD, ICP and SPH jointly. SPH led the formal analysis and wrote the original draft.*

Abstract

Wildfires are an intrinsic part of the Earth system, affected by people, vegetation and climate. However, extreme fire years and their impacts on people are of increasing concern. Understanding wildfire frequency is challenging across timescales, both due to stochasticity in individual wildfire occurrences and because significant climate variability in fire weather conditions is poorly sampled by the short observational record. This thesis characterises patterns in wildfire occurrence over the contiguous United States of America (USA) accounting for these two sources of uncertainty. First, developing a probabilistic model to account for the randomness of individual wildfire events. And second, using a large ensemble (LE) to account for the wider distribution of possible driving conditions in a reference (2000-2009) and future (+2°C) climate. Mean annual wildfire occurrences are projected to increase with climate change, though variability between fire years increases at a faster rate. An ensemble of model training runs and the LE application of the wildfire occurrence model enabled key drivers of daily and annual wildfire frequency to be found. Vegetation productivity was a key effect at both timescales, and an increasing control on variability in annual wildfire occurrences due to the emerging limitation of fuel availability on wildfire likelihood in dry regions of the USA. Climate variability is partially predictable from climate modes, which have been linked to increased wildfire in some regions. Multiple modes were found to have widespread, statistically significant associations with annual USA wildfire patterns, with these associations mostly strengthening in response to future climate change. This thesis advances wildfire occurrence modelling and quantification of interannual wildfire variability using LEs, both useful to global wildfire models. It is the first study to quantify the spatially varying effect of climate modes on USA wildfire likelihood, of potentially major utility in projecting seasonal fire danger.

Contents

Introduction and Literature Review

Wildfires are an intrinsic part of the Earth system and have been present since the emergence of vascular plants on Earth (Scott, 2000). Frequent wildfire is necessary to maintain the biodiversity of many fire-adapted ecosystems (Moritz et al., 2014), but wildfires are also a fundamental part of the disturbance regime and can initiate succession in the dominant vegetation type (Stickney, 1986). However, the increase in extreme wildfires in recent years, the rising socioeconomic impacts of wildfires in human occupied fire-prone areas (MunichRe, 2024) and effect of tropical deforestation fires on carbon cycles (Van der Werf et al., 2017) has prompted concern about the occurrence of wildfires and how they may worsen under future climate and land-use change.

One difficulty in understanding wildfires is that their occurrence is influenced by many interacting factors. Meteorological factors and vegetation properties are both important influences on fire occurrence. For example, immediate weather conditions that influence fuel dryness determine whether initial ignitions are suppressed or propagate into a fire. And vegetation type and biomass influence fuel availability. However, on timescales of months to decades, the vegetation properties that determine fuel loads are conditioned by weather and climate (Pausas et al., 2025). Furthermore, vegetation properties themselves influence both local and global climate, via modulating land-atmosphere exchanges of water, energy, and through carbon uptake and storage. The situation is further complicated because human activities can influence the occurrence of wildfires (Balch et al., 2017). People start wildfires either deliberately or accidentally. Planned or controlled human-set fires can cause wildfires through escapes into natural vegetation. Human activities can also have positive effects, minimising the spread of wildfires through fragmenting the landscape and creating artificial firebreaks (Bowring et al., 2024). However, the effectiveness of landscape fragmentation in minimising wildfires is itself dependent on the type of the ecosystem (Harrison et al., 2021). Finally, there are feedbacks from wildfires to all of these controls. Wildfires modify vegetation properties (Pausas and Moreira, 2012), they impact climate immediately through the release of greenhouse gases and particulates (Ward et al., 2012), and in the longer term through changes in carbon storage and uptake (Harrison et al., 2018).

There is an urgent need to understand these complex interactions in the face of ongoing climate, land-use and climate-induced vegetation change. The threat that extreme wildfire events will

be more likely and more intense, and occur in environments in which they have been historically rare (Cunningham et al., 2024) gives added impetus to this. These issues are addressed in this thesis, with a focus on the contiguous United States. Specifically, the thesis examines the importance of different controls in order to develop an empirical model of wildfire occurrence. It then uses this model to examine how wildfire occurrence is likely to change in the future, taking into account the inherent stochasticity of wildfire and the internal variability of the climate. Finally, it looks at the relationship between wildfire occurrence and climate modes, an approach which could provide a way of enhancing the short-term predictability of wildfire occurrence and facilitate better wildfire preparedness.

In the rest of this introduction, I discuss the environmental controls on wildfire, how these have changed over time and how they may be expected to change in future. I then discuss the impacts of wildfire on people and the environment, and the broader role of wildfire in the Earth system. I then present an overview of existing wildfire models and some of their limitations. This material informed the development of the occurrence model (Chapter 2), as well as motivating a more comprehensive study of wildfire interannual variability than currently presented by existing models (Chapter 3). I then introduce large ensemble methods and their potential utility in characterising a fuller distribution of possible wildfire danger, the benefits and limitations of which are then explored in Chapters 3 and 4.

Terminology:

In this thesis, 'wildfire' is defined as any uncontrolled vegetation fire. Risk, and terms relating to risk are relevant to the interpretation of results throughout this thesis. 'Risk' is used to refer to the overall probability and consequence of different types of wildfire events (Brown et al., 2024) at a specific time and place. Risk can be conceptualised as summing the probability of different hazard severities multiplied by exposure (for example of people, property or an ecosystem) and the vulnerability of that exposure to wildfire. 'Hazard' is used here to describe the likely properties of wildfires at a location, in the context of potential negative impacts. 'Exposure', relates to the amount and type of different wildfire-vulnerable categories. 'Vulnerability', relates to the expected impacts wildfire would have on a particular exposed category. This framework is particular to catastrophe risk modelling, which is only relevant to the estimated negative impact of wildfire. The focus of this thesis is more generally on patterns in wildfire, so the broader term 'wildfire danger' is used when discussing the general

conduciveness of conditions to a wildfire event without connoting a risk perspective (as in, e.g., Dupuy et al., 2020; Chuvieco et al., 2023).

1.1 Wildfire Across Scales

Individual wildfires can be up to 10,000s of square kilometres in size. But the distribution of wildfire sizes is long-tailed, varying from a log-normal to power-law distribution depending on environment (Hantson et al., 2016) – meaning that the majority of wildfires are very small. The scale of an individual wildfire is determined by natural and artificial barriers such as rivers and roads, how fast the fire spreads, and multi-day wildfire persistence. The impact of a wildfire on vegetation and in emissions is affected by the intensity of the wildfire, controlled by the flammability, moisture and biomass of the burning vegetation. Wildfire intensity and size can contribute to the impact of a wildfire on people and property, but location and the speed of spread are often more important. For example, in the Lahaina (2023) and Los Angeles (2025) wildfires (Figure 1) relatively small, rapidly spreading wildfires overwhelmed evacuation and suppression capabilities. This led to penetration of suburban areas with widespread impacts on the surrounding area and economy and recovery often taking months. At a larger scale, high impact wildfires affecting a large area can occur when multiple extreme wildfires arise due to synoptic-scale weather conditions. These conditions include low humidity, high windspeeds and high temperatures that persist at a location for consecutive days. In highly productive environments this can result in extensive ecosystem damage and harmful air-quality effects over the surrounding region (e.g. the Pantanal and Indonesia, Figure 1). The greatest impacts of wildfire at a continental scale result from seasonal (e.g. Canada, Figure 1) to multiannual (e.g. the Arctic, Figure 1) periods of high fire activity associated with long-term fire-prone conditions. Such events are influenced by climate change and annual to multiannual climate oscillations that influence regional temperatures and precipitation patterns.

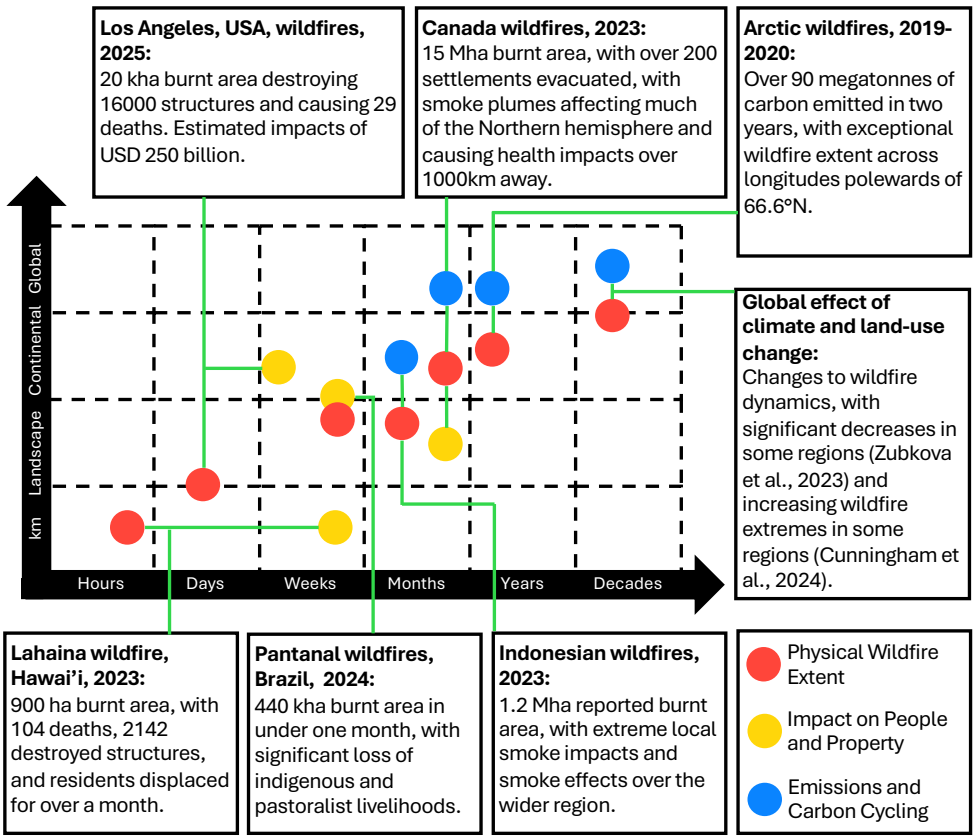

Figure 1: Recent examples of wildfire events and the variation in scale of their impacts and extent, adapted from Hamilton et al. (2024). Los Angeles, 2025 (Barnes et al., 2025), Canada, 2023 (Jain et al., 2024), Arctic, 2019-2020 (Copernicus, 2022), global change (Zubkova et al., 2023; Cunningham et al., 2024), Indonesia, 2023 (Copernicus, 2023; UNDRR, 2024), Pantanal, 2024 (Barnes et al., 2024), Lahaina, 2023 (Maui County, 2023).

1.2 Controls on Wildfire

Three conditions must be met for a wildfire to occur. First, there must be an ignition source. Second, there must be fuel available to burn. Third, the fuel must be sufficiently flammable for a wildfire to develop. These simple conditions give rise to complex interactions. The two principal causes of wildfire ignition are lightning and human activity. Most lightning occurs during rainfall events (Wickramasinghe et al., 2024), which decreases susceptibility to wildfire. However, precipitation creates more favourable conditions for vegetation growth and hence fuel accumulation in the long term. Humans ignite fires, either deliberately or accidently, but human activities are also associated with suppression of fires, vegetation fragmentation which limits spread, and creation of monocultures vulnerable to wildfire (Bousfield et al., 2025). Long-term wildfire suppression can also have a secondary impact on the fire regime, resulting in higher fuel loads and more intense wildfires (MacDonald et al., 2023). Fuel production is higher in moist conditions, but these conditions also lower combustibility from wet fuels and

increase the rate of dead fuel decay (Moore, 1986) reducing fuel loads. Wind also has multiple effects on wildfire. Wind increases evapotranspiration and fuel drying, transports embers long distances increasing fire starts (Wang, 2011), drives a faster rate of wildfire spread (Moritz et al., 2010) and influences lower atmospheric instability which can cause extreme fire behaviour (Werth, 2011).

Globally, most burnt area results from human ignitions. Wildfires in tropical grasslands and savannah are the greatest contributors to global burnt area (Jones et al., 2022, Janssen et al., 2023). In highly developed landscapes such as Europe (Dijkstra et al., 2022), the contiguous US (Balch et al., 2017), and southeastern Australia (Collins et al., 2015), ignitions by people are especially prevalent. Short (2014) categorises human ignitions in the United States of America (USA) as resulting from commercial or industrial activity such as heavy equipment use, infrastructure such as railways or powerlines, and debris or agricultural burning. Ignitions can also occur due to accidents such as poor cigarette disposal, campfires, children playing, or structural fires, ceremonial activities such as bonfires and fireworks, or arson or protest. Ignitions from powerline networks or rail lines are predictable from mapped infrastructure, but ignition rates from the other sources can be harder to predict. Modelling wildfire ignitions therefore requires predictors that approximate the penetration of people into natural landscapes, such as population or road densities. Specific behaviours associated with different types of ignition likelihood can be predicted by variables for human behaviour such as hiking trails or cropland. Some moderately inhabited environments are exposed to very large numbers of ignition sources. In such environments, the effect of ignitions on overall burnt area can plateau (Guyette et al., 2006, Archibald et al., 2009). Anthropogenic ignition sources can also result in an expansion of the natural conditions in which wildfire occurs – human-caused wildfires in the USA occur at higher average fuel moistures than those associated with lightning ignitions (Balch et al., 2017).

Lightning ignitions contribute more to burnt area than human ignitions in less habited regions such as the northern extratropical forests, Amazonia, the Congo basin, and interior Australia (Veraverbeke et al., 2017; Jones et al., 2022; Janssen et al., 2023). As lightning is associated with higher rainfall, high lightning seasons and regions can be less wildfire prone overall, an effect that is especially strong in Africa (Janssen et al., 2023). There do exist high quality lightning datasets (WWLLN and Vaisala) but these data are not freely available and cover a limited amount of time. This means that predictors for lightning and dry-lightning activity such

as convective available potential energy (CAPE) must be used as a proxy with precipitation controlled for (Saleh et al., 2023).

Precipitation is an important meteorological control on wildfire, with different effects on different timescales. At daily timescales, precipitation can rapidly wet fine fuels, decreasing the probability that an ignition will propagate. Precipitation events can also extinguish active fires. Dry spells are an important shorter-term control on wildfire because bulky litter and deep fuel beds require longer periods to dry (van Wagner, 1974; Cohen and Deeming, 1985). Over monthly timescales, drought can strongly affect live fuel moisture. Canopy moisture content decreases at lower water potentials (Scarff et al., 2021) increasing the likelihood of crown fire. Extreme drought can also cause plant mortality from hydraulic failure (McDowell et al., 2008) leading to higher dry, dead fuel loads and more intense wildfires (Stephens et al., 2018). At seasonal and longer timescales, precipitation acts primarily as an influence on other variables such as plant productivity and snow cover. Long periods of high precipitation promote plant growth, increasing wildfire likelihood if followed by dry conditions. Snow cover can suppress wildfire likelihood (Hessilt et al., 2024), and earlier snowmelt has been linked to a longer pre-season drying period and greater burnt area in some regions (O'Leary et al., 2016). Despite being influenced by precipitation, these effects can be accounted for directly.

Evapotranspiration is the loss of moisture to the atmosphere, via transpiration from plants and evaporation form the soil. When water is available in the soil, evapotranspiration increases with radiation, wind, and the vapour pressure deficit (VPD) (FAO, 1998). These three variables determine water vapour loss through the leaves when stomata are open, and evaporation from dead fuels and soil. VPD directly relates to the difference between the atmospheric absolute humidity capacity, the vapour mass at a relative humidity of 100%, and its actual ambient value. VPD is therefore the key control on the diffusive force between saturated air adjacent to a moisture source and the surrounding atmosphere (Anderson, 1936). Accumulated VPD can be used as a measure of the long-term drying potential on a landscape and determines live fuel drying and plant mortality during dry periods (Grossiord et al., 2020). VPD is strongly influenced by temperature, so is generally high in the day and lower during the night (Swain et al., 2025). Low VPD at night is an extinction 'barrier' for wildfires, since at low VPD plant moisture levels can increase to a point where fire cannot propagate (Balch et al., 2022). Alternately, extreme VPD maxima can drive very low fine fuel moistures associated with extreme wildfire behaviour (Matthews, 2014; Resco de Dios et al., 2022). Whilst VPD and fuel

drying increase in response to warmer temperatures, cold temperatures can also desiccate plants – freezing otherwise available moisture in the ground and plant tissues resulting in more combustible plants (Davies et al., 2010).

Wind is a control on fuel drying, but it is also important for driving wildfire spread and causing large wildfires (Moritz et al., 2010; Srock et al., 2018). Surface wind is also associated with atmospheric instability, which increases vertical motion in the atmosphere. Wildfires can also generate their own wind systems, an effect controlled by atmospheric instability – which relates to the ease of vertical motion of air in the atmosphere. Higher instability allows for a greater updraft from a wildfire, which can allow for extreme fire behaviour. This could be a greater indraft to the fire front leading to faster fire spread (Haines, 1988), or more exotic behaviour such as the formation of fire whorls (Forthofer and Goodrick, 2011). Once large, wildfires self-generate atmospheric instability through a convective plume. In rare cases such plumes may collapse, causing an intense downdraft and extreme fire behaviour (Werth, 2011). Whilst atmospheric instability is complex, it can be characterised by CAPE.

Through these meteorological controls on fuel conditions and fire dynamics, climate is an emergent control on wildfire. Atmospheric moisture capacity responds exponentially to temperature (Manabe and Weatherald, 1967) making VPD extremes much more likely in warmer climates. Drought and very wet years are both more likely with high atmospheric moisture capacity (Swain et al., 2025). This increases the likelihood of years with beneficial growing conditions and high fuel productivity followed by drought, which can lead to an extreme fire season (Madakumbura et al., 2025). Patterns of climate variability such as El Niño Southern Oscillation or the Arctic Oscillation are known to influence the jet position, which can influence midlatitude weather patterns and storm tracks (Eichelberger and Hartmann, 2007; Soulard et al., 2019) and have a resulting effect on pre-fire-season fuel moisture. Atmospheric blocking events resulting in persistent hot conditions have been linked to extreme fire seasons in the extratropics (Gedalof et al., 2005; Antokhina et al., 2023), the frequency and intensity of which has also been linked to global climate modes (Barriopedro et al., 2006).

Fuel availability is another essential factor for wildfire occurrence. Fuel availability is limited in urban areas, rocky and snow-covered terrain, but is also limited in tundra, deserts and semi-arid areas. Wildfire spread is limited by vegetation connectivity. Discontinuity in vegetation cover can control fire development due to natural barriers such as bodies of water or less

flammable vegetation, or due to human development such as roads and fire breaks (O'Donnell et al., 2010; Janssen and Veraverbeke, 2025). Changes in landscape fragmentation by people limits the size of wildfires but also can result in drying at vegetation edges and the introduction of more ignitions. Road fragmentation therefore results in an overall global decline in burnt area but an increase in fire occurrences and intensity (Bowring et al., 2024). The regional effect on burnt area depends on whether an ecosystem is fire-adapted or not (Harrison et al., 2021). In ecosystems more adapted to wildfire fragmentation reduces burnt area, while in non-adapted environments fragmentation leads to increased fuel drying and wind speeds causing increased wildfire. Though this effect does not apply in the most fire-prone environments, as human fragmentation has little additional effect on open and grass dominated vegetation. In fire-prone forests, wildfires create a mosaic of unburnt and burnt vegetation that limits subsequent wildfire size and intensity by areas of no vegetation (Kolden et al., 2012). This is the basis of mosaic or patch burning practices to mitigate wildfire danger.

The amount of vegetation ultimately determines the available fuel load. The productivity of vegetation is therefore a key determinant of the amount of live and dead fuel, with recent work finding that ecosystem-level productivity is of rivalling predictive power to meteorological drivers in wildfire models (Haas et al., 2024; Harrison et al., 2025b). At a given fuel moisture level, higher GPP and consequent fuel loads would mean more frequent and intense wildfire. However, high productivity requires a moist environment that suppresses fuel combustibility and results in less wildfire. Similarly, in highly flammable dry conditions, low productivity limits wildfire (Van der Werf et al., 2008). Due to transpiration, nondormant live vegetation is moister and less ignitable than dead vegetation, meaning that dead fuel availability is the primary fuel control on wildfire viability in the growing season (Chuvieco et al., 2004; Little et al., 2024). This dead fuel is an unstable energy pool, which can be released either through rotting or burning. Dead fuel loads are determined by the productivity rate of vegetation and how long it takes for this material to decay. Decomposition rates are determined by an environments moisture and temperature (Bunnell et al., 1977) and the litter's lignin and nitrogen levels on decomposition (Aerts, 1997; Grootemaat et al., 2015)

Plant traits influence flammability, fire dynamics and post-fire ecosystem recovery. Plant traits that convey adaptations to fire can be subdivided into four categories (Pausas et al., 2017; Popović et al., 2021). Firstly, there are traits that result in faster fire spread and consequently less burnt biomass per area. This increases survival chances and benefits plants that flower post-

wildfire. These include leaf traits that result in finer, less densely packed fuels such as through higher specific leaf area (SLA), curled leaves, and higher leaf surface to volume ratio, as well as the presence of volatile organic compounds (VOCs) (Burton et al., 2020; Chen et al., 2023). Mixed sources of leaf litter combine non-additively, with the spread rate driven by the most flammable leaf type (de Magalhães and Schwilk, 2012). Secondly, there are traits affecting plant survival of wildfires in these faster spreading, lower intensity fire regimes, such as savannah. Thicker or lower density bark (Pellegrini et al., 2017; Nolan et al., 2020) increases trunk resilience to scorching. When the base of the canopy is higher, the chance of fire affecting the branches is reduced (Blauw et al., 2017). A higher canopy base or thicker bark comes with a higher carbon cost and reduces but does not eliminate plant combustibility. Such traits are therefore most common where fires are frequent but less intense (Pausas et al., 2017), where they confer the greatest difference between plant mortality and survival. Resprouting of new shoots after a plant is damaged is also more common in more fire-prone environments (Shen et al., 2023). Resprouting is possible from the plant base and stem (Clarke et al., 2012) though can be limited by water stress (Resco de Dios et al., 2020). Though in very frequent fire environments, seeding grasses are more competitive (Simpson et al., 2020) as carbon stored in the meristem by resprouters can be depleted beyond that the plant has been able to invest. Thirdly, there are traits associated with higher heat release and plant mortality, which favour species that can rapidly regrow or re-establish. The amount of fuel concurrently burning determines the fire intensity. Intensity is therefore higher when there is more fuel, coarser fuels that burn for longer, and ladder fuels that promote crown fire. Whilst fuel loads and structure are also controlled by other environmental factors, plant traits contribute through effects on canopy bulk density, litter packing and branch structure (Pausas et al., 2017, Blauw et al., 2017). Litter decomposability, which affects fuel loads, has been found to be decoupled from leaf size and shape traits that affect litter density and the rate of wildfire spread (der et al., 2017). The litter load and litter density can therefore be treated as independent plant-trait driven effects on surface flammability. Fourthly, there are traits affecting post-wildfire regrowth in severely burnt areas. These include serotiny, the triggering of germination of dormant seeds by heat or smoke, or resprouting from below-ground meristems.

Vegetation structure is a key influence on whether wildfires are primarily surface fires or transition to crown (or canopy) fires. Surface fires burn vegetation close to the ground and occur primarily in grassland and shrubland, although they can also occur in lower energy forest wildfires. Crown fires are more intense and fast spreading (Rothermel, 1983). They result in

more ignitions from radiative transfer and ember transport (Cohen and Butler, 1996) and are harder to manage. The likelihood of a transition from a surface to crown fire is more likely in denser forest, or where there are ladder fuels, lower basal branches, and higher canopy dry mass (Alexander, 1988). Ground fires can also occur in high biomass organic soils such as peatlands and wetlands. These must be subject to significant drying to ignite and are slow burning because of limited availability of oxygen. Consequently, ground fires can persist for very long periods and result in significant net emissions (de Groot, 2012). The likelihood of fire spreading from intense crown fires to ignite organic soils in boreal forest is affected by species variation in structure and chemistry (Blauw et al., 2017).

While people are an important source of ignitions, they also reduce the occurrence of large wildfires. This can be intentional through suppression of active fires through fire-fighting activities or through pre-fire vegetation management to reduce fuel loads or create firebreaks. Wildfire suppression is limited in extreme wildfire conditions, with the most extreme fires able to cross firebreaks, resist suppression, and pass through heavily developed land cover (Jacobo, 2025). Human suppression can also be unintentional: the use of land for infrastructure or agricultural fragments the landscape and creates artificial firebreaks. Long term wildfire suppression can result in an increasingly connected landscape with high fuel loads outside of the natural equilibrium, which can cause more severe and impactful wildfire events (Moritz et al., 2014; Kreider et al., 2024). Fire-excluding suppression policies in many regions have had a significant effect on the fire regime, increasing the chance of extreme wildfire late in the dry season and changing the fuel profile (Moura et al., 2019). Many societies have a historic culture of vegetation fire use (Smith et al., 2022), with changes to these practices resulting in permanent changes to ecosystems and human-fire relationships (Bowman et al., 2020).

One key influence on the wildfire regime is human fire use. Intentional fires can escape and evolve into wildfires (Perkins et al., 2024), as well as reducing fuel loads and altering the vegetation cover. Smith et al. (2022) identify multiple types of intentional human fire use globally. First, agricultural fire use has been used historically across the globe to clear land for semi-permanent or swidden agriculture (Temudo et al., 2020), to establish permanent farms and plantations (Temudo et al., 2020), and to clear weeds and pests (Ditomaso et al., 2006). Second, pastoralists use fire to clear land and decrease predation rates for grazing livestock, as well as to promote high-quality forage from post-fire regrowth (Butz, 2009; Thapa et al., 2022). Third, fire is used to improve conditions for hunted species (Vaarzon-Morel and Gabrys, 2009), as a

hunting tool (Welch, 2014), and to increase accessibility for fishing (Sletto, 2011). Fourth, fire can be employed as a tool in gathering and foraging to improve visibility and production of desirable plants (Long et al., 2017), and to aid in the collection of wild honey (Mulder et al., 2000). Fifth, fire can be used to produce fuel and charcoal for cooking fires (Butz, 2009) and to speed the drying of bulky fuels (Kepe, 2012). Sixth, fire can be used to reduce the risk of wildfires to people, with prescribed fire commonly used to combat wildfires and reduce future wildfire risk (Manzello et al., 2020). Seventh, fire also has sociocultural uses for signalling (Lewis and Clark, 1805), in arson and protest (Seijo, 2005), and in cultural practices (McKemey et al., 2019). Many of these types of fire use have substantial impacts on the fire regime through the intentional reduction of tall grasses, shrubs and trees, resulting in a lower intensity grassland fire regime. Each fire use has a different associated likelihood of escape, with fire use with no control measures, pasture management and vegetation clearance having the highest associated rates of escape (Perkins et al., 2024).

Given the large number of effects driving changes in ignition likelihood, the fuel regime, and wildfire development, it can be complex to identify the optimal set of predictors for a wildfire event. Predictors selection is often based on a general understanding of important effects or is simply based on previous studies (Haas et al., 2024) – capturing the key categories of effect, but not the large number of specific variables that could be used. In this thesis, the conceptual understanding of the different controls on wildfire are each accounted for by a range of candidate predictors for each type of effect (given in Table 1, with more detail in Chapter 2, Table A1).

Table 1: This table shows the categories of different types of control on wildfire discussed in this section, and how they map onto the predictors used in the wildfire occurrence model described in Chapter 2. Indirect predictors of wildfire control types are shown in italics – these were used either due to data quality and availability issues for variables describing direct effects, or because the variable also describes a different causal effect on wildfire. A detailed overview of the exact predictors used in Chapter 2 is available in Chapter 2, Table A1.

Type of Control on Wildfire	**Predictors Considered in Chapter 2**
Accidental Anthropogenic Ignition	*Population density (rural and total), Landscape access (roads, trails, roughness), Industry (powerlines, railroads), Land-use (cropland)*

Human Suppression and Intentional Fire Use	*Population density (rural and total), Landscape access (roads, trails, roughness), Land-use (cropland)*
Lightning	*Convective available potential energy (dry days and all days)*
Recent Precipitation	Dry days, Precipitation volume (daily, 5-daily), *Soil moisture (multiple layers), Snow cover*
Seasonal Precipitation	*Plant productivity (over different antecedent time periods), Aridity and annual soil moisture*
Evapotranspiration	Temperature (mean, maximum, minimum and range), Vapour pressure deficit (day, night, and over different antecedent time periods), Relative humidity, Insolation, *Elevation*
Wind and atmospheric instability	Surface windspeed, Convective available potential energy
Fuel Continuity	*Population density (rural and total), Landscape fragmentation (roads, trails, railroads, roughness), Plant productivity*
Fuel Amount	Plant productivity (over annual to multiannual time periods), *Aridity and annual soil moisture*
Live Fuel Moisture	Plant productivity (over different recent time periods)
Plant Flammability Traits	*Plant cover type, Aridity and annual soil moisture*
Veg Structure	Plant cover type

The best combination of predictors in a wildfire model can be comprehensively tested with a flexible variable selection algorithm. Ultimately, models converge on a set of important variables (figure 2). Annual or multiannual productivity and recent productivity are both important, predicting fuel loads and live fuel moisture respectively. Key meteorological predictors relate to atmospheric heat, humidity and recent precipitation. And the important effects of sparse populations are captured through rural population density, roads and cropland. For most of these models, snow cover and vegetation type fractions are also selected. Adding additional variables results in a more predictive model, but increased model complexity can also result in overfitting and difficulty in interpreting the model output. The most appropriate number of variables can therefore be selected using an information criterion which balances model fit against the number of variables used in the model.

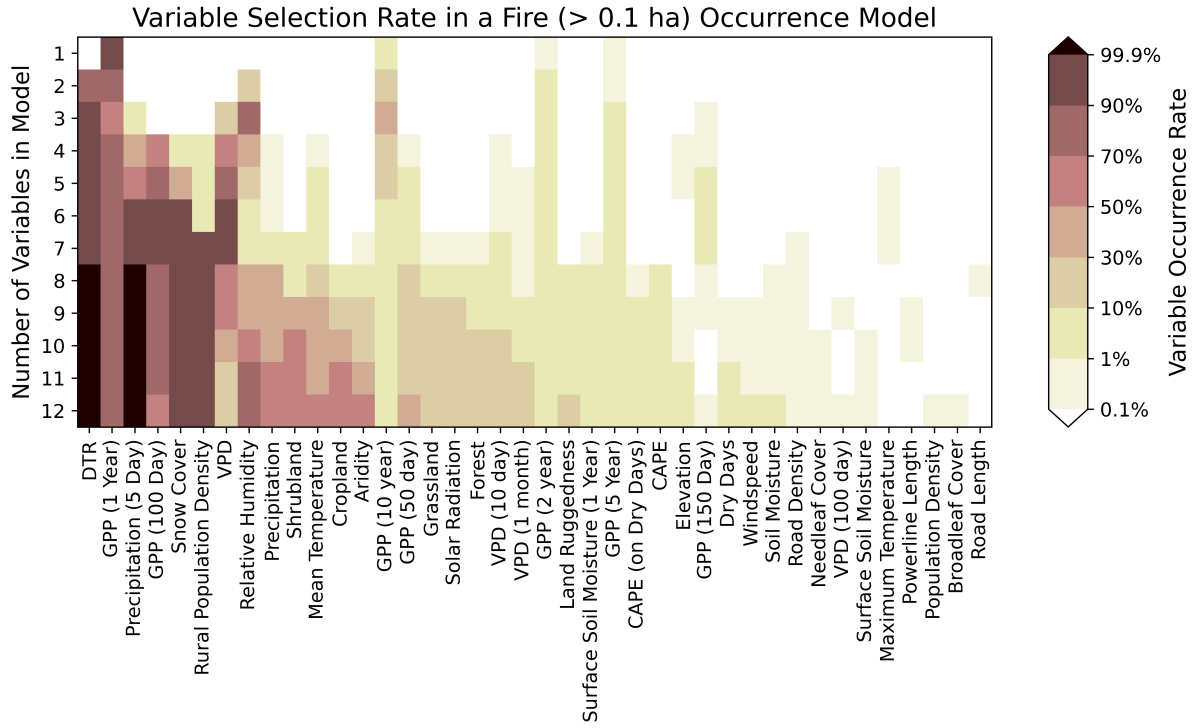

Figure 2: Occurrence rate of selected predictors for 1000 n-variable fire occurrence models trained in the contiguous United States. The number of variables considered was up to twelve, after which key drivers were roughly stable. Models were based on a generalised linear model (GLM), predicting the daily likelihood of a wildfire occurrence >0.1ha. Each model was trained on one million randomly sampled data points. Acronyms used are DTR (diurnal temperature range), GPP (gross primary productivity), VPD (vapour pressure deficit), CAPE (convective available potential energy). Adapted from work derived from this thesis, presented in Haas et al. (2024).

Many factors influence the occurrence of wildfires, but these factors cannot be applied in isolation and the interactions between them gives rise to emergent relationships. The intermediate fire occurrence-intensity hypothesis (Van der Werf et al., 2008) states that in high productivity environments wildfire occurrence and intensity are low due to high moistures, and in dry, low productivity environments wildfire occurrences are low due to a fuel limitation but more intense due to the dry fuel. The consequence of this is that wildfire occurrence is highest in moderately moist, moderately productive environments that are associated with intermediate fire intensity. Across annual GPP and VPD gradients, wildfire daily occurrence frequencies and fire size follow humped relationships in the contiguous USA. The highest burnt area is found in dry but non-arid environments (figure 3). Wildfire size and burnt area decrease in response to higher population density (Bistinas et al., 2014), whilst occurrence likelihood increases then

decreases – shown for the contiguous US in figure 3. Higher ignition rates initially increasing with population density until approximately 200 people per km2, before decreasing in more developed environments.

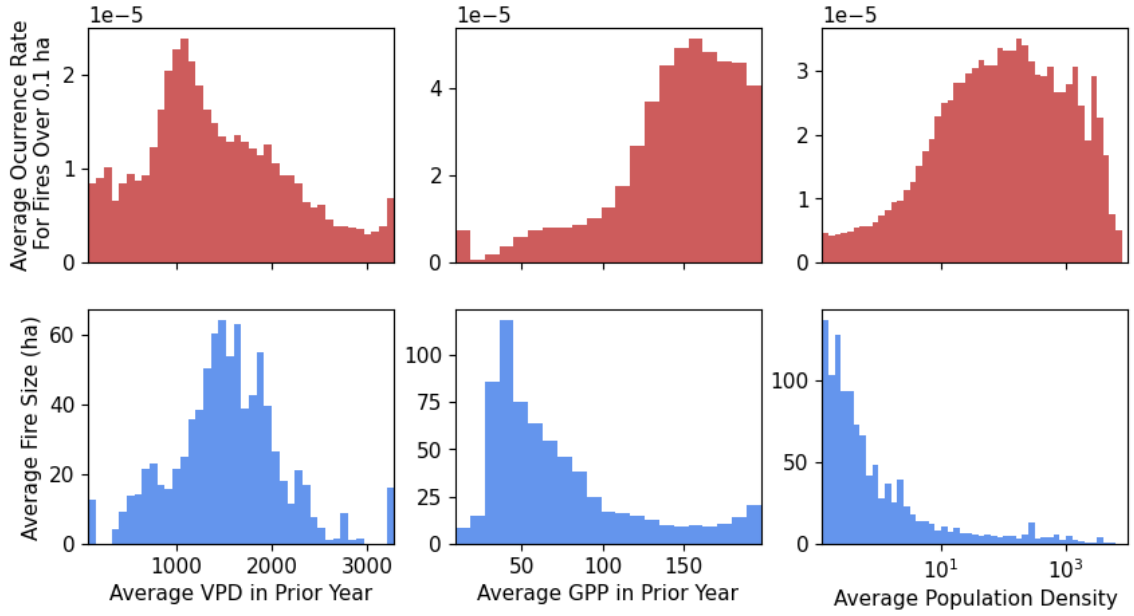

Figure 3: Original results illustrating the humped response of wildfire occurrence and size to predictor variables in the contiguous USA. Top row: mean annual number of fires as a function of daily vapour pressure deficit, GPP over prior year, and population density. Bottom row: mean fire size as a function of daily VPD, total GPP over prior year, and population density. This plot is an original and unpublished result.

1.3 The Past, Present and Future of Wildfire

Wildfire is an integral part of the Earth system, having an effect on, and being affected by, vegetation, people and climate. There is evidence that wildfires have occurred since the emergence of vascular plants (Scott, 2000) and have consequently shaped the evolution of vegetation on Earth (Keeley et al., 2011). People also have co-developed with wildfire. Fire has been used by humans since before the development of agriculture (Pyne, 2001), and with recent population growth and land-use change driving an increase in wildfire from the late 18th century and a subsequent decline in the post-industrial era (Marlon et al., 2008). Current climate and land-use are rapidly shifting, with an effect on wildfire. There is an apparent statistically significant decline in global burnt area (Andela et al., 2017) but this is not consistent across datasets (Forkel et al., 2019a). Rigorous testing of the trend finds no global trend but declining trends at different rates in some regions (Zubkova et al., 2023). Despite this apparent decrease

in area, the most intense wildfires have more than doubled in frequency and intensity globally in the last two decades (Cunningham et al., 2024), with this trend expected to continue in the future.

The first appearance of charcoal in the fossil record is at approximately 420 Myr BP, about 10 Myr after the first evidence of higher-biomass vascular plants (Berner, 2006; Harrison and Morris, 2017). Thereafter, wildfires occur throughout the fossil record whenever atmospheric oxygen is sufficient for ignition, at about 13%. Wildfires became widespread after the emergence of forests (Scott, 2000), especially when atmospheric oxygen concentrations were above 25% (Scott and Glasspool, 2006). Given this fire history, plants have evolved a range of adaptations to fire that can in turn affect the wildfire regime. Over geologic timescales, it has been suggested that the emergence of fire-adapted grasslands has affected regional climate, further promoting wildfire. Specifically, an increase in wildfires with the emergence the savannah biome has been linked to increases in regional drought through a reduction in evapotranspiration and cloud duration (Beerling and Osborne, 2006).

Early humans originated in the highly wildfire-prone African savannah approximately 2 Myr BP. The origin of human fire-use (Bowman et al., 2009) and the evolution of our relative tolerance to air pollution (Platek et al., 2002) have both been linked to the prevalence of fire in this environment. Evidence that fire has influenced human evolution is the divergence in the hominoid molar size, indicating cooking fire use up to 1.9 Myr BP (Organ et al., 2011), and the first archaeological evidence of cooking fires 780 kyr BP (Zohar et al., 2022). In recent geologic time wildfire activity has varied considerably, with disagreement as to the extent of the human role in these trends (Bowman et al., 2011). Since the end of the Last Glacial Maximum (LGM), approximately 22 kyr BP, there has been an increasing trend in wildfire activity. This can be explained almost entirely by the changes in climate and CO_2 levels (Daniau et al., 2010; Daniau et al., 2012; Haas et al., 2023). As human populations have been low until recent centuries, the impact of human fire use is likely small. Haas et al. (2023) constrain the contribution of people to LGM burnt area as less than 5% in Europe, Africa and Australia. In the last two millennia global fire activity declined until approximately 1750, rapidly rose until 1870, before sharply declining again. These trends are visible in both the ice core and charcoal records. These trends can be respectively attributed to cooler northern hemisphere temperatures, early land use change and population expansion, and landscape fragmentation (Marlon et al., 2008; Marlon et al., 2013).

Global burnt area is mostly driven by fire in sub-Saharan Africa, with secondary contributions from Central and South America, Central and Southeast Asia, and Australia (Figure 4). Linearly fitting the 1998-2015 Global Fire Emissions Database (GFED4s) satellite record, there is an approximately 25% decline in global burnt area (Andela et al., 2017). However, Forkel et al. (2019a) found that the global trend is not statistically significant for all satellite fire datasets. Furthermore, the slope of each trend is very sensitive to the start and end dates of the observation period. Using the MCD64A1 MODIS record, Zubkova et al. (2023) identified significant declining trends in Europe, sub-Saharan Africa and Central Asia but no significant trend in other regions of the world. Even though burnt area has declined over the past two decades, the frequency and intensity of extreme wildfires has strongly increased in the same period. The frequency of the 99.9th percentile of wildfire by intensity (summed fire radiative power) has increased 2.2 times from 2003-2023 and the average intensity of the 20 most intense annual wildfire events has increased 2.3 times (Cunningham et al., 2024). This increase in extreme wildfires is a consequence of emerging fire weather extremes driven by climate change (Abatzoglou et al., 2018). Whilst climate attribution studies have to this point only considered the meteorological component of the wildfire hazard, the concurrent fire weather observed with wildfire extremes has been attributed to climate change in Canada (Kirchmeier-Young et al., 2019; Barnes et al., 2023), Mediterranean France (Barbero et al., 2020), California (Williams et al., 2019, Barnes et al., 2025a), Australia (van Oldenborgh, 2021), the Pantanal (Barnes et al., 2024), and Korea (Barnes et al., 2025b).

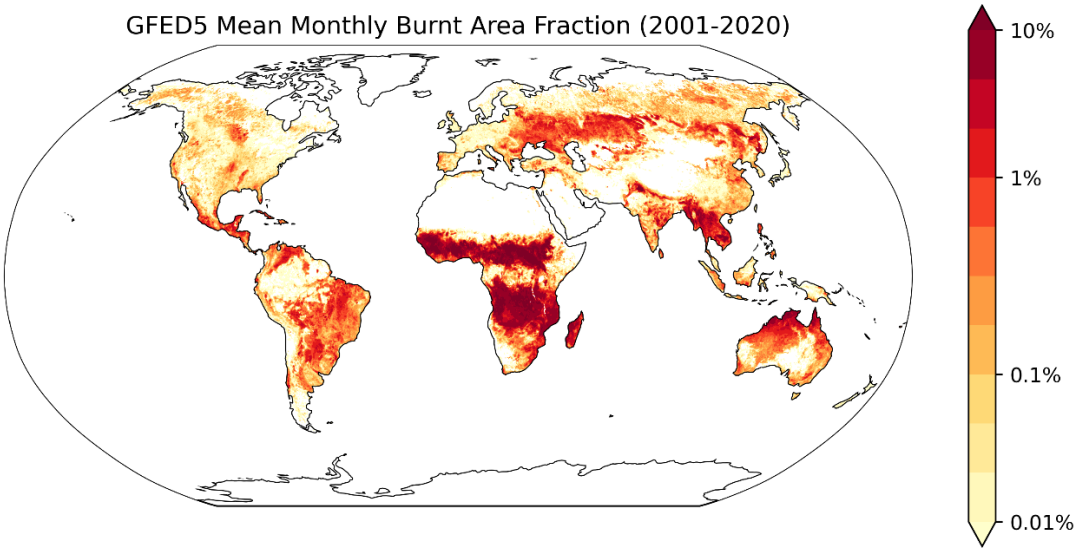

Figure 4: Total monthly mean burnt area from version 5 of the Global Fire Emissions Database (GFED5) (Chen et al., 2023)

There is a strong interest in understanding and projecting future wildfire, motivated by the regional changes in burnt area and emerging wildfire extremes. and extreme fire weather (Abatzoglou et al., 2018). A UN Environment Programme report (Sullivan et al., 2022) also predicted a global rise in burnt area, and an increase in the likelihood of extreme wildfire events of 31-57% by 2100. The uncertainty on this estimate accounts for possible model parameters and Representative Concentration Pathways RCP2.6 and RCP6.0. However, this study does not account for the additional aleatoric uncertainty that results from the stochastic nature of fire.

1.4 Impacts of Fire on People

The most substantial overall impact of wildfire on physical health comes from the exposure of communities to smoke. Wildfire smoke contains irritant and carcinogenic gases including carbon monoxide, nitrogen oxides and polycyclic aromatic hydrocarbons; as well as microscopic particulates smaller than 2.5μm (PM2.5) that can penetrate and inflame the respiratory system, causing a range of range of respiratory and cardiovascular health impacts (Naeher et al., 2006). Large-scale wildfire events can result in very high PM2.5 levels. During the 2023 wildfire season in Canada, PM2.5 concentrations of over 100μg/m^3 were recorded in all Canadian provinces (Jain et al., 2024), as well as in Oregon and California (Dinavahi and Archer, 2025). In the 2019/2020 Australian Black Summer, concentrations of over 1000μg/m^3 were recorded in densely populated areas (Johnston et al., 2020). Extreme PM2.5 concentrations are driven by smoke transport and stagnation, and the volume of biomass burnt. In the Central Californian Valley, for example, persistent pollution occurs when smoke is trapped by high-pressure systems, prevailing winds and the surrounding mountains (LaDochy and Witiw, 2023). Extreme concentrations resulting from high volumes of burnt biomass from Indonesian peat burning affects air quality in cities such as Singapore and Pekanbaru (Crippa et al., 2016) and has produced PM2.5 concentrations of over 7000μg/m^3 in Sumatra (Fujii et al., 2014). Elevated PM2.5 levels are the primary driver of negative health effects from vegetation fire, which is defined here as both wildfire and human fire use. PM2.5 has been linked to the exacerbation of asthma, chronic obstructive pulmonary disease, respiratory infections, cardiac failure and heart disease, lower birthweights and more young infant deaths, and the toxic inflammation of lung cells (Reid et al., 2016). The mortality from vegetation fire smoke, not including cooking fires, has been estimated at 260-600,000 annual excess deaths globally (Johnston et al., 2012), with the greatest concentrations in sub-Saharan Africa and Southeast Asia. Modelling indicates vegetation fire PM2.5 caused 3.8 million annual excess

deaths in 749 cities from 2000-2016 – an approximate 2% increase in all-cause mortality for every 10μg/m^3 increase in vegetation fire related PM2.5 (Chen et al., 2021). This is likely a conservative global estimate, as Chen et al. (2021) do not include rural areas and have poor coverage of cities in sub-Saharan Africa and India. Higher mortality rates have been estimated for some regions, for example a 3% effect per 10μg/m^3 found for Brazil (Ye et al., 2022).

Direct wildfire deaths from asphyxiation, burning or impact are low compared to those from smoke. Though global estimates are unreliable, in the USA, there were an average of 18 direct annual deaths for 2007-2020, in comparison to an estimated 11,415 annual deaths from wildfire smoke exposure (Ma et al., 2024). In addition to deaths and physical health consequences, wildfire events have been associated with mental health effects, including increased post-fire rates of post-traumatic stress disorder, depression and anxiety (Moosavi et al., 2019; To et al., 2021). Following the Black Saturday wildfires in 2009 that killed 173 people and destroyed 2133 houses in Victoria, Australia (Pascoe et al., 2010), rates of post-fire depression and alcohol abuse remained high even ten years after the event although post-fire stress disorders moderately declined in the same period (Bryant et al., 2021).

Wildfire can also have financial consequences. Annual losses from wildfires globally have increased since 1960. From 2020-2023, they were approximately 0.012% of the global gross domestic product (GDP) (Poduška and Stajić, 2024). Wildfire can also affect long term economic growth. In southern Europe, if a region experiences a wildfire, GDP growth is on average reduced by 0.1-0.2% (Meier et al., 2023). However, global data on the economic impacts of wildfires is often strongly biased towards rich developed countries, especially the USA. The main mechanism through which financial losses are reported is via insurance claims. These are much better represented in developed economies with high property values and where insurance against wildfire is widespread. The USA provides an example of how financial risk from wildfire has changed in a highly developed, fire-prone country. From 2011-2024 the average annual number of structures destroyed by wildfire was 6,900 (NICC, 2025). The average annual insured losses were 3.7 billion USD (at 2025 equivalent rates, MunichRe, 2024). However, annual wildfire losses in the USA are highly variable and are characterised by large, rare events. There have been only three years since 1980 with USA insured losses over 5 billion USD, but these years had average losses of 18 billion USD (MunichRe, 2024). The 2025 Los Angeles wildfires are estimated to have caused property and capital losses between 95 to 165 billion USD, with 75 billion USD insured (Li and Yu, 2025). If these claims are realised, insured

losses from these wildfires would equal approximately 0.07% of the global GDP in 2024. There has been a trend in regions of increasingly extreme climate-related risk, for insurers to exit these markets. This is the case in Californian, with state-backed programmes having to act as last resort insurers at high public cost (NPR, 2025).

An additional cost of wildfire is to business interruption through loss of infrastructure, employment and customer base. This has not been well documented in the case of wildfire, though Thomas et al. (2017) made comparisons between wildland-urban interface (WUI) wildfires and low intensity hurricanes in their average business-interruption impacts, at an average of 140 billion USD (Burrus et al., 2002). Industries reliant on an intact landscape are especially vulnerable to wildfire, with significant losses in the tourism industry associated with large wildfire events (Carruthers, 2020). Wildfires also harm to agroforestry resources. In the USA, wildfire accounted for 14% of forest stock carbon removals from 1941 to 2017 (Magerl et al., 2023). Wildfire smoke exposure can also ruin vine harvests (Madhusoodanan, 2021).

Reported USA fire statistics show a minor decreasing trend in wildfire events and a minor increasing trend in burnt area over the last four decades (Figure 5, top panel) as a result of the increasing potential for larger fires in the US with climate change (Barbero et al., 2015). However, the impacts of wildfire have increased in the same time period, driven by high-cost wildfires in the WUI. The WUI expanded in the USA between 1990 to 2010, both in area and the number of structures. The WUI housing density further increased from 2010 to 2020 (figure 5, middle panel). Impacts are particularly high in the Western USA wildland/rural urban interface due to the intermediate population density, as catastrophic wildfires are less likely in the more densely populated regions like Mediterranean Europe in comparison to less populated but similarly fire-prone regions such as the western USA or southeastern Australia (Moritz et al., 2014; Bowman et al., 2017).

Suppression costs, structures destroyed and insured losses have all increased significantly in real terms (figure 5, bottom panel). Though the dependence of losses on extreme destructive wildfire events in high value areas does introduce considerable noise into the timeseries. The 2018 Camp fire, for example, which resulted in 16 of the total 23 billion USD annual losses. Media reporting of wildfire events often uses explicitly apocalyptic language (Reilly, 2025; Willis, 2025; Sherriff, 2025). Doerr and Santín (2016) show that there was no clear increasing trend in global wildfire losses up to 2012 but that awareness of wildfire in the West has

increased with rising WUI exposure and suppression costs. They argue that this framing of wildfire as a "problem" is a consequence of human settlement in fire-prone regions, or introduction of fire into non-adapted regions. This effect is a key driver of the increasing prominence of wildfire in the public-consciousness and increasing insurance losses. However, there have been a large number of extreme and highly damaging wildfire events globally since 2012, which have been attributable to climate change (Kirchmeier-Young et al., 2019; Barbero et al., 2020, Williams et al., 2019, Barnes et al., 2025a, van Oldenborgh, 2021, Barnes et al., 2024, Barnes et al., 2025b).

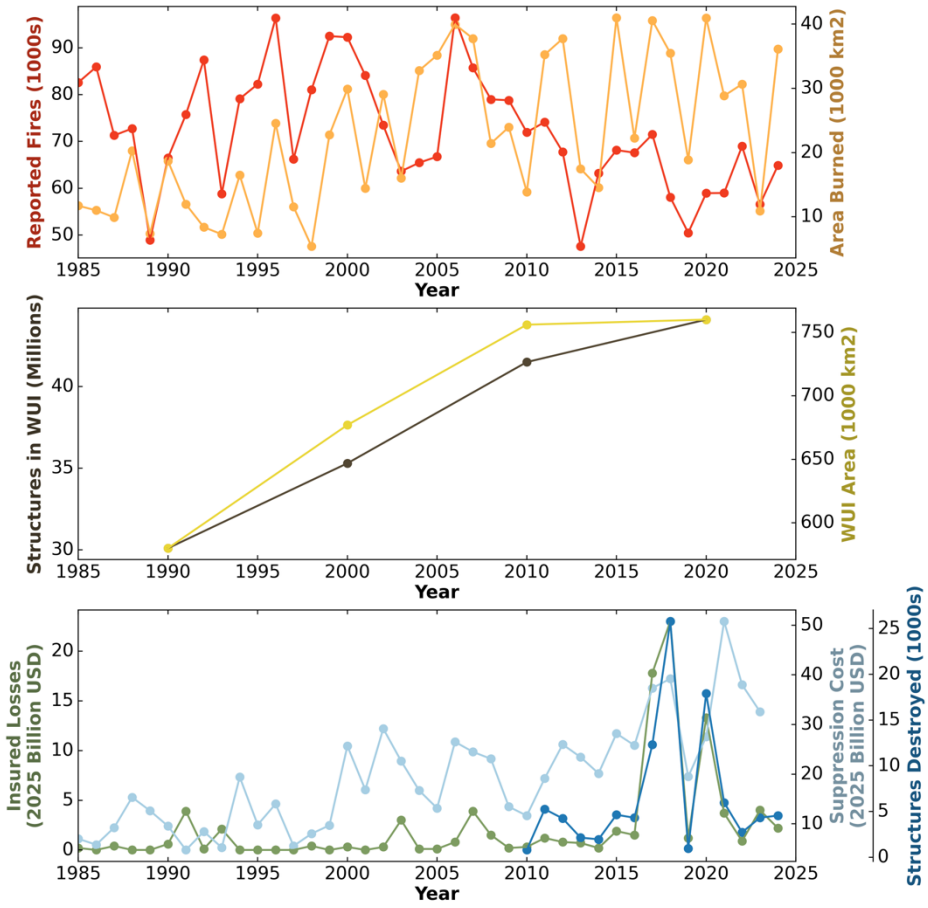

Figure 5: Illustration of the hazard, exposure and impact of wildfires. Top panel, annual trends in US fire numbers and burnt area (NIFC, 2024). Middle panel, annual trends in the US wildland urban interface area and number of properties (USDA, 2023). Bottom panel, insured losses (MunichRe), structures destroyed (NICC, 2025), and suppression costs (NIFC, 2024).

Wildfire can also impact people indirectly by exacerbating other natural hazards. Wildfire events can diminish soil integrity, increasing the likelihood of landslides (Cannon et al., 2010). Wildfires can enhance water repellence at the soil surface (Arcenegui et al., 2008) increasing run-off and consequent flood volume (Soulis, 2017). Large wildfires have been linked to

warmer surface temperature due to the destruction of temperate and boreal forest, increasing the likelihood of extreme heat hazards (Zhao et al., 2024). Wildfire activity is also increased by other natural hazards such as volcanic eruption, drought, lightning, extreme heat, and meteoric impact (Gill and Malamud, 2014).

1.5 Impacts on the Earth System

Climate change has increased fire-prone conditions (Smith et al., 2020), but wildfire can also affect climate change through the land surface energy budget and atmospheric chemistry. The surface energy budget can be altered by wildfire through albedo-induced changes in shortwave radiation absorption. Wildfires affect albedo directly by darkening the surface (Zhao et al., 2024). In snow covered regions, wildfire reduces the albedo of non-forested land through carbon deposition but increases forest albedo through canopy loss exposing the underlying snow (Gersh et al., 2022). The immediate reduction in albedo in grasslands is followed by an overall brightening through regrowth, resulting in a net albedo increase (Flegrová and Brindley, 2025).

CO_2 emissions from wildfire result in higher atmospheric greenhouse gas concentrations, even when discounting net wildfire emissions from long-term carbon sinks through peatland or deforestation fire. This is because the reduction in land carbon pools must be balanced by an increase in carbon resident in the atmosphere. Harrison et al. (2018) find that the overall increase in wildfire per degree of warming results in an additional 2.4-8.8 ppm CO_2. This positive feedback was estimated by Burton et al. (2024a) to decrease the global carbon budgets required to maintain temperatures below 1.5°C or 2°C by approximately 5%. Wildfires also emit other greenhouse gases (Ito et al., 2007), including methane, and nitrogen oxides which are a very strong greenhouse gases that can also react with VOCs to increase tropospheric ozone (Xu et al., 2021). Microscopic particles emitted by wildfires impact the global energy budget by acting as cloud condensation nuclei and increasing cloud cover and also by directly scattering incoming shortwave radiation (Jiang et al., 2020). In addition to these cooling effects, absorbative black carbon particulates can have a warming effect in the middle and lower atmosphere (Liu et al., 2014).

Total annual emissions from wildfires are approximately 2.1 PgC (van Wees et al., 2022), with net annual emissions from deforestation and peat fire equivalent to approximately 0.4 PgC (van der Werf et al., 2017) which is about 1% of total annual emissions from fossil-fuels and land-

use change (Ritchie and Roser, 2020). The sign of the overall effect of wildfire on global temperature is dependent on balancing the warming effect of terrestrial biomass loss to atmospheric carbon and the cooling effects of aerosols. There is high uncertainty on both of these effects in models (Hantson et al., 2020; Hamilton et al., 2025), and on the observed effect of aerosols (Liu et al., 2014), meaning that the overall effect of wildfire on climate is highly uncertain.

Post-wildfire conditions and vegetation loss can impact a range of localised meteorological and hydrological processes. Firstly, wildfire can result in an increase in local temperature. Lower albedo from canopy loss and scorched soil has been linked to increased local surface temperatures through greater absorption of shortwave radiation in the extratropics (Zhao et al., 2024). Further, reduced evapotranspiration from vegetation mortality (Ma et al., 2020; Nolan et al., 2013) can decrease cooling from latent heat transport, resulting in warmer surface temperature and lower humidity. Secondly, depending on burn completeness and the resulting vegetation fragmentation, wildfire can either increase or decrease surface roughness (Crompton et al., 2021). Large continuous burns that result in lower surface roughness have been linked to higher surface windspeeds (Wever, 2012), which contribute to evaporation (FAO, 1998). Thirdly, post-wildfire conditions can alter surface water runoff. Fire can increase soil hydrophobicity when vapourised organic compounds coat soil particles in a hydrophobic film (DeBano, 1981). This increases run-off most strongly in loose or sandy soils and can be enhanced by the destruction of otherwise absorptive litter and vegetation (Doerr et al., 2005). However, post-fire ash deposits can absorb water (Cerda and Doer, 2008) and wildfire can reduce water repellence in soils that are already highly hydrophobic (Doerr et al., 2005).

Wildfire is important for maintaining open vegetation, such as grasslands, and fire-adapted ecosystems, such as savannas. In the absence of fire, these ecosystems are likely to become forests. The effect of fire on global vegetation cover has been assessed using dynamic global vegetation models (DGVMs) in fire-enabled simulations and counterfactual simulations without fire. An early estimate (Bond et al., 2004) suggested that forest cover was reduced by 50% by fire, resulting in a loss of global biodiversity and a reduction in C_4 grasslands. However, recent work using an ensemble of more sophisticated models only showed a 10% reduction in overall tree cover, but with great losses in some regions including a 17% reduction in savannahs (Lasslop et al., 2020).

The impact of wildfires on biodiversity is dependent on the degree to which the ecosystems are adapted to fire. In fire-adapted ecosystems, fire suppression or a climate change driven reduction in fire occurrence, will reduce biodiversity. Excluding wildfire from a fire-adapted environment disrupts the natural vegetation and its associated habitats (Noss et al., 2006; Moritz et al., 2014). However, since ecosystems show different levels of adaptation to fire, increases in wildfire occurrence beyond the level to which they are adapted will also cause reductions in biodiversity. Changes to the fire regime driven by climate change and increased fuel loads from reduced grazing or fire exclusion is a threat to 28% of the endangered or vulnerable taxa identified by the IUCN (Kelly et al., 2020), with species native to savannah, grassland, shrubland and rocky environments most exposed to this hazard. However, the impact of wildfires on biodiversity can be influenced by other factors. Driscoll et al. (2024), for example, found that the 2019-2020 wildfires in Australia increased species richness in some areas, but had negative impacts in environments already stressed by previous drought or fires. In less fire-adapted ecosystems, wildfires initiate succession and allows fast-growing pioneer species to invade, and this can lead to an overall increase in biodiversity. Wildfires rarely burn an ecosystem completely (Kolden et al., 2012), and the resultant mosaic of burnt and unburnt vegetation tends to create greater landscape diversity in forest ecosystems than would be present in the absence of fires.

Wildfire also has a strong effect on biodiversity at higher trophic levels. Moritz et al. (2023) analysed the effect of fire activity and net primary productivity (NPP) on bird, mammal and amphibian species richness per area using a mixed effect model. They showed that fire has a stronger additional effect than NPP on mammal richness and an equivalent effect to NPP on bird richness. The modelled findings are supported by field studies, with burnt ecosystems showing greater species richness for birds (Jorge et al., 2022), mammals and reptiles (Pastro et al., 2011) – and a mixed response for amphibians (Hossack and Pilliod, 2011).

Wildfire also plays a key role in nutrient cycling, which can also influence vegetation cover and biodiversity. Fire releases nutrients from vegetation, resulting in a significant increase in nutrient availability (Chorover et al., 1994). In addition to local release of nutrients, benefitting post-fire recovery, nutrients can be transported either through runoff or atmospheric transport (Olsen et al., 2023) and thus become available over a much larger region. The Central African (Bauters et al., 2017) and Amazon rainforests (Barkley et al., 2019) both benefit from nutrients transported from African savannah wildfires. Similarly, phytoplankton in the Atlantic and

Southern Oceans are fertilised by African and Australian wildfires (Barkley et al., 2019; Weis et al., 2022).

1.6 Wildfire and Earth System Feedbacks

There are multiple feedbacks between wildfires and other components of the Earth system. These feedbacks operate on different timescales. At annual to decadal timescales, wildfires result in feedbacks to climate through emissions and changes in carbon storage. At decadal to millennial timescales wildfires can result in environmental changes through vegetation succession and migration, which then affect the fire regime. On longer, multi-millennial timescales, the vegetation can become adapted to the wildfire regime. Over geologic timescales, wildfire plays an important role in Earth system chemistry through phosphorous weathering, deep carbon sequestration, and regulation of atmospheric oxygen concentrations (Archibald et al., 2018).

Vegetation evolves traits in partial response to wildfire, which in turn affects the fire regime. It has been argued that the evolution of C_4 savannah grasses 8 Myr BP was due to their high flammability which created fire conditions that enhanced their competitiveness (Beerling and Osbourne, 2006). A species with advantageous traits post-disturbance such as rapid growth, resprouting or serotiny will experience an evolutionary advantage if it can make an ecosystem more flammable. This evolutionary pressure to develop more flammable and intensely burning fuels (Bond and Midgley, 1995) has been a major influence on plants such as pines and obligate seeders (He et al., 2012; Pausas and Moreira, 2012). Wildfire activity can also pressure the evolution of fire-adapted traits for fire resilience and rapid regrowth, though these traits can also develop in response to climate (Rosell, 2016) or grazing (Pellew, 1983). That vegetation flammability is a primary determinant of the fire regime is questionable. This is because the viability of such strategies is also controlled by climate-driven effects on plant productivity and fuel moisture, and truly similar environments should see similar convergent adaptations (Pausas et al., 2025). It is nonetheless helpful to consider wildfire as an ecosystem process that acts as one contributor to the viability of certain vegetation traits in addition to other environmental conditions.

Over daily to multimillennial timescales, wildfires can create conditions that increase or diminish the likelihood of subsequent wildfires. At the shortest timescales, extreme wildfires can cause the ignition of other wildfires or overwhelm human fire suppression systems

(Abatzogolou et al., 2020; Magnussen and Taylor, 2012). Depending on the speed of ecosystem recovery, the destruction of vegetation by wildfire reduces the likelihood of wildfire at multiannual timescales, while the lack of wildfire has the opposite effect (Parks et al., 2015). However, fires can lead to local increases in surface temperature and humidity via a post-fire decrease in albedo and reduction in evapotranspiration. This increases shortwave radiation absorption and reduces latent heat transport to the atmosphere by evapotranspiration (Zhao et al., 2024; Liu et al., 2019). The increase in the average surface temperature results in higher temperature extremes, which are linked to greater wildfire danger (Gutierrez et al., 2021). Wildfire can also reduce surface roughness which increases average windspeed, which again increases the likelihood of wildfire (Crompton et al., 2021; Wever, 2012; Rayner, 2007). The increases or decreases in wildfire activity, however, generally only have a decadal-scale impact because of vegetation regrowth.

Wildfires influence global mean surface temperatures by altering the Earth's energy budget. Ward et al. (2012) model the radiative forcing effect by vegetation fire to be about -0.5 Wm^{-2} due to the cooling effect of aerosols. Ward et al. (2012) used the Community Atmospheric Model, which has a high estimate of the aerosol cooling effect (Hamilton et al., 2025) and this may thus be a lower bound. The effect of wildfire on the carbon cycle and atmospheric CO_2 is warming, because a world without fire would have more carbon stored in live terrestrial biomass that would otherwise be emitted by burning. The consequence of this is an increase in wildfire emissions from terrestrial biomass as fire prone conditions increase with climate change, resulting in higher atmospheric CO_2 levels (Harrison et al., 2018; Burton et al., 2024a). Thus, wildfire has a cooling effect on global temperatures through aerosol effects, and a warming effect through the limitation on terrestrial carbon pools. Arneth et al. (2010) find that the overall effect of wildfire on climate change is uncertain in sign and much smaller than other biogeochemical feedbacks. However, a change in the climate and resulting burn conditions could significantly shift this forcing in either direction.

Under ongoing climate change, wildfires have an additional warming effect through the destruction of large carbon sinks such as peatland and rainforests. Aerosols and black carbon can also result in greater ice melt which reduces mid-latitude albedo and increases warming (Kang et al., 2020). On longer, multimillion year, timescales wildfires reduce atmospheric oxygen levels. Wildfires occur regardless of moisture levels when O_2 is higher than 35% and cannot occur when levels are lower than 13% (Scott and Glasspool, 2006), resulting in a

regulation of atmospheric oxygen. However, wildfire is a minor feedback over geologic timescales, lagging changes in the global energy budget forced by the impact changes in solar changes on climate.

1.7 Overview of Wildfire Models

Current, rapid changes to the global fire regime (Section 1.3) are important to understand, especially given the widespread impacts these changes are having, and could have, on people (Section 1.4) and the Earth System (Section 1.5). Wildfire modelling is a key part of current global assessments of the present and future of wildfire (Sullivan et al., 2022; Kelley et al., 2025), developed to best capture the complex network of weather, human and vegetation drivers and feedbacks with wildfire (Section 1.2, 1.6). Simulations of current or projected wildfires are made using fire models integrated into dynamic global vegetation models (DGVMs) forced by climate model inputs, which in turn may be integrated into a fully coupled Earth System Model (ESM). These fire models, differently implemented in different DGVMs – presented in Table 2 – vary in approach and complexity. Figure 6 gives an overview of the DGVM-integrated fire modelling schemes that took place in the first round of the Fire Model Intercomparison Project (FireMIP1) (Rabin et al., 2017; Hantson et al., 2020).

Table 2: Overview of the combinations of DGVMs and global fire models used in FireMIP1 and presented in Figure 6. Acronyms and full names are given, as well as citations for each DGVM-fire model implementation.

DGVMs		Fire Models		References
LPJ-GUESS	Lund-Potsdam-Jena General Ecosystem Simulator	GlobFIRM	Global Fire Model	Thonicke et al. (2001)
		SPITFIRE	Spread and Intensity of Fire	Lehsten et al. (2009), Pfeiffer et al. (2013)
		SIMFIRE-BLAZE	Simulated Fire Induced Land-Atmosphere Flux Estimator	Knorr et al. (2014)
CLM	Community Land Model	Li	The Li Scheme	Li et al. (2013)
		GlobFIRM	Global Fire Model	Kloster et al. (2010)
JULES	Joint UK Land Environment Simulator	INFERNO	Interactive Fires and Emissions Algorithm for Natural Environments	Mangeon et al. (2016)
MC2	Second Mapped Atmosphere-Plant-Soil	MC-FIRE	Mapped Atmosphere-Plant-Soil System Soil Organic	Conklin et al. (2016)

	System Soil Organic Matter and Biogeochemistry Model		Matter and Biogeochemistry Model Fire Model	
ORCHIDEE	Organizing Carbon and Hydrology In Dynamic Ecosystems	SPITFIRE	Spread and Intensity of Fire	Yue et al. (2014)
JSBACH	Jena Scheme for Biosphere-Atmosphere Coupling in Hamburg	SPITFIRE	Spread and Intensity of Fire	Lasslop et al. (2014)
CTEM	Canadian Terrestrial Ecosystem Model	CTEM	Canadian Terrestrial Ecosystem Model	Melton and Arora (2016)

Each fire model consists of a series of modules. Firstly, the fire models include an occurrence or wildfire viability module, this predicts the number of wildfires or wildfire-viable days depending on the modelling scheme. GlobFIRM, SIMFIRE-BLAZE and MC-Fire have wildfire viability modules, where a binary wildfire event is assumed per grid-cell given appropriate that fuel conditions. The other models simulate number of wildfire occurrence, either as a probability (CTEM) or an expected number of fires (Li, SPITFIRE, INFERNO). All the schemes account for fuel moisture, with the occurrence-based modules also containing an ignition-frequency sub-module which accounts for human (except SPITFIRE in LPJ-LMfire) and lightning ignitions. The occurrence/viability modules can also contain a suppression sub-module limiting occurrences, which is included in the SIMFIRE-BLAZE, INFERNO, CTEM and SPITFIRE models. The wildfire model presented in Chapter 2 predicts the daily probability of fire, and could be a viable replacement to any of the probability or count-based wildfire occurrence modules.

Secondly, the fire models contain a fire size or spread module. Models that estimate likely wildfire size are termed ‘empirical’ and those that directly simulate wildfire duration and spread are known as ‘process-based’. This categorisation is independent of the structure of the occurrence module, meaning the occurrence model presented in this thesis could be of utility to both empirical and process-based methods. Process-based models simulate wildfire duration and spread using Rothermel’s equations (Rothermel, 1972) (SPITFIRE and MC-Fire) or via a wind and fuel driven fire spread scheme for each plant functional type (PFT) (Li, CTEM). Empirical models (SIMFIRE-BLAZE, GlobFIRM, INFERNO) predict overall fire size for each fire based on wildfire susceptibility and suppression conditions. Human extinction of fires as a function of population density or GDP is included in the Li and CTEM process-based models. MC-Fire includes a process-based module to simulate fire size, but calculates overall burnt area by an alternate method. Thirdly and fourthly, these fire models also include wildfire emissions

and vegetation mortality modules, for use in fully-coupled ESMs, which are beyond the scope of this thesis. Overall, fire-enabled DGVMs represent the spatial distribution of fire reasonably, but do not represent interannual variability and the timing and spread of the fire season throughout the year well (Hantson et al., 2020).

Figure 6 (overleaf): An overview of the structure of global fire models assessed in FireMIP1, as described in the paragraphs above. This diagram is based on the papers cited in Table 2, and was checked against overviews presented in Rabin et al. (2017) and Haas et al. (2024).

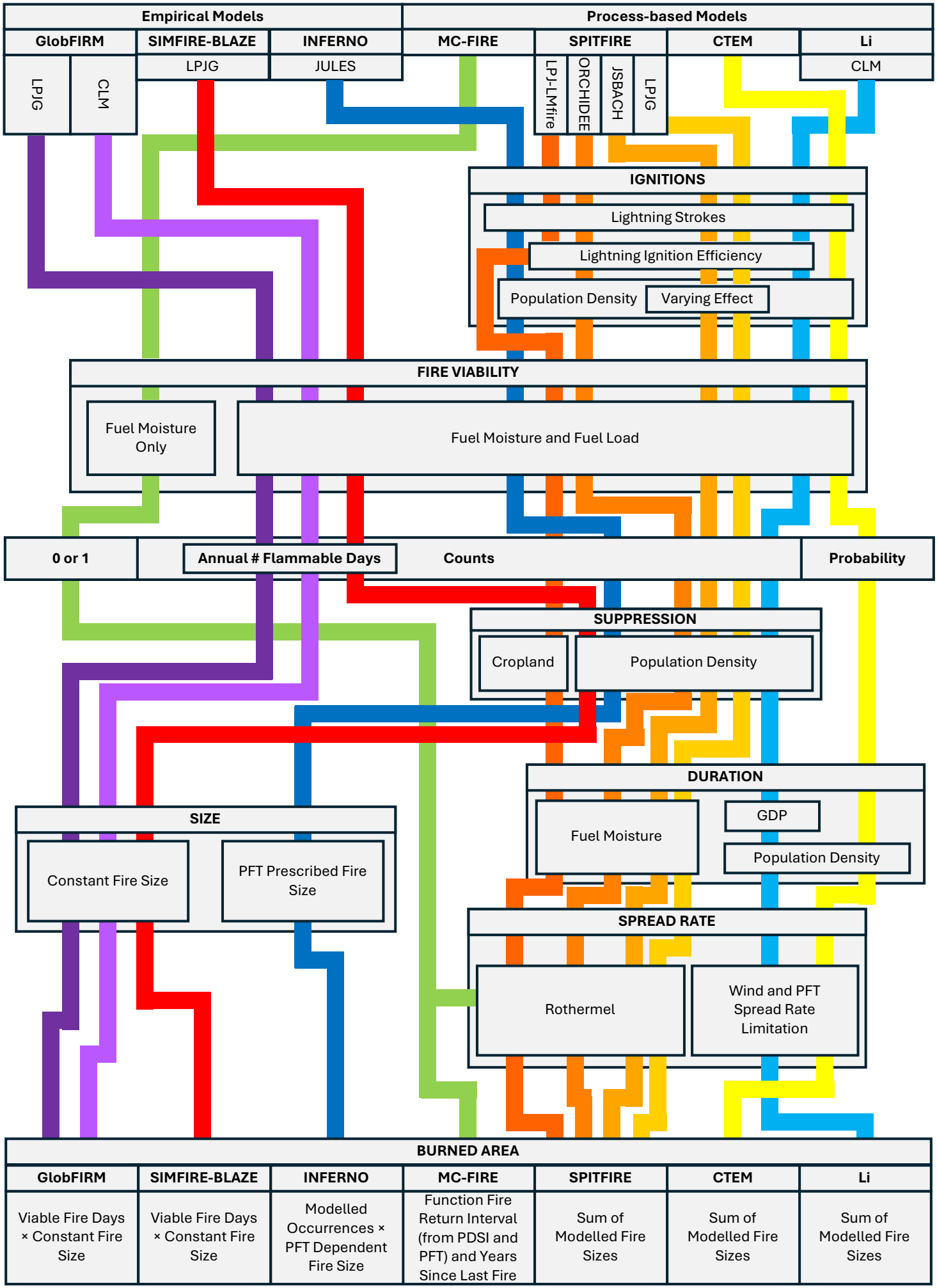
Empirical Models
Process-based Models
GlobFIRM
SIMFIRE-BLAZE
INFERNO
MC-FIRE
SPITFIRE
CTEM
Li
LPJG
CLM
LPJG
JULES
LPJ-LMfire
ORCHIDEE
JSBACH
LPJG
CLM
IGNITIONS
Lightning Strokes
Lightning Ignition Efficiency
Population Density
Varying Effect
FIRE VIABILITY
Fuel Moisture Only
Fuel Moisture and Fuel Load
0 or 1
Annual # Flammable Days
Counts
Probability
SUPPRESSION
Cropland
Population Density
DURATION
Fuel Moisture
GDP
Population Density
SIZE
Constant Fire Size
PFT Prescribed Fire Size
SPREAD RATE
Rothermel
Wind and PFT Spread Rate Limitation
BURNED AREA
GlobFIRM
SIMFIRE-BLAZE
INFERNO
MC-FIRE
SPITFIRE
CTEM
Li
Viable Fire Days × Constant Fire Size
Viable Fire Days × Constant Fire Size
Modelled Occurrences × PFT Dependent Fire Size
Function Fire Return Interval (from PDSI and PFT) and Years Since Last Fire
Sum of Modelled Fire Sizes
Sum of Modelled Fire Sizes
Sum of Modelled Fire Sizes

Fire-enabled DGVMs integrated into ESMs are adapted to run at shorter time-steps and have often been tuned using more recent global fire products (Li et al., 2024). Seven of the twelve fire-enabled ESMs in CMIP5 (Kloster and Lasslop, 2017) used GlobFIRM, while the remaining models used simpler approaches, including defining fire as a linear function of soil-moisture and biomass (Moorcroft et al., 2001), or as implicit in either heterotrophic respiration (Raddatz et al., 2007) or all-cause plant mortality (Brovkin et al., 2009). CMIP5 ESMs estimated global burnt area to be less than half of the GFED4s estimate though modelled global fire emissions fell within the GFED4s range. The disjunct between burnt area and emissions implies the use of unphysical emissions factors. CMIP6 fire-enabled ESMs (Li et al., 2024) used a wider array of fire models, specifically several different versions of the Li, SPITFIRE, and GlobFIRM schemes. The representation of burnt area is better in the CMIP6 models, improving from a 0.30 to 0.69 spatial correlation with the average burnt area from GFED5, FireCCI5.1 and MODIS C6. Emissions for most models are within the observational range.

The ability to simulate wildfire realistically depends on the strength of the causal relationships between driving variables and modelled fire outcomes. Forkel et al. (2019b) find that variation over time in modelled wildfire does not correspond well to the satellite record in semi-arid and temperate ecosystems for FireMIP1 models. Furthermore, these global fire models only show agreement with observed burnt area relationships for some meteorological variables, and for population density in some models. Other factors, especially vegetation-related variables do not show their relationships reflected well in the models. This raises questions about their reliability and use for future projections. Estimates of burnt area and emissions totals have shifted significantly over the last two decades. GFED4s identified 11% more emissions and 37% burnt area than GFED3 (van der Werf, 2017), and GFED5 found 61% more burnt area than GFED4s (Chen et al., 2023). This makes it hard to assess the extent to which the improvement between CMIP5 and CMIP6 identified by Li et al. (2024) has come from modelling improvements rather than better tuning of model parameters. The concern that these models are not adequately representing the key processes driving global change in the fire regime (Forkel et al., 2019b) is further supported by the finding that CMIP6 fire-enabled ESMs generally do not show the correct sign for the global trend in burnt area (Li et al., 2024).

Empirical models have been used to simulate wildfires with some success. Generalised linear models (GLMs) are statistical models that fit a sum of continuous variable effects to a specified function of the target variable. Haas et al. (2022) used a GLM to model global spatial trends in

wildfire, which outperformed the FireMIP models in geospatial burnt area patterns. They used the same methodology to predict fire size and intensity. Forrest et al (2024) develop two GLMs to model cropland and non-cropland burnt area in Europe. These models also performed within the benchmarked range of the FireMIP models. The success of GLM-based modelling of wildfires indicates scope for considerable improvements to fire simulation through simple continuously varying effects. This is a different strategy to the discontinuous PFT and environmental-threshold effects used in the FireMIP1 models. Machine learning methods have also been used to represent nonlinear combined effects successfully on sub-continental (Elia et al., 2020), continental (Boulanger et al., 2018), and global scales (McNorton et al., 2024; Zhang et al., 2021). Whilst it is possible to explain key effects in a machine learning model (Korving and Van Marle, 2025), the opacity of machine learning methods makes it harder to protect against overfitting. Boulanger et al. (2018) address this by using multiple statistical and machine learning (ML) modelling methods to find consensus – balancing respective underfitting and overfitting issues. McNorton et al. (2024) start with a limited framework of strong causal effects, limiting the possibility of spurious effects being introduced.

1.8 Limitations of Wildfire Models

One limitation of fire-enabled DGVMs is in their simulation of the human contributions to fire. These processes are exclusively accounted for as ignitions and suppressions, and are modelled using simple, globally homogeneous relationships. In reality, human fire-use is widespread and spatially diverse (Smith et al., 2022). The poor representation (Forkel et al., 2019b) of human effects in fire models contributes to the divergences between fire-enabled DGVMs – which even disagree over whether historic population and land-use changes have contributed positively or negatively to global burnt area (Teckentrup et al., 2019). The total effect of human fire-use is uncertain due to small fire sizes and subsequent disturbance of the fire scar, but is estimated to have been between 60 and 120 Mha/yr in the last two decades (Chen et al., 2023) in comparison to annual totals of 450 to 800 Mha/yr (Li et al., 2024). Perkins et al. (2024) have integrated human land management and fire use into JULES-INFERNO by modelling human relationships with fire as determined by socio-ecological conditions. These relationships control tendencies towards different types of managed fire-use, each of which has an associated likelihood of escape. The split approach by Forrest et al. (2024) also targets this problem by modelling natural vegetation and cropland fires using different predictor variables over a relatively socioeconomically homogeneous region.

Some key wildfire processes cannot be effectively captured because of the spatial and temporal scales of global fire models. Fire-enabled DGVMs are run at spatial resolutions from 0.5° to 2.8° (Li et al., 2019; Hantson et al., 2020), with fire-enabled ESMs run at similar resolutions (Li et al., 2024). Such resolutions are too coarse to resolve the variation in land cover and topography – which are critical in wildfire evolution and extinction (Janssen and Veraverbeke, 2025). Further, regridding of input variables to these scales can smear the nonlinear effects of sharp variations in population density, vegetation productivity and vegetation type on wildfire. The temporal scale of fire models is dependent on whether there is a process-based or empirical fire size scheme. Process-based fire models such as SPITFIRE simulate the spread of wildfire occurrences and are thus necessarily run at a sub-daily timesteps (Li et al., 2024), whilst empirical models such as GlobFIRM and INFERNO are trained with monthly accumulations – though this may be divided over each ESM timestep in the model output (Mangeon et al., 2016). For process-based models, the coarse spatial scale of the model means that spatially varying wildfire dynamics associated with wildfire evolution at a sub-daily timestep are not captured. On the other hand, empirical schemes trained on monthly data can miss the dynamics driving seasonal variation in wildfire outcomes, as very large fires shaped by daily-scale weather extremes drive burnt area totals (Stavros et al., 2014; Abatzoglou et al., 2014; Barnes et al., 2023)

Fire models make deterministic predictions of wildfire given environmental conditions and are often applied in a single ESM or DGVM run, resulting in an underrepresentation of wildfire stochasticity. Firstly, global fire models used in DGVMs and ESMs predict the expected burnt area per timestep, not capturing the uncertainty of an individual wildfire outcome. At finer spatial scales, many locations will see years with no fire interspersed with large wildfire events, due to the aleatoric uncertainty of wildfire ignition and survival. Secondly, there is also epistemic uncertainty on the precise effect of model drivers at the scales at which these models are run. Other disciplines such as flood modelling account for this uncertainty with an ensemble of possible models that incorporate the spread of possible model parameters (Ziliani et al., 2019). Thirdly, global fire models have mostly been applied in individual fully-coupled ESMs (Li et al., 2024) or run offline with reanalysis data (Burton et al., 2024b; Hantson et al., 2020). This does not account for the inherent variability in the climate system. A single realisation of the climate in either an ESM or reality is a very limited sample of the distribution of possible weather. The use of a large ensemble to characterise the distribution of possible drivers is

standard in other climate impact disciplines such as floods (Cloke et al., 2013), cyclones (Roberts et al., 2015), and heat extremes (Vautard et al., 2013).

1.9 Large Ensemble Methods

The atmosphere is a chaotic system (Lorenz, 1972). This chaotic behaviour means that errors in deterministic models of the atmosphere grow rapidly with time such that model predictions become less reliable (Lorenz, 1969). Current cutting-edge forecasts meet skill benchmarks up to 9-10 days forward of the initial state (ECMWF, 2023). Climate can be defined as the distribution of all possible weather states given external solar forcing and the composition of the land, ocean, cryosphere and atmosphere. Under stable conditions, the climate could be simulated with a single, sufficiently long simulation. In a changing climate, the only way to approximate the set of possible weather states is through an ensemble of model runs. There has therefore been broad adoption of large ensemble approaches when making weather predictions (Bowler et al., 2008), in seasonal forecasting (Johnson et al., 2019), and in projecting future climate scenarios (Maher et al., 2021).

Large ensembles (LEs) can be generated by combining outputs from multiple climate models, or by perturbation of the initial conditions or physics scheme of an individual model. Single model initial-condition large ensembles (SMILEs) run one climate model with variation introduced in the initial model conditions (Figure 7), allow the model to sample the internal variability of the climate more fully (Deser et al., 2020). Projecting changes in predictable climate modes of variability cannot be done by a single model. SMILEs characterise this change within a self-consistent modelling scheme. Multi-model ensembles (MMEs) run multiple GCMs (global circulation models) or GCM and RCM (regional climate model) combinations. Variability between the models arises from differences in initial conditions and in the physics schemes of each model (Figure 7). Whilst SMILEs account solely for aleatoric uncertainty, MMEs are also affected by epistemic uncertainty in how the model represents the relevant processes. SMILEs generally resolve aleatoric uncertainty in the climate system more completely than MMEs because they involve many more ensemble members (Maher et al., 2021; Muntjewerf et al., 2023).

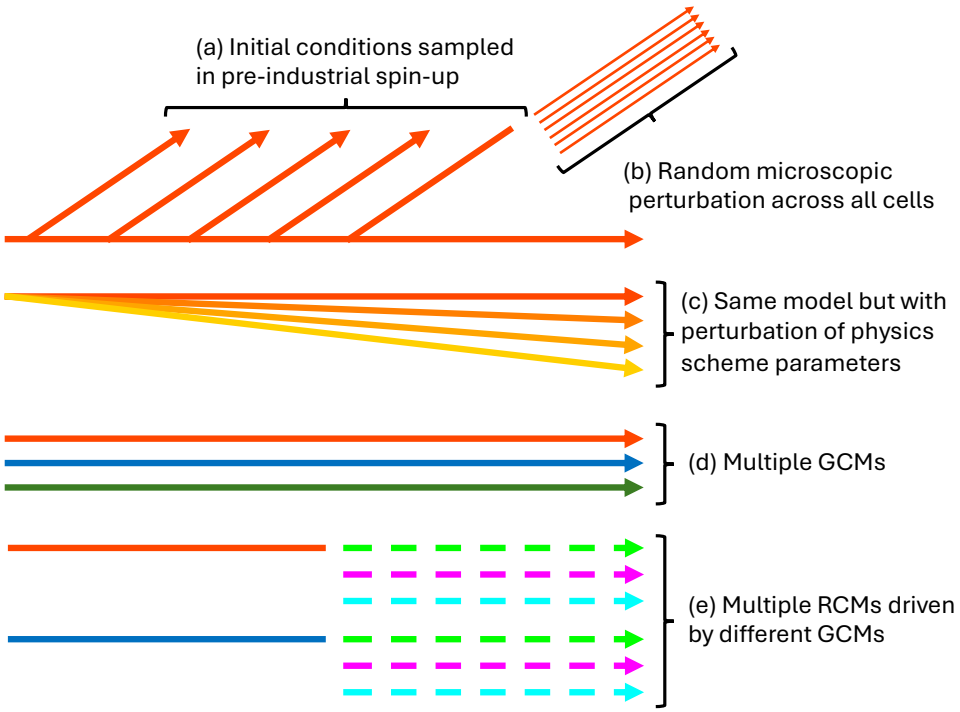

Figure 7: An overview of the different types of climate ensemble. SMILEs can be initialised (a) by sampling the model spin-up at decadal scale timesteps ensuring better sampling of structured modes of climate variability, or (b) by an instantaneous micro-perturbation of model fields such as temperature or pressure in every grid cell, which can allow for more ensemble members and reducing the demand on computational resources. LEs can also (c) run one model with perturbations on physics parameters to represent uncertainty in unknown driving effects. Finally, multiple GCM runs (d) can be combined separately for comparison, with the combination (e) of driving GCMs to multiple RCMs allowing for more ensemble members and a higher model resolution.

LEs sample rare, extreme events much better than single models or smaller ensembles. They have therefore been widely adopted in climate impacts research to understand changes in the likelihood and intensity of extreme events. LEs have been used, for example, to characterise changes to extreme summer temperatures in Europe with global warming (Suarez-Gutierres et al., 2018), the intensity of extreme flooding and drought events (Van der Wiel et al., 2019), annual maximum amounts of snowfall (Sasai et al., 2019), and the likelihood of observed extremes in fire weather and drought (Squire et al., 2021). LEs can also be used to estimate the changing distributions of weather variables (Haugen et al., 2018). They have been used to show the large variability in possible near-term trends in regional weather extremes, including characterisation of the likelihood of observing multidecadal trends opposite in sign to those

expected globally with climate change (Fischer et al., 2013). Although fire weather has been analysed using large ensemble methods, fire models have not previously been run using an LE. This is likely due to the computational demands of running a DGVM many times to obtain necessary vegetation inputs to the fire model.

1.10 Research Rationale

The aim of this thesis is to fully characterise the wildfire occurrence regime in the United States and understand its drivers, with an emphasis on variation between fire years. To do this, it was first necessary to develop a model for the daily probability of wildfire events. This was to enable the meaningful analysis of the fire hazard and its response to daily and slower-varying conditions – instead of solely focussing on realised events. Interannual wildfire variability in the present climate is poorly understood due to rapidly changing land-use and climate conditions and the resulting small sample of analogous fire years. To gain insight into this, the wildfire occurrence model was applied to an LE to assess patterns and drivers of interannual variability in the US – both in a recent and future climate. Clear spatial patterns in interannual wildfire variability and its chief controls prompted the question of the extent to which fire year variability and its drivers are controlled by climate modes – which can strongly influence the likelihood of different weather and vegetation conditions.

To gain a better understanding of patterns in wildfire occurrence over the US, this research project targets two key sources of uncertainty, generating synthetic data to better understand the real world. Firstly, daily wildfire occurrence probabilities are generated to present a more complete understanding of realised wildfire occurrence that is not skewed by a small sample of realised but low probability events. Secondly, synthetic fire years are generated for the recent (and a future) climate, so that the distribution of possible fire years can be analysed without spurious results being introduced due to the small sample size. With these sources of stochasticity over two very different temporal scales addressed by the model, patterns of variability in the annual number of wildfires and structure of the fire season can then be analysed.

The first research item was to develop a simple probabilistic model for wildfire occurrence. Wildfire has a central role in key Earth system processes such as nutrient cycling, the energy budget, and ecosystem composition (Sections 1.5, 1.6). It can also have extreme impacts on people's health, livelihoods and property (Section 1.4). As global wildfire has changed

dramatically in response to past climate and land-use change (section 1.3), and as these factors are currently changing rapidly, the development of high-quality wildfire models to understand current and future trends is crucial. This thesis focusses on an occurrence model, as this is the essential first module to a full fire model, and because occurrence modules are relatively undeveloped in existing global fire models (Section 1.8). A probability model was needed because actual wildfire events are rare and extremely stochastic – whilst daily probabilities of occurrence can be accumulated to account for seen and unseen events to better identify trends. Although the primary focus of this thesis is on the interannual patterns in the wildfire signal, a daily likelihood model was necessary to account for the strong contribution of extreme weather days to annual totals. Such a model needed to be developed due to the relatively undeveloped state of wildfire occurrence modelling (Section 1.7), not accounting for very recent developments in the field (Di Giuseppe et al., 2025). The focus was on developing a model of combined, simple variable effects. This was to facilitate the explanatory use of the model, and to have a simpler and more interpretable set of high confidence variable effects to better ensure applicability to out-of-sample scenarios. The use of some machine learning methodologies can achieve greater in-sample accuracy, but the inclusion of complex interacting terms means that identified relationships may be overfit and not hold true outside of the training sample.

The second research item was to use this occurrence model to understand patterns of interannual variability in wildfire occurrences due to climate and climate-induced vegetarian variability. This focus on interannual variability was prompted by the particular contribution of extreme fire years as a source of wildfire impacts. For example, the Australian Black Summer of 2019/2020, the Canadian fire season of 2023, and the Indonesian fire season of 2015 (NHRA 2023, Jain et al., 2024; Crippa et al., 2016). Despite growing scrutiny on regional fire season extremes, leading assessments of trends in global wildfire (e.g. Sullivan et al., 2022; Burton et al., 2024b; Kelley et al., 2025) have focussed on the projection of the fire regime mean burnt area, as opposed to a consideration of extremes or the full distribution of possible years. Additionally, global fire models perform poorly in reproducing interannual variability (Hantson et al., 2020). This does not interfere with their primary function of modelling average wildfire-related emissions and vegetation mortality in ESMs. Interannual variability in the wildfire record is well established as a key characteristic of the wildfire regime (Van der Werf et al., 2006; Tang et al., 2021), however there is currently a significant gap in the fire-modelling and projections literature exploring interannual variability and its future changes. This is of particular utility due to the shortness of the existing wildfire record in analogous climate

conditions, especially given the increasing rapidity of climate change seen in recent decades (Forster et al., 2024). Better understanding interannual wildfire variability would enable the likelihood of both observed and unseen events to be better estimated.

The third research item was to explore the extent to which fire years are associated with the phase of different climate modes. Climate modes are persistent or recurrent patterns identified in the climate system on interannual to multi-decadal timescales. Examples include the ENSO, a naturally occurring climate pattern that reflects ocean atmosphere interactions in the tropical Pacific Ocean with a multi-year oscillation, and the Pacific Decadal Oscillation (PDO) which has an even longer oscillation scale. This research topic flowed from the fact that the spread of annual wildfire occurrences was found to be greater than the mean predicted value, with strong spatial patterns in this relative variability. Associating higher wildfire occurrence years at a high spatial resolution with specific climate modes has utility from a hazard forecasting perspective, with climate modes often predictable months in advance. Climate modes were focussed on for this analysis, as it is already well established that the causal drivers of wildfire (Section 1.2) such as moist conditions (favourable for vegetation growth) and dry-heat are strongly influenced by climate modes over the US (Gershunov, 1998; Wang and Asefa, 2018). There is an existing literature establishing statistically significant links between wildfire and climate modes in the contiguous US (Heyerdahl et al., 2002; Kipfmueller et al., 2012; Simard et al., 2012). However, existing studies have not identified geographically varying patterns of association over the region due to the short satellite record necessitating either site-based tree ring data (e.g. Westerling and Swetnam, 2003) or aggregated federal data over a large region (e.g. Goodrick and Hanley, 2009). However, the applicability of LE methods to this problem is not well explored.

The three research questions (Section 1.11) all target two questions related to the stochasticity of wildfire. First, what processes drive wildfire occurrence? And second, what are the spatial and temporal patterns of wildfire occurrences as a consequence of those drivers? Chapter 2 answers these questions at a daily timescale using realised weather conditions in recent years. Then, Chapter 3 examines patterns in the distribution of possible years from which the small sample of realised years in an analogous recent climate are drawn, as well as in a climate subject to future global warming. This chapter examines patterns of variability between fire years, and which variables contribute most to that variability in different regions. Finally, Chapter 4 then explores the extent to which this variability can be explained by predictable

global climate modes, and how those associations might strengthen or weaken with future climate change.

1.11 Research Overview

How should a simple probabilistic model for wildfire occurrence be built?

In this thesis I focus on modelling the probability of wildfire occurrence, a first and necessary step in constructing the next generation of probabilistic global fire models. Building on previous work elucidating the drivers of wildfire (Parisien and Moritz, 2009; Harrison et al., 2010; Knorr et al., 2014, Bistinas et al., 2014; Forkel et al., 2017, Forkel et al., 2019b; Harrison et al., 2021; Kuhn-Regnier et al., 2021, Chuvieco, et al., 2021, Mukunga et al., 2023), I aim to build an empirical fire likelihood model that performs as well as existing models, operates at a higher spatial resolution, and resolves the strong daily response of fire to changing weather conditions.

The model was developed with the dual objects of predictive capability and a basis in simple driving effects (justified in Section 1.10). This chapter therefore aimed to identify the necessary alterations to a model of combined linear effects such that it was of adequate predictive capability for wildfire occurrence modelling. To do this I focus on a region with high-quality data spanning a wide range of fire regimes. The contiguous USA has a comprehensive federal record of fire occurrences (Short, 2014) and good representation of global fire regimes. Harrison et al. (2025b) have shown that pyroclimates delineated on the basis of GPP and VPD, controlling fuel loads and drying, are characterised by 18 distinct fire regimes. The contiguous US has 10 of these 18 global pyroclimates (mostly the extratropical pyroclimates) covering over 100,000 km^2 of the USA total area (Figure 8).

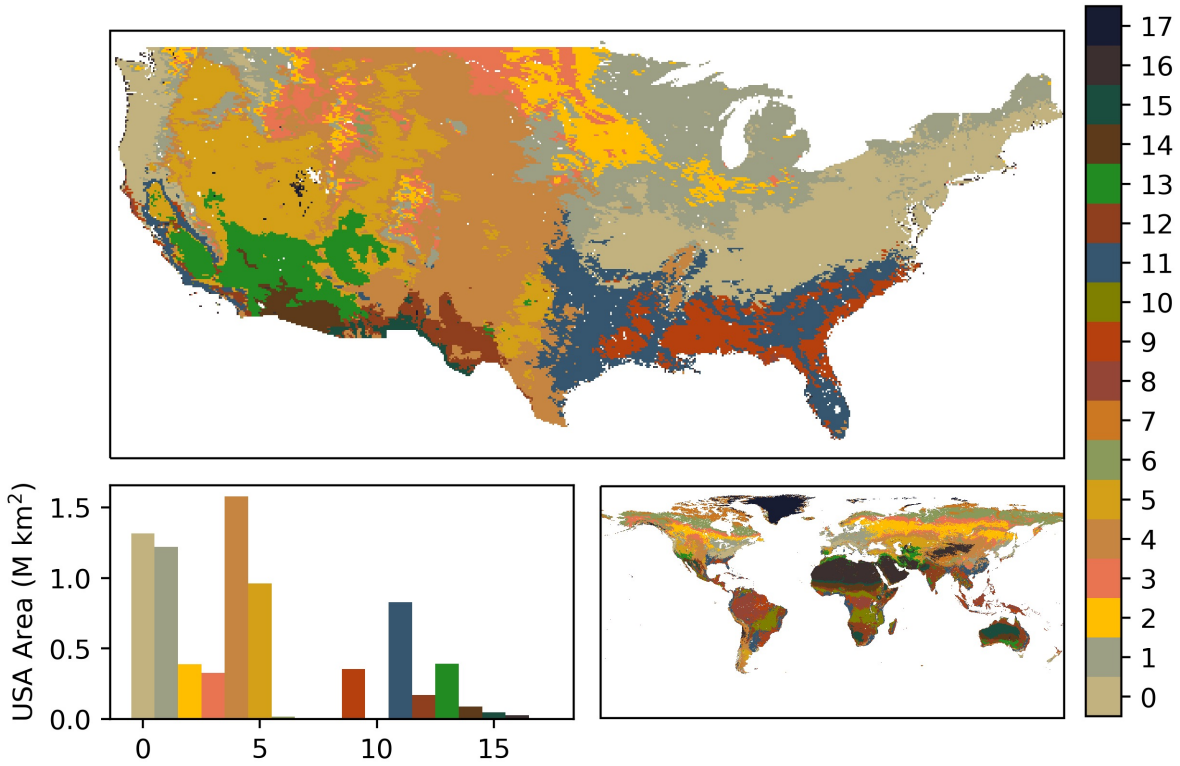

Figure 8: Globally clustered pyroclimates as delineated by VPD and GPP have been shown to reflect distinct fire regimes by Harrison et al. (2025b), with the 18 clustered pyroclimates identified in that study reproduced here. The top panel shows a map of these pyroclimates for the contiguous USA. The lower left panel shows the total area of the contiguous USA occupied by each pyroclimate. The lower right panel shows the global map of pyroclimates identified by Harrison et al. (2025b) for comparison.

What is the interannual variability of wildfire occurrence due to climate and climate-induced vegetation variability?

Defining the wildfire occurrence distribution can provide a better understanding of the modern fire regime. A distribution of possible fire years allows for observed extremes to be contextualised, unrealised fire-years to be accounted for, and the drivers of high and low fire years to be identified. Observed wildfire and reanalysis driven fire models, though useful as a benchmark, do not provide a sufficiently large sample of years to define the wildfire occurrence distribution robustly, especially potential extremes. This chapter is chiefly intended to (1) define spatial patterns in wildfire interannual variability and its drivers, and (2) assess the broad additional utility of LE methods in understanding these processes. Importantly, using an LE to define the distribution of possible fire years in the recent climate also allows for a like-for-like comparison with future projections of the distribution. In this chapter I focus on the

meteorological effects and climate-driven changes in vegetation productivity on wildfire occurrence, holding demographic and land-use change constant to target climate-related variability only.

Can interannual variability in wildfire occurrence be predicted by climate modes?

Given that there is significant interannual variability in wildfire occurrence, the final question is to what extent this is predictable. This chapter explores the effect of eleven climate modes, selected by association with global-scale weather patterns or strong effects over the US specifically – each with an oscillation period of a year or longer. The area of statistically significant effect of each mode, and geographic patterns of the magnitude of this effect on annual wildfire events was tested for each mode. Following these associations, the effect of the most impactful modes of variability on driving wildfire conditions was then also tested. The extent to which such associations were identifiable from reanalysis data was also explored, establishing the additional benefit of LEs in understanding associations between climate modes and regional wildfire patterns.

1.12 References

Aerts R (1997) Climate, Leaf Litter Chemistry and Leaf Litter Decomposition in Terrestrial Ecosystems: A Triangular Relationship. *Oikos* 79(3), 439. https://doi.org/10.2307/3546886

Alexander ME (1988). Help with Making Crown Fire Hazard Assessments. In: Protecting People and Homes from Wildfire in the Interior West: Proceedings of the Symposium and Workshop. *USDA, Forest Service* 147–156.

Andela N, Morton DC, Giglio L, Chen Y, van der Werf GR, et al. (2017) A Human-Driven Decline in Global Burned Area. *Science* 356(6345), 1356-1362. https://doi.org/10.1126/science.aal4108

Anderson DB (1936) Relative Humidity or Vapor Pressure Deficit. *Ecology* 17(2), 277-282. https://doi.org/10.2307/1931468

Antokhina OY, Antokhin PN, Belan BD, Gochakov AV, Martynova YV, et al. (2023) Effects of Rossby Waves Breaking and Atmospheric Blocking Formation on the Extreme Forest Fire and Floods in Eastern Siberia 2019. *Fire* 6(3), 122. https://doi.org/10.3390/fire6030122

Arcenegui V, Mataix-Solera J, Guerrero C, Zornoza R, Mataix-Beneyto J, et al. (2008) Immediate effects of wildfires on water repellency and aggregate stability in Mediterranean calcareous soils. *Catena* 74(3), 219-226. https://doi.org/10.1016/j.catena.2007.12.008

Archibald S, Roy DP, Van Wilgen BW, Scholes RJ (2009) What Limits Fire? An Examination of Drivers of Burnt Area in Southern Africa. *Glob. Chang. Biol.* 15(3), 613-630. https://doi.org/10.1111/j.1365-2486.2008.01754.x

Archibald S, Lehmann CER, Belcher CM, Bond WJ, Bradstock RA, et al. (2018) Biological and Geophysical Feedbacks with Fire in the Earth System. *Environ. Res. Lett.* 13(3), 033003. https://doi.org/10.1088/1748-9326/aa9ead

Arneth A, Harrison SP, Zaehle S, Tsigaridis K, Menon S, et al. (2010) Terrestrial Biogeochemical Feedbacks in the Climate System. *Nat. Geosci.* 3, 525-532. https://doi.org/10.1038/ngeo905

Balch JK, Bradley BA, Abatzoglou JT, Nagy RC, Fusco EJ, et al. (2017) Human-Started Wildfires Expand the Fire Niche Across the United States. *Proc. Natl. Acad. Sci. U.S.A.* 114(11), 2946-2951. https://doi.org/10.1073/pnas.1617394114

Balch JK, Abatzoglou JT, Joseph MB, Koontz MJ, Mahood AL, et al. (2022) Warming Weakens the Night-Time Barrier to Global Fire. *Nat.* 602, 442-448. https://doi.org/10.1038/s41586-021-04325-1

Barbero R, Abatzoglou JT, Larkin NK, Kolden CA, Stocks B (2015) Climate Change Presents Increased Potential for Very Large Fires in the Contiguous United States. *Int. J. Wildland Fire* 24(7), 892. https://doi.org/10.1071/WF15083

Barbero R, Abatzoglou JT, Pimont F, Ruffault J, Curt T (2020) Attributing Increases in Fire Weather to Anthropogenic Climate Change Over France. *Front. Earth Sci.* 8 104. https://doi.org/10.3389/feart.2020.00104

Barkley AE, Prospero JM, Mahowald N, Hamilton DS, Popendorf KJ, et al. (2019) African Biomass Burning is a Substantial Source of Phosphorus Deposition to the Amazon, Tropical Atlantic Ocean, and Southern Ocean. *Proc. Natl. Acad. Sci. U.S.A.* 116(33), 16216-16221. https://doi.org/10.1073/pnas.1906091116

Barnes C, Boulanger Y, Keeping T, Gachon P, Gillett N, et al. (2023) Climate Change More than Doubled the Likelihood of Extreme Fire Weather Conditions in Eastern Canada. *Imp. Coll.* https://doi.org/10.25561/105981

Barnes C, Santos F, Libonati R, Keeping T, Rodrigues R, et al. (2024) Hot, Dry and Windy Conditions that Drove Devastating Pantanal Wildfires 40% more Intense due to Climate Change. *Imp. Coll.* https://doi.org/10.25561/113726

Barnes C, Keeping T, Madakumbura G, Abatzoglou J, Williams P, et al. (2025) Climate Change Increased the Likelihood of Wildfire Disaster in Highly Exposed Los Angeles Area. *Imp. Coll.* https://www.worldweatherattribution.org/wp-content/uploads/WWA-scientific-report-LA-wildfires-1.pdf

Barnes C, Lee JY, Yang, YM, Seo YW, Yun JE et al. (2025) Climate Change Made Weather Conditions Leading to Deadly South Korean Wildfires about Twice as Likely. *Imp. Coll*. https://www.worldweatherattribution.org/wp-content/uploads/Scientific-report-Korea-wildfires.pdf

Barriopedro D, García-Herrera R, Lupo AR, Hernández E (2006) A climatology of Northern Hemisphere blocking. *J. Clim.* 19(6), 1042-1063. https://doi.org/10.1175/JCLI3678.1

Beerling DJ, Osborne CP (2006) The Origin of the Savanna Biome. *Glob. Chang. Biol.* 12(11), 2023-2031. https://doi.org/10.1111/j.1365-2486.2006.01239.x

Berner RA (2006) GEOCARBSULF: A Combined Model for Phanerozoic Atmospheric O_2 and CO_2. *Geoch. Cosm. Act.* 70(23), 5653-5664. https://doi.org/10.1016/j.gca.2005.11.032

Bistinas I, Harrison SP, Prentice IC, Pereira JMC (2014) Causal Relationships versus Emergent Patterns in the Global Controls of Fire Frequency. *Biogeosciences* 11, 5087-5101. https://doi.org/10.5194/bg-11-5087-2014

Blauw LG, van Logtestijn RS, Broekman R, Aerts R, Cornelissen JHC (2017) Tree Species Identity in High-latitude Forests Determines Fire Spread through Fuel Ladders from Branches to Soil and Vice Versa. *For. Ecol. Manag.* 400, 475-484. https://doi.org/10.1016/j.foreco.2017.06.023

Bond WJ, Midgley JJ (1995) Kill Thy Neighbour: An Individualistic Argument for the Evolution of Flammability. *Oikos* 73(1), 79-85. https://doi.org/10.2307/3545728

Bond WJ, Woodward FI, Midgley GF (2004) The Global Distribution of Ecosystems in a World Without Fire. *New Phytol.* 165(2), 525-538. https://doi.org/10.1111/j.1469-8137.2004.01252.x

Boulanger Y, Parisien M, Wang X (2018) Model-Specification Uncertainty in Future Area Burned by Wildfires in Canada. *Int. J. Wildland Fire* 27(3), 164. https://doi.org/10.1071/WF17123

Bousfield CG, Morton O, Lindenmayer DB, Pellegrini AFA, Hethcoat MG, et al. (2025) Global Risk of Wildfire across Timber Production Systems. *Nat. Commun.* 16, 4204. https://doi.org/10.1038/s41467-025-59272-6

Bowler NE, Arribas A, Mylne KR, Robertson KB, Beare SE (2008) The MOGREPS Short-Range Ensemble Prediction System. *Q. J. R. Meteorol. Soc.* 134, 703-722. https://doi.org/10.1002/qj.234

Bowman DMJS, Balch JK, Artaxo P, Bond WJ, Carlson JM, et al. (2009) Fire in the Earth System. *Science* 324, 481-484. https://doi.org/10.1126/science.1163886

Bowman DMJS, Balch J, Artaxo P, Bond WJ, Cochrane MA, et al. (2011) The Human Dimension of Fire Regimes on Earth. *J. Biogeogr.* 38(12), 2223-2236. https://doi.org/10.1111/j.1365-2699.2011.02595.x

Bowman DMJS, Williamson GJ, Abatzoglou JT, Kolden CA, Cochrane MA, et al. (2017) Human Exposure and Sensitivity to Globally Extreme Wildfire Events. *Nat. Ecol. Evol.* 1, 0058. https://doi.org/10.1038/s41559-016-0058

Bowman DMJS, Kolden CA, Abatzoglou JT, Johnston FH, van der Werf GR, et al. (2020) Vegetation Fires in the Anthropocene. *Nat. Rev. Earth Environ.* 1, 500-515. https://doi.org/10.1038/s43017-020-0085-3

Bowring SP, Li W, Mouillot F, Rosan TM, Ciais P (2024). Road Fragment Edges Enhance Wildfire Incidence and Intensity, while Suppressing Global Burned Area. *Nat. Commun.* 15, 9176. https://doi.org/10.1038/s41467-024-53460-6

Brown S, Calkin D, Clark N, Cooper N, Dillon G, et al. (2024) Wildfire risk 101. Science You Can Use 101. Fort Collins, CO: US Department of Agriculture, Forest Service, Rocky Mountain Research Station.

Bryant RA, Gibbs L, Colin Gallagher H, Pattison P, Lusher D, et al. (2021) The Dynamic Course of Psychological Outcomes Following the Victorian Black Saturday Bushfires. *Aust. NZ J. Psychiatry* 55, 666-677. https://doi.org/10.1177/0004867420969815

Bunnell FL, Tait DEN, Flanagan PW, Van Clever K (1977) Microbial Respiration and Substrate Weight Loss: A General Model of the Influences of Abiotic Variables. *Soil boil. biochem.* 9(1) 33-40. https://doi.org/10.1016/0038-0717(77)90058-X

Burrus RT, Dumas CF, Farrell CH, Hall WW (2002) Impact of Low-Intensity Hurricanes on Regional Economic Activity. *Nat. Hazards Rev.* 3(3). https://doi.org/10.1061/(ASCE)1527-6988(2002)3:3(118)

Burton JE, Cawson JG, Filkov AI, Penman TD (2020) Leaf Traits Predict Global Patterns in the Structure and Flammability of Forest Litter Beds. *J. Ecol.* 109(3), 1344-1355. https://doi.org/10.1111/1365-2745.13561

Burton CA, Kelley DI, Burke E, Mathison C, Jones CD, et al. (2024a) Fire Weakens Land Carbon Sinks Before 1.5 °C. *Nat. Geosci.* 17, 1108-1114. https://doi.org/10.1038/s41561-024-01554-7

Burton C, Lampe S, Kelley DI, Thiery W, Hantson S, et al. (2024b) Global Burned Area Increasingly Explained by Climate Change. *Nat. Clim. Chang.* 14, 1186-1192. https://doi.org/10.1038/s41558-024-02140-w

Butz RJ (2009) Traditional Fire Management: Historical Fire Regimes and Land Use Change in Pastoral East Africa. *Int. J. Wildland Fire* 18(4) 442. https://doi.org/10.1071/WF07067

Cannon SH, Gartner JE, Rupert MG, Michael JA, Rea AH, et al. (2010) Predicting the Probability and Volume of Postwildfire Debris Flows in the Intermountain Western United States. *Geol. Soc. Am. Bull.* 122(1-2), 127-144. https://doi.org/10.1130/B26459.1

Carruthers F (2020) Tourism Loses $4.5b to Bushfires as Overseas Visitors Cancel. Available at: https://www.afr.com/companies/tourism/tourism-loses-4-5b-to-bushfires-as-overseas-visitors-cancel-20200116-p53s0s (Accessed 30/5/2025)

Cerdà A, Doerr SH (2008) The Effect of Ash and Needle Cover on Surface Runoff and Erosion in the Immediate Post-Fire Period. *Catena* 74(3), 256-263. https://doi.org/10.1016/j.catena.2008.03.010

Chen F, Si L, Zhao F, Wang M (2023) Volatile Oil in Pinus Yunnanensis Potentially Contributes to Extreme Fire Behavior. *Fire* 6(3), 113. https://doi.org/10.3390/fire6030113

Chen G, Guo Y, Yue X, Tong S, Gasparrini A, et al. (2021) Mortality Risk Attributable to Wildfire-Related PM2.5 Pollution: a Global Time Series Study in 749 Locations. *Lancet Planet. Health* 5(9), e579-e587. https://doi.org/10.1016/S2542-5196(21)00200-X

Chen Y, Hall J, van Wees D, Andela N, Hantson S, et al. (2023) Multi-Decadal Trends and Variability in Burned Area from the Fifth Version of the Global Fire Emissions Database (GFED5). *Earth Syst. Sci. Data* 15, 5227-5259. https://doi.org/10.5194/essd-15-5227-2023

Chuvieco E, Pettinari ML, Koutsias N, Forkel M, Hantson S, et al. (2021) Human and Climate Drivers of Global Biomass Burning Variability. *Sci. Tot. Env.* 779, 146361. https://doi.org/10.1016/j.scitotenv.2021.146361

Chuvieco E, Yebra M, Martino S, Thonicke K, et al. (2023) Towards an integrated approach to wildfire risk assessment: when, where, what and how may the landscapes burn. *Fire* 6(5), 215. https://doi.org/10.3390/fire6050215

Clarke PJ, Lawes MJ, Midgley JJ, Lamont BB, Ojeda F, et al. (2012) Resprouting as a Key Functional Trait: how Buds, Protection and Resources Drive Persistence after Fire. *New Phytol.* 197(1), 19-35. https://doi.org/10.1111/nph.12001

Cloke HL, Wetterhall F, He Y, Freer JE, Pappenberger F (2013) Modelling Climate Impact on Floods with Ensemble Climate Projections. *Q.J.R. Meteorol. Soc.* 139(671), 282-297. https://doi.org/10.1002/qj.1998

CNFDB (2024) Canadian National Fire Database (CNFDB). Available at: https://cwfis.cfs.nrcan.gc.ca/ha/nfdb (Accessed 30/5/2025)

Cohen JD, Deeming JE (1985) The National Fire-Danger Rating System: Basic Equations. *USDA, Forest Service*. https://doi.org/10.2737/PSW-GTR-82

Cohen JD, Butler BW (1996) Modeling Potential Structure Ignitions from Flame Radiation Exposure with Implications for Wildland/Urban Interface Fire Management. *13th Fire and Forest Meteorology Conference.*

Collins KM, Price OF, Penman TD (2015) Spatial Patterns of Wildfire Ignitions in South-Eastern Australia. *Int. J. Wildland Fire* 24(8), 1098. https://doi.org/10.1071/WF15054

Conklin DR, Lenihan JM, Bachelet D, Neilson RP, Kim JB (2016) MCFire Model Technical Description. *USDA, Forest Service*. https://doi.org/10.2737/PNW-GTR-926

Copernicus (2022) Wildfire Carbon Emissions. Available at: https://climate.copernicus.eu/esotc/2022/arctic-wildfires (Accessed 30/5/2025)

Copernicus (2023) 2023: A Year of Intense Global Wildfire Activity. Available at: https://atmosphere.copernicus.eu/2023-year-intense-global-wildfire-activity (Accessed 30/5/2025)

Cornelissen JHC, Grootemaat S, Verheijen LM, Cornwell WK, van Bodegom PM, et al. (2017) Are Litter Decomposition and Fire Linked through Plant Species Traits? *New Phytol.* 216(3), 653-669. https://doi.org/10.1111/nph.14766

Crippa P, Castruccio S, Archer-Nicholls S, Lebron GB, Kuwata M, et al. (2016) Population Exposure to Hazardous Air Quality due to the 2015 Fires in Equatorial Asia. *Sci. Rep.* 6, 37074. https://doi.org/10.1038/srep37074

Crompton O, Corrêa D, Duncan J, Thompson S (2021) Deforestation-Induced Surface Warming is Influenced by the Fragmentation and Spatial Extent of Forest Loss in Maritime Southeast Asia. *Environ. Res. Lett.* 16, 114018. https://doi.org/10.1088/1748-9326/ac2fdc

Cunningham CX, Williamson GJ, Bowman DMJS (2024) Increasing Frequency and Intensity of the Most Extreme Wildfires on Earth. *Nat. Ecol. Evol.* 8, 1420-1425. https://doi.org/10.1038/s41559-024-02452-2

Daniau AL, d'Errico F, Sánchez Goñi MF (2010) Testing the Hypothesis of Fire Use for Ecosystem Management by Neanderthal and Upper Palaeolithic Modern Human Populations. *PLoS One*, 5(2) e9157. https://doi.org/10.1371/journal.pone.0009157

Daniau A, Bartlein PJ, Harrison SP, Prentice IC, Brewer S, et al. (2012) Predictability of Biomass Burning in Response to Climate Changes. *Glob. Biogeochem. Cycles* 26(4). https://doi.org/10.1029/2011GB004249

Davies G, Legg C, O'Hara R, MacDonald A, Smith A (2010) Winter desiccation and rapid changes in the live fuel moisture content of Calluna vulgaris. *Plant Ecol. Divers.* 3(3), 289-299. https://doi.org/10.1080/17550874.2010.544335

de Groot (2012) Peatland Fires and Carbon Emissions. Available at: https://publications.gc.ca/collections/collection_2012/rncan-nrcan/Fo122-1-50-2012-eng.pdf (Accessed 30/5/2025)

de Magalhães RMQ, Schwilk DW (2012) Leaf Traits and Litter Flammability: Evidence for Non-additive Mixture Effects in a Temperate Forest. *J. Ecol.* 100, 1153-1163. https://doi.org/10.1111/j.1365-2745.2012.01987.x

Deser C, Lehner F, Rodgers KB, Ault T, Delworth TL, et al. (2020) Insights from Earth System Model Initial-condition Large Ensembles and Future Prospects. *Nat. Clim. Chang*., 10(4) 277-286. https://doi.org/10.1038/s41558-020-0731-2

Di Giuseppe F, McNorton J, Lombardi A, Wetterhall F (2025) Global data-driven prediction of fire activity. *Nat. Commun.* 16(1), 2918. https://doi.org/10.1038/s41467-025-58097-7

Dijkstra J, Durrant T, San-Miguel-Ayanz J, Veraverbeke S (2022) Anthropogenic and Lightning Fire Incidence and Burned Area in Europe. *Land* 11(5), 651. https://doi.org/10.3390/land11050651

Dinavahi S, Archer CL (2025) Air quality in the US during the 2023 wildfire season. *Bull. Atmos. Sci. Tech.* 6(1), 6. https://doi.org/10.1007/s42865-025-00093-2

Ditomaso JM, Brooks ML, Allen EB, Minnich R, Rice PM, et al. (2006) Control of Invasive Weeds with Prescribed Burning. *Weed technol.* 20, 535-548. https://doi.org/10.1614/WT-05-086R1.1

Doerr SH, Shakesby R, Blake W, Chafer C, Humphreys G, et al. (2005) Effects of Differing Wildfire Severities on Soil Wettability and Implications for Hydrological Response. *J. Hydrol.* 319(1-4), 295-311. https://doi.org/10.1016/j.jhydrol.2005.06.038

Doerr SH, Santín C (2016) Global Trends in Wildfire and its Impacts: Perceptions versus Realities in a Changing World. *Phil. Trans. R. Soc. B* 371(1696), 20150345. https://doi.org/10.1098/rstb.2015.0345

Driscoll DA, Macdonald KJ, Gibson RK, Doherty TS, Nimmo DG, et al. (2024) Biodiversity Impacts of the 2019–2020 Australian Megafires. *Nat.* 635, 898-905. https://doi.org/10.1038/s41586-024-08174-6

Dupuy JL, Fargeon H, Martin-StPaul N, Pimont F, Ruffault J, et al. (2020) Climate change impact on future wildfire danger and activity in southern Europe: a review. Ann. Forest Sci. 77(2), 35. https://doi.org/10.1007/s13595-020-00933-5

ECMWF (2023) Annual Report 2023. Available at: https://www.ecmwf.int/sites/default/files/elibrary/062024/81569-annual-report-2023.pdf (Accessed 30/5/2025)

Eichelberger SJ, Hartmann DL (2007) Zonal Jet Structure and the Leading Mode of Variability. *Ametsoc.* 20(20), 5149-5163. https://doi.org/10.1175/JCLI4279.1

Elia M, D'Este M, Ascoli D, Giannico V, Spano G, et al. (2020) Estimating the Probability of Wildfire Occurrence in Mediterranean Landscapes using Artificial Neural Networks. *Env. Impact Ass. Rev.* 85, 106474. https://doi.org/10.1016/j.eiar.2020.106474

FAO (1998) Crop evapotranspiration - Guidelines for Computing Crop Water Requirements. Available at: https://www.fao.org/4/X0490E/x0490e00.htm (Accessed 30/5/2025)

Fischer EM, Beyerle U, Knutti R (2013) Robust Spatially Aggregated Projections of Climate Extremes. *Nat. Clim. Change* 3, 1033-1038. https://doi.org/10.1038/nclimate2051

Flegrová M, Brindley H (2025) Two decades of fire-induced albedo change and associated short-wave radiative effect over sub-Saharan Africa. *J. Geophys. Res. Atmos.* 130(2), e2024JD041491. https://doi.org/10.1029/2024JD041491

Forkel M, Dorigo W, Lasslop G, Teubner I, Chuvieco E, et al. (2017) A Data-Driven Approach to Identify Controls on Global Fire Activity from Satellite and Climate Observations (SOFIA V1). *Geosci. Model Dev.* 10, 4443-4476. https://doi.org/10.5194/gmd-10-4443-2017

Forkel M, Dorigo W, Lasslop G, Chuvieco E, Hantson S, et al. (2019a) Recent Global and Regional Trends in Burned Area and their Compensating Environmental Controls. *Environ. Res. Commun.* 1(5), 051005. https://doi.org/10.1088/2515-7620/ab25d2

Forkel M, Andela N, Harrison SP, Lasslop G, van Marle M, et al. (2019b) Emergent Relationships with Respect to Burned Area in Global Satellite Observations and Fire-Enabled Vegetation Models. *Biogeosciences* 16(1), 57-76. https://doi.org/10.5194/bg-16-57-2019

Forrest M, Hetzer J, Billing M, Bowring SPK, Kosczor E, et al. (2024) Understanding and Simulating Cropland and Non-Cropland Burning in Europe Using the BASE (Burnt Area Simulator for Europe) Model. *Geosci. Model Dev.* 21(23), 5539-5560 https://doi.org/10.5194/egusphere-2024-1973

Forster PM, Smith C, Walsh T, Lamb WF, Lamboll R (2024) Indicators of Global Climate Change 2023: annual update of key indicators of the state of the climate system and human influence. *ESSD* 16(6), 2625-2658. https://doi.org/10.5194/essd-17-2641-2025

Forthofer JM, Goodrick SL (2011) Review of Vortices in Wildland Fire. *J Combust.* 1, 984363 https://doi.org/10.1155/2011/984363

Fujii Y, Iriana W, Oda M, Puriwigati A, Tohno S, et al. (2014) Characteristics of Carbonaceous Aerosols Emitted from Peatland Fire in Riau, Sumatra, Indonesia. *Atmos. Env.* 87, 164-169. https://doi.org/10.1016/j.atmosenv.2014.01.037

Gedalof ZE, Peterson DL, Mantua NJ (2005) Atmospheric, climatic, and ecological controls on extreme wildfire years in the northwestern United States. *Ecol. Appl.* 15(1), 154-174. https://doi.org/10.1890/03-5116

Gersh M, Gleason KE, Surunis A (2022) Forest Fire Effects on Landscape Snow Albedo Recovery and Decay. *Remote Sens.* 14(16), 4079. https://doi.org/10.3390/rs14164079

Gershunov A (1998) ENSO influence on intraseasonal extreme rainfall and temperature frequencies in the contiguous United States: Implications for long-range predictability. J. Clim. 11(12), 3192-3203. https://doi.org/10.1175/1520-0442(1998)011<3192:EIOIER>2.0.CO;2

Gill JC, Malamud BD (2014) Reviewing and Visualizing the Interactions of Natural Hazards. *Rev. Geophys.* 52(4), 680-722. https://doi.org/10.1002/2013RG000445

Goodrick SL, Hanley DE (2009) Florida wildfire activity and atmospheric teleconnections. Int. J Wild. Fire 18, 476-482. https://doi.org/10.1071/WF07034

Grootemaat S, Wright IJ, van Bodegom PM, Cornelissen JHC, Cornwell WK (2015) Burn or Rot: Leaf Traits Explain why Flammability and Decomposability are Decoupled across Species. *Func. Ecol.* 29(11), 1486-1497. https://doi.org/10.1111/1365-2435.12449

Grossiord C, Buckley TN, Cernusak LA, Novick KA, Poulter B, et al. (2020) Plant responses to rising vapor pressure deficit. *New Phyt.* 226(6), 1550-1566. https://doi.org/10.1111/nph.16485

Gutierrez AA, Hantson S, Langenbrunner B, Chen B, Jin Y, et al. (2021) Wildfire Response to Changing Daily Temperature Extremes in California's Sierra Nevada. *Sci. Adv.* 7(47) 6417. https://doi.org/10.1126/sciadv.abe6417

Guyette RP, Dey DC, Stambaugh MC, Muzika RM (2006) Fire Scars Reveal Variability and Dynamics Of Eastern Fire Regimes. *USDA, Forest Service*, GTR-NRS-P-1.

Haas O, Prentice IC, Harrison SP (2022) Global Environmental Controls on Wildfire Burnt Area, Size, and Intensity. *Environ. Res. Lett.* 17, 065004. https://doi.org/10.1088/1748-9326/ac6a69

Haas O, Prentice IC, Harrison SP (2023) The Response of Wildfire Regimes to Last Glacial Maximum Carbon Dioxide and Climate. *Biogeosciences* 20(18), 3981-3995. https://doi.org/10.5194/bg-20-3981-2023

Haas O, Keeping T, Gomez-Dans J, Prentice IC, Harrison SP (2024) The Global Drivers of Wildfire. *Front. Environ. Sci.* 12 438262. https://doi.org/10.3389/fenvs.2024.1438262

Haines DA (1988) A Lower Atmospheric Severity Index for Wildlife Fires. *Fire Weather* 13, 3.

Hamilton DS, Kelley D, Perron MM, Llort J, Burton C, et al. (2024) Igniting Progress: Outcomes from the FLARE Workshop and Three Challenges for the Future of Transdisciplinary Fire Science. *Fut. Earth*. https://doi.org/10.5281/zenodo.12634068

Hamilton D, Kasoar M, Bergas-Massó E, Dalmonech D, Hantson S, et al. (2025) Global Warming Increases Fire Emissions but Resulting Aerosol Forcing is Uncertain. *Sci. Rep.* https://doi.org/10.21203/rs.3.rs-4567012/v1 [in review]

Hantson S, Pueyo S, Chuvieco E (2016) Global Fire Size Distribution: from Power Law to Log-Normal. *Int. J. Wildland Fire* 25(4), 403-412. https://doi.org/10.1071/WF15108

Hantson S, Kelley DI, Arneth A, Harrison SP, Archibald S, et al. (2020) Quantitative Assessment of Fire and Vegetation Properties in Simulations with Fire-Enabled Vegetation Models from the Fire Model Intercomparison Project. *Geosci. Model Dev.* 13(7), 3299-3318. https://doi.org/10.5194/gmd-13-3299-2020

Harrison SP, Marlon JR, Bartlein PJ (2010) Fire in the Earth System. *Springer Netherlands* 21-48. https://doi.org/10.1007/978-90-481-8716-4_3

Harrison CJ, Morris JL (2017) The Origin and Early Evolution of Vascular Plant Shoots and Leaves. *Phil. Trans. R. Soc. B* 373(1739), 20160496. https://doi.org/10.1098/rstb.2016.0496

Harrison SP, Bartlein PJ, Brovkin V, Houweling S, Kloster S, et al. (2018) The Biomass Burning Contribution to Climate–Carbon-Cycle Feedback. *Earth Syst. Dyn.* 9(2), 663-677. https://doi.org/10.5194/esd-9-663-2018

Harrison SP, Prentice IC, Bloomfield KJ, Dong N, Forkel M, et al. (2021) Understanding and Modelling Wildfire Regimes: an Ecological Perspective. *Environ. Res. Lett.* 16, 125008. https://doi.org/10.1088/1748-9326/ac39be

Harrison SP, Haas O, Bartlein PJ, Sweeney L, Zhang G (2025a) Climate, Vegetation, People: Disentangling the Controls of Fire at Different Timescales. *Phil. Trans. R. Soc. B* 380(1924). https://doi.org/10.1098/rstb.2023.0464

Harrison SP, Shen Y, Haas O, Sandoval DC, Sapkota D, et al. (2025b) An eco-evolutionary approach to defining wildfire regimes. *Comm. Earth Environ.* [in review]

Haugen MA, Stein ML, Moyer EJ, Sriver RL (2018) Estimating Changes in Temperature Distributions in a Large Ensemble of Climate Simulations Using Quantile Regression. *J. Clim.* 31, 8573-8588. https://doi.org/10.1175/JCLI-D-17-0782.1

He T, Pausas JG, Belcher CM, Schwilk DW, Lamont BB (2012) Fire-Adapted Traits of Pinus Arose in the Fiery Cretaceous. *New Phyt.*, 194(3), 751-759. https://doi.org/10.1111/j.1469-8137.2012.04079.x

Hessilt TD, Rogers BM, Scholten RC, Potter S, Janssen TAJ, et al. (2024) Geographically Divergent Trends in Snow Disappearance Timing and Fire Ignitions across Boreal North America. *Biogeosciences* 21(1), 109-129. https://doi.org/10.5194/bg-21-109-2024

Heyerdahl EK, Brubaker LB, Agee JK (2002) Annual and decadal climate forcing of historical fire regimes in the interior Pacific Northwest, USA. Holocene 12, 597–604. https://doi.org/10.1191/0959683602hl570rp

Hossack BR, Pilliod DS (2011) Amphibian Responses to Wildfire in the Western United States: Emerging Patterns from Short-Term Studies. *Fire Ecol.*, 7(2), 129-144. https://doi.org/10.4996/fireecology.0702129

IPBES (2019) Global Assessment Report on Biodiversity and Ecosystem Services of the Intergovernmental Science-Policy Platform on Biodiversity and Ecosystem Services. *IPBES Secretariat*. https://doi.org/10.5281/zenodo.3831673

IPCC (2023) Climate Change 2023: Synthesis Report. Contribution of Working Groups I, II and III to the Sixth Assessment Report of the Intergovernmental Panel on Climate Change. *IPCC*, Geneva, Switzerland. https://doi.org/10.59327/IPCC/AR6-9789291691647

Ito A, Sudo K, Akimoto H, Sillman S, Penner JE (2007) Global Modeling Analysis of Tropospheric Ozone and its Radiative Forcing from Biomass Burning Emissions in the Twentieth Century. *J. Geophys. Res.* 112(D24). https://doi.org/10.1029/2007JD008745

Jacobo J (2025) Why the California Wildfires were Nearly Impossible to Contain. Available at: https://abcnews.go.com/US/california-wildfires-impossible/story?id=117506137 (Accessed 30/5/2025).

Jain P, Barber QE, Taylor SW, Whitman E, Castellanos Acuna D, et al. (2024) Drivers and Impacts of the Record-Breaking 2023 Wildfire Season in Canada. *Nat. Commun.* 15, 6764. https://doi.org/10.1038/s41467-024-51154-7

Janssen TAJ, Jones MW, Finney D, van der Werf GR, van Wees D, et al. (2023) Extratropical Forests Increasingly at Risk due to Lightning Fires. *Nat. Geosci.* 16, 1136-1144. https://doi.org/10.1038/s41561-023-01322-z

Janssen TAJ, Veraverbeke S (2025) What Are the Limits to the Growth of Boreal Fires? *Glob. Chang. Biol.* 31. https://doi.org/10.1111/gcb.70130

Jiang Y, Yang X, Liu X, Qian Y, Zhang K, et al. (2020) Impacts of Wildfire Aerosols on Global Energy Budget and Climate: The Role of Climate Feedbacks. *Ametsoc.* 33(8), 3351-3366. https://doi.org/10.1175/JCLI-D-19-0572.1

Johnson SJ, Stockdale TN, Ferranti L, Balmaseda MA, Molteni F, et al. (2019) SEAS5: the New ECMWF Seasonal Forecast System. *Geosci. Model Dev.* 12(3), 1087-1117. https://doi.org/10.5194/gmd-12-1087-2019

Johnston FH, Henderson SB, Chen Y, Randerson JT, Marlier M, et al. (2012) Estimated Global Mortality Attributable to Smoke from Landscape Fires. *Environ. Health Perspect.* 120(5), 695-701. https://doi.org/10.1289/ehp.1104422

Johnston FH, Borchers-Arriagada N, Morgan GG, Jalaludin B, Palmer AJ, et al. (2020) Unprecedented Health Costs of Smoke-related PM2.5 from the 2019–20 Australian Megafires. *Nat. Sustain.* 4, 42-47. https://doi.org/10.1038/s41893-020-00610-5

Johnston FH, Williamson G, Borchers-Arriagada N, Henderson SB, Bowman DM (2024) Climate Change, Landscape Fires, and Human Health: A Global Perspective. *Ann. Rev.* 45, 295-314. https://doi.org/10.1146/annurev-publhealth-060222-034131

Jones MW, Abatzoglou JT, Veraverbeke S, Andela N, Lasslop G, et al. (2022) Global and Regional Trends and Drivers of Fire Under Climate Change. *Rev. Geophys.* 60(3) e2020RG000726. https://doi.org/10.1029/2020RG000726

Jorge MH, Conner LM, Garrison EP, Cherry MJ (2022) Avian Species Richness in a Frequently Burned Ecosystem: a Link between Pyrodiversity and Biodiversity. *Land. Ecol.*, 37(4), 983-996. https://doi.org/10.1007/s10980-022-01399-8

Kang S, Zhang Y, Qian Y, Wang H (2020) A Review of Black Carbon in Snow and Ice and its Impact on the Cryosphere. *Earth Sci. Rev.* 210, 103346. https://doi.org/10.1016/j.earscirev.2020.103346

Keeley JE, Pausas JG, Rundel PW, Bond WJ, Bradstock RA (2011) Fire as an Evolutionary Pressure Shaping Plant Traits. *Trends Plant Sci.* 16(8), 406-411. https://doi.org/10.1016/j.tplants.2011.04.002

Kelley DI, Burton C, Di Giuseppe F, Jones MW, Barbosa ML, et al. (2025) State of wildfires 2024–25. *ESSD Discuss.* 17, 1-179. https://doi.org/10.5194/essd-17-5377-2025

Kelly LT, Giljohann KM, Duane A, Aquilué N, Archibald S, et al. (2020) Fire and Biodiversity in the Anthropocene. *Science* 370(6519). https://doi.org/10.1126/science.abb0355

Kepe T (2005) Grasslands ablaze: vegetation burning by rural people in Pondoland, South Africa. *S. Afr. Geogr. J.* 87(1), 10-17. https://doi.org/10.1080/03736245.2005.9713821

Kipfmueller KF, Larson ER, St. George S (2012) Does proxy uncertainty affect the relations inferred between the Pacific Decadal Oscillation and wildfire activity in the western United States?, Geophys. Res. Lett. 39, 04703, https://doi.org/10.1029/2011GL050645

Kirchmeier-Young MC, Gillett NP, Zwiers FW, Cannon AJ, Anslow FS (2019) Attribution of the Influence of Human-Induced Climate Change on an Extreme Fire Season. *Earth Fut.* 7(1), 2-10. https://doi.org/10.1029/2018EF001050

Kloster S, Mahowald NM, Randerson JT, Thornton PE, Hoffman FM, et al. (2010) Fire Dynamics during the 20th Century Simulated by the Community Land Model. *Biogeosciences* 7, 1877-1902. https://doi.org/10.5194/bg-7-1877-2010

Kloster S, Lasslop G (2017) Historical and Future Fire Occurrence (1850 to 2100) Simulated in CMIP5 Earth System Models. *Glob. Planet. Chang.* 150, 58-69. https://doi.org/10.1016/j.gloplacha.2016.12.017

Knorr W, Kaminski T, Arneth A, Weber U (2014) Impact of Human Population Density on Fire Frequency at the Global Scale. *Biogeosciences* 11, 1085-1102. https://doi.org/10.5194/bg-11-1085-2014

Kolden CA, Lutz JA, Key CH, Kane JT, van Wagtendonk JW (2012) Mapped versus Actual Burned Area within Wildfire Perimeters: Characterizing the Unburned. *For. Ecol. Manag.* 286, 38-47. https://doi.org/10.1016/j.foreco.2012.08.020

Korving H, Van Marle M (2025) Decoding Wildfires - Extracting Interpretations and Causal Pathways of Catalysts for Wildfire Occurrence from Machine Learning Models. *EGU Gen. Assemb.* EGU25-12889. https://doi.org/10.5194/egusphere-egu25-12889, 2025.

Kreider MR, Higuera PE, Parks SA, Rice WL, White N, et al. (2024) Fire Suppression makes Wildfires more Severe and Accentuates Impacts of Climate Change and Fuel Accumulation. *Nat. Commun.* 15, 2412. https://doi.org/10.1038/s41467-024-46702-0

Kuhn-Régnier A, Voulgarakis A, Nowack P, Forkel M, Prentice IC, et al. (2021) The Importance of Antecedent Vegetation and Drought Conditions as Global Drivers of Burnt Area. *Biogeosciences* 18(12), 3861-3879. https://doi.org/10.5194/bg-18-3861-2021

LaDochy S, Witiw M (2023) Fire and Rain: California's Changing Weather and Climate. *Springer Nature.*

Lasslop G, Hantson S, Harrison SP, Bachelet D, Burton C, et al. (2020) Global Ecosystems and Fire: Multi-Model Assessment of Fire-Induced Tree-Cover and Carbon Storage Reduction. *Glob. Chang. Biol.* 26(9), 5027-5041. https://doi.org/10.1111/gcb.15160

Lehsten V, Tansey K, Balzter H, Thonicke K, Spessa A, et al. (2009) Estimating Carbon Emissions from African Wildfires. *Biogeosciences* 6(3), 349-360. https://doi.org/10.5194/bg-6-349-2009

Lewis and Clark (1805) Journals of the Lewis & Clark Expedition. Available at: https://lewisandclarkjournals.unl.edu/item/lc.jrn.1805-07-20 (Accessed 30/5/2025)

Li F, Levis S, Ward DS (2013) Quantifying the Role of Fire in the Earth System – Part 1: Improved Global Fire Modeling in the Community Earth System Model (CESM1). *Biogeosciences* 10(4), 2293-2314. https://doi.org/10.5194/bg-10-2293-2013

Li F, Val Martin M, Andreae MO, Arneth A, Hantson S, et al. (2019) Historical (1700–2012) Global Multi-Model Estimates of the Fire Emissions from the Fire Modeling Intercomparison Project (FireMIP). *Atmos. Chem. Phys.* 19(19), 12545-12567. https://doi.org/10.5194/acp-19-12545-2019

Li F, Song X, Harrison SP, Marlon JR, Lin Z, et al. (2024) Evaluation of Global Fire Simulations in CMIP6 Earth System Models. *Geosci. Model Dev.* 17(23), 8751-8771. https://doi.org/10.5194/gmd-17-8751-2024

Li Z, Yu W (2025) Economic Impact of the Los Angeles Wildfires. Prevention Web. Available at: https://www.preventionweb.net/news/economic-impact-los-angeles-wildfires (Accessed 30/5/2025)

Little K, Graham LJ, Flannigan M, Belcher CM, Kettridge N (2024) Landscape Controls on Fuel Moisture Variability in Fire-Prone Heathland and Peatland Landscapes. *Fire Ecol.* 20, 14. https://doi.org/10.1186/s42408-024-00248-0

Liu Y, Goodrick S, Heilman W (2014) Wildland Fire Emissions, Carbon, and Climate: Wildfire–Climate Interactions. *For. Ecol. Manag.* 317, 80-96. https://doi.org/10.1016/j.foreco.2013.02.020

Liu Z, Ballantyne AP, Cooper LA (2019) Biophysical Feedback of Global Forest Fires on Surface Temperature. *Nat. Commun.* 10, 214. https://doi.org/10.1038/s41467-018-08237-z

Long JW, Goode RW, Gutteriez RJ, Lackey JJ, Anderson MK (2017) Managing California Black Oak for Tribal Ecocultural Restoration. *J. For.* 115(5), 426-434. https://doi.org/10.5849/jof.16-033

Lorenz EN (1969) The Predictability of a Flow which Possesses many Scales of Motion. *Stockholm University Press* 21, 289. https://doi.org/10.3402/tellusa.v21i3.10086

Lorenz EN (1972) Predictability: Does the Flap of a Butterfly's Wings in Brazil Set Off a Tornado in Texas. *AAAS*.

Ma Q, Bales RC, Rungee J, Conklin MH, Collins BM, et al. (2020) Wildfire Controls on Evapotranspiration in California's Sierra Nevada. *J. Hydrol.* 590, 125364. https://doi.org/10.1016/j.jhydrol.2020.125364

Ma Y, Zang E, Liu Y, Wei J, Lu Y, et al. (2024) Long-Term Exposure to Wildland Fire Smoke PM2.5 Mortality in the Contiguous United States. *Proc. Natl. Acad. Sci. U.S.A.* 121(40) e2403960121. https://doi.org/10.1073/pnas.2403960121

MacDonald G, Wall T, Enquist CAF, LeRoy SR, Bradford JB, et al. (2023) Drivers of California's Changing Wildfires: a State-of-the-Knowledge Synthesis. *Int. J. Wildland Fire* 32(7), 1039-1058. https://doi.org/10.1071/WF22155

Madakumbura G, Thackeray C, Hall A, Williams P, Norris J, et al. (2025) Climate Change A Factor In Unprecedented LA Fires. *UCLA Sustainable LA Grand Challenge.* Available at: https://sustainablela.ucla.edu/2025lawildfires (Accessed 30/5/2025)

Madhusoodanan J (2021) Wildfires pose a burning problem for wines and winemakers. *PNAS* 118(34), e2113327118. https://doi.org/10.1073/pnas.2113327118

Magerl A, Gingrich S, Matej S, Cunfer G, Forrest M, et al. (2023) The Role of Wildfires in the Interplay of Forest Carbon Stocks and Wood Harvest in the Contiguous United States During the 20th Century. *Glob. Biogeochem. Cycl.* 37(8) e2023GB007813 https://doi.org/10.1029/2023GB007813

Magnussen S, Taylor SW (2012) Inter- and Intra-Annual Profiles of Fire Regimes in the Managed Forests of Canada and Implications for Resource Sharing. *Int. J. Wildland Fire* 21(4) 328-341. https://doi.org/10.1071/WF11026

Maher N, Milinski S, Ludwig R (2021) Large Ensemble Climate Model Simulations: Introduction, Overview, and Future Prospects for Utilising Multiple Types of Large Ensemble. *Earth Syst. Dynam.* 12(2), 401-418. https://doi.org/10.5194/esd-12-401-2021

Manabe S, Wetherald RT (1967) Thermal Equilibrium of the Atmosphere with a Given Distribution of Relative Humidity. *J. Atmos. Sci.* 24(3), 241-259. https://doi.org/10.1175/1520-0469(1967)024%3c0241:TEOTAW%3e2.0.CO;2

Mangeon S, Voulgarakis A, Gilham R, Harper A, Sitch S, et al. (2016) INFERNO: A fire and emissions scheme for the UK Met Office's Unified Model. *Geosci. Model Dev.*, 9(8), 2685-2700. https://doi.org/10.5194/gmd-9-2685-2016

Manzello SL (2020) Encyclopedia of Wildfires and Wildland-Urban Interface (WUI) Fires. *Springer Int. Pub.*. https://doi.org/10.1007/978-3-319-52090-2

Marlon JR, Bartlein PJ, Carcaillet C, Gavin DG, Harrison SP, et al. (2008) Climate and Human Influences on Global Biomass Burning over the Past Two Millennia. *Nat. Geosci.* 1, 697-702. https://doi.org/10.1038/ngeo313

Matthews, S. (2013) Dead Fuel Moisture Research: 1991–2012. *Int. J. Wildland Fire* 23(1), 78-92. https://doi.org/10.1071/WF13005

Maui County (2023) Pacific Disaster Center and the Federal Emergency Management Agency releases Fire Damage. Available at: https://web.archive.org/web/20230812204557/https:/www.mauicounty.gov/CivicAlerts.aspx?aid=12683 (Accessed 30/5/2025)

McDowell N, Pockman WT, Allen CD, Breshears DD, Cobb N, et al. (2008) Mechanisms of Plant Survival and Mortality during Drought: Why do some Plants Survive while Others Succumb to Drought? *New Phytol.* 178(4), 719-739. https://doi.org/10.1111/j.1469-8137.2008.02436.x

McKemey MB, Patterson M, Rangers B, Ens EJ, Reid NC, et al. (2019) Cross-cultural monitoring of a cultural keystone species informs revival of indigenous burning of country in South-Eastern Australia. *Human Ecol.* 47(6), 893-904. https://doi.org/10.1007/s10745-019-00120-9

McNorton JR, Giuseppe FD, Pinnington EM, Chantry M, Barnard C (2024) A Global Probability-of-Fire (PoF) Forecast. *Geophys. Res. Lett.* 51(12) e2023GL107929 https://doi.org/10.1029/2023GL107929

Meier S, Elliott RJ, Strobl E (2023) The Regional Economic Impact of Wildfires: Evidence from Southern Europe. *J. Env. Econ. Manag.* 118, 102787. https://doi.org/10.1016/j.jeem.2023.102787

Melton JR, Arora VK (2016) Competition Between Plant Functional Types in the Canadian Terrestrial Ecosystem Model (CTEM) v. 2.0. *Geosci. Model Dev.* 9(1), 323-361. https://doi.org/10.5194/gmd-9-323-2016

Moorcroft PR, Hurtt GC, Pacala SW (2001) A Method for Scaling Vegetation Dynamics: The Ecosystem Demography Model. *Ecol. Monogr.* 71(4), 557-586. https://doi.org/10.1890/0012-9615(2001)071%5b0557:AMFSVD%5d2.0.CO;2

Moore A (1986) Temperature and Moisture Dependence of Decomposition Rates of Hardwood and Coniferous Leaf Litter. *Soil Biol. Biochem.* 18(4), 427-435. https://doi.org/10.1016/0038-0717(86)90049-0

Moosavi S, Nwaka B, Akinjise I, Corbett SE, Chue P, et al. (2019) Mental Health Effects in Primary Care Patients 18 Months After a Major Wildfire in Fort McMurray: Risk Increased by Social Demographic Issues, Clinical Antecedents, and Degree of Fire Exposure. *Front. Psychiatry* 10, 683. https://doi.org/10.3389/fpsyt.2019.00683

Moritz MA, Moody TJ, Krawchuk MA, Hughes M, Hall A (2010) Spatial Variation in Extreme Winds Predicts Large Wildfire Locations in Chaparral Ecosystems. *Geophys. Res. Lett.* 37(4). https://doi.org/10.1029/2009GL041735

Moritz MA, Batllori E, Bradstock RA, Gill AM, Handmer J, et al. (2014) Learning to Coexist with Wildfire. *Nat.* 515, 58-66. https://doi.org/10.1038/nature13946

Moritz MA, Batllori E, Bolker BM (2023) The Role of Fire in Terrestrial Vertebrate Richness Patterns. *Ecol. Lett.* 26(4), 563-574. https://doi.org/10.1111/ele.14177

Moura LC, Scariot AO, Schmidt IB, Beatty R, Russell-Smith J (2019) The Legacy of Colonial Fire Management Policies on Traditional Livelihoods and Ecological Sustainability in Savannas: Impacts, Consequences, New Directions. *J. Environ. Manag.* 232, 600-606. https://doi.org/10.1016/j.jenvman.2018.11.057

Mukunga T, Forkel M, Forrest M, Zotta RM, Pande N, Schlaffer S, Dorigo W (2023) Effect of Socioeconomic Variables in Predicting Global Fire Ignition Occurrence. *Fire* 6(5), 197. https://doi.org/10.3390/fire6050197

Mulder V, Heri V, Wickham T (2000) Traditional Honey and Wax Collection with Apis Dorsata in the Upper Kapuas Lake Region, West Kalimantan. *Borneo Res. Bull*. 31, 246–261.

Muntjewerf L, Bintanja R, Reerink T, van der Wiel K (2023) The KNMI Large Ensemble Time Slice (KNMI–LENTIS). *Geosci. Model Dev.* 16(15), 4581-4597. https://doi.org/10.5194/gmd-16-4581-2023

Naeher LP, Brauer M, Lipsett M, Zelikoff JT, Simpson CD, et al. (2006) Woodsmoke Health Effects: A Review. *Inhal. Toxicol.* 19(1), 67-106. https://doi.org/10.1080/08958370600985875

Naser MZ, Kodur V (2025) Vulnerability of Structures and Infrastructure to Wildfires: a Perspective into Assessment and Mitigation Strategies. *Nat. Hazards.* 121, 9995–10015. https://doi.org/10.1007/s11069-025-07168-5

NICC (2025) NICC Annual Reports. Available at: https://www.nifc.gov/nicc/predictive-services/intelligence (Accessed 30/5/2025)

NIFC (2024) Suppression Costs. Available at: https://www.nifc.gov/fire-information/statistics/suppression-costs (Accessed 30/5/2025)

Nolan RH, Lane PNJ, Benyon RG, Bradstock RA, Mitchell PJ (2013) Changes in Evapotranspiration following Wildfire in Resprouting Eucalypt Forests. *Ecohydrol.* 7(5), 1363-1377. https://doi.org/10.1002/eco.1463

Nolan RH, Rahmani S, Samson SA, Simpson-Southward HM, Boer MM, et al. (2020) Bark Attributes Determine Variation in Fire Resistance in Resprouting Tree Species. *For. Ecol. Manag.* 474, 118385. https://doi.org/10.1016/j.foreco.2020.118385

Noss RF, Franklin JF, Baker WL, Schoennagel T, Moyle PB (2006) Managing Fire-Prone Forests in the Western United States. *Front. Ecol. Environ.* 4(9), 481-487. https://doi.org/10.1890/1540-9295(2006)4%5b481:MFFITW%5d2.0.CO;2

NPR (2025) As Insurance Companies Leave High-risk Areas, Many Turn to 'Last Resort' Insurance. Available at: https://www.wkar.org/2025-01-18/as-insurance-companies-leave-high-risk-areas-many-turn-to-last-resort-insurance (Accessed 30/5/2025)

O'Donnell AJ, Boer MM, McCaw WL, Grierson PF (2010) Vegetation and Landscape Connectivity Control Wildfire Intervals in Unmanaged Semi-Arid Shrublands and Woodlands in Australia. *J. Biogeogr.* 38(1), 112-124. https://doi.org/10.1111/j.1365-2699.2010.02381.x

O'Leary DS, Bloom TD, Smith JC, Zemp CR, Medler MJ (2016) A New Method Comparing Snowmelt Timing with Annual Area Burned. *Fire Ecol.* 12, 41-51. https://doi.org/10.4996/fireecology.1201041

Olson NE, Boaggio KL, Rice RB, Foley KM, LeDuc SD (2023) Wildfires in the Western United States are Mobilizing PM2.5-Associated Nutrients and May be Contributing to Downwind Cyanobacteria Blooms. *Environ. Sci. Proc. Impact.* 25(6), 1049-1066. https://doi.org/10.1039/D3EM00042G

Organ C, Nunn CL, Machanda Z, Wrangham RW (2011) Phylogenetic Rate Shifts in Feeding Time During the Evolution of Homo. *Proc. Natl. Acad. Sci. U.S.A.* 108(35), 14555-14559. https://doi.org/10.1073/pnas.1107806108

Parisien M, Moritz MA (2009) Environmental Controls on the Distribution of Wildfire at Multiple Spatial Scales. *Ecol. Monogr.* 79(1), 127-154. https://doi.org/10.1890/07-1289.1

Parks SA, Miller C, Parisien M, Holsinger LM, Dobrowski SZ, et al. (2015) Wildland Fire Deficit and Surplus in the Western United States, 1984–2012. *Ecosphere* 6(12), 1-13. https://doi.org/10.1890/ES15-00294.1

Pastro LA, Dickman CR, Letnic M (2011) Burning for Biodiversity or Burning Biodiversity? Prescribed Burn vs. Wildfire Impacts on Plants, Lizards, and Mammals. *Ecol. Appl.*, 21(8), 3238-3253. https://doi.org/10.1890/10-2351.1

Pascoe S (2010) The 2009 Victorian Bushfires Royal Commission: Lessons for the Conduct of Inquiries in Australia. *AJPA* 69 392-400. https://doi.org/10.1111/j.1467-8500.2010.00702.x

Pausas JG, Moreira B (2012) Flammability as a Biological Concept. *New Phytol.*, 194(3), 610-613. https://doi.org/10.1111/j.1469-8137.2012.04132.x

Pausas JG, Keeley JE, Schwilk DW (2017) Flammability as an Ecological and Evolutionary Driver. *J. Ecol.* 105(2), 289-297. https://doi.org/10.1111/1365-2745.12691

Pausas JG, Keeley JE, Syphard AD (2025) Are Fire Regimes the Result of Top-Down or Bottom-Up Drivers?. *Phil. Trans. R. Soc. B* 380(1924), 20230447. https://doi.org/10.1098/rstb.2023.0447

Pellegrini AFA, Anderegg WRL, Paine CET, Hoffmann WA, Kartzinel T, et al. (2017) Convergence of Bark Investment According to Fire and Climate Structures Ecosystem Vulnerability to Future Change. *Ecol. Lett.* 20(3), 307-316. https://doi.org/10.1111/ele.12725

Pellew RAP (1983) The Impacts of Elephant, Giraffe and Fire upon the *Acacia Tortilis* Woodlands of the Serengeti. *Afr. J. Ecol.* 21(1), 41-74. https://doi.org/10.1111/j.1365-2028.1983.tb00311.x

Perkins O, Kasoar M, Voulgarakis A, Smith C, Mistry J, et al. (2024) A Global Behavioural Model of Human Fire Use and Management: WHAM! v1.0. *Geosci. Model Dev.* 17(9), 3993-4016. https://doi.org/10.5194/gmd-17-3993-2024

Pfeiffer M, Spessa A, Kaplan JO (2013) A Model for Global Biomass Burning in Preindustrial Time: LPJ-LMfire (v1.0). *Geosci. Model Dev.* 6(3), 643-685. https://doi.org/10.5194/gmd-6-643-2013

Platek S, Gallup G, Fryer B (2002) The Fireside Hypothesis: was there Differential Selection to Tolerate Air Pollution during Human Evolution? *Med. Hyp.* 58(1), 1-5. https://doi.org/10.1054/mehy.2001.1385

Poduška Z, Stajić S (2024) The Cost of Forest Fires: A Socioeconomic Analysis. In: Fire Hazards: Socio-economic and Regional Issues (123-135). *Springer International Publishing.*

Popović Z, Bojović S, Marković M, Cerdà A (2021) Tree Species Flammability based on Plant Traits: A synthesis. *Sci. Tot. Env.* 800, 149625. https://doi.org/10.1016/j.scitotenv.2021.149625

Pyne SJ (2001) Fire: A Brief History. *University of Washington Press.*

Rabin SS, Melton JR, Lasslop G, Bachelet D, Forrest M, et al. (2017) The Fire Modeling Intercomparison Project (FireMIP), phase 1: Experimental and Analytical Protocols with Detailed Model Descriptions. *Geosci. Model Dev.* 10(3), 1175-1197. https://doi.org/10.5194/gmd-10-1175-2017

Raddatz TJ, Reick CH, Knorr W, Kattge J, Roeckner E, et al. (2007) Will the Tropical Land Biosphere Dominate the Climate–Carbon Cycle Feedback during the Twenty-First Century? *Clim. Dyn.* 29, 565-574. https://doi.org/10.1007/s00382-007-0247-8

Randerson JT, Chen Y, van der Werf GR, Rogers BM, Morton DC (2012) Global Burned Area and Biomass Burning Emissions from Small Fires. *J. Geophys. Res.* 117(G4). https://doi.org/10.1029/2012JG002128

Rayner DP (2007) Wind Run Changes: The Dominant Factor Affecting Pan Evaporation Trends in Australia. *Ametsoc.* 20(14), 3379-3394. https://doi.org/10.1175/JCLI4181.1

Reid CE, Brauer M, Johnston FH, Jerrett M, Balmes JR, et al. (2016) Critical Review of Health Impacts of Wildfire Smoke Exposure. *Environ. Health Perspect.* 124(9), 1334-1343. https://doi.org/10.1289/ehp.1409277

Reilly R (2025) Apocalypse Los Angeles. Available at: https://www.washingtonpost.com/opinions/2025/01/08/wildfires-los-angeles-disaster-la/ (Accessed 30/5/2025)

Resco de Dios V, Arteaga C, Peguero-Pina JJ, Sancho-Knapik D, Qin H, et al. (2020) Hydraulic and photosynthetic limitations prevail over root non-structural carbohydrate reserves as drivers of resprouting in two Mediterranean oaks. *Plant Cell Environ.* 43(8),1944-1957. https://doi.org/10.1111/pce.13781

Resco de Dios V, Cunill Camprubí À, Pérez-Zanón N, Peña JC, Martínez del Castillo E, et al. (2022) Convergence in Critical Fuel Moisture and Fire Weather Thresholds Associated with Fire Activity in the Pyroregions of Mediterranean Europe. *Sci. Tot. Env.* 806(4), 151462. https://doi.org/10.1016/j.scitotenv.2021.151462

Ritchie H, Roser M (2020) CO_2 emissions. Available at: https://ourworldindata.org/co2-emissions (Accessed 30/5/2025)

Roberts MJ, Vidale PL, Mizielinski MS, Demory M, Schiemann R, et al. (2015) Tropical Cyclones in the UPSCALE Ensemble of High-Resolution Global Climate Models. *Ametsoc.* 28(2), 574-596. https://doi.org/10.1175/JCLI-D-14-00131.1

Rosell JA (2016) Bark Thickness across the Angiosperms: More than Just Fire. *New Phytol.*, 211(1), 90-102. https://doi.org/10.1111/nph.13889

Rothermel (1972) A Mathematical Model for Predicting Fire Spread in Wildland Fuels. *USDA, Forest Service.*

Rothermel (1983) How to Predict the Spread and Intensity of Forest and Range Fires. *USDA, Forest Service.*

Sadegh M, Abatzoglou JT, AghaKouchak A, Seydi ST (2025) Ignition Matters. *Nat. Sustain.* 8, 327-328. https://doi.org/10.1038/s41893-025-01527-7

Saleh N, Gharaylou M, Farahani MM, Alizadeh O (2023) Performance of Lightning Potential Index, Lightning Threat Index, and the Product of CAPE and Precipitation in the WRF Model. *Earth Space Sci.* 10(9) e2023EA003104. https://doi.org/10.1029/2023EA003104

Scarff FR, Lenz T, Richards AE, Zanne AE, Wright IJ, et al. (2021) Effects of Plant Hydraulic Traits on the Flammability of Live Fine Canopy Fuels. *Func. Ecol.* 35(4), 835-846. https://doi.org/10.1111/1365-2435.13771

Scott A (2000) The Pre-Quaternary History of Fire. Palaeogeography, Palaeoclimatology, *Palaeoecol.* 164(1-4), 281-329. https://doi.org/10.1016/S0031-0182(00)00192-9

Scott AC, Glasspool IJ (2006) The Diversification of Paleozoic Fire Systems and Fluctuations in Atmospheric Oxygen Concentration. *Proc. Natl. Acad. Sci. U.S.A.* 103(29), 10861-10865. https://doi.org/10.1073/pnas.0604090103

Seijo F (2005) The Politics of Fire: Spanish Forest Policy and Ritual Resistance in Galicia, Spain. *Env. Pol.* 14(3), 380-402. https://doi.org/10.1080/09644010500087665

Shen Y, Cai W, Prentice IC, Harrison SP (2023) Community Abundance of Resprouting in Woody Plants Reflects Fire Return Time, Intensity, and Type. *For.* 14(5), 878. https://doi.org/10.3390/f14050878

Sherriff L (2025) I Saw the Beginning of Hell: What Started as Small Flames Engulfed my City and My Life. Available at: https://nymag.com/intelligencer/article/palisades-california-fires-climate-reporter-essay.html (Accessed 30/5/2025)

Short KC (2014) A Spatial Database of Wildfires in the United States, 1992-2011. *Earth Syst. Sci. Data* 6(1), 1-27. https://doi.org/10.5194/essd-6-1-2014

Simard AJ, Haines DA, Main WA (1985) Relations between El Nino/Southern Oscillation anomalies and wildland fire activity in the United States. Agr. For. Met. 36, 93-104, https://doi.org/10.1016/0168-1923(85)90001-2

Simpson KJ, Jardine EC, Archibald S, Forrestel EJ, Lehmann CER, et al. (2020) Resprouting Grasses are Associated with Less Frequent Fire than Seeders. *New Phytol.* 230(2), 832-844. https://doi.org/10.1111/nph.17069

Sletto B (2011) Conservation Planning, Boundary-Making and Border Terrains: The Desire for Forest and Order in the Gran Sabana, Venezuela. *Geoforum.* 42(2), 197-210. https://doi.org/10.1016/j.geoforum.2010.12.006

Smith AJP, Jones MW, Abatzoglou JT, Canadell JG, Betts RA (2020) Climate Change Increases the Risk of Wildfires. *Science Brief.*

Smith C, Perkins O, Mistry J (2022) Global Decline in Subsistence-Oriented and Smallholder Fire Use. *Nat. Sustain.* 5, 542-551. https://doi.org/10.1038/s41893-022-00867-y

Soulard N, Lin H, Yu B (2019) The Changing Relationship between ENSO and its Extratropical Response Patterns. *Sci. Rep.* 9, 6507. https://doi.org/10.1038/s41598-019-42922-3

Soulis KX (2017) Estimation of SCS Curve Number Variation following Forest Fires. *Hydrol. Sci.* 63(9), 1332-1346. https://doi.org/10.1080/02626667.2018.1501482

Squire DT, Richardson D, Risbey JS, Black AS, Kitsios V, et al. (2021) Likelihood of Unprecedented Drought and Fire Weather during Australia's 2019 Megafires. *NPJ Clim. Atmos. Sci.* 4, 64. https://doi.org/10.1038/s41612-021-00220-8

Srock AF, Charney JJ, Potter BE, Goodrick SL (2018) The Hot-Dry-Windy Index: A New Fire Weather Index. *Atmos.* 9(7), 279. https://doi.org/10.3390/atmos9070279

Stavros EN, Abatzoglou J, Larkin NK, McKenzie D, Steel EA (2014) Climate and Very Large Wildland Fires in the Contiguous Western USA. *Int. J. Wildland Fire* 23(7), 899. https://doi.org/10.1071/WF13169

Stephens SL, Collins BM, Fettig CJ, Finney MA, Hoffman CM, et al. (2018) Drought, Tree Mortality, and Wildfire in Forests Adapted to Frequent Fire. *Biocci.* 68(2) 77-88. https://doi.org/10.1093/biosci/bix146

Stickney PF (1986) First Decade Plant Succession Following the Sundance Forest Fire, Northern Idaho. *USDA, Forest Service.*

Stocker BD, Wang H, Smith NG, Harrison SP, Keenan TF, et al. (2020) P-model v1.0: an Optimality-Based Light Use Efficiency Model for Simulating Ecosystem Gross Primary Production. *Geosci. Model Dev.* 13(3), 1545-1581. https://doi.org/10.5194/gmd-13-1545-2020

Suarez-Gutierrez L, Li C, Müller WA, Marotzke J (2018) Internal Variability in European Summer Temperatures at 1.5 °C and 2 °C of Global Warming. *Environ. Res. Lett.* 13, 064026. https://doi.org/10.1088/1748-9326/aaba58

Sullivan A, Baker E, Kurvits T, Popescu A, Paulson AK, et al. (2022) Spreading like Wildfire: The Rising Threat of Extraordinary Landscape Fires. *UNEP*.

Swain DL, Prein AF, Abatzoglou JT, Albano CM, Brunner M, et al. (2025) Hydroclimate Volatility on a Warming Earth. *Nat. Rev. Earth Environ.* 6, 35-50. https://doi.org/10.1038/s43017-024-00624-z

Tang R, Mao J, Jin M, Chen A, Yu Y, et al. (2021) Interannual variability and climatic sensitivity of global wildfire activity. *Adv. Clim. Change Res.* 12(5), 686-695. https://doi.org/10.1016/j.accre.2021.07.001

Teckentrup L, Harrison SP, Hantson S, Heil A, Melton JR, et al. (2019) Response of simulated burned area to historical changes in environmental and anthropogenic factors: a comparison of seven fire models. *Biogeosci.* 16(19), 3883-3910. https://doi.org/10.5194/bg-16-3883-2019

Temudo MP, Oom D, Pereira JM (2020) Bio-cultural fire regions of Guinea-Bissau: Analysis combining social research and satellite remote sensing. *Appl. Geogr.* 118, 102203. https://doi.org/10.1016/j.apgeog.2020.102203

Thapa SK, de Jong JF, Hof AR, Subedi N, Joshi LR, et al. (2022) Fire and Forage Quality: Postfire Regrowth Quality and Pyric Herbivory in Subtropical Grasslands of Nepal. *Ecol. Evol.* 12(4) e8794. https://doi.org/10.1002/ece3.8794

Thomas D, Butry D, Gilbert S, Webb D, Fung J (2017) The Costs and Losses of Wildfires: a Literature Survey. *Nat. Inst. Stand. Tech.* https://doi.org/10.6028/NIST.SP.1215

Thonicke K, Venevsky S, Sitch S, Cramer W (2001) The role of fire disturbance for global vegetation dynamics: coupling fire into a Dynamic Global Vegetation Model. *Glob. Ecol. Biogeog.*, 10(6), 661-677. https://doi.org/10.1046/j.1466-822X.2001.00175.x

To P, Eboreime E, Agyapong VIO (2021) The Impact of Wildfires on Mental Health: A Scoping Review. *Behav. Sci.* 11(9), 126. https://doi.org/10.3390/bs11090126

UNDRR (2024) Indonesia wildfires, 2023 - Forensic analysis. Available at: https://www.undrr.org/resource/indonesia-wildfires-2023-forensic-analysis (Accessed 30/5/2025)

USDA (2023) Understanding the Wildland-Urban Interface (1990-2020). Available at: https://storymaps.arcgis.com/stories/6b2050a0ded0498c863ce30d73460c9e (Accessed 30/5/2025)

Vaisala (2025) Lightning Data and Mapping. Available at: https://www.xweather.com/weather-api/lightning-api (Accessed 30/5/2025)

van der Werf GR, Randerson JT, Giglio L, Collatz GJ, Kasibhatla PS, et al. (2006) Interannual variability in global biomass burning emissions from 1997 to 2004. *Atmos. Chem. Phys.* 6(11), 3423-3441. https://doi.org/10.5194/acp-6-3423-2006

Van Der Werf GR, Randerson JT, Giglio L, Gobron N, Dolman AJ (2008) Climate Controls on the Variability of Fires in the Tropics and Subtropics. *Glob. Biogeochem. Cycl.*, 22(3). https://doi.org/10.1029/2007GB003122

van der Werf GR, Randerson JT, Giglio L, van Leeuwen TT, Chen Y, et al. (2017) Global Fire Emissions Estimates During 1997–2016. *Earth Syst. Sci. Data* 9(2), 697-720. https://doi.org/10.5194/essd-9-697-2017

van der Wiel K, Wanders N, Selten FM, Bierkens MFP (2019) Added Value of Large Ensemble Simulations for Assessing Extreme River Discharge in a 2 °C Warmer World. *Geophys. Res. Lett.* 46(4), 2093-2102. https://doi.org/10.1029/2019GL081967

van Oldenborgh GJ, Krikken F, Lewis S, Leach NJ, Lehner F, et al. (2021) Attribution of the Australian Bushfire Risk to Anthropogenic Climate Change. *Nat. Hazards Earth Syst. Sci.* 21(3), 941-960. https://doi.org/10.5194/nhess-21-941-2021

van Wagner CE (1974) Structure of the Canadian Forest Fire Weather Index. Available at: https://meteo-wagenborgen.nl/wp/wp-content/uploads/2019/08/van-Wagner-1974.pdf (Accessed 30/5/2025)

van Wees D, van der Werf GR, Randerson JT, Rogers BM, Chen Y, et al. (2022) Global Biomass Burning Fuel Consumption and Emissions at 500m Spatial Resolution based on the Global Fire Emissions Database (GFED). *Geosci. Model Dev.* 15(22), 8411-8437. https://doi.org/10.5194/gmd-15-8411-2022

van Wilgen BW, Biggs HC, O'Regan SP, Maré N (2000) A Fire History of the Savanna Ecosystems in the Kruger National Park, South Africa, between 1941 and 1996. *SA J. Sci.*, 96.

Vaarzon-Morel P, Gabrys K (2009) Fire on the Horizon: Contemporary Aboriginal Burning Issues in the Tanami Desert, Central Australia. *Geo J.* 74(5), 465-476. https://doi.org/10.1007/s10708-008-9235-8

Vautard R, Gobiet A, Jacob D, Belda M, Colette A, et al. (2013) The simulation of European heat waves from an ensemble of regional climate models within the EURO-CORDEX project. *Clim. Dyn.* 41(9), 2555-2575. https://doi.org/10.1007/s00382-013-1714-z

Veraverbeke S Rogers BM, Goulden ML, Jandt RR, Miller CE, et al. (2017) Lightning as a major driver of recent large fire years in North American boreal forests. *Nat. Clim. Change* 7(7), 529-534. https://doi.org/10.1038/nclimate3329

Wang H (2011) Analysis on Downwind Distribution of Firebrands Sourced from a Wildland Fire. *Fire Technol.* 47, 321-340. https://doi.org/10.1007/s10694-009-0134-4

Wang H, Asefa T (2018) Impact of different types of ENSO conditions on seasonal precipitation and streamflow in the Southeastern United States. Int. J. Climatol. 38(3), 1438-1451. https://doi.org/10.1002/joc.5257

Ward DS, Kloster S, Mahowald NM, Rogers BM, Randerson JT (2012) The Changing Radiative Forcing of Fires: Global Model Estimates for Past, Present and Future. *Atmos. Chem. Phys.* 12(22), 10857-10886. https://doi.org/10.5194/acp-12-10857-2012

Weis J, Schallenberg C, Chase Z, Bowie AR, Wojtasiewicz B, et al. (2022) Southern Ocean Phytoplankton Stimulated by Wildfire Emissions and Sustained by Iron Recycling. *Geophys. Res. Lett.* 49(11) e2021GL097538. https://doi.org/10.1029/2021GL097538

Welch JR (2014) Xavante Ritual Hunting: Anthropogenic Fire, Reciprocity, and Collective Landscape Management in the Brazilian Cerrado. *Hum. Ecol.* 42, 47-59. https://doi.org/10.1007/s10745-013-9637-1

Werth PA, Potter BE, Clements CB, Finney MA, Goodrick SL, et al. (2011) Synthesis of Knowledge of Extreme Fire Behavior: Volume I for Fire Managers. *JFSP Research Project Reports* 75.

Westerling AL, Swetnam TW (2003) Interannual to decadal drought and wildfire in the western United States. *Trans. AGU* 84(49), 545-555. https://doi.org/10.1029/2003EO490001

Wever N (2012) Quantifying Trends in Surface Roughness and the Effect on Surface Wind Speed Observations. *J. Geophys. Res.* 117(D11). https://doi.org/10.1029/2011JD017118

Wickramasinghe AMK, Boer MM, Cunningham CX, Nolan RH, Bowman DMJS, et al. (2024) Modeling the Probability of Dry Lightning-Induced Wildfires in Tasmania: A Machine Learning Approach. *Geophys. Res. Lett.* 51(16) e2024GL110381. https://doi.org/10.1029/2024GL110381

Williams AP, Abatzoglou JT, Gershunov A, Guzman-Morales J, Bishop DA, et al. (2019) Observed Impacts of Anthropogenic Climate Change on Wildfire in California. *Earth Fut.* 7(8), 892-910. https://doi.org/10.1029/2019EF001210

Willis D (2025) What it's like inside LA's real life apocalypse movie. Available at: https://www.bbc.co.uk/news/articles/c86w61839pyo (Accessed 30/5/2025)

WWLLN (2025) World Wide Lightning Location Network. Available at: https://wwlln.net/ (Accessed 30/5/2025)

Xu L, Crounse JD, Vasquez KT, Allen H, Wennberg PO, et al. (2021) Ozone Chemistry in Western U.S. Wildfire Plumes. *Sci. Adv.* 7(50) eabl3648 https://doi.org/10.1126/sciadv.abl3648

Ye T, Xu R, Yue X, Chen G, Yu P, et al. (2022) Short-Term Exposure to Wildfire-Related PM2.5 Increases Mortality Risks and Burdens in Brazil. *Nat. Commun.* 13, 7651. https://doi.org/10.1038/s41467-022-35326-x

Yue C, Ciais P, Cadule P, Thonicke K, Archibald S, et al. (2014) Modelling the Role of Fires in the Terrestrial Carbon Balance by Incorporating SPITFIRE into the Global Vegetation Model ORCHIDEE – Part 1: Simulating Historical Global Burned Area and Fire Regimes. *Geosci. Model Dev.* 7(6), 2747-2767. https://doi.org/10.5194/gmd-7-2747-2014

Zhang G, Wang M, Liu K (2021) Deep Neural Networks for Global Wildfire Susceptibility Modelling. *Ecol. Indic.* 127, 107735. https://doi.org/10.1016/j.ecolind.2021.107735

Zhao J, Yue C, Wang J, Hantson S, Wang X, et al. (2024) Forest Fire Size Amplifies Postfire Land Surface Warming. *Nat.* 633, 828-834. https://doi.org/10.1038/s41586-024-07918-8

Ziliani MG, Ghostine R, Ait-El-Fquih B, McCabe MF, Hoteit I (2019) Enhanced flood forecasting through ensemble data assimilation and joint state-parameter estimation. *J. Hydrol.* 577, 123924. https://doi.org/10.1016/j.jhydrol.2019.123924

Zohar I, Alperson-Afil N, Goren-Inbar N, Prévost M, Tütken T, et al. (2022) Evidence for the Cooking of Fish 780,000 Years Ago at Gesher Benot Ya'aqov, Israel. *Nat. Ecol. Evol.* 6, 2016-2028. https://doi.org/10.1038/s41559-022-01910-z

Zubkova M, Humber ML, Giglio L (2023) Is Global Burned Area Declining due to Cropland Expansion? How Much do we Know Based on Remotely Sensed Data? *Int. J. Rem. Sens.* 44(4), 1132-1150. https://doi.org/10.1080/01431161.2023.2174389

Modelling the Daily Probability of Wildfire Occurrence in the Contiguous United States

This chapter was originally published in *Environmental Research Letters* in February 2024. As it was published as an independent article, I provide a cover page here with information on how this chapter links to the rest of the thesis, how research published since may affect the chapter's interpretation, as well as additional information on modelling methods and training data strategies that were not included in the original article.

This chapter is foundational to the research project of this thesis, which is to understand the short and long-term patterns of wildfire variability and their drivers. As detailed in Section 1.10, an occurrence model is necessary for this project. The high stochasticity of individual wildfire events and driving weather conditions in combination with the relatively short observational record render observational data insufficient for answering key questions about wildfire occurrence patterns and their drivers. The occurrence model is also necessary for Chapters 3 and 4, where it is applied to future climate data, as well as unrealised years in the present climate. In this chapter, there is also a systematic establishment of the key drivers of wildfire occurrence in the contiguous US. The model identifies smooth, monotonic changes over a subsection of each selected variable's domain. Simple variable effects can therefore be identified and assessed, both to answer scientific questions about the drivers of wildfire (see Haas et al., 2024) and to improve the existing occurrence modules in leading global fire models (Section 1.7).

This chapter answers the question: *how should a simple probabilistic model for wildfire occurrence be built?* It does this by starting with a simple model framework commonly used in statistical modelling, a generalised linear model (GLM). The chapter then details the three necessary adaptations to address a specific limitation of GLMs in modelling wildfire likelihood. First, identifying which variables are most predictive when there are many candidate effects. Second, addressing the fact that different variables can have different strengths of effect on wildfire likelihood at different parts of their domain. Third, resolving the tendencies of GLMs to compress rare events toward the centre of a distribution. The performance of the resultant model is then extensively assessed by an ensemble of model training runs. Lower and upper bounds on the model's performance across benchmarks were found, allowing for a stricter point of comparison against other wildfire modelling methods, and that the best performing models

could be identified. The rate at which variables are selected can also be identified using the training ensemble, which also presents the relative importance of different predictors.

The model presented here is utilisable as an independent regional model for the daily likelihood of wildfire events in the contiguous USA. The methodology is also applicable to wildfire occurrence modelling generally. Applied to global wildfire data, this could be used to improve the simple occurrence modules currently used in global fire models – independent of whether the subsequent size/spread module is empirical or process-based (Section 1.7). The methodology also offers significant operational benefits over fire weather indices, as it incorporates seasonally variations in vegetation and multiannual trends in land-use, demography and vegetation. Whilst some fire weather indices are highly predictive of wildfire likelihood and intensity, they were not considered as inputs. This is because such indices are either already the combination of simple meteorological variables (e.g. the Hot-Dry-Windy Index or Angström Index) or are sophisticated indices that assume vegetation structure and fuel drying dynamics (e.g. the Canadian Fire Weather Index or USA Burning Index) that may be highly predictive in some environments and anti-correlated with wildfire in others (Jones et al., 2022).

Since the publication of this chapter, Di Giuseppe et al. (2025) published ECMWF's operational probability of fire model (PoF). PoF predicts wildfire likelihood using an ML method (XGBoost) trained on globally available satellite data. Unlike previous fire danger products from weather services, this product uses vegetation, land cover and population data, as well as new modelled fuel load and moisture input variables (McNorton and Di Giuseppe, 2024). Whilst the model is not benchmarked analogously to the model in this chapter, Di Giuseppe et al. (2025) report a separability statistic (AUC) of 0.94 globally, and 0.69 to 0.96 across key regions, in comparison to the 0.85–0.87 found in Chapter 2 over the contiguous US. Generally, ML methods are able to achieve higher predictive power than statistical models, due to a much higher degree of freedom in how they can fit to the training data. The objective of the model in this chapter, is to present a model with simple, robust and falsifiable variable effects. By constraining the model to simple variable effects, and then optimising for predictive power, the model can be better used to explain key associations with wildfire frequency and to improve existing modelling methods.

As model development is an exploratory process, not all tests undertaken in model development could be included in the following chapter. For example, other modelling techniques were also compared including zero-inflated GLMs, and hierarchical Bayesian models. These methods were assessed for explanatory clarity and increase in model performance and were not selected. Similarly, including cross-terms in the GLM was assessed, but did not provide a commensurate improvement in model performance to outweigh increased model complexity. The time period for variables in which multiple antecedences were considered (precipitation, gross primary productivity, vapour pressure deficit) were selected by graphing the changing model likelihood in response to different antecedent timescales, with commonly selected variables included as covariates. Model training datasets were either 10^6 or 10^7 datapoints, with test datasets 25% of that size again. Test and training data were randomly sampled across all days and grid cells, and were unweighted by season, region, or the presence or absence of a wildfire event.

ENVIRONMENTAL RESEARCH
LETTERS

LETTER

Modelling the daily probability of wildfire occurrence in the contiguous United States

Theodore Keeping[1,2,*], **Sandy P Harrison**[1,2] and **I Colin Prentice**[2,3]

[1] Geography & Environmental Science, University of Reading, Whiteknights, Reading RG6 6AH, United Kingdom
[2] Leverhulme Centre for Wildfires, Environment and Society, Imperial College London, South Kensington, London SW7 2BW, United Kingdom
[3] Georgina Mace Centre for the Living Planet, Department of Life Sciences, Imperial College London, Silwood Park Campus, Buckhurst Road, Ascot SL5 7PY, United Kingdom
[*] Author to whom any correspondence should be addressed.

E-mail: t.r.keeping@pgr.reading.ac.uk

Keywords: wildfire risk, wildfire occurrence modeling, natural hazards, contiguous United States, generalised linear models, social-ecological systems

Supplementary material for this article is available online

OPEN ACCESS

RECEIVED
1 October 2023

REVISED
12 December 2023

ACCEPTED FOR PUBLICATION
22 January 2024

PUBLISHED
2 February 2024

Abstract

The development of a high-quality wildfire occurrence model is an essential component in mapping present wildfire risk, and in projecting future wildfire dynamics with climate and land-use change. Here, we develop a new model for predicting the daily probability of wildfire occurrence at 0.1° (∼10 km) spatial resolution by adapting a generalised linear modelling (GLM) approach to include improvements to the variable selection procedure, identification of the range over which specific predictors are influential, and the minimisation of compression, applied in an ensemble of model runs. We develop and test the model using data from the contiguous United States. The ensemble performed well in predicting the mean geospatial patterns of fire occurrence, the interannual variability in the number of fires, and the regional variation in the seasonal cycle of wildfire. Model runs gave an area under the receiver operating characteristic curve (AUC) of 0.85–0.88, indicating good predictive power. The ensemble of runs provides insight into the key predictors for wildfire occurrence in the contiguous United States. The methodology, though developed for the United States, is globally implementable.

1. Introduction

Wildfire poses a significant risk to both the natural environment and people. Wildfires are increasing in many parts of the world, including the United States, the northern boreal zone, southern Europe, Amazonia, and Australia (Smith *et al* 2020) in response to ongoing climate change, which has been associated with a strong drying effect on vegetation fuels (Ellis *et al* 2022). Wildfire is also an important earth system process. In addition to the effects of radiative forcing and carbon emissions on climate (Liu *et al* 2014), wildfire has been found to influence Amazon regrowth after deforestation (Drüke *et al* 2023), to be a major driver of permafrost thaw (Gibson *et al* 2018); and to cause significant ocean fertilisation events (Weis *et al* 2022). It is thus critical to be able to make quick and robust predictions of the likelihood of wildfire events, both to characterise wildfire risk and to better understand wildfire's complex role in the earth system.

Wildfire occurrence can be defined as the development of an unplanned fire over a certain size. Occurrence, in conjunction with fire size, controls annual burned area—the cumulative footprint of wildfire on the landscape. The rate of wildfire occurrence is related to fire intensity (Luo *et al* 2017), a key determinant for the severity of a burn event. The likelihood of fire occurrence is the first component in process-based fire models used in dynamic global vegetation models (Rabin *et al* 2017). Wildfire occurrence is also of importance from a fire management perspective because of the need to identify and control smaller wildfire events in high-risk areas.

Wildfire occurrence is driven by many factors, reflecting the multiple conditions that must be

met for ignition and initial fire spread: an ignition source, fuel availability, fuel dryness, and atmospheric conditions (Krawchuk *et al* 2009, Harrison *et al* 2010). Ignitions may be caused by lightning or humans, but there are many human sources of ignitions including recreation, smoking, debris burning, arson, machinery, railroads and powerlines (Short 2014). However, humans also suppress wildfires, either directly through fuel management and firefighting, or indirectly through the impacts of land-use and landscape fragmentation on fuel availability and continuity (Harrison *et al* 2021). Fuel accumulation is also determined by vegetation characteristics, including primary production and dominant plant type (Harrison *et al* 2010, Forkel *et al* 2019). Meteorological drivers such as precipitation, atmospheric moisture, and temperature influence fire occurrence through their effect on fuel moisture, while topography and wind strength influence the rate of spread (Parisien and Moritz 2009). In addition to current conditions, antecedent vegetation growth and drought also influence the occurrence of wildfires through their effect on fuel availability (Kuhn-Régnier *et al* 2021). Given the large number of potential influences on wildfire occurrence, it is important to consider which are most important in order to define a parsimonious set of predictors to incorporate into a wildfire occurrence model.

The probability of wildfire occurrence is primarily modelled as a monthly to decadal landscape susceptibility to wildfire. Highly resolved, regional fire susceptibility maps account for local effects driving fire likelihood in different regions based on either statistical models, machine-learning or maximum entropy approaches (D'Este *et al* 2020, Gholamnia *et al* 2020, Chen *et al* 2021). Daily timescale variability in the probability of wildfire occurrence is often accounted for using fire danger rating systems, risk indices that are largely based on modelling meteorological effects, with some limited integration of remote sensing and fuel mapping products (Zacharakis and Tsihrintzis 2023).

In this paper we introduce an adapted Generalised Linear Model (GLM) methodology to model the daily probability of wildfire. GLMs are statistical models that establish the most likely linear relationship between a dependent variable and a set of predictors, taking into account the statistical properties of the dependent variable. The approach was adopted here because it provides more easily interpretable results than machine learning or non-linear statistical methods and is also less susceptible to overfitting, which is important given the highly stochastic nature of wildfire occurrence. We then apply this in an ensemble of models to determine the spread of model performance, and to identify which predictors are most essential to modelling the likelihood of daily fire occurrence. We evaluate the model's performance across geospatial and seasonal trends, and its representation of interannual variability.

2. Methods

2.1. Data

2.1.1. Fire occurrence data

The target fire occurrence variable was developed from the fire programme analysis fire-occurrence database (FPA FOD) (Short 2021), a synthesis of wildfire occurrence across the United States from data provided by federal, state and local fire organisations covering the period 1992–2018. Prescribed burns are not included in the dataset, but escaped fires that result from prescribed burns are included. The fire start location is given to a resolution of 1.6 km. We use data from 2002 onwards because the quality of non-federal reporting systems is better after this date (Short 2014). We define a fire occurrence as an unplanned fire greater than 0.25 acres (0.1 ha)—the lowest non-zero U.S. National Wildfire Coordinating Group fire size classification. The binary data (occurrence, non-occurrence) were gridded at daily, 0.1° resolution.

2.1.2. Predictors

A total of 47 predictors representing meteorological, vegetation and human factors affecting the probability of fire occurrence were used (supplementary table A1). Precipitation and temperature-related variables were obtained from the PRISM Climate Group (2019), with additional meteorological variables taken from ERA5-Land (Muñoz-Sabater *et al* 2021). These data were used to derive predictors (e.g. antecedent precipitation) associated with antecedent conditions over several different time periods. Convective available potential energy data, a predictor of lightning occurrence, was sourced from the National Centres for Environmental Prediction's North American Regional Reanalysis (NCEP-NAAR: Mesinger *et al* 2006). Rural and total population density were obtained from version 4 of the Global Population of the World dataset (CIESIN 2016). Road density was obtained from version 4 of the Global Roads Inventory Project data set (Meijer *et al* 2018) and additional measures of human activity (e.g. powerline length per area) from OpenStreetMap (OSM Contributors 2022). The land-cover fraction of different vegetation types (e.g. herbaceous cover) was obtained from the European Space Agency Climate Change Initiative data set (Defourny *et al* 2019). Gross primary production (GPP) was derived using a light-use efficiency model (P model: Stocker *et al* 2020) driven by the remotely-sensed fraction of absorbed photosynthetically active radiation (Jiang and Ryu 2016), photosynthetic photon flux density (Ryu *et al* 2018) and climate data. Antecedent effects on fuel

accumulation, fuel drying and fuel wetting, represented by antecedent GPP, vapour pressure deficit (VPD) and precipitation respectively, were included through testing different timescales for each predictor through test runs of the model at varying antecedences. All the predictor variables were re-gridded to 0.1° resolution and linearly interpolated to a daily timescale.

2.2. Modelling approach

We used a binomial GLM to model the binary outcome of whether a wildfire greater than 0.25 acres occurred on a given day at a given location. GLMs provide highly interpretable results distinguishing the effect of each predictor when other predictors are held constant (Nelder and Wedderburn 1972) and provide a measure of variable significance in the form of t-values (McCullagh and Nelder 1989). There are well-established frameworks for evaluation of model performance and predictors, including the Akaike information criterion (AIC) (Akaike 1974) and the variance inflation factor (VIF) (Allison 1999) used in this study. We used the area under the receiver operating characteristic curve (AUC) as an overall performance metric. GLMs have been widely applied to model wildfire, both in a global context (e.g. Bistinas *et al* 2014, Haas *et al* 2022), and in regional fire occurrence modelling (e.g. Vilar *et al* 2010, Lan *et al* 2023).

We developed our new model in Python, using the statsmodels module. The standard bionomial approach was modified in three ways for this application (figure 1). We introduced an objective predictor selection procedure, given the large number of potential predictors (table A1), in order to minimise multicollinearity in the predictors and overfitting the model. A stepwise variable selection algorithm (Chowdhury and Turin 2020) was applied, starting from a constant model with no predictors and then iteratively (1) finding the best performing new variable to add by minimising the AIC (the forwards step), before (2) checking whether removing any of the existing predictors for an unused variable minimises the AIC further (the backwards step). Predictor variables that produced VIFs >5 were ignored in both steps, to prevent inclusion of highly correlated predictors. Improvements in predictivity (AUC) were negligible after 12 predictors; this was therefore taken as the maximum number of predictors to reduce the likelihood of overfitting.

Predictors may only influence fire occurrence probability in a certain range. For example, small increments in daily precipitation are more likely to impact fire occurrence probability when the precipitation rate is low. Predictors may also have different effects on the probability of fire in different parts of their range. Aridity, for example, lowers fuel moisture and leads to higher fire risk, but further increases in aridity leads to less vegetation growth, decreasing fuel availability and fuel continuity and hence leading to lower fire risk. We determined the appropriate range of influence for each predictor through an algorithm that truncated the predictor ranges through optimisation of the AIC. The algorithm (given in supplementary material, figure A1) iteratively tested the improvement of the model by clipping the upper or lower bound of each predictor. The final set of predictor domains is defined as the set of upper and lower bounds on each predictor from which there is no further significant improvement in AIC—with an AIC difference of two taken as a substantial difference in models (Burnham and Anderson (2004)).

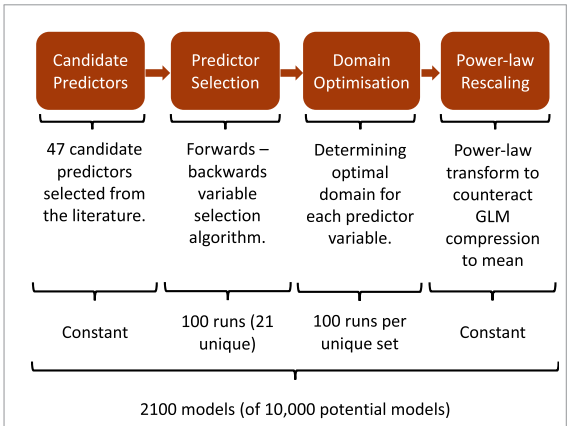

Figure 1. An overview of the GLM architecture and the ensemble application of the modelling methodology. The inputs and adaptations to a basic GLM application are detailed in the top two layers, with the second two layers showing 100 predictor selection runs, and subsequent 100 runs of the predictor domain optimisation algorithm.

GLMs have a known tendency to compress predicted values towards the middle of the sampled range and to under-represent high and low extremes (Hastie *et al* 2009) due to the assumption of linearity with the log odds of the target variable. Whilst a good ranking of high and low fire risk was achieved in the model (i.e. high AUC), compression was observed in the geospatial mean of the probability of fire occurrence between 2002–2018. We applied a power-law transformation to the output daily probability of fire occurrence, optimising to reduce the residuals in the distribution of the observed and modelled geospatial means.

2.3. Ensemble application of model

We created an ensemble of models by running the predictor selection algorithm 100 times with a training dataset of 10^7 datapoints and running the predictor range optimisation algorithm 100 times for each unique set of selected predictors with a training dataset of 10^6 datapoints. This produced an ensemble of 2100 members. This ensemble allows us to characterise the spread of model performance and to evaluate whether the model performs well given

the uncertainties introduced by variable selection and range optimisation. We use the mean of the Pareto superior subset (Jahan *et al* 2016) of the ensemble, which is less likely to be overfit than a single 'best performing' ensemble member, to represent fire probability. The Pareto superior subset is defined as the set of all Pareto efficient models across the four model benchmarks defined in section 2.4. An additional 2000-member ensemble was created by running the predictor selection algorithm with a training dataset of 10^6 datapoints to identify the rate at which each of the candidate predictor variables was selected. The higher number of runs was required due to the low rate of selection for some variables and to better assess whether some core variables were always selected, the smaller training dataset was a necessary cost due to the relatively higher number of runs.

2.4. Evaluation metrics

We used the AUC statistic to assess predictive power through separability—the extent to which the model can separate between wildfire occurrence and non-occurrence (Hanley and McNeil 1982). The normalised mean error (NME) between the modelled and observed mean rate of wildfire occurrence for each cell over the study period of 2002–2018 was used to assess performance with respect to geospatial trends. The NME of the total number of wildfire occurrences was used to assess the representation of interannual variability. Seasonal effects were evaluated in terms of seasonal concentration and seasonal phase (Hantson *et al* 2020). Seasonal concentration is the extent to which fire occurrence is clustered in the year, where 0 indicates that there are the same number of fires each month and 1 indicates fires occur in a single month; this was assessed using NME. Seasonal phase is the peak timing the fire season, and is most meaningful when the season is characterised by a single, symmetrical peak. Seasonal phase was assessed using the mean phase difference (MPD) (Hantson *et al* 2020). NME and MPD were calculated as follows:

$$\mathrm{NME} = \frac{\sum_i A_i \left| X_i^{\mathrm{mod}} - X_i^{\mathrm{obs}} \right|}{\sum_i A_i \left| X_i^{\mathrm{obs}} - \overline{X^{\mathrm{obs}}} \right|} \quad (1)$$

$$\mathrm{MPD} = \frac{1}{\pi} \frac{\sum_i A_i \arccos\left[\cos\left(\varphi_i^{\mathrm{mod}} - \varphi_i^{\mathrm{obs}}\right)\right]}{\sum_i A_i} \quad (2)$$

where A_i are cell areas, φ is seasonal phase, and X is either the mean rate of fire occurrence per site, the total annual number of fires, or the seasonal concentration. An NME value of 0 corresponds to perfect performance, whilst a value of 1 means performance equal to a null model predicting a constant value of X for all datapoints. An MPD of 0 means the model and observation are in perfect phase, whilst a value of 1 would mean perfect antiphase.

3. Results

The overall performance of the model as measured by the AUC is good (table 1). All the models have an AUC of >0.85, higher than the threshold of 0.8 generally taken as indicating 'very good' model performance (McCune *et al* 2002). The Pareto subset of models have an AUC of >0.86.

The model has a geospatial NME for the Pareto subset of the ensemble of 0.44, considerably better than a null model assuming the mean value of fire probability across all cells. The poorest NME score from the full ensemble (0.49) is also very good. The model identifies key features of the geospatial patterns shown by the mean of the model output from 2002 to 2018 (figure 2), such as the broad regions of lower fire likelihood in the Mississippi Valley, the Corn Belt and the Great Plains, and the areas of higher fire likelihood such as the Southeastern and Texas Plains and the West Coast. These patterns are also observed in the daily outputs (see figure A2 for examples). Even at a finer scale, the model generally captures the high and low fire areas within a region. However, the model output is smoother than the observations. The area with $<10^{-4}$ average daily probability of wildfire occurrence is 37% smaller than for the observations, and the model shows none of the discontinuities at State boundaries seen in the observations, such as those seen at the New York and North Carolina state borders.

As with the geospatial patterns, the model also produces reasonable spatial patterns for wildfire seasonality (figure 3). The mean MPD value for the Pareto subset of 0.14 for seasonal phase indicates that the phasing of the fire season is well captured. Model performance for seasonal concentration is less good, with a mean NME value for the Pareto subset of 0.78. Nevertheless, the model identifies the early spring phase for wildfire in the southeast, the late spring phase in the northeast, and the late spring/summer phase in the west. It also correctly identifies the less concentrated fire season in the Southeastern and Great Plains, as well as towards the coasts. However, the observations are considerably noisier than the model, particularly in low fire regions. Figures A3–A5 in the supplementary material show the three most observed seasonal patterns, a spring fire season; a spring/autumn bimodal fire season; and a summer fire season respectively.

The model is also able to predict high and low fire years (figure 4). The model has an interannual NME for total annual fire counts for the Pareto subset of the ensemble of 0.67, much better than a null model assuming the mean value of fire probability across all years. Figure A6 in the supplementary material contrasts the mean modelled and observed rate of fire in the years with highest (2006) and lowest (2003) number of fire occurrences.

Table 1. AUC and benchmark metrics for all ensemble members, the Pareto superior subset and the highest AUC model of the Pareto superior subset (the 'best model').

	All ensemble members			Pareto superior subset			
	Min	Mean	Max	Min	Mean	Max	Best Model
Separability (AUC)	0.85	0.87	0.87	0.86	0.87	0.87	0.87
Geospatial (NME)	0.43	0.45	0.49	0.43	0.44	0.46	0.44
Annual fire count (NME)	0.66	0.67	0.68	0.66	0.67	0.67	0.67
Seasonal concentration (NME)	0.70	0.83	1.02	0.70	0.78	0.88	0.74
Seasonal phase (MPD)	0.13	0.15	0.17	0.13	0.14	0.16	0.15

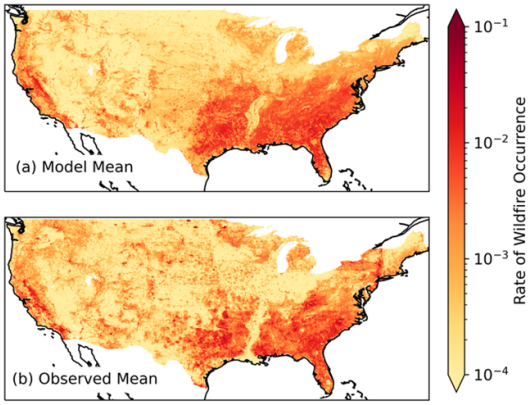

Figure 2. Comparison of (a) modelled and (b) observed mean of daily modelled probability of wildfire occurrence over the period 2002–2018. The model results are the average across the Pareto superior set of ensemble members. Both maps are plotted on a logarithmic scale.

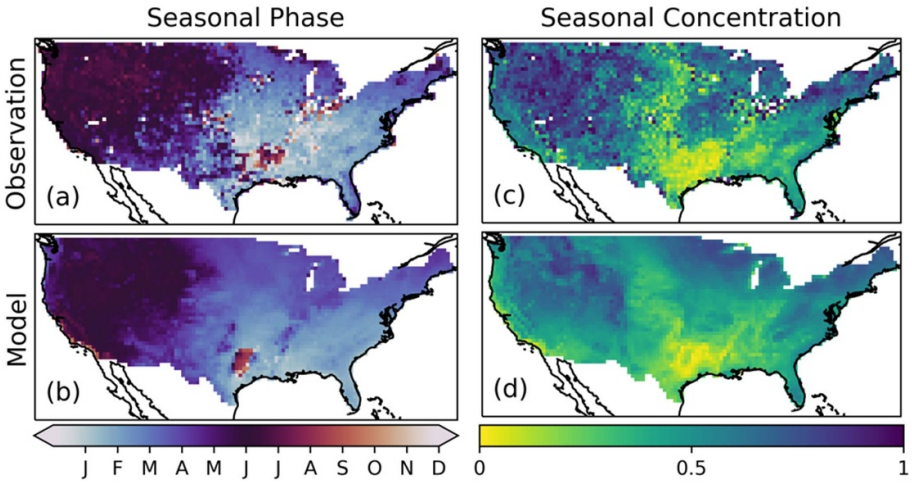

Figure 3. Comparison of (a) observed and (b) modelled seasonal phase and (c) observed and (d) modelled seasonal concentration of wildfire occurrence.

Analysis of the 2000-model ensemble of the predictor selection component of the model (figure 5) shows that several variables are identified as important predictors in all the runs. Rural population density, snow-cover fraction, precipitation over the prior five days, and the diurnal temperature range (DTR) were selected in all 2000 models, and nighttime VPD was selected in 98% of the runs. A further seven predictors are selected in more than 50% of the runs: GPP over the antecedent year and over the antecedent 50 d, tree cover fraction, shrub cover fraction, herb cover fraction, aridity and daily precipitation—emphasising the importance of vegetation and moisture controls on wildfire occurrence probability. However, some predictors were rarely or never selected, including ruggedness, soil moisture and measures of human infrastructure.

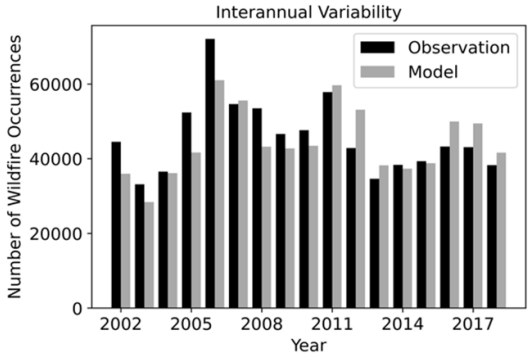

Figure 4. Annual total modelled and observed fire occurrences in the contiguous United States from 2002–2018.

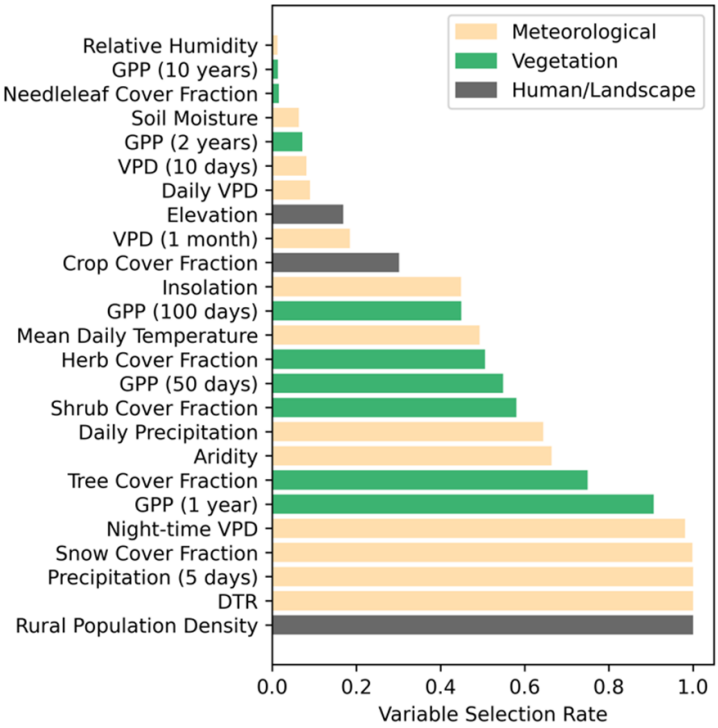

Figure 5. Rate of selection of individual predictor variables in the 2000-member ensemble from the stepwise variable selection algorithm. Only variables that were selected in more than 1% of the ensemble members are shown.

4. Discussion

We have presented a model to predict the daily probability of wildfire occurrence which has good predictive power. All models have an AUC of greater than 0.85, higher than the threshold of 0.8 for 'very good' model performance taken in other studies (McCune *et al* 2002). Similarly good performance has been obtained with models focusing on more limited regions, for example a daily lightning fire occurrence model for Daxinganling Mountains (AUC = 0.87) (Chen *et al* 2015), and an hourly forest fire risk index developed for South Korea (AUC = 0.84) (Kang *et al* 2020). However, both of these studies focus on a relatively short time period (6 years) and more climatologically and ecologically homogeneous regions. Our research shows that reliable predictions of the daily probability of wildfire occurrence can be made using statistical models through careful adaptation of a GLM methodology, and provides a roadmap for how to do so.

Whilst there is good correspondence between the modelled and observed geospatial patterns (figure 2), there are also regions of disagreement. The most marked difference between the modelled and observed mean rate of wildfire occurrence is in the northeast US. This may reflect a problem with the FPA FOD data for fire numbers since there is poor agreement, except for New York state, between these data and annual fire count estimates from the

National Interagency Coordination Centre (NICC) (Short 2014). However, despite the poor match in the predicted rate of fire in the northeast and the FPA FOD data, the model still identifies key regional effects, including the greater amount of fire on the New England coast compared to inland, and the comparatively low rate of fire in the upstate New York boreal highlands. The model tends to identify more fire in agriculturally intensive regions such as the corn belt and the Mississippi valley. This may reflect more systematic fuel removal and landscape management in these regions. However, this region includes states where the FPA FOD dataset predicts a lower rate of wildfire than the NICC estimates (Missouri, Indiana and Ohio), so it may be that the FPA FOD dataset is under-reporting wildfire counts in these regions whilst the model is correctly responding to causal factors associated with a higher mean rate of fire occurrence.

We have shown that there is good first-order correspondence between the observed and modelled seasonal concentration and phase of wildfires. The match is less good in low fire regions, where the noisiness of the observational records affects the reliability of the metric. There is also a major disagreement between the modelled and observed seasonality in the Pacific Northwest, where the model incorrectly predicts a late spring peak in wildfires compared to the observed early summer phasing. One potential reason for this mismatch is that evergreen forests are less susceptible to spring wildfires than deciduous forests, since the canopy protects leaf litter from drying out (Tamai 2001). However, this cannot be the only explanation for the poor model performance in the Pacific Northwest because the wildfire seasonality in other regions where evergreen forests are dominant is predicted reasonably well. The largest mismatches between the predicted and observed timing of fire peak occur in grid cells with extremely high annual precipitation, with values >99.5th percentile in the overall data set. It is to be expected that the model has more difficulty in capturing extremes that are poorly represented in the training data but it is clear that the power-law transformation used to minimise the impact of outliers has not overcome this limitation completely.

The ensemble of 2000 predictor selection runs showed that rural population density is an important predictor in all models whereas total population density is not. Total population density has been used as a predictor of wildfires both in global statistical models (e.g. Bistinas *et al* 2014, Haas *et al* 2022) and in fire-enabled dynamic global vegetation models (Rabin *et al* 2017). Despite the fact that Fusco *et al* (2016) discounted population density as a meaningful predictor at local scales in the U.S. compared to land-use predictors, our study shows that rural population density is an informative metric. Specifically, increases in rural population lead to an increased probability of fire occurrence. This is consistent with the findings of Balch *et al* (2017) that human ignitions occur on days and in regions that are wetter than those under which fires start naturally, thus creating an expansion of the 'fire niche'.

The ensemble of predictor selection runs emphasises the importance of meteorological variables in controlling fire occurrence. Both night-time VPD and DTR were identified as important predictors, reflecting the different effects on daily fluctuations in fuel moisture from the dampening effect of the antecedent night-time moisture barrier (Goens 1989) and the drying effect from warming throughout the day. GPP was found to be an important control on wildfire occurrence at both annual and seasonal antecedences—reflecting the effects of consequently higher fuel load and live fuel moisture respectively. This supports the conclusions of Kuhn-Régnier *et al* (2021) that including antecedent conditions for vegetation predictors produces more accurate predictions of burnt area.

There are several potential applications of the model and modelling approach described here. The probability of fire occurrence over the short-term at a regional scale for the purposes of fire and landscape management is usually predicted using fire index models which rely on detailed fuel catalogues and drying models (e.g. Preisler *et al* 2014). Similar predictions can be made with our model even in the absence of detailed fuel load information. Furthermore, the model could be applied to predict likely future changes in wildfire occurrence using ensembles of climate model projections and without assuming static (modern observed) fuel loads. Near term prediction of the occurrence of fires over a given size would be useful to stakeholders exposed to wildfire risk, including the insurance sector and land managers. Although our model was originally developed for the contiguous United States, because of the availability of high-quality data particularly on variables related to potential human influences on wildfires, the final set of selected variables are obtainable from readily available global data sets. Thus, the same modelling approach could be employed to assess fire risks in other regions and how these might change with a changing climate. It would be interesting to compare different regions of the world to determine how the key drivers of wildfire vary regionally, as has been suggested by several previous studies (e.g. Bistinas *et al* 2014, Forkel *et al* 2019). The model may also have utility in the context of fire-enabled dynamic vegetation models. The current generation of fire-enabled dynamic vegetation models do not predict the seasonality or interannual variability of wildfires well (Hantson *et al* 2020). This is a major limitation given that these models are now included in earth system models used to predict future climate changes in order to simulate the feedback associated with fire emissions (Park *et al* 2023, Wang *et al* 2023).

Our modelling approach could be used to provide a way of realistically predicting fire starts, replacing the simplistic ignition assumptions currently based on lightning strikes or a human population density, that could then be coupled to the process-based fire spread component of the global fire models.

5. Conclusion

We have presented a new model to predict the probability of wildfire occurrence that produces realistic predictions at a daily timescale and 0.1° resolution for the contiguous United States. It captures the geographic differences both in the numbers and the seasonal occurrence of fires, as well as predicting high and low fire years. The most important predictors of the probability of wildfire occurrence are rural population, meteorological variables (short-term drying, precipitation and snow cover) and vegetation properties (plant type cover and antecedent GPP). The model is easily applicable and, given that all the variables are available in global data sets, could be applied to predict fire risk worldwide under a changing climate.

Data availability statement

All of the data sets used in the analysis are publicly available from the references cited in table A1. The outputs of the model and the code are available from https://zenodo.org/record/8392712.

The data that support the findings of this study are openly available at the following URL/DOI: https://doi.org/10.5281/zenodo.8392712.

Acknowledgments

We thank Hannah Cloke for suggestions about the ensemble approach, Wenjia Cai for assistance with the P model. We also thank Ted Shepherd, colleagues from AXA-XL Ioana Dima-West and Alec Vessey, and colleagues at the Leverhulme Centre for Wildfires, Environment and Society for discussions of the results. This work is a contribution to the LEMONTREE (Land Ecosystem Models based On New Theory, obseRvations and ExperimEnts) project, funded through the generosity of Eric and Wendy Schmidt by recommendation of the Schmidt Futures program (T R K, S P H, I C P). T R K also acknowledges support from the SCENARIO NERC Doctoral Training Programme (NE/S007261/1). I C P also acknowledges support from the ERC-funded project REALM (Re-inventing Ecosystem And Land-surface Models, Grant No. 787203). We acknowledge computational resources and support provided by the Imperial College Research Computing Service.

Author contributions

Concepts, strategy and interpretation were developed by T R K, S P H and I C P jointly. T R K was responsible for data curation, processing and analysis, and produced the graphics and tables. T R K wrote the original draft and all authors contributed to the final version.

Conflict of interest

The authors declare that they have no conflict of interest.

ORCID iDs

Theodore Keeping https://orcid.org/0000-0002-5603-6980
Sandy P Harrison https://orcid.org/0000-0001-5687-1903
I Colin Prentice https://orcid.org/0000-0002-1296-6764

References

Akaike H 1974 A new look at the statistical model identification *IEEE Trans. Autom. Control* **19** 716–23
Allison P D 1999 *Multiple Regression: A Primer* (Pine Forge Press)
Balch J K, Bradley B A, Abatzoglou J T, Nagy R C, Fusco E J and Mahood A L 2017 Human-started wildfires expand the fire niche across the United States *Proc. Natl Acad. Sci.* **114** 2946–51
Bistinas I, Harrison S P, Prentice I C and Pereira J M C 2014 Causal relationships versus emergent patterns in the global controls of fire frequency *Biogeosciences* **11** 5087–101
Burnham K P and Anderson D R 2004 Multimodel inference: understanding AIC and BIC in model selection *Sociol. Methods Res.* **33** 261–304
Center for International Earth Science Information Network—CIESIN—Columbia University 2016 Gridded population of the World, version 4 (GPWv4): administrative unit center points with population estimates (NASA Socioeconomic Data and Applications Center (SEDAC)) (https://doi.org/10.7927/H4F47M2C)
Chen B, Jin Y, Scaduto E, Moritz M A, Goulden M L and Randerson J T 2021 Climate, fuel, and land use shaped the spatial pattern of wildfire in California's Sierra Nevada *J. Geophys. Res.* **126** e2020JG005786
Chen F, Du Y, Niu S and Zhao J 2015 Modeling forest lightning fire occurrence in the Daxinganling Mountains of Northeastern China with MAXENT *Forests* **6** 1422–38
Chowdhury M Z I and Turin T C 2020 Variable selection strategies and its importance in clinical prediction modelling *Fam. Med. Commun. Health* **8** e000262
D'Este M, Ganga A, Elia M, Lovreglio R, Giannico V, Spano G, Colangelo G, Lafortezza R and Sanesi G 2020 Modeling fire ignition probability and frequency using Hurdle models: a cross-regional study in Southern Europe *Ecol. Process.* **9** 1–14
Defourny P ESA Land Cover CCI project team 2019 ESA land cover climate change initiative (Land_Cover_cci): global land cover maps, version 2.0.7 (Centre for Environmental Data Analysis) (available at: https://catalogue.ceda.ac.uk/uuid/b382ebe6679d44b8b0e68ea4ef4b701c) (Accessed 15 September 2022)

Drüke M, Sakschewski B, von Bloh W, Billing M, Lucht W and Thonicke K 2023 Fire may prevent future Amazon forest recovery after large-scale deforestation *Commun. Earth Environ.* **4** 248

Ellis T M, Bowman D M, Jain P, Flannigan M D and Williamson G J 2022 Global increase in wildfire risk due to climate-driven declines in fuel moisture *Glob. Change Biol.* **28** 1544–59

Forkel M *et al* 2019 Emergent relationships with respect to burned area in global satellite observations and fire-enabled vegetation models *Biogeosciences* **16** 57–76

Fusco E J, Abatzoglou J T, Balch J K, Finn J T and Bradley B A 2016 Quantifying the human influence on fire ignition across the western USA *Ecol. Appl.* **26** 2390–401

Gholamnia K, Gudiyangada Nachappa T, Ghorbanzadeh O and Blaschke T 2020 Comparisons of diverse machine learning approaches for wildfire susceptibility mapping *Symmetry* **12** 604

Gibson C M, Chasmer L E, Thompson D K, Quinton W L, Flannigan M D and Olefeldt D 2018 Wildfire as a major driver of recent permafrost thaw in boreal peatlands *Nat. Commun.* **9** 3041

Goens D W 1989 Forecast guidelines for fire weather and forecasters, how nighttime humidity affects wildland fuels

Haas O, Prentice I C and Harrison S P 2022 Global environmental controls on wildfire burnt area, size, and intensity *Environ. Res. Lett.* **17** 065004

Hanley J A and McNeil B J 1982 The meaning and use of the area under a receiver operating characteristic (ROC) curve *Radiology* **143** 29–36

Hantson S *et al* 2020 Quantitative assessment of fire and vegetation properties in simulations with fire-enabled vegetation models from the fire model intercomparison project *Geosci. Model Dev.* **13** 3299–318

Harrison S P *et al* 2021 Understanding and modelling wildfire regimes: an ecological perspective *Environ. Res. Lett.* **16** 125008

Harrison S P, Marlon J R and Bartlein P J 2010 *Fire in the Earth System* (Springer) pp 21–48

Hastie T, Tibshirani R, Friedman J H and Friedman J H 2009 *The Elements of Statistical Learning: Data Mining, Inference, and Prediction* vol 2 (Springer) pp 1–758

Jahan A, Edwards K L and Bahraminasab M 2016 *Multi-criteria Decision Analysis for Supporting the Selection of Engineering Materials in Product Design* (Butterworth-Heinemann)

Jiang C and Ryu Y 2016 Multi-scale evaluation of global gross primary productivity and evapotranspiration products derived from breathing earth system simulator (BESS) *Remote Sens. Environ.* **186** 528–47

Kang Y, Jang E, Im J, Kwon C and Kim S 2020 Developing a new hourly forest fire risk index based on catboost in South Korea *Appl. Sci.* **10** 8213

Krawchuk M A, Moritz M A, Parisien M A, Van Dorn J and Hayhoe K 2009 Global pyrogeography: the current and future distribution of wildfire *PLoS One* **4** e5102

Kuhn-Régnier A, Voulgarakis A, Nowack P, Forkel M, Prentice I C and Harrison S P 2021 The importance of antecedent vegetation and drought conditions as global drivers of burnt area *Biogeosciences* **18** 3861–79

Lan Y, Wang J, Hu W, Kurbanov E, Cole J, Sha J, Jiao Y and Zhou J 2023 Spatial pattern prediction of forest wildfire susceptibility in Central Yunnan Province, China based on multivariate data *Nat. Hazards* **116** 565–86

Liu Y, Goodrick S and Heilman W 2014 Wildland fire emissions, carbon, and climate: wildfire–climate interactions *For. Ecol. Manage.* **317** 80–96

Luo R, Hui D, Miao N, Liang C and Wells N 2017 Global relationship of wildfire occurrence and fire intensity: a test of intermediate wildfire occurrence-intensity hypothesis *J. Geophys. Res.* **122** 1123–36

McCullagh P and Nelder J A 1989 *Generalized Linear Models* 2nd edn (Chapman and Hall)

McCune B, Grace J B and Urban D L 2002 *Analysis of Ecological Communities* (MjM Software Design, Oregon, USA)

Meijer J R, Huijbregts M A, Schotten K C and Schipper A M 2018 Global patterns of current and future road infrastructure *Environ. Res. Lett.* **13** 064006

Mesinger F *et al* 2006 North American regional reanalysis *Bull. Am. Meteorol. Soc.* **87** 343–60

Muñoz-Sabater J *et al* 2021 ERA5-Land: a state-of-the-art global reanalysis dataset for land applications *Earth Syst. Sci. Data* **13** 4349–83

Nelder J A and Wedderburn R W 1972 Generalized linear models *J. R. Stat. Soc.* A **135** 370–84

OpenStreetMap contributors 2022 © *OpenStreetMap contributors Available under the Open Database Licence from: openstreetmap.org* (OpenStreetMap Foundation) (Accessed 13 September 2022)

Parisien M A and Moritz M A 2009 Environmental controls on the distribution of wildfire at multiple spatial scales *Ecol. Monogr.* **79** 127–54

Park C Y, Takahashi K, Li F, Takakura J, Fujimori S, Hasegawa T, Ito A, Lee D K and Thiery W 2023 Impact of climate and socioeconomic changes on fire carbon emissions in the future: sustainable economic development might decrease future emissions *Glob. Environ. Change* **80** 102667

Preisler H K, Eidenshink J and Howard S 2014 Forecasting distribution of numbers of large fires *Proc. Large Wildland Fires Conf.* vol 181 p RMRS-P-73

PRISM Climate Group Oregon State University (available at: https://prism.oregonstate.edu,datacreated01/01/2019) (Accessed 08 July 2022)

Rabin S S *et al* 2017 The fire modeling intercomparison project (FireMIP), phase 1: experimental and analytical protocols with detailed model descriptions *Geosci. Model Dev.* **10** 1175–97

Ryu Y, Jiang C, Kobayashi H and Detto M 2018 MODIS-derived global land products of shortwave radiation and diffuse and total photosynthetically active radiation at 5 km resolution from 2000 *Remote Sens. Environ.* **204** 812–25

Short K C 2014 A spatial database of wildfires in the United States, 1992–2011 *Earth Syst. Sci. Data* **6** 1–27

Short K C 2021 Spatial wildfire occurrence data for the United States, 1992–2018 FPA_FOD_20210617

Smith A J, Jones M W, Abatzoglou J T, Canadell J G and Betts R A, 2020 Climate change increases the risk of wildfires: 2020 *ScienceBrief*

Stocker B D, Wang H, Smith N G, Harrison S P, Keenan T F, Sandoval D, Davis T and Prentice I C 2020 P-model v1. 0: an optimality-based light use efficiency model for simulating ecosystem gross primary production *Geosci. Model Dev.* **13** 1545–81

Tamai K 2001 Estimation model for litter moisture content ratio on forest floor. In soil-vegetation-atmosphere transfer schemes and large-scale hydrological models *Proc. an Int. Symp., Held during the Sixth IAHS Scientific Assembly* (*Maastricht, Netherlands, 18–27 July 2001*) (IAHS Press) pp 53–57

Vilar L, Nieto H and Martín M P 2010 Integration of lightning-and human-caused wildfire occurrence models *Hum. Ecol. Risk Assess.* **16** 340–64

Wang S S-C, Leung L R and Qian Y 2023 Projection of future fire emissions over the contiguous US using explainable artificial intelligence and CMIP6 models *J. Geophys. Res. Atmos.* **128** e2023JD039154

Weis J, Schallenberg C, Chase Z, Bowie A R, Wojtasiewicz B, Perron M M, Mallet M D and Strutton P G 2022 Southern Ocean phytoplankton stimulated by wildfire emissions and sustained by iron recycling *Geophys. Res. Lett.* **49** e2021GL097538

Zacharakis I and Tsihrintzis V A 2023 Environmental forest fire danger rating systems and indices around the globe: a review *Land* **12** 194

2.7 Supplementary: Modelling the daily probability of wildfire occurrence in the contiguous United States

The supplementary material contains the following figures and tables:

Table A1: An overview of all candidate predictors considered in the variable selection algorithm, their sources and how they were processed.

Figure A1: A flowchart of the variable domain clipping process referred to in figure 1.

Figure A2: Examples of the daily probability of fire occurrence maps. Here we show the mean of the Pareto superior subset of models for one day from each week in 2010.

Figure A3-A5: Examples of the modelled and observed seasonal cycle for three regions with one of three characteristic seasonal cycles. These being a spring peak; a summer peak; a bimodal cycle with spring and autumn peaks.

Figure A6: The mean rate of wildfire occurrence in the highest (2006) and lowest (2003) modelled fire years.

Table A1: An overview of all candidate predictors considered in the variable selection algorithm, their sources and how they were processed.

Variable	Code	Source	Available Time Period	Original Resolution	Processing
Dry Days	dd	PRISM *(PRISM Climate Group, 2019)*	1981-present	Daily, 4km	Derived from min., max. daily temperature and total daily precipitation. Dry day threshold 0.1mm.
Diurnal Temperature Range	DTR				
Maximum Daily Temperature	MaxT				
Minimum Daily Temperature	MinT				
Precipitation	precip				
Mean Daily Vapour Pressure Deficit	VPD	ERA5 *(Muñoz-Sabater et al., 2021)*	1950-present	Daily, 0.1°	Hourly VPD data calculated using Buck (1981). Aridity calculated annually using Priestley and Taylor (1972).
Priestley-Taylor Aridity	alpha_mean				
Minimum night-time VPD	minVPD_night				
Relative Humidity	RH				
Surface Windspeed	sfcWind				
Snow Cover Fraction	snow_cover				
Mean Daily Temperature	T				
Mean night-time VPD	VPD_night				
Soil moisture (0-7cm)	Vsoil1				
Soil moisture (7-28cm)	Vsoil2				
Soil moisture (28-100cm)	Vsoil3				

Convective Available Potential Energy	CAPE	NCEP NARR *(Mesinger et al., 2006)*	1979-present	Daily, 0.3°	Interpolated to 0.1°
Population Density	PopDens	GPWv4 *(CIESIN, 2016)*	2000-present	5 yearly, 0.0083°	Interpolated to 0.1° and daily data. Rural population density clipped at 25 persons per km^2. Threshold derived from definition of an urban cluster definition of more than 2500 persons (Ratcliffe et al., 2016) and approximate cell areas of 100km^2.
Rural Population Density	PopDens_rural				
Road Density	RoadDens	GRIP4 *(Meijer et al., 2018)*	2018	Static, 0.083°	Interpolated to 0.1°
Powerline length per area	powerline_length	OpenStreetMap *(OSM Contributors, 2022)*	Present	Static, spatial resolution not applicable	Length per unit area calculated by the total length of structure per grid cell area.
Railroad length per area	rail_length				
Walking trail length per area	trail_length				
Road length per area	road_length				
Herbaceous land-cover fraction	HERB	ESA CCI *(Defourny et al., 2019)*		Annual, 300m	Interpolated to 0.1° and daily data. Vegetation types calculated using the conversion factors
Tree land-cover fraction	TREE				
Cropland land-cover fraction	CROP				

Needleleaf land-cover fraction	NEEDLELEAF				from Forkel et al. (2017)
Shrub land-cover fraction	SHRUB				
Broadleaf land-cover fraction	BROADLEAF				
Elevation	elevation	GMTED2010 (*Danielson and Gesch, 2011*)		0.0083°	Interpolated to 0.1°
Vector Roughness Metric	VRM				
Insolation	solar_insolation	Climlab (*Rose, 2018*)			
Dry Day CAPE	dry_CAPE	Derived from other variables			
Cumulative VPD over dry spell	drying				
5-day antecedent precipitation	precip_5d	Antecedent data derived from other variables.			GPP calculated using ERA5 data, observations from Ryu et al. (2018), Jiang and Ryu (2016); Keeling et al. (2001); using the p-model method in Stocker et al. (2020).
1-year antecedent GPP	GPP_1yr				
2-year antecedent GPP	GPP_2yr				
5-year antecedent GPP	GPP_5yr				
10-year antecedent GPP	GPP_10yr				
50-day antecedent GPP	GPP_50d				
100-day antecedent GPP	GPP_100d				
150-day antecedent GPP	GPP_150d				
10-day antecedent VPD	VPD_10d				

30-day antecedent VPD	VPD_30d				
100-day antecedent VPD	VPD_100d				
1-year antecedent soil moisture	Vsoil1_365d				

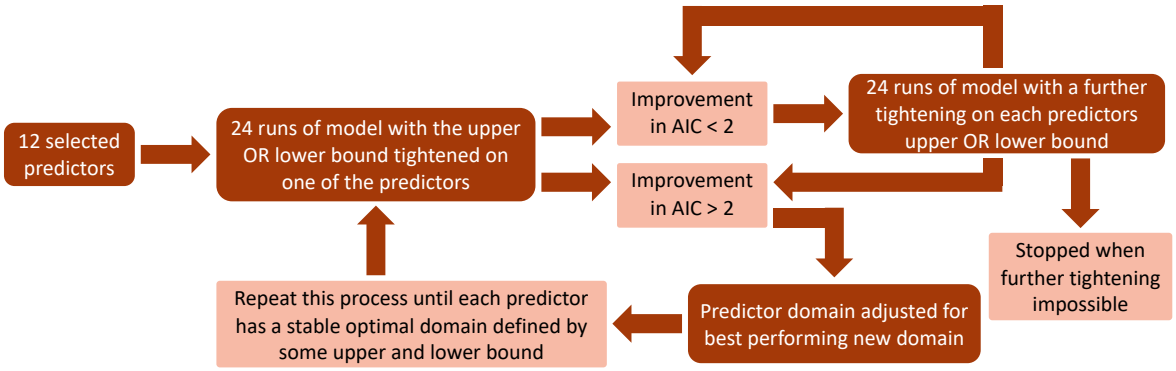

Figure A1: Flowchart of the variable domain clipping process referred to in figure 1. Tightening was done in increments of one quarter of a standard deviation between the 0.01st and 99.99th percentiles (to account for long-tailed distributions such as population density)

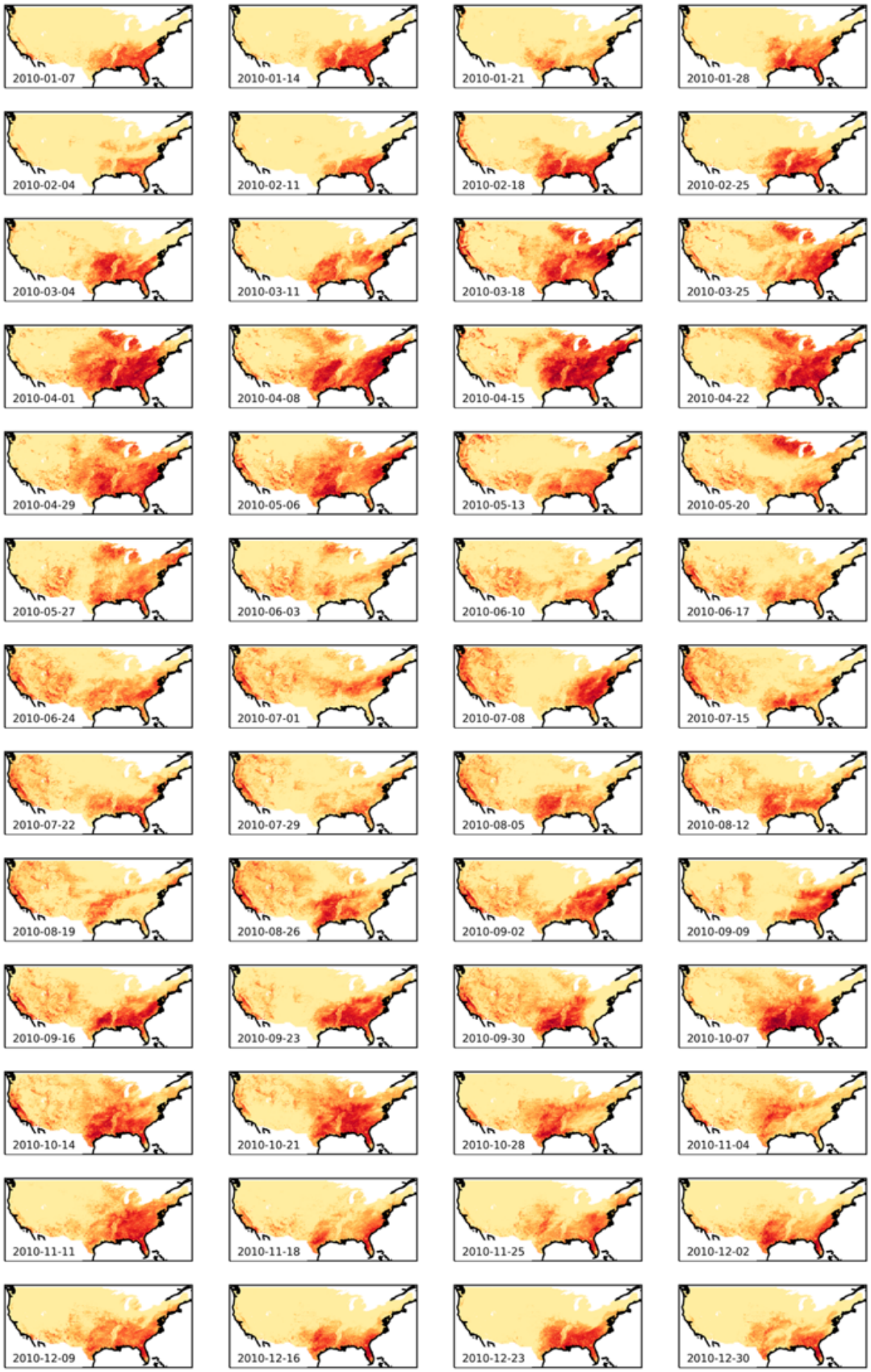

Figure A2: Examples of the daily probability of fire occurrence maps. Here we show the mean of the Pareto superior subset of models for one day from each week in 2010.

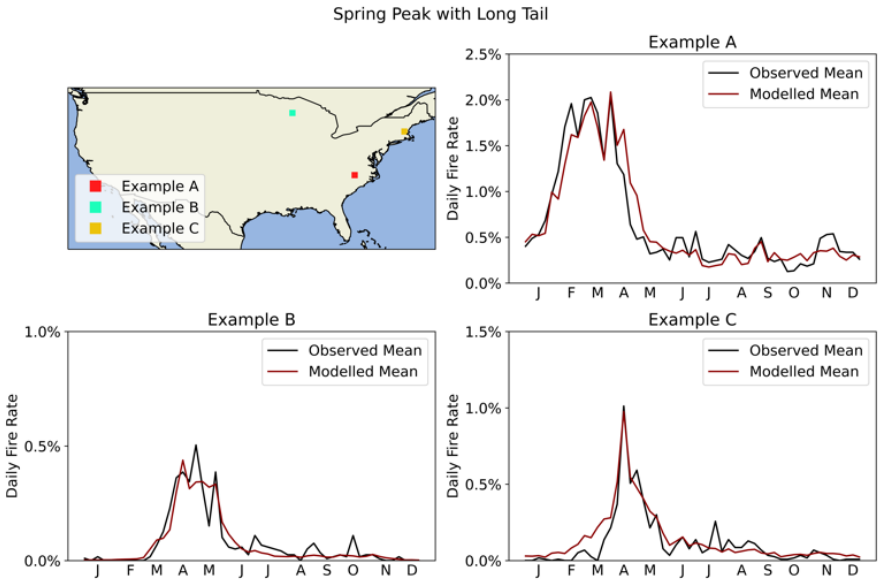

Figure A3: Examples of the modelled (red) and observed (black) mean rate of fire occurrence in a region over the study period, giving the seasonal cycle for three example regions. This figure shows regions exhibiting a characteristic spring peak in the fire season, which is primarily found in the northeast United States.

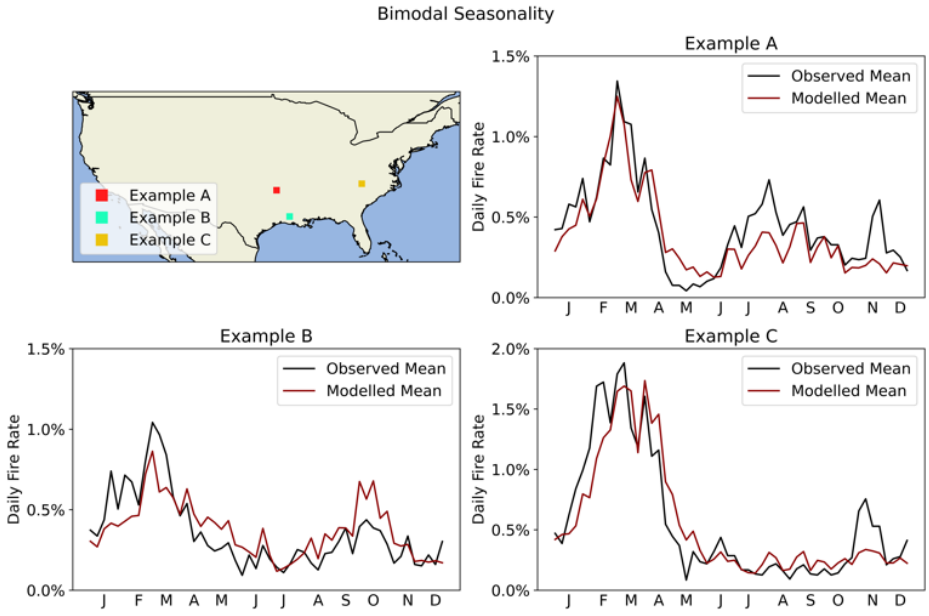

Figure A4: Examples of the modelled (red) and observed (black) mean rate of fire occurrence in a region over the study period, giving the seasonal cycle for three example regions. This figure shows regions exhibiting a bimodal seasonality with a spring and autumn peak in the fire season, which is primarily found in the southern United States.

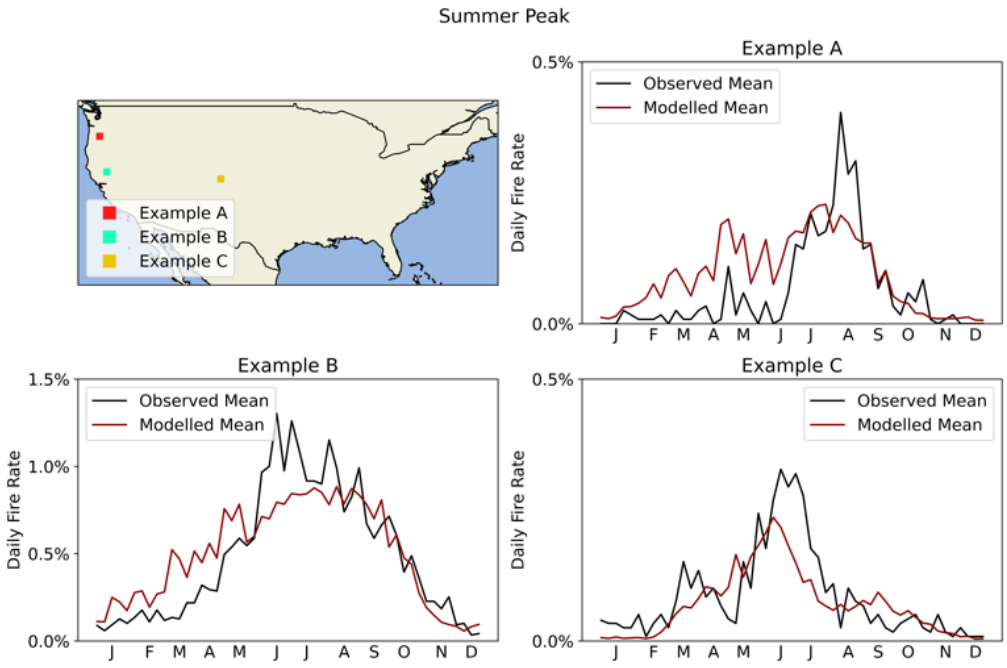

Figure A5: Examples of the modelled (red) and observed (black) mean rate of fire occurrence in a region over the study period, giving the seasonal cycle for three example regions. This figure shows regions exhibiting a summer peak in the fire season, which is primarily found in the western United States.

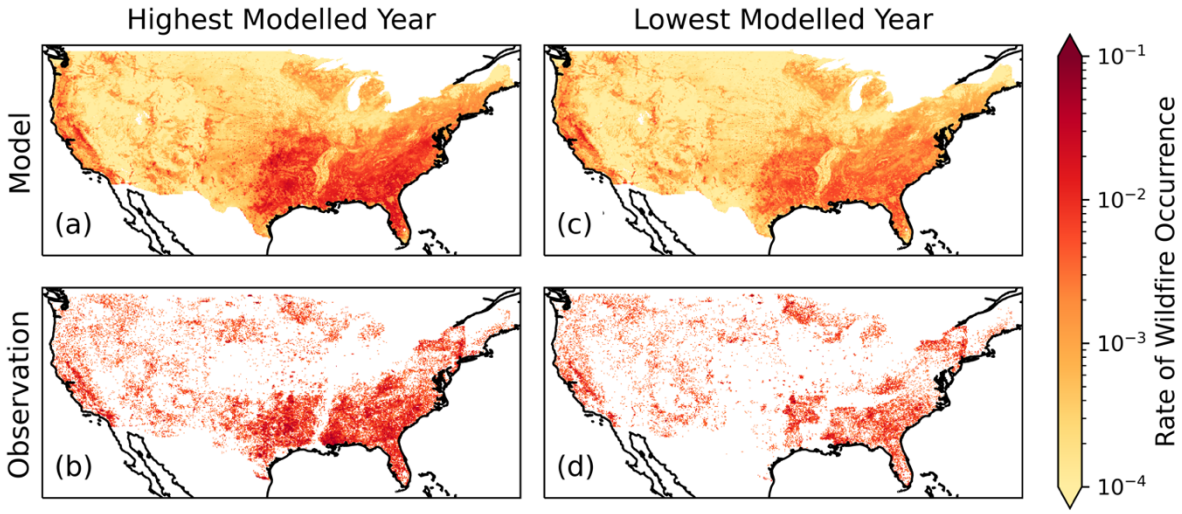

Figure A6: The mean rate of wildfire occurrence in (a, b) the highest (2006) and (c, d) lowest (2003) modelled fire years in the study period of 2002-2018

2.6.1 Supplementary and Cover Page References

Buck AL (1981) New equations for computing vapor pressure and enhancement factor. *J. Appl. Meteorol. Climatol.* 20(12), 1527-1532.

CIESIN Gridded Population of the World, Version 4 (GPWv4). Available at: http://dx.doi.org/10.7927/H4F47M2C (Accessed 14/08/2022).

Danielson JJ, Gesch DB (2011) Global multi-resolution terrain elevation data 2010 (GMTED2010).

Di Giuseppe F, McNorton J, Lombardi A, Wetterhall F (2025) Global data-driven prediction of fire activity. *Nat. Commun.* 16(1), 2918. https://doi.org/10.1038/s41467-025-58097-7

ESA Land Cover CCI project team: Defourny P (2019) ESA Land Cover Climate Change Initiative: Global Land Cover Maps, Version 2.0.7. Centre for Environmental Data Analysis, https://catalogue.ceda.ac.uk/uuid/b382ebe6679d44b8b0e68ea4ef4b701c (Accessed 15/09/2022)

Forkel M, Dorigo W, Lasslop G, Teubner I, Chuvieco E et al. (2017) A data-driven approach to identify controls on global fire activity from satellite and climate observations (SOFIA V1). *Geosci. Model Dev.* 10(12), 4443-4476. https://doi.org/10.5194/gmd-10-4443-2017

Haas O, Keeping T, Gomez-Dans J, Prentice IC, Harrison SP (2024) The global drivers of wildfire. *Front. Environ. Sci.* 12, 1438262. https://doi.org/10.3389/fenvs.2024.1438262

Jiang C, Ryu Y (2016) Multi-scale evaluation of global gross primary productivity and evapotranspiration products derived from Breathing Earth System Simulator (BESS). *Remote Sens. Environ.* 186, 528-547. https://doi.org/10.1016/j.rse.2016.08.030

Jones MW, Abatzoglou JT, Veraverbeke S, Andela N, Lasslop G, et al. (2022) Global and Regional Trends and Drivers of Fire Under Climate Change. Rev. Geophys. 60(3) e2020RG000726. https://doi.org/10.1029/2020RG000726

McNorton, J. R., Di Giuseppe, F (2024) A global fuel characteristic model and dataset for wildfire prediction. *Biogeosci*. 21:1, 279–300

Meijer JR, Huijbregts MAJ, Schotten CGJ, Schipper AM (2018) Global patterns of current and future road infrastructure. *Environ. Res. Lett.* 13, 064006. https://doi.org/10.1088/1748-9326/aabd42

Mesinger F, DiMego G, Kalnay E, Mitchell K, Shafran PC, et al. (2006) North American regional reanalysis. *Bull. Am. Meteorol. Soc.* 87(3), 343-360.

Muñoz-Sabater J, Dutra E, Agustí-Panareda A, Albergel C, Arduini G, et al. (2021) ERA5-Land: A state-of-the-art global reanalysis dataset for land applications. *Earth Syst. Sci. Data* 13(9) 4349-4383. https://doi.org/10.5194/essd-13-4349-2021

OpenStreetMap contributors. OpenStreetMap Foundation: Cambridge, UK; 2022. © OpenStreetMap contributors. Available under the Open Database Licence from: openstreetmap.org (Accessed 13/09/2022)

Poulter B, MacBean N, Hartley A, Khlystova I, Arino O, et al. (2015) Plant functional type classification for earth system models: results from the European Space Agency's Land Cover Climate Change Initiative. *Geosci. Model Dev.* 8(7), 2315-2328. https://doi.org/10.5194/gmd-8-2315-2015

Priestley CHB, Taylor RJ (1972) On the assessment of surface heat flux and evaporation using large-scale parameters. *Mon. Wea. Rev.* 100(2), 81-92.

PRISM Climate Group, Oregon State University, https://prism.oregonstate.edu, data created 01/01/2019 (Accessed 08/07/2022)

Ratcliffe M, Burd C, Holder K, Fields A (2016) Defining rural at the US Census Bureau. *Am. Commun. Surv.* 1(8), 1-8.

Rose BE (2018) CLIMLAB: a Python toolkit for interactive, process-oriented climate modeling. *J. Open Source Softw.* 3(24), 659. https://doi.org/10.21105/joss.00659

Ryu Y, Jiang C, Kobayashi H, Detto M (2018). MODIS-derived global land products of shortwave radiation and diffuse and total photosynthetically active radiation at 5 km resolution from 2000. *Remote Sens. Environ.* 204, 812-825. https://doi.org/10.1016/j.rse.2017.09.021

Stocker BD, Wang H, Smith NG, Harrison SP, Keenan TF, et al. (2020) P-model v1. 0: an optimality-based light use efficiency model for simulating ecosystem gross primary production. *Geosci. Model Dev.* 13(3), 1545-1581. https://doi.org/10.5194/gmd-13-1545-2020

Keeling CD, Piper SC, Bacastow RB, Wahlen M, Whorf TP, et al. (2001) Exchanges of atmospheric CO_2 and $^{13}CO_2$ with the terrestrial biosphere and oceans from 1978 to 2000. Scripps Institution of Oceanography, San Diego.

Present and future interannual variability in wildfire occurrence: a large ensemble application to the United States

This chapter was originally published in *Frontiers in Forests and Global Change* in April 2025. The chapter answers the question, w*hat is the interannual variability of wildfire occurrence due to climate and climate-induced vegetation variability?* The wildfire occurrence model developed in Chapter 2 is applied to a large number of modelled years in the recent climate. Meteorological inputs, and vegetation productivity controlled by CO2 levels and meteorological data, were used to drive the wildfire occurrence model. Land cover and anthropogenic variables were held constant, specifically targeting the question as to the climate variability driven contribution to wildfire occurrence interannual variability. This product allowed questions to be answered on geographic differences in fire year variability and its drivers that could not be resolved by the observational record, which is an extremely small sample of fire years by comparison. The wildfire occurrence model is also applied to a future climate, answering questions about how regional fire variability can be expected to change, and difference in magnitude of the effects of internal climate variability and future climate change on wildfire totals.

Chapter 2 identifies regional hotspots for wildfire occurrence over the contiguous US, as well as considerable interannual variability between fire years over the last two decades. Chapter 3 extends this characterisation of the wildfire occurrence hazard over the contiguous US, by characterising geographic patterns in interannual variability. This is also extended to include variability in season length and the presentation of the full distribution of regional annual wildfire counts. Chapter 2 also provides an overview of the key predictors of daily wildfire occurrences over the full study region. Chapter 3 extends this analysis of wildfire drivers by identifying the primary regional controls of the annual number of wildfires, for both the overall spread of fire year outcomes and the determinants of the most extreme years. This interannual analysis is then foundational to Chapter 4, which explores the link between the global climate mode phases and increased annual wildfire occurrences.

frontiers | Frontiers in Forests and Global Change

TYPE Original Research
PUBLISHED 16 April 2025
DOI 10.3389/ffgc.2025.1519836

OPEN ACCESS

EDITED BY
Ana Cristina Russo,
University of Lisbon, Portugal

REVIEWED BY
Rita Margarida Cardoso,
University of Lisbon, Portugal
Luciana Ghermandi,
National Scientific and Technical Research Council (CONICET), Argentina
Thomas Adam Coates,
Virginia Tech, United States

*CORRESPONDENCE
Theodore R. Keeping
✉ t.r.keeping@pgr.reading.ac.uk

RECEIVED 30 October 2024
ACCEPTED 31 March 2025
PUBLISHED 16 April 2025

CITATION
Keeping TR, Zhou B, Cai W, Shepherd TG, Prentice IC, van der Wiel K and Harrison SP (2025) Present and future interannual variability in wildfire occurrence: a large ensemble application to the United States.
Front. For. Glob. Change 8:1519836.
doi: 10.3389/ffgc.2025.1519836

Present and future interannual variability in wildfire occurrence: a large ensemble application to the United States

Theodore R. Keeping[1,2]*, Boya Zhou[3], Wenjia Cai[3], Theodore G. Shepherd[4], I. Colin Prentice[2,3], Karin van der Wiel[5] and Sandy P. Harrison[1,2]

[1]Geography and Environmental Science, University of Reading, Reading, United Kingdom, [2]Leverhulme Centre for Wildfires, Environment and Society, Imperial College London, London, United Kingdom, [3]Georgina Mace Centre for the Living Planet, Department of Life Sciences, Imperial College London, Ascot, United Kingdom, [4]Department of Meteorology, University of Reading, Reading, United Kingdom, [5]Royal Netherlands Meteorological Institute (KNMI), De Bilt, Netherlands

Realistic projections of future wildfires need to account for both the stochastic nature of climate and the randomness of individual fire events. Here we adopt a probabilistic approach to predict current and future fire probabilities using a large ensemble of 1,600 modelled years representing different stochastic realisations of the climate during a modern reference period (2000–2009) and a future characterised by an additional 2°C global warming. This allows us to characterise the distribution of fire years for the contiguous United States, including extreme years when the number of fires or the length of the fire season exceeded those seen in the short observational record. We show that spread in the distribution of fire years in the reference period is higher in areas with a high mean number of fires, but that there is variation in this relationship with regions of proportionally higher variability in the Great Plains and southwestern United States. The principal drivers of variability in simulated fire years are related either to interannual variability in fuel production or atmospheric moisture controls on fuel drying, but there are distinct geographic patterns in which each of these is the dominant control. The ensemble also shows considerable spread in fire season length, with regions such as the southwestern United States being vulnerable to very long fire seasons in extreme fire years. The mean number of fires increases with an additional 2°C warming, but the spread of the distribution increases even more across three quarters of the contiguous United States. Warming has a strong effect on the likelihood of less fire-prone regions of the northern United States to experience extreme fire years. It also has a strong amplifying effect on annual fire occurrence and fire season length in already fire-prone regions of the western United States. The area in which fuel availability is the dominant control on fire occurrence increases substantially with warming. These analyses demonstrate the importance of taking account of the stochasticity of both climate and fire in characterising wildfire regimes, and the utility of large climate ensembles for making projections of the likelihood of extreme years or extreme fire seasons under future climate change.

KEYWORDS

wildfire, wildfire risk, wildfire occurrence, climate variability, large ensembles, LES, climate impacts, interannual variability

1 Introduction

Recent wildfire events have prompted concern about future changes in wildfire regimes. Analyses of remotely sensed burned area show significant declines since 2001 in Europe, sub-Saharan Africa, southern Africa and Central Asia, but no significant trends in other regions of the world (Zubkova et al., 2023). However, there has been an overall increase in burned area as a result of wildfires in the United States between 1983 and 2022 (EPA, 2024). Other aspects of the fire regime are also changing. Extreme wildfire events have become more frequent and intense globally (Cunningham et al., 2024) and the fire season has lengthened significantly in many regions over the past four decades (Smith et al., 2020). There has been a strong response of fire regimes to warming and land-use change during past centuries (Sayedi et al., 2024). A similar response is expected with future global warming, with fire risk projected to increase over the 21st century as a result of changes in meteorological conditions (Arias et al., 2021). Fuel accumulation is also projected to increase with warming (Lu et al., 2024), and fuel moisture is projected to decrease across the plant productivity gradient (Ellis et al., 2022).

A recent UNEP report (Sullivan et al., 2022), using outputs from four climate models under the RCP2.6 and RCP6.0 scenarios, predicted a significant increase in burned area globally in the 21st century and an increasing trend in the likelihood of extreme wildfire events from 2020 to 2100. That study reflects the spread of burned area outcomes given modelled conditions - based on the distribution of possible model parameters from the training data (Kelley et al., 2019) - but does not reflect the full spread due to the chance of different realisations of weather that affect the likelihood of wildfire occurrence. This second component of the uncertainty can be addressed by using a large ensemble (LE) of climate simulations. As the drivers of wildfire likelihood (such as temperature, moisture, and vegetation productivity) vary between years in a given climate, considering a large distribution of simulated years for a given global mean temperature, or climate state, allows the full variability in potential fire years to be defined (Van der Wiel et al., 2021). Modelling this aleatoric component of the uncertainty allows us to characterise the otherwise unknown spread of the annual wildfire distribution that arises from the limited length of the recent wildfire record, and to understand the possible extremes of the modern fire regime through better resolution of the tails of the distribution.

LEs are a standard method in climate and climate impact science where ensemble runs are used to represent the distribution of possible outcomes and extremes. LEs have been widely adopted in flood modelling (Cloke and Pappenberger, 2009) and have been used to predict extremes for heavy snowfall (Sasai et al., 2019), drought (Van der Wiel et al., 2021), extreme heat (Suarez-Gutierrez et al., 2020), and fire weather (Squire et al., 2021). This approach is very applicable in the context of fire, which is sensitive to meteorological variability between years (Chuvieco et al., 2021) and to changes in vegetation properties caused by this variability. LE methods have been adopted for projection or attribution of extreme fire weather events (Touma et al., 2022; Squire et al., 2021), but have not been applied to other factors influencing fire regimes. Significant spread has been shown between General Circulation Model (GCM) predictions of wildfire in California (Dye et al., 2023; Yue et al., 2014) and the northern United States (Kerr et al., 2018). These studies represent a combination of aleatoric and systematic uncertainty, and hence cannot be interpreted probabilistically (Shepherd, 2019). It is important to understand how this uncertainty impacts projections, particularly given the rapidly moving target due to climate and land-use change.

Accounting for interannual stochasticity in modelling wildfire under present-day and future conditions is important in model products designed for the wider fire community. Fire management is often based on the extrapolation of observed incidence, meaning that the effect of future environmental change on the fire regime is viewed in terms of increasing risk relative to local operational experience. However, this approach ignores the possibility that the observed occurrence of fires does not provide a full representation of the potential fire regime - including unseen extremes. The modern observational record does not necessarily reflect the mean response to climate since it is strongly influenced by variability due to the small sample of years considered. Adopting an LE allows a characterisation of the distribution of possible events, meaning that the likelihood of extremes can be more robustly determined. Additionally, climate change can have a different effect on average versus extreme fire years. LEs allow a robust characterisation of the full distribution of fire years to define vulnerability to extremes as well as changes to the landscape's expected average susceptibility to wildfire.

Here, we apply a previously established modelling methodology for the likelihood of wildfire occurrence using an LE to assess the distribution of the expected number of fires per year for the contiguous United States. We then assess the regional drivers of fire variability and variability in the length of the fire season across North American ecological regions, or ecoregions (Commission for Environmental Cooperation (Montréal, Québec) and Secretariat, 1997). Finally, we consider how these distributions change when subject to an additional 2°C of warming, identifying regionally distinct effects of climate change on both the mean and spread of fire year outcomes.

2 Methods

We use a model that predicts the daily likelihood of fire as a function of meteorological, vegetation, and human-activity variables. We take bias-corrected meteorological variables from the Royal Netherlands Meteorological Institute Large Ensemble Time Slice (KNMI-LENTIS) ensemble for a "modern" period (2000–2009) and a hypothetical future (+2°C global warming relative to the modern ensemble). We also use these bias-corrected variables as input to a light-use efficiency model to derive gross primary production (GPP). Factors related to land cover and human activities are held constant. We then analyse the ensemble distribution of fire years under modern and future conditions, using a climate reanalysis-driven model as a baseline, focusing on how the variability between years varies spatially; extreme fire years; and variation in the length of the fire season.

2.1 Fire modelling approach

We use an existing model for the daily probability of fire occurrence at 0.1° spatial resolution for the contiguous United States (Keeping et al., 2024), trained on occurrence data from the Fire Programme Analysis fire-occurrence database (Short, 2022). The original model selects 12 variables from a suite of 47 candidate variables associated with the likelihood of wildfire occurrence,

including instantaneous and antecedent predictors of weather conditions, plant productivity, plant type, population, and landscape development. The selected variables are then used to predict the daily likelihood of a wildfire occurrence using a power-law rescaled generalized linear model. Here, a reduced set of 31 candidate predictors (Supplementary Table 1) are used because some of the original variables could not be obtained from the KNMI-LENTIS ensemble, and some were eliminated because they were not selected across 1,000 randomly sampled training datasets. The selected ensemble-derived variables were GPP, precipitation, vapour pressure deficit (VPD), snow cover, diurnal temperature range (DTR), and windspeed across a range of antecedences. Inputs derived from KNMI-LENTIS were downscaled to the resolution of the fire model since the effect of wildfire drivers varies across spatial scales (Parisien and Moritz, 2009) and the modelled relationships and the thresholds used for these relationships would therefore not necessarily be appropriate at coarser scale.

The reanalysis model based on the reduced set of variables performs as well as the original model. It shows good separability for fire occurrence, with an area under the receiver operating characteristic curve (AUC) statistic of 0.89. It also performs well spatially, with a geospatial normalised mean error (NME) of 0.46, in predicting both how concentrated the fire season is (seasonal concentration NME = 0.78) and when the peak of the fire season occurs (mean seasonal phase difference = 0.13), and in predicting interannual variability (interannual NME = 0.67). The model driven by reanalysis data provides a point of comparison for the realised likelihood of wildfire given the weather that occurred. However, as a reanalysis derived product, it cannot include the full stochasticity of the actual weather.

2.2 KNMI-LENTIS ensemble

KNMI-LENTIS (Muntjewerf et al., 2023) provides a large ensemble run of EC-Earth3 (Döscher et al., 2021) for two climate periods, 2000–2009 and +2°C warming from this "modern" period (2075–2084 under SSP2-4.5 in EC-Earth3). Each ensemble consists of 160 simulations of 10 years. These 160 ensemble members are created combining "macro" initialization and "micro" perturbations, with 16 different starting conditions created by starting the model at 25-year intervals in the pre-industrial spin-up, and running long transient (historical and SSP2-4.5) simulations. Each of these 16 runs is then subject to nine very small perturbations to the atmospheric temperature field at the start of the modern and modern + 2°C decades to produce two ensembles of 160 members each. These 160 members yield 1,600 years of data for two climates that are considered relatively stable (the 2000s and that climate subject to +2°C warming) since any climate trend will be limited in a 10-year period. Antecedent GPP over the preceding year was selected as a predictor, although none of the longer antecedent GPP predictors was found to be important in the model training. Antecedent 1-year GPP was calculated by repeating the first year of the ensemble following Van der Wiel et al. (2019).

2.3 Bias correction and generation of input data

The KNMI-LENTIS outputs were bias-corrected and downscaled by the climate imprint (CI) method (Hunter and Meentemeyer, 2005) using ERA5-Land data (Muñoz-Sabater et al., 2021) for the period 1990–2019 at 0.1° (~10 km resolution). Bias-correction of the meteorological and plant growth predictors reduces the general overestimation of GPP and the under/over-estimation of windspeed and snow cover in some regions (Supplementary Figure 6) which, because of the threshold relationships inherent in the fire probability model, would result in the prediction of unrealistically high likelihoods of fire occurrence (Supplementary Figure 7).

Although KNMI-LENTIS and ERA5-Land are both ECMWF products, the core atmospheric modules are different (IFS Cy36r4 and Cy45r1 respectively), IFS Cy45r1 performs better then IFS Cy36r4 (ECMWF, 2025), and ERA5-Land also uses observational data assimilation. Thus, the modelling schemes and implementation are sufficiently different for ERA5-Land to be considered as an independent source for bias-correction and downscaling of EC-Earth3. Whilst reanalysis products are an imperfect representation of reality and can be subject to bias, assessments of ERA5-Land show that it performs better than other products in reproducing extratropical northern hemisphere land temperatures (Muñoz-Sabater et al., 2021), United States temperature extremes (Ibebuchi et al., 2024), precipitation in the northeastern United States (Crossett et al., 2020) and extratropical precipitation patterns more generally (Lavers et al., 2022). The representation of precipitation extremes is not as good (Lavers et al., 2022) but this is not important since the wildfire model is not sensitive to precipitation exceeding 13 mm/day (Keeping et al., 2024).

The reanalysis data were averaged by the day-of-year and smoothed by a 31-day centred window, thus preserving the seasonality but eliminating error introduced by limited sampling of stochastically varying years (on leap-years, day 366 was grouped with day 365 for this reason). Modern ensemble data was converted into single delta values relative to the ensemble day-of-year mean. Zero-bounded variables, such as precipitation, were treated multiplicatively whilst non-bounded variables, such as temperature, were treated additively. This delta version of the ensemble was then bilinearly downscaled and applied to the day-of-year averaged and smoothed reanalysis data. The bias correction was applied to all variables separately. The same procedure was followed for the +2°C ensemble data, but the difference was between the future ensemble data and the modern ensemble day-of-year mean. As some ensemble variables have a 3-h resolution, times of day were bias-corrected separately to respect potentially different distributions in different parts of the diurnal cycle.

The 0.1°, 3-hourly or daily bias corrected data were used to generate climate predictors for the fire model. Diurnal temperature range was derived from the difference between the daily minimum and maximum temperature. Daily and 5-daily precipitation were derived from daily precipitation data. Windspeed was derived from the daytime mean of 3-hourly windspeed data, which in turn had been calculated from westerly and northerly components prior to the bias correction. Snow cover was derived from daily data. Vapour pressure deficit was calculated according to the Buck formula (Buck, 1981) from 3-hourly temperature and dewpoint data, which was then used to derive the daytime mean value.

The top four moments (mean, variance, skewness and kurtosis) were calculated for the reanalysis and bias-corrected ensemble data aggregated by time of day; month; and 2π the ensemble resolution. The mean and variance showed good agreement for all the bias-corrected variables except windspeed (Supplementary Table 2a). A

single-value variance rescaling was thus applied to further correct windspeed (Supplementary Table 2b).

2.4 The GPP model

Predictions of GPP were made using a light-use efficiency model (the P model) that combines the Farquhar-von Caemmerer-Berry photosynthesis model for instantaneous biochemical processes with two eco-evolutionary hypotheses to account for the spatial and temporal acclimation of carboxylation and stomatal conductance to environmental variations at weekly to monthly time scales (Wang et al., 2017; Stocker et al., 2020). The model uses an empirical function to take account of the effect of soil moisture stress on photosynthesis, as defined in Stocker et al. (2020). The inputs to the P model are air temperature (°C), VPD (Pa), air pressure (Pa), incident photosynthetic photon flux density (PPFD, μmol m^{-2} s^{-1}), the fraction of absorbed photosynthetically active radiation (fAPAR), and ambient CO_2 concentration. The meteorological inputs to drive the P model were the bias-corrected and downscaled variables from the KNMI-LENTIS ensemble, with the +2°C scenario using CO_2 concentrations corresponding to the SSP2-4.5 scenario for 2075–2084. fAPAR was derived from a prognostic model of the seasonal cycle of the leaf area index (LAI) (Zhou et al., 2025), since fAPAR can be derived from LAI using Beer's law. This model derived the steady-state LAI timeseries from the GPP time course based on a general linear relationship between "steady-state" LAI, the LAI when environmental conditions remain unchanging, and GPP. The actual estimated LAI is then calculated as the time-lagged average of the steady-state LAI. A seasonal maximum fAPAR model was embedded in this model to limit seasonal LAI predictions (Zhu et al., 2023; Cai et al., 2025).

2.5 Ecoregions

To conduct regional analyses of wildfire patterns, we aggregated data using the Level I Ecological Regions of North America (Commission for Environmental Cooperation (Montréal, Québec) and Secretariat, 1997). Two ecoregions that occupy relatively small areas in the contiguous United States were merged with a closely related ecoregion, following Balik et al. (2024). Specifically Tropical Wet Forests (in southern Florida) were merged with Eastern Temperate Forests, and Southern Semi-arid Highlands (in southeastern Arizona) were merged with Temperate Sierras. The eight ecoregions used here are: Eastern Temperate Forests; Great Plains; Marine West Coast Forest; Mediterranean California; North American Deserts; Northern Forests; Northwestern Forested Mountains; and Temperate Sierras (Supplementary Figure 1a). When describing more specific geographical regions, we followed the naming convention of the United States Census Bureau (Supplementary Figure 1b).

2.6 Fire year metrics

The ensemble-driven fire model is compared to the reanalysis-driven fire model rather than to the observations to provide a like-for-like comparison of the contemporary probability of wildfire, because of the stochasticity of the realised wildfire record. The fire occurrence model is daily, accounting for the daily extremes that drive the annual likelihood of fire, but the analysis here is annual to focus on variability between fire seasons and not on daily scale variability in weather. The spread of the ensemble is defined as the 1st to 99th percentile of the ensemble fire years by grid cell since this is more robust than the maximum and minimum of the distribution (Supplementary Figure 2). A leave-one-out (LOO) approach was used to identify the predictor that contributes most to interannual variability in fire occurrence. A version of the ensemble was generated for each of the eight climate predictors by taking the average for each day of the year across the full ensemble to eliminate interannual variability of that predictor. This approach preserves seasonality but means that all years are identical for that predictor across ensemble members. The mean absolute difference between the original and LOO annual number of fires was used to measure the contribution of that predictor to variability. The length of the fire season was defined as the number of days exceeding a threshold of 50% of the average of the week with the most fires at each location in the reanalysis model. We also compared the reanalysis maximum fire years (from the 1990s, 2000s and 2010s) to the 160 ensemble decades by ecoregion to determine whether the observed decadal maximum falls in the distribution of possible decadal maxima for a similar environment. This also allows us to examine if there was a trend in the reanalysis period that could affect the comparison with the ensemble model.

3 Results

3.1 Modern day fire regimes

The spatial pattern of number of fires in the reanalysis-based model is broadly consistent with the observational record (Short, 2022), although as expected the observed map is less smooth (Figure 1). Despite the good overall agreement with observations, there are some differences - for example the greater extent of wildfires in northern parts of the Mountain West and East North Central, and the sharper boundaries of regions where wildfire does not occur in heavily farmed regions of the East North Central (the Corn Belt) and East South Central (the Mississippi Valley). The model is a reliable predictor for the probability of wildfire occurrence, and the reanalysis-based model mean shows good agreement ($R^2 = 0.96$) with the KNMI-LENTIS modern ensemble mean, indicating that the bias-corrected ensemble data is also reliable. Without bias-correction and downscaling, the fire model shows the correct geographic patterns but seriously overestimates the probability of fire in high-likelihood regions (Supplementary Figure 7).

The absolute spread of the 1,600-year ensemble for the expected annual number of fires (Figure 1d) is largest in regions with a high mean number of fires. The regions most susceptible to wildfire occurrence over a long period also show the highest absolute spread in fire occurrence on a year-to-year basis, with extreme years contributing substantially to the higher-than-average rate of wildfire. As the mean and spread of the ensemble distribution are strongly associated spatially, the ratio between them (the relative spread) indicates where the skewed fire year distribution (Supplementary Figure 2) is longer tailed, and where there is a different response in the spread and mean of the distribution to warming. The relative spread (Figure 1e) is highest in the Great Plains,

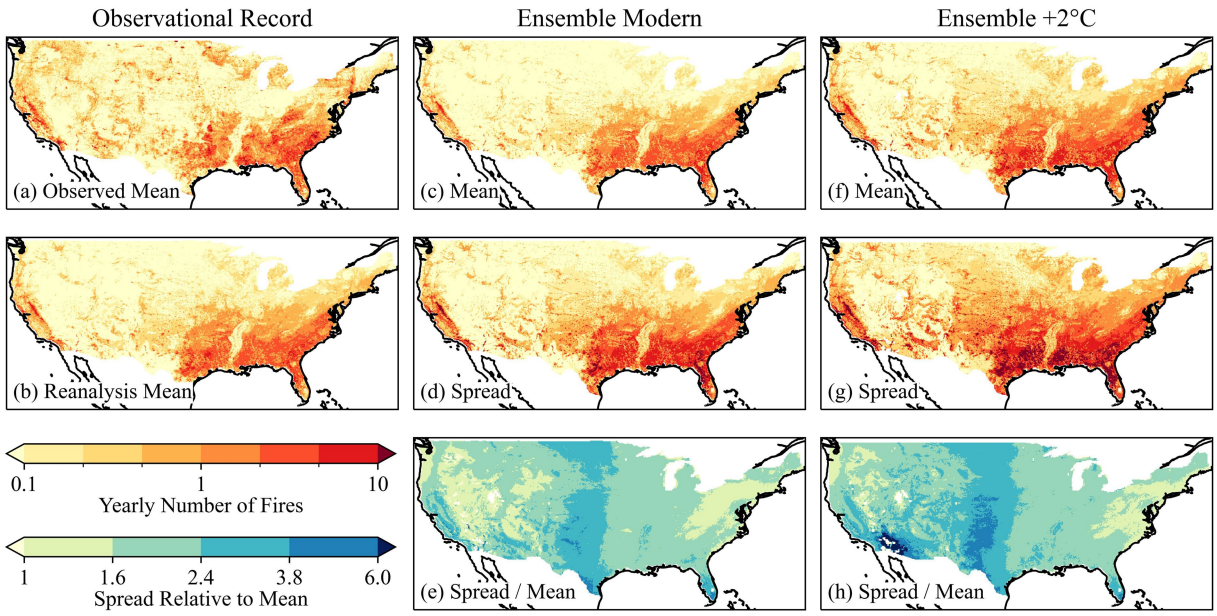

FIGURE 1
Modelled and observed patterns in the annual number of wildfires greater than 0.1 hectares, with both the mean and 1st-99th percentile spread shown. The plots show **(a)** the observed annual mean of the wildfire occurrence record for 1992–2020; **(b)** the modelled reanalysis mean for 1990–2019; **(c)** the modelled ensemble mean for the modern (2000–2009 climate); **(d)** the modelled ensemble spread for the modern; **(e)** the ratio of model spread and mean for the ensemble modern; **(f)** the +2°C ensemble mean (2000–2009 climate plus 2°C of warming); **(g)** the +2°C ensemble spread; and **(h)** the ratio of model spread and mean for the +2°C ensemble.

the Warm Deserts, the coast and hills of Mediterranean California, and southern Florida. In contrast, a large region of the eastern United States has a high mean number of expected fire events but low relative spread. The relative spread identifies regions where previously unseen extremes could be substantially above the recent mean, with Mediterranean California and the southern Great Plains being characterised by particularly high mean annual fires and relative spread.

The model predictors can be categorised into static variables (rural population density, shrubland cover, needleleaf cover, cropland cover) and dynamic variables that vary with time, including meteorological (mean daytime VPD, DTR, mean daytime windspeed, snow cover, precipitation in the prior 5-days, and daily precipitation) and vegetation (GPP in the prior year and GPP in the prior 50-days) variables. The four most influential variables in the model (Supplementary Table 1) were annual GPP, VPD, rural population density and 50-day GPP, respectively.

Comparison of the original fire year ensemble and the ensemble with the interannual variability of individual variables fixed showed that the primary driver of interannual fire variability reflects two sets of controls: atmospheric drying (VPD, DTR) and fuel availability (GPP) (Figures 2a, 3a). Fuel availability is the most important control on interannual variability in the eastern Great Plains, Eastern Temperate Forests, Mediterranean California, Temperate Sierras, and the southern North American Deserts. Atmospheric drying is most important in the lower fire-occurrence areas of the Mountain West and northern Pacific West. VPD and annual GPP control fire year variability across most of the United States, but DTR is more important in the Marine West Coast Forest, the northeastern Northern Forest, and a small area west of the Great Lakes. These three regions have the lowest interannual variability in VPD, whilst DTR variability is more homogeneous in the surrounding areas. GPP in the prior 50 days is also an important control in much of the Northwestern Forested Mountains. Interannual variability in VPD is the most important control of variability in severe fire years, as indexed by the top 1% of fire years (Figure 2c), except in the southwestern United States (Figure 3c) where fuel availability is the main control.

The mean fire season length is < 30 days over much of the United States (reanalysis-model, Supplementary Figure 4a; modern ensemble, Figure 4a), except for the southwestern North American Deserts where the season can be up to 4 months long. There is considerable variation in the extremes of the distribution in fire season length (Figure 4c) and this can be significantly higher than the maximum registered in the 30-year reanalysis period (Supplementary Figure 4b). The East South Central and southern South Atlantic regions can experience long fire seasons of up to 120 days. However, most of the region with long fire seasons in severe years – often multiple times longer than the mean fire season – lies west of the 100th meridian: the Warm Deserts and southern Mediterranean California see increases from 10–120 to 120–240 days in extreme years. Although these regions are characterised by a long fire season, they are also the most exposed to unseen extremes.

There are large differences in the spread of the distribution of the decadal maximum fire year across the 160 ensemble-based simulations (Figure 5), with Mediterranean California, the Temperate Sierras, and the Great Plains showing the largest spread and Marine West Coast Forest, Northwestern Forested Mountains, Northern Forests, and Eastern Temperate Forests showing a relatively confined distribution. The distribution of the decadal maximum fire year in the simulations is congruent with the maximum for each decade in the

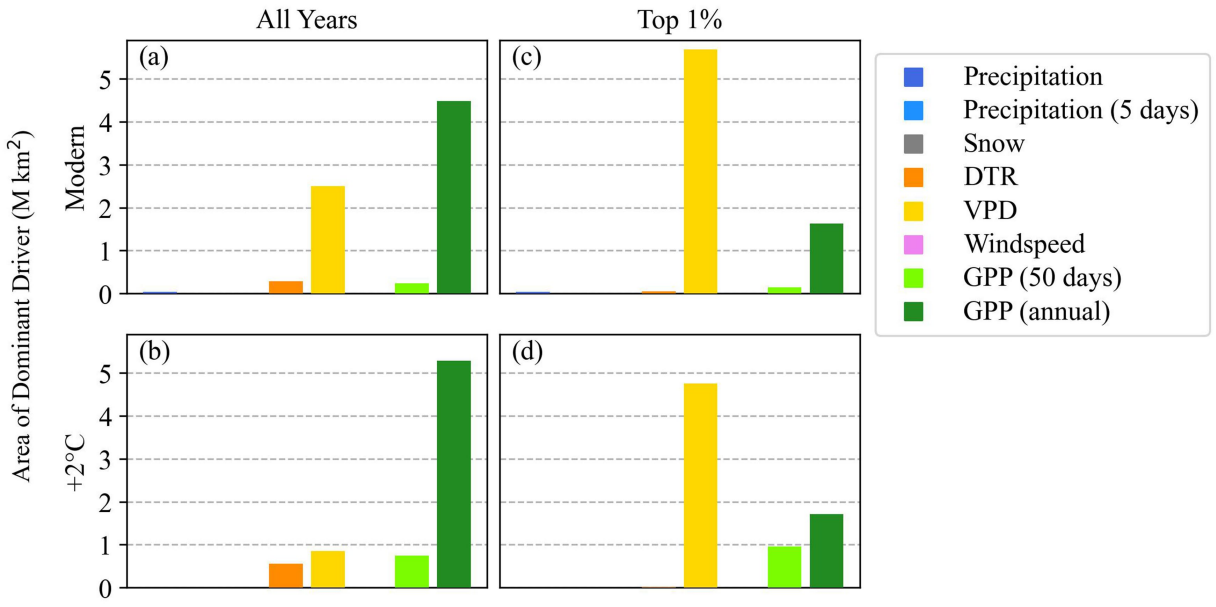

FIGURE 2
Relative importance (as measured by the area where the variable is the dominant effect) of different drivers for the variability in the modelled number of wildfires per year as shown by the leave-one-out analysis. The top plots show the drivers in the modern (2000–2009) ensemble for **(a)** all fires and **(c)** the top 1% of fire years. The bottom plots show the drivers in the +2°C ensemble, for **(b)** all fires and **(d)** the top 1% of fire years. DTR is the diurnal temperature range, VPD is vapour pressure deficit, GPP is gross primary production.

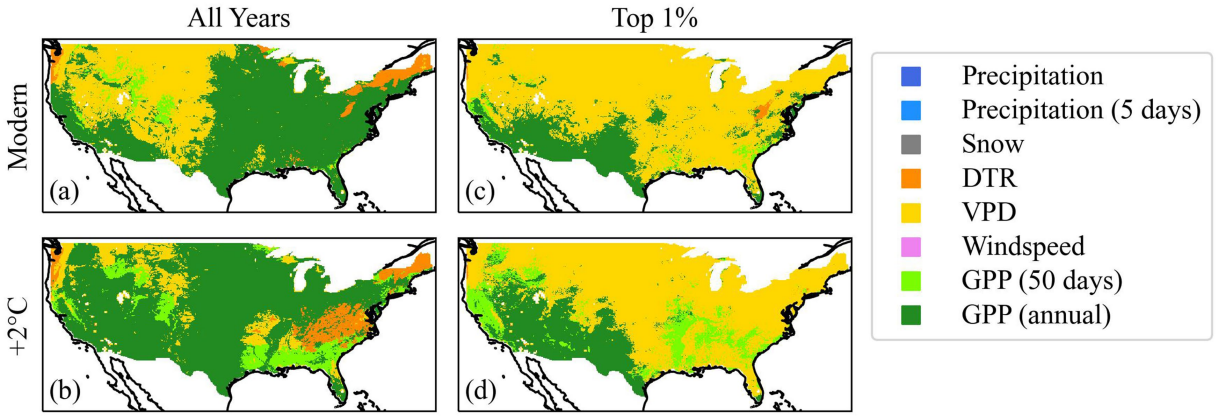

FIGURE 3
Maps showing the areas where each variable is the dominant driver of interannual variability between fire years. The top plots show the drivers in the modern (2000–2009) ensemble for **(a)** all fires and **(c)** the top 1% of fire years. The bottom plots show the drivers in the +2°C ensemble, for **(b)** all fires and **(d)** the top 1% of fire years. DTR is the diurnal temperature range, VPD is vapour pressure deficit, GPP is gross primary production.

reanalysis-based model for some ecoregions (Figure 5), most notably in the Great Plains and the Eastern Temperate Forests. However, the tail of the simulated decadal maximum fire year in Mediterranean California, the North American Deserts, and the Temperate Sierras greatly exceeds the maximum in the reanalysis-based model. There is only one region, Northern Forests, where the maximum in the reanalysis-based model lies outside the ensemble-based distribution. The extremes from each of the three reanalysis decades differ (Figure 5), reflecting the observed warming trend since the 1990's. This highlights the unreliability of estimating extremes from the reanalysis model rather than the ensemble-based model.

3.2 Future fire

There is an increase in both the mean and spread of total annual wildfires across all regions of the United States in the +2°C ensemble-based simulations (Figure 1, Supplementary Figure 5). The mean annual number of fires is more than double in the Midwest and Northeast. However, the greatest changes are in the West (Supplementary Figure 5) and most pronounced in the higher fuel-load environments of the Northwestern Forested Mountains. The increase in the spread is generally greater than the increase to the mean (Figure 1h): 78% of the contiguous United States shows an

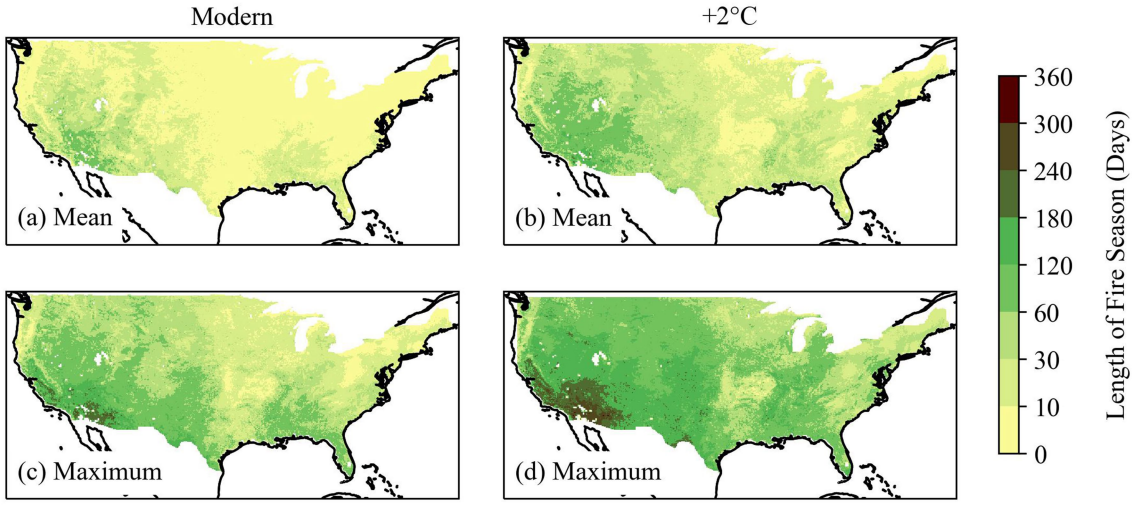

FIGURE 4
Maps of fire season length. The mean for **(a)** the modern ensemble and **(b)** + 2°C ensemble, and the resolvable maximum (99th percentile) for **(c)** the modern ensemble and **(d)** + 2°C ensemble number of days exceeding a threshold of 50% of the average of the modern ensemble week with the most fires at each location. This number of locally relatively fire-prone days is considered as the effective fire season length.

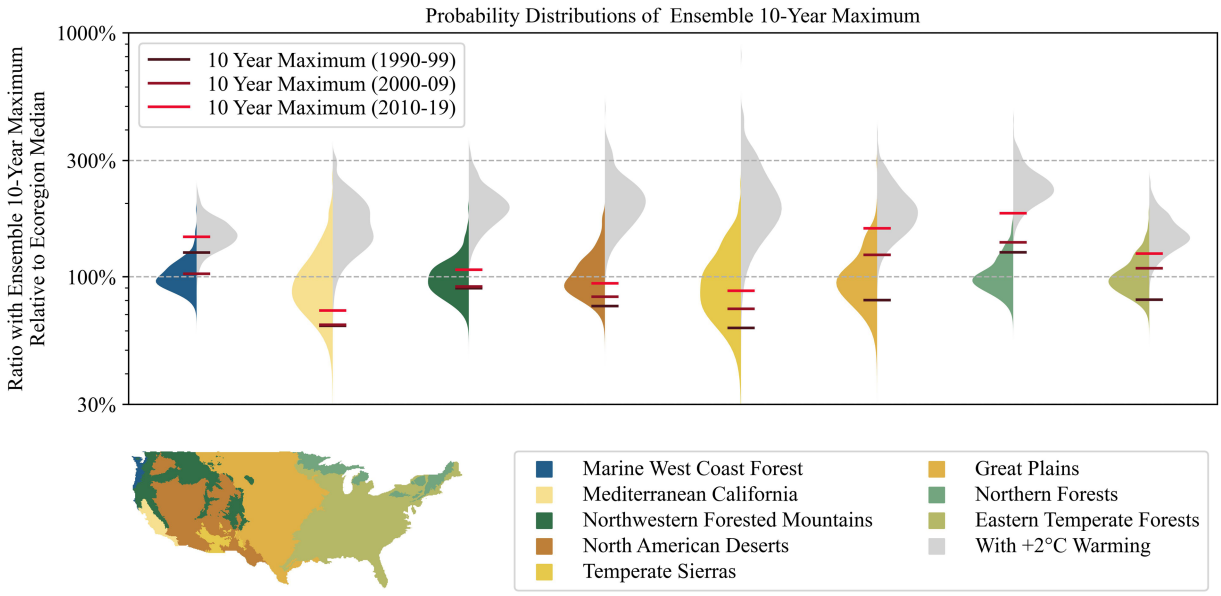

FIGURE 5
Coloured histograms show the distribution of the maximum number of fires in a year per ensemble member (i.e., one simulated decade) in different ecoregions; the grey histograms show the distribution of the 10-year maximum in the same ecoregion after an additional +2°C warming. The maximum number of fires per decade in the reanalysis-based model are shown by horizontal lines. The map shows the area covered by each ecoregion.

increase in spread greater than that of the mean in the +2°C ensemble, and the spread increases by > 1.2 times the mean over 34% of the region (Supplementary Figure 3). Fire years are consistently most variable relative to the mean annual number of fires in the Great Plains, Warm Deserts, and Mediterranean California. There is also a marked increase in relative spread in the southern Great Plains and Warm Deserts. The southeastern United States has the most limited increase in both mean annual number of fires and interannual spread.

GPP and atmospheric drying (VPD and DTR) are the most important drivers of interannual variability in the +2°C ensemble-based simulations (Figure 2). However, GPP is the predominant control on fire year variability over 71% of the contiguous United States in the +2°C ensemble compared to 60% in the modern ensemble. Much of the expansion of the region where GPP is the primary control is in the West. In the +2°C ensemble scenario, the modelled average annual GPP increases across the contiguous United States, with a mean increase of 41% compared to a 49% increase in the average CO_2

concentration, and with 99% of the contiguous United States showing an increase in GPP relative to the modern ensemble. The +2°C scenario also shows a GPP response of greater variance between years relative to the modern ensemble scenario across 99% of the contiguous United States, with 66% of the area of the contiguous United States showing an increase in the variability relative to the mean as shown by coefficients of variation of the modern and +2°C ensembles. Variables related to atmospheric drying become more important in the southeastern United States, where interannual variability is almost entirely controlled by GPP in the modern ensemble (Figure 3). DTR emerges as a more significant effect than in the modern ensemble. The area where it is the most important factor doubles. The region where VPD is the primary control decreases to one third of its extent in the modern ensemble. GPP over the prior 50 days becomes a more important driver of interannual variability than annual GPP in much of the South. GPP in the prior 50 days also replaces VPD as the dominant driver for the top 1% of fire years in parts of the same region – indicating an increase in the importance of low-productivity intervals (for example drought) for driving interannual variability.

The length of the fire season is increased in the 2°C ensemble compared to the modern ensemble (Figure 4), with increases to the mean fire season in the West and East South Central regions. There are regions of the southwestern North American Deserts and southern Mediterranean California where the top percentile of the distribution of fire season length is > 300 days. More northerly regions, such as the Northwestern Forested Mountains, are projected to experience fire seasons that would be normally associated with more southerly fire regimes. All ecoregions show a strong increase in the distribution of decadal extreme fire years (Figure 5). The Northern Forests ecoregion shows the greatest change: there is virtually no overlap between the 2000–2009 and the +2°C extreme distributions. A similar but less extreme difference occurs in the Northwestern Forested Mountains.

4 Discussion

The interannual spread of number of fires is greater than the mean expected number in the modern ensemble, meaning that the annual wildfire occurrence distribution can be described as highly variable and sensitive to interannual climate variability. Areas with a higher mean expected number of fires are likely to have a correspondingly higher spread in the distribution of annual number of fires, however there are geospatially distinct patterns in the spread of the distribution relative to the mean. There is an apparent effect of warming on the most extreme fire year per decade (across all eight ecoregions) over the past 30 years. The distribution of modelled decadal maxima in the modern climate consistently exceeds the reanalysis decadal maxima in all ecoregions. Drier ecoregions show higher spread between decadal maxima relative to the median decadal maximum of the ensemble. This effect could arise from the widespread variability in aggregated fire risk that can occur due to widespread drought affecting a large portion of an ecoregion, an established amplifier of wildfire risk in the West (Richardson et al., 2022). Whilst wildfire occurrence is high in the South and in highly populated areas, the southern West and southern Great Plains are the regions where relatively extreme years and extreme fire seasons are most likely under both the modern ensemble and +2°C ensemble scenarios.

The interannual variability in fire is largely controlled by the interannual variability in daily VPD or annual GPP, which correspond to variability in fuel moisture content and fuel availability, respectively. In the modern ensemble, fuel availability is consistently the most important driver in the southwestern United States, even for the top 1% of fire years which are primarily controlled by VPD in other regions. The response of GPP to climate change in the future scenario shows that the generally positive effects of CO_2 on average outweigh the negative effect of increasing incidence of soil moisture stress on net primary production. This is consistent with the findings of Cai and Prentice (2020) that in the United States the predominant controls on GPP are plant cover (fAPAR) and CO_2, as well as matching recent (Jeong et al., 2024) and projected (Knauer et al., 2023) trends in GPP. GPP becomes more variable in the +2°C ensemble scenario, even relative to the increase in the mean. The overall effect of this is to increase fuel production, increasing fire likelihood given equivalent weather conditions, and to increase the variability in fuel production between years, enhancing the impact of GPP variability in driving variability between fire years. This is seen in the increasing area of the West in the +2°C ensemble scenario for which GPP is the primary control of interannual wildfire variability – consistent with the findings of Abatzoglou et al. (2021) that the fires in the western United States are increasingly constrained by increasing fuel availability with near-term future warming, despite increases in fire likelihood. Fuel limitation is also characteristic of the Great Plains, where annual GPP is the dominant control of interannual variability in fire occurrence in both the modern and the +2°C ensembles. The herbaceous fuels in this region have a shorter lifespan and are more sensitive to aridity (McGranahan and Wonkka, 2024), meaning that years of low productivity associated with lower moisture strongly reduce fire likelihood (Guyette et al., 2015; Knapp, 1998). VPD is a well-established control on the daily likelihood of wildfire (Mueller et al., 2020) but even in fuel-availability controlled regions, the top 1% of fire years in both the modern ensemble and +2°C scenarios are often controlled by VPD. Even though annual GPP is the chief control of interannual variability, the interannual variation in VPD controls whether an extreme fire year occurs, consistent with its influence on extreme burned area in the West (Williams et al., 2019).

We identified DTR as the primary driver of interannual variability in the Northeast in the modern ensemble and in the Northeast and Appalachia (the mountainous inland region that extends parallel to the coast down from the Northeast) in the +2°C ensemble. Seager et al. (2015) showed there is strong interannual variability in summer VPD in all of the United States except for Florida and the Northeast, and that VPD does not exert a strong effect on soil dryness in the Northeast and Appalachia. Physically, DTR and mean daily VPD are strongly linked, with VPD having an exponential response to temperature (through saturation vapour pressure, SVP) modulated by relative humidity; VPD = SVP (1 – RH/100). The exponential response of SVP to temperature means that, physically, DTR corresponds to the daytime increase in SVP whilst VPD corresponds directly to the rate of vegetation drying by diffusive evaporation, separate from thermal or photomolecular vaporisation (Tu et al., 2023). Thus, one explanation for the emergence of DTR as a more important contributor to interannual wildfire variability in regions where VPD is less variable could be related to increased atmospheric

instability and increased cloud-free days, which result in greater night-time cooling and daytime warming: both of which are associated with elevated wildfire risk (Haines, 1988; Williams et al., 2018). Increases in the expected area per year of the Northern Hemisphere affected by atmospheric blocking (Nabizadeh et al., 2019) could also contribute to this. Atmospheric blocking is associated with long-term cloud-free conditions (Lupo, 2021), which are in turn associated with periods of higher-than-average DTR (Dai et al., 2001), so an increase in blocking events with climate change could explain greater interannual variation in DTR. The fact that DTR becomes a more widespread control after warming shows that despite VPD being an effective predictor of wildfire risk (Sedano and Randerson, 2014) and widely used in empirical fire models (Haas et al., 2024), other metrics for atmospheric drying are more appropriate regionally.

Cumulated GPP over the 50 prior days is the primary control in the more fire-prone regions of the Northwest Forested Mountains, and it is also important over much of the South in the +2°C ensemble. Extreme fires have been linked to short-term acute drought in the South (Barbero et al., 2014), which may explain why variability in short-term vegetation productivity influences fire year variability in such relatively high productivity regions. The increase in importance of this control in the +2°C ensemble, particularly in the top 1% of fire years for occurrences, may reflect the increasing vulnerability to severe drought in some regions with warmer climates.

It was necessary to ensure that the ensemble climate data was directly comparable to the reanalysis data in order to compare the ensemble and reanalysis wildfire models. We bias-corrected and downscaled the climate ensembles to map the climate ensemble onto the local reanalysis distribution using a relatively simple approach. The analyses show that this reduces but does not eliminate bias in the ensemble. The CI downscaling method used in this study can result in some distortion of the spatial covariance of climate variables, but preserves the temporal dynamics and representation of extremes (Maraun, 2013; Hnilica et al., 2017; Sobie and Murdock, 2017). More complex methods of bias correction (e.g., quantile mapping, Grillakis et al., 2017; or multivariate techniques, François et al., 2020) can produce a more precise correspondence but they impose a greater change on the climate-model distribution. The method used here is intended to be more robust by not making extreme – and thus more likely unphysical – alterations to the underlying distribution of the original climate ensemble (see Karger et al., 2023; Tefera et al., 2024; Mosier et al., 2014).

The moments of the ensemble GPP distribution correlate less well to the reanalysis than for other bias-corrected variables (Supplementary Tables 2a,b), and this may help to explain why the reanalysis decadal maxima is consistently lower than the median in more arid ecosystems such as Mediterranean California, the North American Deserts, and the Temperate Sierras. This effect could be because GPP variability is not well reflected in the ensemble, possibly because the simulated fAPAR is based on an optimal response to environmental conditions during a given year and does not take account of prior disturbances or multi-annual changes in soil moisture. Therefore, whilst the ensemble GPP serves as a best estimate for an undisturbed vegetation regime, environments identified as primarily driven by variability in dryness-related predictors would naturally still be controlled by vegetation abundance or productivity in the case of high levels of disturbance, such as deforestation or prior wildfires.

The stochastic realisation of individual fire year conditions drives differences in potential outcomes from an impacts and management perspective. LE approaches have been adopted by the climate impacts community (e.g., Cloke and Pappenberger, 2009; Bevacqua et al., 2023; Van der Wiel et al., 2020), and bring benefits for wildfire modelling, both in gauging the likelihood of fire extremes and in contextualising the observational record. However, there are two difficulties that may limit the use of LEs for wildfire. Firstly, wildfire is influenced by vegetation properties and human-activities more than many other climate-related hazards. The impact of human activities in particular is difficult to simulate reliably. Secondly, as in the case of the renewable energy community (Craig et al., 2022), there is often a need in wildfire studies to look at spatial resolutions finer than available from accessible climate datasets. Despite these difficulties, there are clear benefits to employing LE methods in wildfire modelling – allowing for the better estimation of resource demand in possible extreme years, and characterisation of the interannual variability inherent to a fire regime.

From a fire management perspective, the LE provides information about potential extremes that are not captured in the relatively short observational record and which might therefore pose a challenge for existing wildfire management resources. The approach can be employed to define regions susceptible to very long fire seasons, of use for planning suppression capacity in extreme years. In the southwestern United States, for example, the existing trend of a lengthening fire-season (Jain et al., 2017) continues with future warming. LEs can also be used to understand emerging issues in vulnerability and exposure to wildfire. The proneness of the southern West and southern Great Plains to extreme fire years corresponds to areas of shrubland and grassland, where the development of the wildland urban interface has been greatest (Radeloff et al., 2023). Given the increasing concern about the increasing costs of changing fire regimes in the United States and the likelihood that these will continue to worsen in coming years (Lee et al., 2015; Melvin et al., 2017; Schoennagel et al., 2017; Murphy et al., 2018; Iglesias et al., 2022), the LE approach provides a more robust management framework for assessing fire occurrence and extremes than currently available.

5 Conclusion

The application of an LE approach to wildfire occurrence modelling provides a more robust characterisation of fire regime properties than provided by the observational record. This makes it possible to estimate the likelihood of extreme fire years – as seen both in the probability of fire occurrence and the length of the fire season. Climate warming extends the area that experiences wildfires. More importantly, climate warming affects the average probability of fire occurrence in fire-prone regions and can cause even larger shifts in extremes in some regions. Interannual variability in fire occurrence is largely controlled by factors affecting fuel availability or fuel drying. The relative importance of these controls varies between regions in the present-day climate. However, fuel availability becomes an even more important control on fire probability under climate warming. Application of an LE approach provides a useful tool for characterising fire regimes and how they might change in the future, and thus a

stronger basis for designing mitigation and adaptation management strategies.

Data availability statement

The source datasets used this study can be found in the KNMI-LENTIS repository https://doi.org/10.5281/zenodo.7573137. The datasets generated, and code used to generate and analyse new data for this study can be found in the repository https://doi.org/10.5281/zenodo.15040670.

Author contributions

TK: Conceptualization, Data curation, Formal analysis, Investigation, Methodology, Writing – original draft, Writing – review & editing. BZ: Methodology, Resources, Writing – review & editing. WC: Methodology, Resources, Writing – review & editing. TGS: Conceptualization, Methodology, Supervision, Writing – review & editing. ICP: Conceptualization, Methodology, Supervision, Writing – review & editing. KW: Resources, Writing – review & editing. SPH: Conceptualization, Funding acquisition, Methodology, Supervision, Writing – review & editing.

Funding

The author(s) declare that financial support was received for the research and/or publication of this article. This research received support through Schmidt Sciences, LLC (TRK, SPH, ICP, BZ, and WC) and contributes to the LEMONTREE (Land Ecosystem Models based On New Theory, obseRvations and ExperimEnts) project. TRK acknowledges support from the SCENARIO NERC Doctoral Training Programme (NE/S007261/1).

Acknowledgments

We thank colleagues at the Leverhulme Centre for Wildfires, Environment and Society for discussions of this work. We acknowledge computational resources and support provided by the Imperial College Research Computing Service.

Conflict of interest

The authors declare that the research was conducted in the absence of any commercial or financial relationships that could be construed as a potential conflict of interest.

Generative AI statement

The authors declare that no Gen AI was used in the creation of this manuscript.

Publisher's note

All claims expressed in this article are solely those of the authors and do not necessarily represent those of their affiliated organizations, or those of the publisher, the editors and the reviewers. Any product that may be evaluated in this article, or claim that may be made by its manufacturer, is not guaranteed or endorsed by the publisher.

Supplementary material

The Supplementary material for this article can be found online at: https://www.frontiersin.org/articles/10.3389/ffgc.2025.1519836/full#supplementary-material

References

Abatzoglou, J. T., Battisti, D. S., Williams, A. P., Hansen, W. D., Harvey, B. J., and Kolden, C. A. (2021). Projected increases in western US forest fire despite growing fuel constraints. *Commun. Earth Environ.* 2, 1–8. doi: 10.1038/s43247-021-00299-0

Arias, P. A., Bellouin, N., Coppola, E., Jones, R. G., Krinner, G., Marotzke, J., et al. (2021). Climate change 2021 – the physical science basis. Cambridge, UK: Cambridge University Press, 35–144.

Balik, J. A., Coop, J. D., Krawchuk, M. A., Naficy, C. E., Parisien, M. A., Parks, S. A., et al. (2024). Biogeographic patterns of daily wildfire spread and extremes across North America. *Front. For. Glob. Change* 7:361. doi: 10.3389/ffgc.2024.1355361

Barbero, R., Abatzoglou, J. T., Kolden, C. A., Hegewisch, K. C., Larkinb, N. K., and Podschwitb, H. (2014). Multi-scalar influence of weather and climate on very large-fires in the eastern United States. *Int. J. Climatol.* 35, 2180–2186. doi: 10.1002/joc.4090

Bevacqua, E., Suarez-Gutierrez, L., Jézéquel, A., Lehner, F., Vrac, M., Yiou, P., et al. (2023). Advancing research on compound weather and climate events via large ensemble model simulations. *Nat. Commun.* 14:2145. doi: 10.1038/s41467-023-37847-5

Buck, A. L. (1981). New equations for computing vapor pressure and enhancement factor. *JAMC*, 20:12 1527–1532. doi: 10.1175/1520-0450(1981)020\u0026lt;1527:NEFCVP\u0026gt;2.0.CO;2

Cai, W., and Prentice, I. C. (2020). Recent trends in gross primary production and their drivers: analysis and modelling at flux-site and global scales. *Environ. Res. Lett.* 15:124050. doi: 10.1088/1748-9326/abc64e

Cai, W., Zhu, Z., Harrison, S. P., Ryu, Y., Wang, H., Zhou, B., et al. (2025). A unifying principle for global greenness patterns and trends. *Nature Communication and Environment* 6:9. doi: 10.1038/s43247-025-01992-0

Chuvieco, E., Pettinari, M. L., Koutsias, N., Forkel, M., Hantson, S., and Turco, M. (2021). Human and climate drivers of global biomass burning variability. *Sci. Total Environ.* 779:146361. doi: 10.1016/j.scitotenv.2021.146361

Cloke, H. L., and Pappenberger, F. (2009). Ensemble flood forecasting: a review. *J. Hydrol.* 375, 613–626. doi: 10.1016/j.jhydrol.2009.06.005

Commission for Environmental Cooperation (Montréal, Québec) and Secretariat (1997). Ecological regions of North America: Toward a common perspective. New York: The Commission.

Craig, M. T., Wohland, J., Stoop, L. P., Kies, A., Pickering, B., Bloomfield, H. C., et al. (2022). Overcoming the disconnect between energy system and climate modeling. *Joule* 6, 1405–1417. doi: 10.1016/j.joule.2022.05.010

Crossett, C. C., Betts, A. K., Dupigny-Giroux, L. A. L., and Bomblies, A. (2020). Evaluation of daily precipitation from the ERA5 global reanalysis against GHCN observations in the northeastern United States. *Climate* 8:148. doi: 10.3390/cli8120148

Cunningham, C. X., Williamson, G. J., and Bowman, D. M. J. S. (2024). Increasing frequency and intensity of the most extreme wildfires on earth. *Nat. Ecol. Evol* 2024:2452. doi: 10.1038/s41559-024-02452-2

Dai, A., Wigley, T. M. L., Boville, B. A., Kiehl, J. T., and Buja, L. E. (2001). Climates of the twentieth and twenty-first centuries simulated by the NCAR climate system model. *J. Clim.* 14, 485–519. doi: 10.1175/1520-0442(2001)014<0485:COTTAT>2.0.CO;2

Döscher, R., Acosta, M., Alessandri, A., Anthoni, P., Arneth, A., Arsouze, T., et al. (2021). The EC-earth3 earth system model for the climate model intercomparison project 6. *Geosci. Model Dev. Discuss.* 15, 2973–3020. doi: 10.5194/gmd-15-2973-2022

Dye, A. W., Gao, P., Kim, J. B., Lei, T., Riley, K. L., and Yocom, L. (2023). High-resolution wildfire simulations reveal complexity of climate change impacts on projected burn probability for Southern California. *Fire Ecol.* 19, 1–19. doi: 10.1186/s42408-023-00179-2

ECMWF. (2025). *Changes to the forecasting system*. ECMWF, Available at: https://confluence.ecmwf.int/display/FCST/Changes+to+the+forecasting+system.

Ellis, T. M., Bowman, D. M., Jain, P., Flannigan, M. D., and Williamson, G. J. (2022). Global increase in wildfire risk due to climate-driven declines in fuel moisture. *Glob. Change Biol.* 28, 1544–1559. doi: 10.1111/gcb.16006

EPA. (2024). *Technical documentation: Wildfires. United States Environmental Protection Agency*. Available online at: https://www.epa.gov/system/files/documents/2024-06/wildfires_documentation.pdf (Accessed 10 Sep 2024).

François, B., Vrac, M., Cannon, A. J., Robin, Y., and Allard, D. (2020). Multivariate bias corrections of climate simulations: which benefits for which losses? *Earth Syst. Dynam.* 11, 537–562. doi: 10.5194/esd-11-537-2020

Grillakis, M. G., Koutroulis, A. G., Daliakopoulos, I. N., and Tsanis, I. K. (2017). A method to preserve trends in quantile mapping bias correction of climate modeled temperature. *Earth Syst. Dynam.* 8, 889–900. doi: 10.5194/esd-8-889-2017

Guyette, R. P., Stambaugh, M. C., Marschall, J., and Abadir, E. (2015). An analytic approach to climate dynamics and fire frequency in the Great Plains. *GPR* 25, 139–150. doi: 10.1353/gpr.2015.0031

Haas, O., Keeping, T., Gomez-Dans, J., Prentice, I. C., and Harrison, S. P. (2024). The global drivers of wildfire. *Front. Environ. Sci.* 12:1438262. doi: 10.3389/fenvs.2024.1438262

Haines, D. A. (1988). A lower atmosphere severity index for wildlife fires. *National Weather Digest* 13, 23–27.

Hnilica, J., Hanel, M., and Puš, V. (2017). Multisite bias correction of precipitation data from regional climate models. *Int. J. Climatol.* 37, 2934–2946. doi: 10.1002/joc.4890

Hunter, R. D., and Meentemeyer, R. K. (2005). Climatologically aided mapping of daily precipitation and temperature. *J. Appl. Meteorol.* 44, 1501–1510. doi: 10.1175/JAM2295.1

Ibebuchi, C. C., Lee, C. C., Silva, A., and Sheridan, S. C. (2024). Evaluating apparent temperature in the contiguous United States from four reanalysis products using artificial neural networks. *JGR* 1:2 e2023JH000102. doi: 10.1029/2023JH000102

Iglesias, V., Balch, J. K., and Travis, W. R. (2022). US fires became larger, more frequent, and more widespread in the 2000s. *Sci. Adv.* 8:11 eabc0020. doi: 10.1126/sciadv.abc0020

Jain, P., Wang, X., and Flannigan, M. D. (2017). Trend analysis of fire season length and extreme fire weather in North America between 1979 and 2015. *Int. J. Wildland Fire* 26, 1009–1020. doi: 10.1071/WF17008

Jeong, S., Ryu, Y., Gentine, P., Lian, X., Fang, J., Li, X., et al. (2024). Persistent global greening over the last four decades using novel long-term vegetation index data with enhanced temporal consistency. *Rem. Sens. Environ.* 311:114282. doi: 10.1016/j.rse.2024.114282

Karger, D. N., Nobis, M. P., Normand, S., Graham, C. H., and Zimmermann, N. E. (2023). CHELSA-TraCE21k–high-resolution (1 km) downscaled transient temperature and precipitation data since the last glacial maximum. *Clim. Past* 19, 439–456. doi: 10.5194/cp-19-439-2023

Keeping, T., Harrison, S. P., and Prentice, I. C. (2024). Modelling the daily probability of wildfire occurrence in the contiguous United States. *Environ. Res. Lett.* 19:024036. doi: 10.1088/1748-9326/ad21b0

Kelley, D. I., Bistinas, I., Whitley, R., Burton, C., Marthews, T. R., and Dong, N. (2019). How contemporary bioclimatic and human controls change global fire regimes. *Nat. Clim. Chang.* 9, 690–696. doi: 10.1038/s41558-019-0540-7

Kerr, G. H., DeGaetano, A. T., Stoof, C. R., and Ward, D. (2018). Climate change effects on wildland fire risk in the northeastern and Great Lakes states predicted by a downscaled multi-model ensemble. *Theor. Appl. Climatol.* 131, 625–639. doi: 10.1007/s00704-016-1994-4

Knapp, P. A. (1998). Spatio-temporal patterns of large grassland fires in the intermountain west, USA. *Glob. Ecol. Biogeo. Lett* 7, 259–272. doi: 10.2307/2997600

Knauer, J., Cuntz, M., Smith, B., Canadell, J. G., Medlyn, B. E., Bennett, A. C., et al. (2023). Higher global gross primary productivity under future climate with more advanced representations of photosynthesis. *Sci. Adv.* 9:eadh9444. doi: 10.1126/sciadv.adh9444

Lavers, D. A., Simmons, A., Vamborg, F., and Rodwell, M. J. (2022). An evaluation of ERA5 precipitation for climate monitoring. *Q. J. R. Meteorol. Soc.* 148:3152. doi: 10.1002/qj.4351

Lee, C., Schlemme, C., Murray, J., and Unsworth, R. (2015). The cost of climate change: ecosystem services and wildland fires. *Ecol. Econ.* 116, 261–269. doi: 10.1016/j.ecolecon.2015.04.020

Lu, Q., Liu, H., Wei, L., Zhong, Y., and Zhou, Z. (2024). Global prediction of gross primary productivity under future climate change. *Sci. Total Environ.* 912:169239. doi: 10.1016/j.scitotenv.2023.169239

Lupo, A. R. (2021). Atmospheric blocking events: a review. *Ann. N. Y. Acad. Sci.* 1504, 5–24. doi: 10.1111/nyas.14557

Maraun, D. (2013). Bias correction, quantile mapping, and downscaling: revisiting the inflation issue. *J. Clim.* 26, 2137–2143. doi: 10.1175/JCLI-D-12-00821.1

McGranahan, D. A., and Wonkka, C. L. (2024). Pyrogeography of the Western Great Plains: a 40-year history of fire in semi-arid rangelands. *Fire* 7:32. doi: 10.3390/fire7010032

Mosier, T. M., Hill, D. F., and Sharp, K. V. (2014). 30-Arcsecond monthly climate surfaces with global land coverage. *Int. J. Climatol.* 34, 2175–2188. doi: 10.1002/joc.3829

Mueller, S. E., Thode, A. E., Margolis, E. Q., Yocom, L. L., Young, J. D., and Iniguez, J. M. (2020). Climate relationships with increasing wildfire in the southwestern US from 1984 to 2015. *For. Ecol. Manag.* 460:117861. doi: 10.1016/j.foreco.2019.117861

Melvin, A. M., Murray, J., Boehlert, B., Martinich, J. A., Rennels, L., and Rupp, T. S. (2017). Estimating wildfire response costs in Alaska's changing climate. *Clim. Chang.* 141, 783–795. doi: 10.1007/s10584-017-1923-2

Muñoz-Sabater, J., Dutra, E., Agustí-Panareda, A., Albergel, C., Arduini, G., Balsamo, et al. (2021). ERA5-land: a state-of-the-art global reanalysis dataset for land applications. *ESSD* 13, 4349–4383. doi: 10.5194/essd-13-4349-2021

Murphy, B. P., Yocom, L. L., and Belmont, P. (2018). Beyond the 1984 perspective: narrow focus on modern wildfire trends underestimates future risks to water security. *Earth's Future* 6, 1492–1497. doi: 10.1029/2018EF001006

Muntjewerf, L., Bintanja, R., Reerink, T., and van der Wiel, K. (2023). The KNMI Large Ensemble Time Slice (KNMI–LENTIS), *Geosci. Model Dev.* 16 4581–4597. doi: 10.5194/gmd-16-4581-2023

Nabizadeh, E., Hassanzadeh, P., Yang, D., and Barnes, E. A. (2019). Size of the atmospheric blocking events: scaling law and response to climate change. *Geophys. Res. Lett.* 46, 13488–13499. doi: 10.1029/2019GL084863

Parisien, M. A., and Moritz, M. A. (2009). Environmental controls on the distribution of wildfire at multiple spatial scales. *Ecol. Monogr.* 79, 127–154. doi: 10.1890/07-1289.1

Radeloff, V. C., Mockrin, M. H., Helmers, D., Carlson, A., Hawbaker, T. J., Martinuzzi, et al. (2023). Rising wildfire risk to houses in the United States, especially in grasslands and shrublands. *Science* 382, 702–707. doi: 10.1126/science.ade9223

Richardson, D., Black, A. S., Irving, D., Matear, R. J., Monselesan, D. P., Risbey, J. S., et al. (2022). Global increase in wildfire potential from compound fire weather and drought. *NPJ Clim. Atmos. Sci.* 5:23. doi: 10.1038/s41612-022-00248-4

Sasai, T., Kawase, H., Kanno, Y., Yamaguchi, J., Sugimoto, S., Yamazaki, et al. (2019). Future projection of extreme heavy snowfall events with a 5-km large ensemble regional climate simulation. *Geophys. Res. Atmos.* 124, 13975–13990. doi: 10.1029/2019JD030781

Sayedi, S. S., Abbott, B. W., Vannière, B., Leys, B., Colombaroli, D., Romera, et al. (2024). Assessing changes in global fire regimes. *Fire Ecol.* 20, 1–22. doi: 10.1186/s42408-023-00237-9

Schoennagel, T., Balch, J. K., Brenkert-Smith, H., Dennison, P. E., Harvey, B. J., Krawchuk, M. A., et al. (2017). Adapt to more wildfire in western north American forests as climate changes. *PNAS* 114, 4582–4590. doi: 10.1073/pnas.1617464114

Seager, R., Hooks, A., Williams, A. P., Cook, B., Nakamura, J., and Henderson, N. (2015). Climatology, variability, and trends in the US vapor pressure deficit, an important fire-related meteorological quantity. *J. Appl. Math. Comput.* 54, 1121–1141. doi: 10.1175/JAMC-D-14-0321.1

Sedano, F., and Randerson, J. (2014). Multi-scale influence of vapor pressure deficit on fire ignition and spread in boreal forest ecosystems. *Biogeo* 11, 3739–3755. doi: 10.5194/bg-11-3739-2014

Shepherd, T. G. (2019). Storyline approach to the construction of regional climate change information. *Proc. Math. Phys. Eng. Sci.* 475:20190013. doi: 10.1098/rspa.2019.0013

Short, K. C. (2022). *Spatial wildfire occurrence data for the United States, 1992–2020 [FPA_FOD_20221014]*. 6th Edn. FS RDA.

Smith, A. J., Jones, M. W., Abatzoglou, J. T., Canadell, J. G., and Betts, R. A. (2020). *Climate change increases the risk of wildfires*. ScienceBrief, Available online at: https://sciencebrief.org/topics/climate-change-science/wildfires/explorer.

Sobie, S. R., and Murdock, T. Q. (2017). High-resolution statistical downscaling in southwestern British Columbia. *J. Appl. Meteorol. Clim.* 56, 1625–1641. doi: 10.1175/JAMC-D-16-0287.1

Squire, D. T., Richardson, D., Risbey, J. S., Black, A. S., Kitsios, V., Matear, R. J., et al. (2021). Likelihood of unprecedented drought and fire weather during Australia's 2019 megafires. *NPJ Clim. Atmos. Sci.* 4:64. doi: 10.1038/s41612-021-00220-8

Stocker, B. D., Wang, H., Smith, N. G., Harrison, S. P., Keenan, T. F., Sandoval, D., et al. (2020). P-model v1. 0: an optimality-based light use efficiency model for simulating ecosystem gross primary production. *GMD* 13:1545. doi: 10.5194/gmd-13-1545-2020

Suarez-Gutierrez, L., Müller, W. A., Li, C., and Marotzke, J. (2020). Hotspots of extreme heat under global warming. *Clim. Dyn.* 55, 429–447. doi: 10.1007/s00382-020-05263-w

Sullivan, A., Baker, E., Kurvits, T., Popescu, A., Paulson, A. K., Cardinal Christianson, A., et al. (2022). Spreading like wildfire: The rising threat of extraordinary landscape fires. Nairobi, Kenya: UNEP.

Tefera, G. W., Ray, R. L., and Wootten, A. M. (2024). Evaluation of statistical downscaling techniques and projection of climate extremes in Central Texas, USA. *Weather Clim. Extrem.* 43:100637. doi: 10.1016/j.wace.2023.100637

Touma, D., Stevenson, S., Swain, D. L., Singh, D., Kalashnikov, D. A., and Huang, X. (2022). Climate change increases risk of extreme rainfall following wildfire in the western United States. *Sci. Adv.* 8:eabm0320. doi: 10.1126/sciadv.abm0320

Tu, Y., Zhou, J., Lin, S., Alshrah, M., Zhao, X., and Chen, G. (2023). Plausible photomolecular effect leading to water evaporation exceeding the thermal limit. *PNAS* 120:e2312751120. doi: 10.1073/pnas.2312751120

Van der Wiel, K., Lenderink, G., and de Vries, H. (2021). Physical storylines of future European drought events like 2018 based on ensemble climate modelling. *Weather Clim. Extrem.* 33:100350. doi: 10.1016/j.wace.2021.100350

Van der Wiel, K., Wanders, N., Selten, F. M., and Bierkens, M. F. P. (2019). Added value of large ensemble simulations for assessing extreme river discharge in a 2 C warmer world. *Geophys. Res. Lett.* 46, 2093–2102. doi: 10.1029/2019GL081967

Van der Wiel, K., Selten, F. M., Bintanja, R., Blackport, R., and Screen, J. A. (2020). Ensemble climate-impact modelling: extreme impacts from moderate meteorological conditions. *Environ. Res. Lett.* 15:034050. doi: 10.1088/1748-9326/ab7668

Wang, H., Prentice, I. C., Keenan, T. F., Davis, T. W., Wright, I. J., Cornwell, W. K., et al. (2017). Towards a universal model for carbon dioxide uptake by plants. *Nat. Plants* 3, 734–741. doi: 10.1038/s41477-017-0006-8

Williams, A. P., Gentine, P., Moritz, M. A., Roberts, D. A., and Abatzoglou, J. T. (2018). Effect of reduced summer cloud shading on evaporative demand and wildfire in coastal southern California. *GRL* 45, 5653–5662. doi: 10.1029/2018GL077319

Williams, A. P., Abatzoglou, J. T., Gershunov, A., Guzman-Morales, J., Bishop, D. A., Balch, J. K., et al. (2019). Observed impacts of anthropogenic climate change on wildfire in California. *Earth's Fut.* 7, 892–910. doi: 10.1029/2019EF001210

Yue, X., Mickley, L. J., and Logan, J. A. (2014). Projection of wildfire activity in southern California in the mid-twenty-first century. *Clim. Dyn.* 43, 1973–1991. doi: 10.1007/s00382-013-2022-3

Zhou, B., Cai, W., Zhu, Z., Wang, H., Harrison, S. P., and Prentice, I. C. (2025). A general model for the seasonal to decadal dynamics of leaf area. *Global Change Biology* e70125. doi: 10.1111/gcb.70125

Zhu, Z., Wang, H., Harrison, S. P., Prentice, I. C., Qiao, S., and Tan, S. (2023). Optimality principles explaining divergent responses of alpine vegetation to environmental change. *Glob. Change Biol.* 29, 126–142. doi: 10.1111/gcb.16459

Zubkova, M., Humber, M. L., and Giglio, L. (2023). Is global burned area declining due to cropland expansion? How much do we know based on remotely sensed data? *Int. J. Rem. Sens.* 44, 1132–1150. doi: 10.1080/01431161.2023.2174389

3.7 Supplementary: Present and future interannual variability in wildfire occurrence: a large ensemble application to the United States

This Supplementary contains the following figures and tables:

Supplementary Figure 1: The regions used to aggregate data in this study.

Supplementary Figure 2: The distribution of the annual number of fires for 16 randomly selected sites.

Supplementary Figure 3: The total annual number of fires for the contiguous US for the modern and modern +2°C periods.

Supplementary Figure 4: The reanalysis fire season length calculated according to the Section 2.5, with the maximum being the 99th percentile of the distribution.

Supplementary Figure 5: The multiplicative increase in the mean and spread of the annual number of fires distribution after a further 2°C warming from the modern.

Supplementary Figure 6: Comparison of the geospatial means of the six dynamic driving variables in KNMI-LENTIS and ERA5-Land.

Supplementary Figure 7: Comparison of: observed wildfire occurrences, reanalysis driven modelled occurrences, the modern ensemble of fire model outputs driven by bias-corrected and downscaled data, the modern ensemble of fire model outputs driven by raw data.

Table 1: Overview of candidate and selected predictor variables.

Tables 2a and **2b**: Bias correction performance statistics.

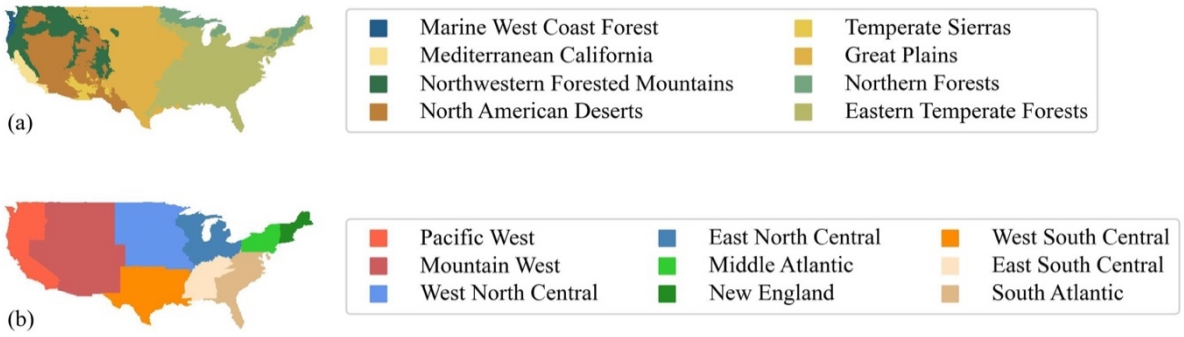

Supplementary Figure 1. The regions used to aggregate data in this study, where (a) shows the ecoregions as defined by of Balik et al. (2024), and (b) shows the US Census Bureau regions. The regions can be further aggregated as West (Pacific West, Mountain West); Midwest (West North Central, East North Central); Northeast (Middle Atlantic, New England); South (West South Central; East South Central; South Atlantic).

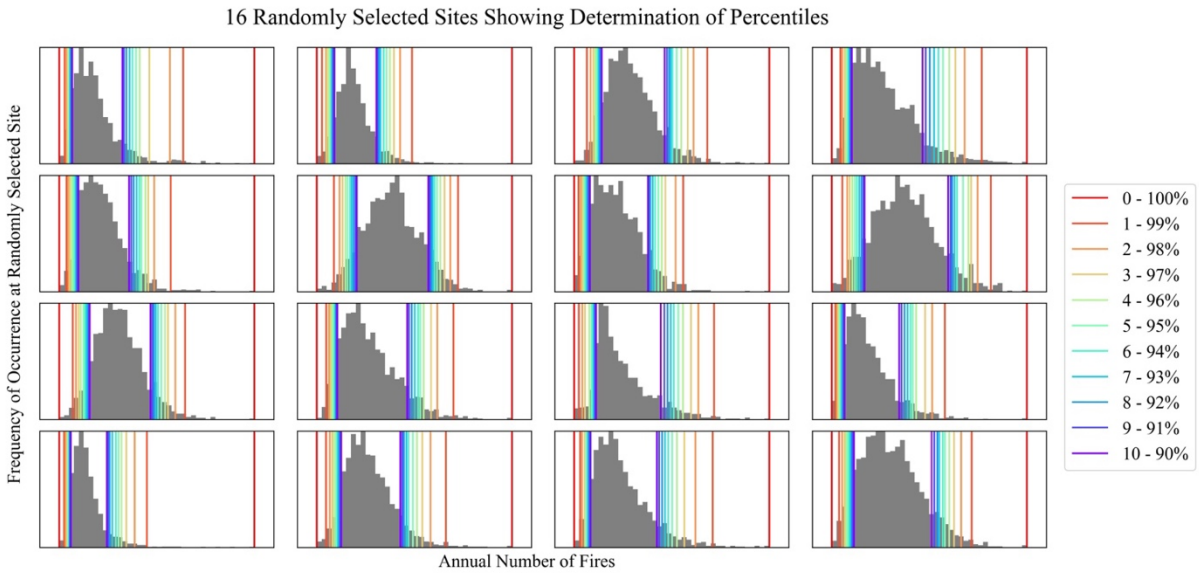

Supplementary Figure 2. The distribution of the annual number of fires for 16 randomly selected sites, showing that the maximum is highly variable but 99th is much more stable.

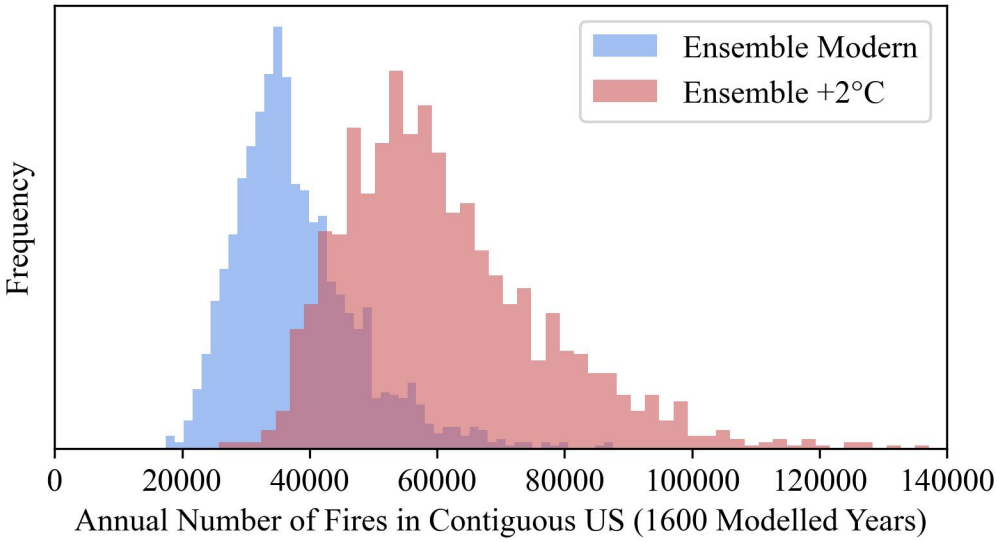

Supplementary Figure 3. The total annual number of fires for the contiguous US for the modern and modern +2°C periods.

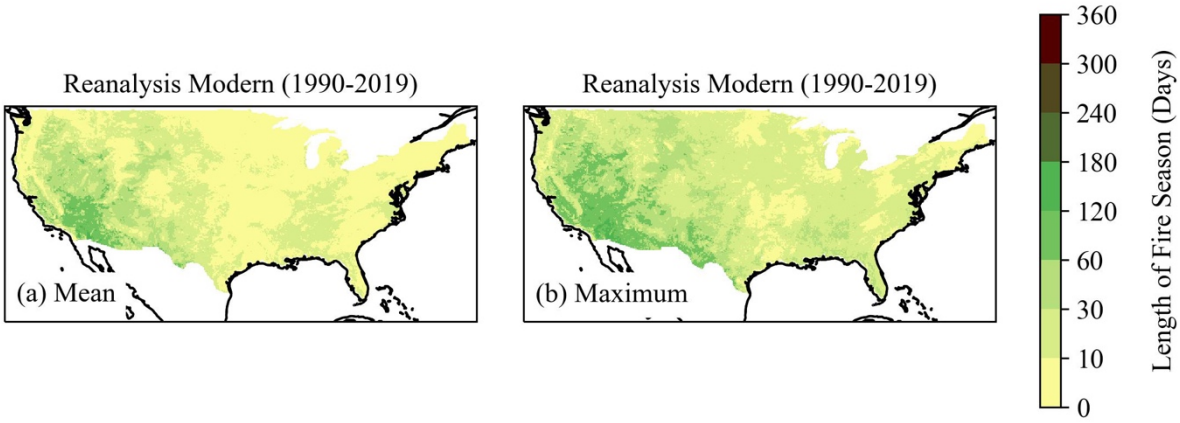

Supplementary Figure 4. The reanalysis fire season length calculated according to the Section 2.5, with the maximum being the 99th percentile of the distribution.

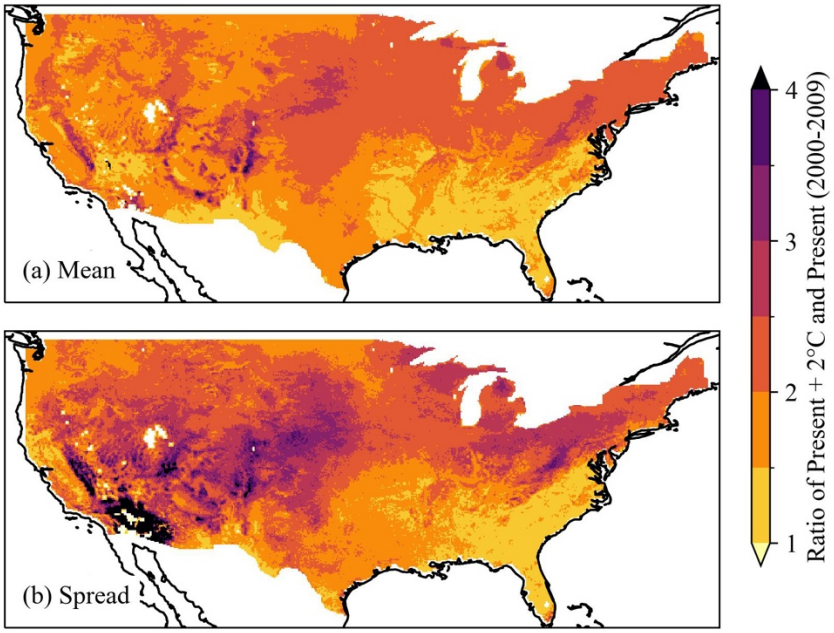

Supplementary Figure 5. The multiplicative increase in the mean and spread of the annual number of fires distribution after a further 2°C warming from the modern.

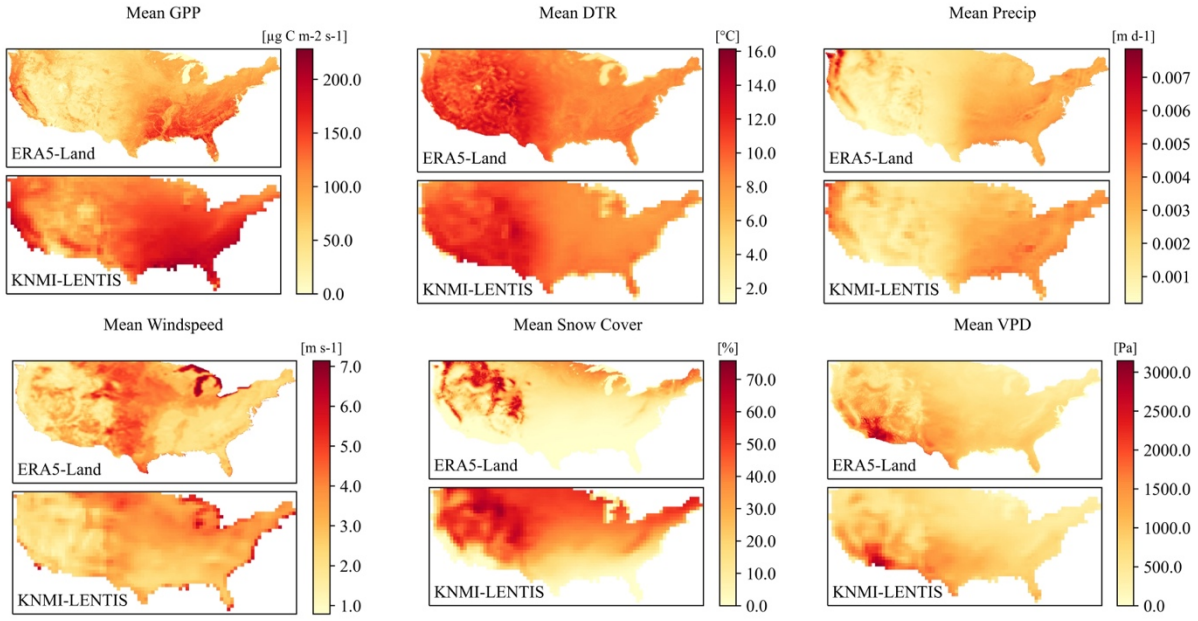

Supplementary Figure 6: Comparison of the 2000-2009 averages of the six dynamic driving variables from KNMI-LENTIS and ERA5-Land.

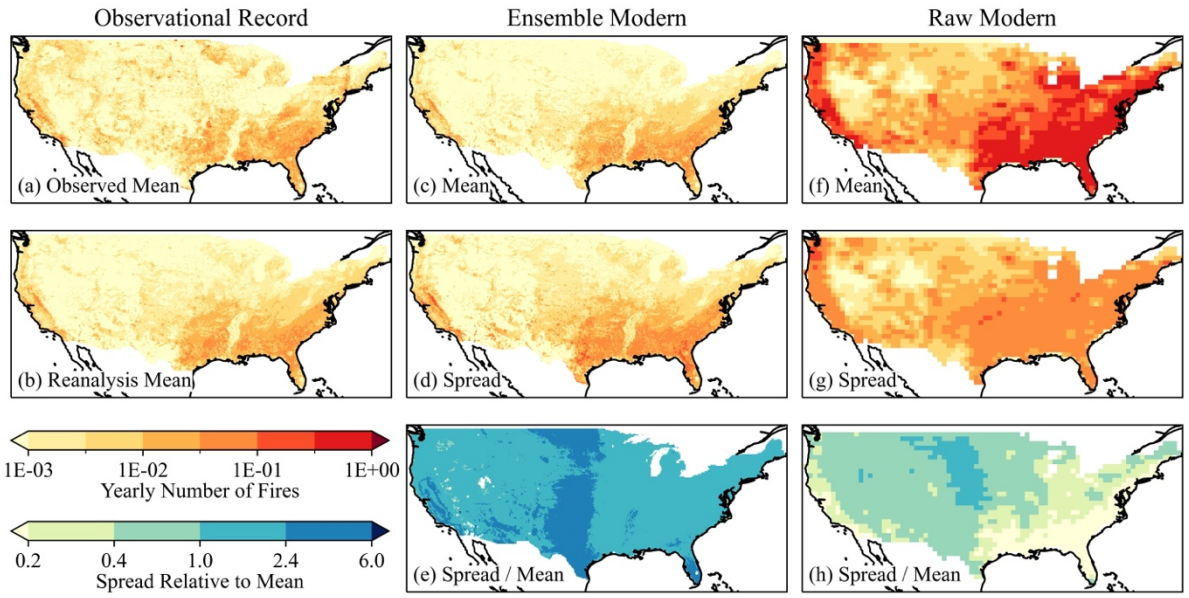

Supplementary Figure 7: Modelled and observed patterns in the annual number of wildfires greater than 0.1 hectares, with both the mean and 1st-99th percentile spread shown. Plots (a) to (e) are taken from Figure 1 in the main text and show (a) the observed annual mean of the wildfire occurrence record for 1992-2020; (b) the modelled reanalysis mean for 1990-2019; (c) the modelled ensemble mean for the modern (2000-2009 climate); (d) the modelled ensemble spread for the modern; (e) the ratio of model spread and mean for the ensemble modern. The remaining plots show the results obtained using outputs from the KNMI-LENTIS before downscaling and bias correction: (f) the modelled ensemble mean for the modern (2000-2009) climate; (g) the modelled ensemble spread for the modern climate, and (h) the ratio of model spread and mean for the ensemble modern climate.

Table 1. Overview of candidate and selected predictor variables. Daytime is defined as 4AM to 8PM local time.

Variable Type:	***Candidates:***	***Selected in model*** ***(t-value in brackets)***
Land-cover	*Cropland fraction; herbaceous fraction; needleleaf fraction; shrubland fraction; forest fraction.*	*Cropland fraction (-6.6); needleleaf fraction (7.3); shrubland fraction (-10.9)*
Plant productivity	*GPP (50-day, 100-day, 150-day, 1-year, 2-year, 5-year, 10-year) - accumulated gross primary productivity*	*50-day GPP (-16.5); 1-year GPP (17.4)*
Topographic	*Elevation; vector ruggedness metric (VRM)*	
Human landscape impact	*Population density; rural population density; road density*	*Rural population density (17.2)*
Meteorological	*Diurnal temperature range; surface soil moisture; precipitation (daily and 5-day total); mean daytime downwelling shortwave radiation; daytime windspeed (mean and maximum); snow cover fraction; daytime temperature (mean and maximum); vapour pressure deficit (daytime mean and maximum, night-time mean and 10-day average).*	*Diurnal temperature range (9.3); daily precipitation (-5.0); 5-day precipitation (-5.5); mean daytime windspeed (8.8); snow cover fraction (-7.0); mean daytime vapour pressure deficit (17.3)*

Tables 2a and 2b. Bias correction performance statistics, based on correlation of statistics for data aggregated at 2π x ensemble resolution and monthly. Table 2a gives the bias correction performance statistics of the raw variables from which predictors were calculated (3-hour timestep for temperature, dewpoint and windspeed, and otherwise daily) and Table 2b the derived predictor variables (daily). The variable abbreviations are: Daily Mean Surface Windspeed (sfcwind); Daily Mean VPD (vpd); Diurnal Temperature Range (DTR); Daily Snow Cover (snc); Daily Total Precipitation (pr); Total Precipitation in Prior 5 days (pr_5d); GPP in Prior 50 Days (GPP_50d); GPP in Prior 1 Year (GPP_1yr).

R^2	Temperature	Dewpoint	Snow Cover	Windspeed	Precipitation	GPP
Mean	0.999	0.999	0.997	0.997	0.987	0.969
Variance	0.762	0.809	0.519	<0	0.789	<0
Skewness	0.463	0.542	0.241	0.134	0.496	<0
Kurtosis	0.085	0.086	<0	<0	0.291	<0

R^2	sfcwind	vpd	dtr	snc	pr	pr_5d	GPP_50d	GPP_1yr
Mean	0.922	0.987	0.983	0.994	0.985	0.985	0.881	0.773
Variance	0.567	0.812	0.684	0.409	0.726	0.771	<0	<0
Skewness	0.073	<0	0.741	0.098	0.110	0.307	<0	0.531
Kurtosis	0.020	<0	0.052	<0	<0	<0	<0	0.266

Influence of global climate modes on wildfire occurrence in the contiguous United States under recent and future climates

This chapter was accepted by *Climate Dynamics* in November 2025. Its content is built on the original research in Chapters 2 and 3, and seeks to further understand the drivers of high wildfire occurrence years by assessing the association of global climate modes and interannual wildfire variability over the contiguous US. Chapter 4 answers the question, *can interannual variability in wildfire occurrence be predicted by climate modes?* This question is answered by analysis of the area of significant effect of each climate mode over the study region, as well as the magnitude of that effect on modelled annual wildfire counts. These associations were found and compared in the recent and future climate fire years defined in Chapter 3, with the analysis also including the effect of the most impactful climate modes on the length and timing of the fire year.

Chapters 2 and 3 both investigate the drivers of higher wildfire activity, at a daily and annual timescale respectively. This chapter then seeks to establish whether the incidence of those driving conditions are sufficiently influenced by persistent climate modes to have a substantial effect on annual wildfire patterns. Chapter 4 is a companion chapter to Chapter 3, identifying operationalisable relationships between predictable and persistent climate modes and regions of higher wildfire activity. It extends the short-term predictive utility of the occurrence model presented in Chapter 2, to a monthly to annual timescale – depending on the predictability of the climate mode. Chapter 4 also includes justification for the use of an LE in understanding wildfire teleconnections, demonstrating that observational data from the recent reanalysis is not sufficient to derive statistically significant relationships between wildfire activity and climate modes. This is proof of concept of the argument made in Chapter 3, that observed fire years can be best understood in the context of the broader distribution of unrealised weather-years in the current climate.

Influence of global climate modes on wildfire occurrence in the contiguous United States under recent and future climates

Theodore R. Keeping*[1,2,3], Theodore G. Shepherd[4], I. Colin Prentice[3,5], Karin van der Wiel[6], Sandy P. Harrison[1,3]

[1]Geography & Environmental Science, University of Reading, Reading, UK

[2]Centre for Environmental Policy, Imperial College London, London, UK

[3]Leverhulme Centre for Wildfires, Environment and Society, Imperial College London, London, UK

[4]Department of Meteorology, University of Reading, Reading, UK

[5]Georgina Mace Centre for the Living Planet, Department of Life Sciences, Imperial College London, Ascot, UK

[6]Royal Netherlands Meteorological Institute (KNMI), De Bilt, The Netherlands

Keywords: wildfire, climate modes, teleconnections, wildfire modelling, climate variability

Predictable modes of climate variability, such as the El Niño Southern Oscillation (ENSO), have a major influence on regional weather patterns, an important control on wildfire occurrence. Although these global climate modes have been associated with historical variability in wildfire occurrence in the United States and are used to forecast seasonal wildfire risk, precise information about the spatial pattern and magnitude of their influence is lacking and the satellite record of wildfires is too short to address these issues. Here we use wildfire occurrence model with a large ensemble of 1600 simulated years from EC-Earth3 in a recent climate (2000-2009) and a future climate corresponding to +2°C global warming, to characterise the impact of specific climate modes on wildfire occurrence in the contiguous US. We show that ENSO, the Indian Ocean Dipole (IOD), and the 1-year lagged Tropical North Atlantic (TNA+1) have the greatest effect on annual fire occurrence – strongly contributed by the effect of these modes on hot, dry conditions in the Great Plains and precipitation in the southwestern US. El Niño is not significantly associated with wildfire occurrence in the northwestern US, contrary to expectation, but is associated with a later (earlier) wildfire season peak in the southwestern (southeastern) US. Under future warming, the AMO and PNA become a significant influence over most of the US, and the magnitude of impact of ENSO and TNA+1 increase strongly.

4.1 Introduction

With climate change, extreme wildfires are occurring at a greater frequency and intensity (Cunningham et al., 2024). Severe fire years often occur when synoptic-scale hot and dry weather events cause extremely wildfire-prone conditions (Gedalof et al., 2005; Barnes et al., 2025), resulting in multiple large wildfire events; the Australian 2019-2020 (NSW EPA, 2021) and the Canadian 2023 (Pelletier et al., 2024) fire seasons are examples of this. Whilst the occurrence of such conditions is generally increasing with climate change, there is a high variability in wildfire activity and its climatic drivers between years (Abatzoglou et al., 2018). This interannual variability is a key property of the wildfire regime, and in the United States (US) – the focus of this study – there are strong geospatial patterns in annual wildfire variability distinct from the mean rate of wildfire (Keeping et al. 2025).

Global modes of climate variability, such as the El Niño Southern Oscillation (ENSO), have been linked to fire year variability. In additional to natural stochasticity in wildfire outcomes, climate variability explains much of the interannual variability in burnt area globally (Abatzoglou et al., 2018; Gincheva et al., 2024). Approximately half of global burnt area is modulated by climate modes (Chen et al., 2016; Cardil et al., 2023) through their influence on rainfall, temperature and spring onset (Dai and Wigley, 2000; Abram et al., 2014; Schwartz et al., 2013). In the US, ENSO and other climate modes have been shown to have a significant influence on wildfire danger (Mason et al., 2017). Climate modes can be used to forecast seasonal wildfire danger (Shen et al., 2019), and ENSO and the Pacific Decadal Oscillation (PDO) are adopted in the published seasonal outlook by the US government (NIFC, 2024a).

There is an extensive tree-ring literature linking historic wildfire events in the western US (west of the 100˚W meridian) and climate modes (see Supplementary Section 1 for more details), primarily focusing on ENSO, the PDO, and the Atlantic Multidecadal Oscillation (AMO). These studies often cover multiple centuries, correlating reconstructed climate modes with tree-ring fire scars. The primary influence on wildfire in the southwestern US is ENSO: tree-ring reconstructions (Kitzberger et al., 2007; Margolis and Swetnam, 2013; Swetnam and Betancourt, 1990; Westerling and Swetnam, 2003) link La Niña years to drought and a higher probability of wildfire. Reanalysis-based studies find the same effect (Mason et al., 2017). Tree-ring reconstructions also link El Niño years to a later southwestern fire-season peak (Kitzberger et al., 2001). In the northwestern US, tree-ring studies link El Niño years to higher wildfire activity (Hessl et al., 2004; Johnston et al., 2017) through a reduction in precipitation

(Westerling and Swetnam, 2003). This effect is linked more strongly to wildfire size than to the rate of occurrence (Heyerdahl et al., 2002). Recent data support the link between El Niño and very large wildfires in this region (Barbero et al., 2015). However, a study of remotely sensed burnt area covering a shorter period but a larger area found that the influence of ENSO on wildfire in the western US is weak compared to other key relationships between wildfire and climate modes globally (Cardil et al., 2023).

The positive phase of the PDO (PDO+) has been linked to greater burnt area in the northwestern US in tree-ring analyses, especially when in conjunction with El Niño (Ascoli et al., 2020; Heyerdahl et al., 2002, Norman and Taylor, 2003; Schoennagel et al., 2005). However, reconstructions of the PDO vary significantly and the effects on US wildfire depend on the specific reconstruction (Kipfmueller et al., 2012). Tree-ring reconstructions also associate the warm AMO+ with increased burnt area in the West, with studies primarily centred on the northwestern US (Ascoli et al., 2020; Kitzberger et al., 2007; Trouet et al., 2010). The positive Pacific/North American (PNA+) mode has also been associated with an earlier spring onset in the West (Ault et al., 2011; Dannenberg et al., 2018).

Tree-ring scars have not been used to reconstruct relationships between wildfire and modes in the southeastern and central US, but shorter timescale federal or state wildfire records have been used. In the southeastern US, state fire records indicate an association between La Niña years and a reduction in precipitation and an increase in burnt area in the early months of the year (Dixon et al., 2008; Goodrick and Hanley, 2009; Simard et al., 1985). Remote sensing data support this finding (Cardil et al., 2021). The PNA- and PDO+ have also been linked with a limited increase in wildfire in the southeastern US (Dixon et al., 2008; Goodrick and Hanley, 2009), whilst the North Atlantic Oscillation (NAO); Arctic Oscillation (AO) and East Atlantic (EA) climate modes are linked to higher evaporative demand in the Southeast – which can increase the likelihood of wildfire (Martens et al., 2018; Cardil et al., 2023). La Niña has also been linked to severe wildfire danger in the southern Great Plains (Lindley et al., 2014; NIFC 2024a) due to vegetation becoming drier in response to droughts (Puxley et al., 2024) associated with La Niña events (Schubert et al., 2004). However, there are no long studies based on long records that firmly establish a link between wildfire and ENSO or any other climate mode in the region.

Site-based tree-ring records can be used to identify robust, long-term relationships between climate modes and wildfire, but are limited in their geographical coverage. Remotely sensed

burned area or state fire records provide more continuous geographical coverage but the small sample size, given the highly stochastic nature of wildfire events, both reduces the probability of obtaining statistically significant relationships between wildfire and climate modes, and introduces a higher risk of spurious correlations due to random variability, especially for longer period modes.

The lack of statistically significant relationships between wildfire and climate modes during the past three decades either in observed (Short et al., 2022; Supplementary Figures 2.2, 2.4) or reanalysis-driven modelled wildfires (Supplementary Figures 2.1, 2.2) reflects the small sample size. Large ensemble (LE) methods, widely used to study other climate impacts (Coburn et al., 2024; Swain et al., 2020; Lopez et al., 2018), overcome the sample-size issue and provide an alternative way of quantifying the relationships between wildfire and climate modes. Thus, using an LE together with a probabilistic model of wildfire occurrence facilitates an assessment of the geographical variation in the relationship between climate modes and wildfire, the strength of these relationships, and how they may be affected by climate change. Here, we investigate the effect of climate modes on US wildfire based on a 1600-year ensemble of modelled annual wildfire occurrence in the contiguous US for two decade-long time slices: the recent (2000-2009) climate and a future climate subject to an additional +2°C global warming. We first identify the most influential modes based on their areal impact under recent climate conditions, and show that their effect is physically plausible. Next, we examine how the magnitude of their effect varies geographically and how they influence fire season length and timing. We also test multivariate effects with ENSO. Finally, we examine how future climate change reduces or increases the area affected and the magnitude of that impact.

4.2 Data and Methods

4.2.1 The Wildfire Occurrence Model

We used a wildfire occurrence model (full description – Keeping et al., 2024) trained on wildfire occurrence data (Short et al., 2022) to model the daily probability of a wildfire greater than 0.1 hectares in extent at 0.1° spatial resolution. This model uses a generalised linear modelling framework but employs a flexible variable selection algorithm to find the optimal set of predictors from a suite of candidate variables related to climate, vegetation, and human factors influencing wildfire, and then optimises the domain of influence of each of the selected variables. In the original derivation of the model 47 candidate predictors were used, but here

we retrained the model starting from 31 candidate predictors for which temporally-varying data were available (per Keeping et al., 2025).

The final selected predictors were cropland fraction, needleleaf fraction, shrub fraction, gross primary production (GPP) in the previous 50 days and the previous year, rural population density, diurnal temperature range, precipitation on that day and in the previous five days, mean daytime windspeed, snow cover fraction, mean daytime vapour pressure deficit (VPD). Lightning ignitions were not included in the model; including convective atmospheric potential energy as a predictor of lightning was assessed but not selected. Meteorological and vegetation properties influence both fuel availability and fuel drying. The inclusion of two GPP terms takes account of both recent and longer-term fuel accumulation. The inclusion of cropland fraction and population density implicitly account for human impacts on wildfire occurrence through ignitions and fragmentation. Although fuel removal or the legacies of fire suppression on fuel accumulation are not take into account explicitly, these are implicit in so far as they are reflected in the fire occurrence data on which the model was trained. The domain over which each variable influences wildfire likelihood was optimised separately. The outputs are then power-law rescaled to minimise the tendency for generalised linear models to underestimate wildfire extremes (Forrest et al., 2024). The model is applied in the recent climate (overlapping with the training period) and in a future climate subject to +2°C global warming. At coarser spatial and temporal resolutions, this could create bias due to out of sample future conditions. However, because the model is trained on daily data across all environments in the contiguous US, almost all days and locations in the +2°C time-slice will have and analogue, or near analogue, in the training data.

The model was tested against wildfire occurrence data (Short et al., 2022) and, when run using reanalysis data (1992-2020), showed good discrimination in its predictions of wildfire events. The reduced variable model performed within the range of the Pareto superior subset of original model training runs (Keeping et al., 2024) across all benchmarks. The area under the receiver operating curve (AUC) score is 0.89, substantially greater than the 0.8 value considered to indicate a good model (McCune et al., 2002). It also reproduced the geographic patterns in wildfire occurrence (Supplementary Figure 3.1; normalised mean error, NME = 0.46), as well as the seasonal concentration (NME = 0.78) and timing of the wildfire season (mean phase difference = 0.13) and the interannual variability (NME = 0.67) in the number of wildfires.

4.2.2 KNMI-LENTIS Derived Inputs and Bias Correction

KNMI-LENTIS (Muntjewerf et al., 2023) is a time-slice single-model initial-condition large ensemble of the EC-Earth3 climate model (Döscher et al., 2022). The pre-industrial spin-up was sampled at 25-year intervals to obtain starting points for 16 transient simulations that were run from the pre-industrial (1850 CE) to the end of the 21st century with historical and SSP2-4.5 forcings. Ensemble members were then derived for 2000-2009 (referred to here as recent) and 2075-2084 (referred to here as future and corresponding to approximately +2°C additional global warming compared to the recent climate), by subjecting each of the 16 transient runs to nine micro-perturbations in global temperature (<5·10-5 K) at the start of each decade. Together with the original transient run, this yielded 10 decade-long simulations, providing 160 ensemble members for each time slice. The 25-year sampling of the macro-perturbations ensures a good sampling of decadal to multidecadal climate oscillations such as the AMO in each ensemble time-slice. Shorter period oscillations such as ENSO are understood to diverge based on initial conditions within a year (Neelin, 2010). EC-Earth3 represents historical trends in precipitation, land-surface temperature and blocking-frequency over the contiguous US well (Döscher et al., 2022). The version used in KNMI-LENTIS was further tuned to improve model performance in the northern hemisphere by reducing a cold bias (Muntjewerf et al., 2023).

The climate predictors from KNMI-LENTIS needed for the wildfire occurrence model were bias- corrected using ERA5-Land reanalysis data (Muñoz-Sabater et al., 2021) and downscaled to 0.1° following the methodology used in Keeping et al. (2025) (Supplementary Section 4). GPP was predicted using a light-use efficiency model (the P model – Wang et al., 2017; Stocker et al., 2020) that simulates photosynthesis, accounting for temporal acclimation of carboxylation and stomatal conductance to environmental conditions. The temperature, VPD, air pressure, incident photosynthetic flux density, and CO_2 concentration inputs to the P model were taken from the bias-corrected and downscaled KNMI-LENTIS ensemble. The fraction of absorbed photosynthetically active radiation (fAPAR) was derived using Beer's law from simulations of the seasonal cycle of leaf area index (LAI), based on the reciprocity between LAI and GPP (Zhou et al., 2024). Annual antecedent GPP is used in the wildfire occurrence model; to calculate this for the first year, the first year of each decade in the climate ensemble was repeated (following Van der Wiel et al., 2019).

4.2.3 Climate Mode Calculation

We initially considered all climate modes thought to influence wildfire danger or evaporative demand over the contiguous US with an annual or longer oscillation timescale, based on previous literature. Climate modes were derived using monthly sea-level pressure (SLP) and sea surface temperature (SST) fields from KNMI-LENTIS. Geopotential height is often used to calculate pressure-based climate modes but was not available for KNMI-LENTIS, so SLP was used instead. Climate mode indices were calculated separately in the recent and +2°C ensembles, in order to represent the effects of variability within the two climates. Modes derived using principal components were checked to ensure they showed the correct sign of effect on their associated SLP or SST trends. The phenomena associated with each climate mode (as defined in Table 1) and their effect on US meteorology are both well-represented compared to observations – refer to Supplementary Section 5 for a complete overview.

Table 1: An overview of the 11 modes considered in this analysis, with the information given on the variable used; the method by which each monthly mode is calculated; and the method by which the annual value of the mode was found.

Mode	Index	Field	Monthly Calculation Method	Annual Index Calculation
El Niño Southern Oscillation (ENSO)	Equatorial Southern Oscillation Index (SOI)	SLP	The difference between the monthly Indo-Pacific [5°S-5°N, 90°E-140°E] and Eastern Pacific [5°S-5°N, 80°W-130°W] standardised anomalies. NOAA (2009).	Monthly values averaged annually
Indian Ocean Dipole (IOD)	Dipole Mode Index (DMI)	SST	The standardised difference between the West [10°S-10°N, 50°E-70°E] and East [10°S-0°N, 90°E-110°E] Indian Ocean anomalies. Saji and Yamagata (2003).	Monthly values averaged annually
Pacific Decadal Oscillation (PDO)	PDO Index	SST	The leading principal component of the SST anomaly over the North Pacific [20°N-70°N, 120°E-100°W]. Newman et al. (2016).	The November to March (NDJFM) mean of the index starting in the previous year
Tropical North Atlantic (TNA)	TNA Index	SST	The monthly anomaly in the North Tropical Atlantic [5°N-25°N, 55°W-15°W]. Enfield et al. (1999).	Monthly values averaged annually

Tropical South Atlantic (TSA)	TSA Index	SST	The monthly anomaly in the South Tropical Atlantic [20°S-0°N, 30°W-10°E]. Enfield et al. (1999).	Monthly values averaged annually
North Atlantic Oscillation (NAO)	NAO Index	SLP	The leading principal component of the monthly anomaly over the North Atlantic [20°N-80°N, 90°W-40°E]. Thornton et al. (2023).	The December to February (DJF) mean of the index starting in the previous year.
East Atlantic (EA)	EA Index	SLP	The second principal component of the monthly anomaly over the North Atlantic [20°N-80°N, 90°W-40°E]. Thornton et al. (2023).	The November to January (NDJ) mean of the index starting in the previous year.
Arctic Oscillation (AO)	AO Index	SLP	The leading principal component of the monthly anomaly north of 20°N. NOAA (2025).	The DJF mean of the index starting in the previous year
Pacific/North American (PNA)	PNA Index	SLP	The leading principal component of the DJF-mean of monthly anomalies over the North Pacific and North America [20°–90°N, 120°E−120°W]. Mori et al. (2024).	The calculation of the DJF mean, starting in the previous year, was taken before the leading principal component was calculated.
Atlantic Multidecadal Oscillation (AMO)	AMO Index	SST	The difference between the annual SST anomalies of the Atlantic [0°N-60°N, 75°W-7.5°W] and the rest of the global ocean. Enfield et al. (2001).	N/A
Southern Annular Mode (SAM)	SAM Index	SLP	The leading principal component of anomalised SLP south of 20°S. NOAA (2025).	The June to August (JJA) mean

4.2.4 Comparison of Climate Mode Effect on US Weather in LE and Reanalysis

A high-resolution wildfire occurrence record is available in the contiguous US from satellite data after 1984 (Eidenshink et al., 2007) or from aggregated state and federal records after 1992 (Short, 2022). This short reanalysis period is not sufficient to capture the major effects of each

climate mode over the contiguous US (Figure 1). The correlation coefficients of climate mode indices and US temperature and precipitation show that there is a large spread in the apparent correlation when 30-year samples from the ensemble are drawn. In most cases, the sign of the observed correlation could be switched and it would still lie within the 95% confidence interval of the model ensemble. The one clear exception is ENSO (note that our ENSO index is the SO index, so the sign is opposite to an SST-based index), where the sign is clear although the magnitude is highly uncertain. This short time period is therefore insufficient to robustly characterise the effect of each mode – justifying the use of modelled wildfires driven by the LE. EC-Earth3 performs well in its representation of ENSO, the NAO and the PNA (Döscher et al., 2022) which are all key controls on North American weather patterns. Comparison of annual US weather and climate mode values between the reanalysis and ensemble (Supplementary Figure 6.2) shows no apparent discrepancies, and strong associations between modes (the TNA, IOD and ENSO) are equally present in the reanalysis and ensemble data (Supplementary Figure 6.1).

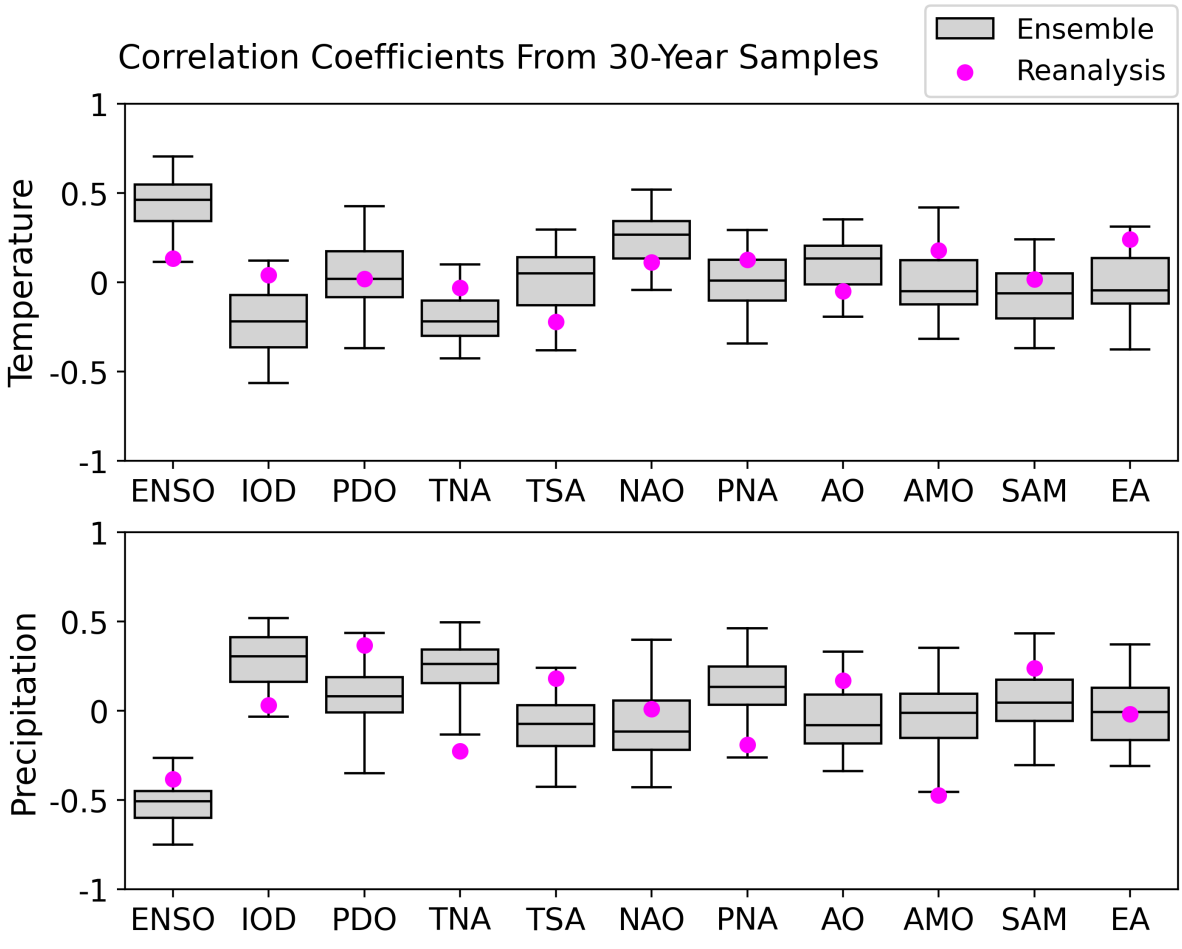

Figure 1: Boxplots of each quartile of the distribution of correlation coefficients between climate mode indices and temperature (upper panel) and precipitation (lower panel) over samples of the recent climate ensemble, and the values from the reanalysis over 1990-2019 (pink dots). To construct the distribution behind the box plots, random samples of 30 years were taken from the ensemble. The outer limits of the boxplots represent the 2.5th and 97.5th percentiles, and the three internal lines correspond to the 25th, 50th and 75th percentiles of the bootstrapped distribution.

4.2.5 Relating Climate Modes to Annual Wildfires

The daily ensemble of modelled wildfire occurrence probabilities was averaged annually for comparison with the yearly phase of each climate mode – though seasonal responses were also checked, see Supplementary Section 7. The positive and negative phase of each climate mode was defined as occurring when its annual-mean index value was a half-standard deviation greater or lesser than zero, respectively; and was otherwise considered to be neutral. Simulated annual wildfire occurrence, aggregated to 0.5°, was regressed against the numerical value of each climate mode index. The relationship found by this regression was only considered in the analysis if it passed a false discovery rate corrected significance level of 0.01, per Wilks (2016). The sign of the climate mode's effect was determined from the regression slope coefficient. The lagged effect of each index on wildfire was also tested by using the index value from the previous year. When mapping geographic patterns in the magnitude of each mode's association with wildfires, the ratio between the number of modelled wildfires in each phase of the mode relative to the mean number at that grid-cell was plotted.

4.2.6 Definition of Fire Season Peak and Length

To determine the effect of climate modes on the peak timing of the fire season, the seasonality was characterised according to Kelley et al. (2013). The wildfire season's mean phase was determined for each grid-cell from the sum of monthly vectors oriented in the complex plane with angles corresponding to the time of year and magnitude proportional to the number of wildfires. The seasonal concentration was defined as the length of that resultant vector, varying between 0 (wildfires equally spread between months) and 1 (all wildfires in one month). The effect on the timing of the seasonal peak was calculated according to the difference between the mean phase over all years and over years in the positive or negative phase of each index. Locations with a seasonal concentration of less than 0.15 were not considered to have a distinct

peak, so were excluded. The effect of climate modes on the length of the fire season was also determined relative to the average annual peak in the fire season, or the ensemble mean of the maximum wildfire month at each location. The mean number of months for which the number of wildfires exceeded half of that average annual peak was defined as the length of the fire season (per Jolly et al., 2015; Abatzoglou et al., 2019).

4.3 Results

4.3.1 Survey of the Modes

The climate modes that show the greatest area of significant (p-value of < 0.01 after controlling for multiple testing) association with wildfire (Figure 2, Table 2) are ENSO, the IOD and annually lagged TNA (TNA+1). The La Niña phase of ENSO has a positive influence on wildfire probability over 91% of the contiguous US. The negative IOD and positive TNA+1 have similarly large areas of significant influence, affecting 90% and 85% respectively. Both of these modes are correlated with (correlation coefficients of -0.61 and -0.32 in the recent ensemble) and causally related to ENSO (Ham et al., 2017; Jiang and Li, 2019). The robustness of the influence of these three modes on US wildfire (Supplementary Section 7), taking a stricter significance threshold of 5.7×10^{-7} (the 5-sigma p-value for a Gaussian distribution), shows that the areal influence of ENSO, IOD and TNA+1 is persistent over most of the US.

Other climate modes exert a significant influence on wildfire but over more limited regions. Eleven modes have a significant influence over an area >20% of the contiguous US: ENSO, IOD, TNA+1, PDO+1, ENSO+1, TNA, AMO+1, TSA, PDO, NAO, and NAO+1. At the stricter significance threshold (Supplementary Section 7), the only modes showing persistent areas of influence on wildfires other than the TNA, IOD and ENSO are the PDO, AMO and NAO. The PDO also has the next most significant control on the distribution of the annual number of wildfires. Of the top eleven modes in areal significance, the TNA, PDO, NAO and ENSO influence wildfire both in the same year and with a one-year lag. For geographical analysis (Figures 4 and 9) we consider the top eight modes by areal influence in the recent time-slice of the LE, eliminating the less influential of each of the unlagged or lagged modes. The top eight modes were ENSO, IOD, TNA+1, PDO+1, AMO+1, TSA, NAO, and PNA. The area influenced by these modes is greatest in the summer, June-August, except for the TSA which has the greatest influence in the spring, March-May (Supplementary Section 7). The AO only

influences a small area (8%) and the SAM+1 only influences 5% of the contiguous US. The EA does not have a significant areal impact.

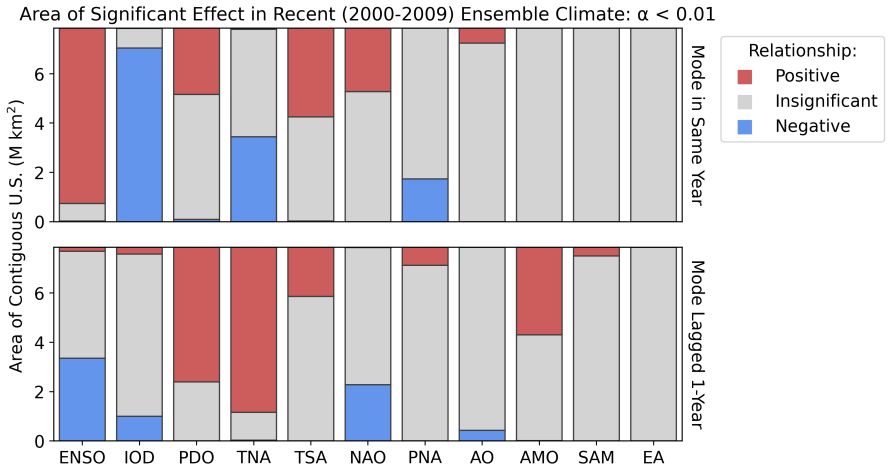

Figure 2: The area of the contiguous US significantly affected by each climate mode. Significance was determined using an FDR corrected significance threshold after Wilks (2016) to a control level of 0.01. The sign of the relationship between the index and the annual number of wildfires is given by the slope of the regression.

Table 2: Percentage of contiguous US area significantly affected by each mode in the recent climate (2000-2009). Two asterisks indicate an area over 50%, one asterisk an area over 20%.

Mode	Area of Effect (Same Year) [%]			Area of Effect (Prior Year) [%]		
	N/A	Positive	Negative	N/A	Positive	Negative
ENSO	9.0	**90.7	0.4	55.3	2.0	*42.7
IOD	10.1	0.2	**89.8	83.7	3.5	12.8
PDO	64.5	*34.3	1.2	30.4	**69.6	0.0
TNA	55.5	0.6	*43.8	14.3	**85.3	0.4
TSA	53.8	*46.0	0.3	74.6	*25.4	0.1
NAO	67.2	*32.8	0.0	70.8	0.1	*29.1
PNA	77.8	0.0	*22.2	90.7	9.3	0.0
AO	92.1	7.9	0.0	94.5	0.0	5.5
AMO	100.0	0.0	0.0	54.7	*45.2	0.1
SAM	100.0	0.0	0.0	95.5	4.5	0.0
EA	100.0	0.0	0.0	100.0	0.0	0.0

4.3.2 Effect of Key Modes

Given the plausibility of the effect of climate modes on US weather in EC-Earth3 (Figure 1, Supplementary Section 5) and the considerable extent of the effect of those modes on US wildfire (Figure 2, Table 2), there is a pertinent question as to the additional utility of the LE approach compared to reanalysis or observed data. There is no location in the US where a climate mode has a significant relationship with observed annual fire occurrences (Supplementary Figure 2.3). Reanalysis-driven modelled fire occurrences also show almost no area of effect (Supplementary Figure 2.1). Of the modes with the largest areas of statistically significant effect, very few climate mode phases result in an effect in the reanalysis significantly outside the distribution of random noise (Figure 3). Only three mode phases are associated with annual wildfire numbers outside of the 95% confidence interval of the bootstrapped distribution from all years. In: La Niña years (positive ENSO phase), El Niño years (negative ENSO phase), and when the prior year had a positive TNA phase. The extent to which these phases exceed the confidence interval is very low in comparison to the

highly significant margin provided by the LE (Supplementary Figure 2.5), due to the different sample sizes.

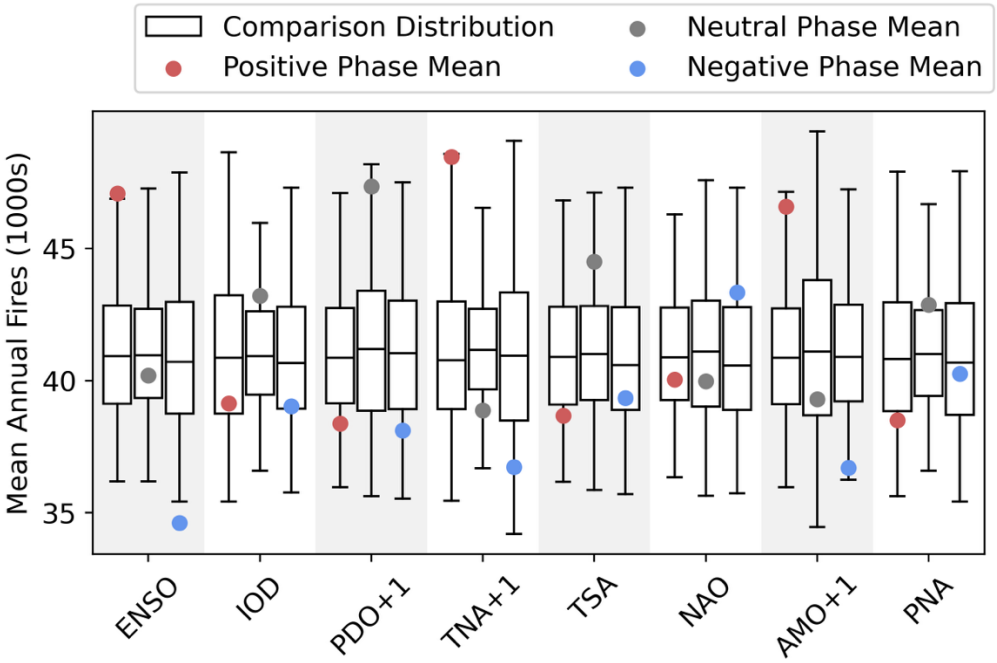

Figure 3: The distribution of the modelled annual number of wildfires for the reanalysis (1990-2019) under different mode phases compared to the distribution of all years, per Shen et al. (2025). The dots show the actual mean value of modelled annual fires. The boxplots show the distribution of the mean number of annual fires, drawn from the distribution of years but with the same sample size as the number of years in that phase in the reanalysis period – repeated 10,000 times. The outer limits of the boxplots represent the 2.5th and 97.5th percentiles, and the three internal lines correspond to the 25th, 50th and 75th percentiles of the bootstrapped distribution.

ENSO has a positive effect on total annual US wildfires in the La Niña phase (Figure 4), with the three areas of greatest relative increase in wildfire occurrence rates being Mediterranean California, the central Great Plains, and southern Florida. The only areas where ENSO has no significant influence on annual wildfire occurrence are in the northwestern and northeastern US. The negative IOD and positive TNA+1 show a very similar association with wildfire to La Niña. The NAO and PNA havepositive and negative impacts on annual wildfires in the southwestern and inland northwestern US respectively. The PDO+1 has a positive influence across the US. The AMO+1 affects a large area in the West and has a localised influence in

southern Florida. ENSO+1 has a strong influence of wildfire occurrence along the southern US border (Supplementary Section 7) – through a control on GPP due to its association with precipitation in this region (see Figure 6). The TNA also shows a substantial effect associated with an increased number of wildfires in the West (including in the northwestern US) and in Florida.

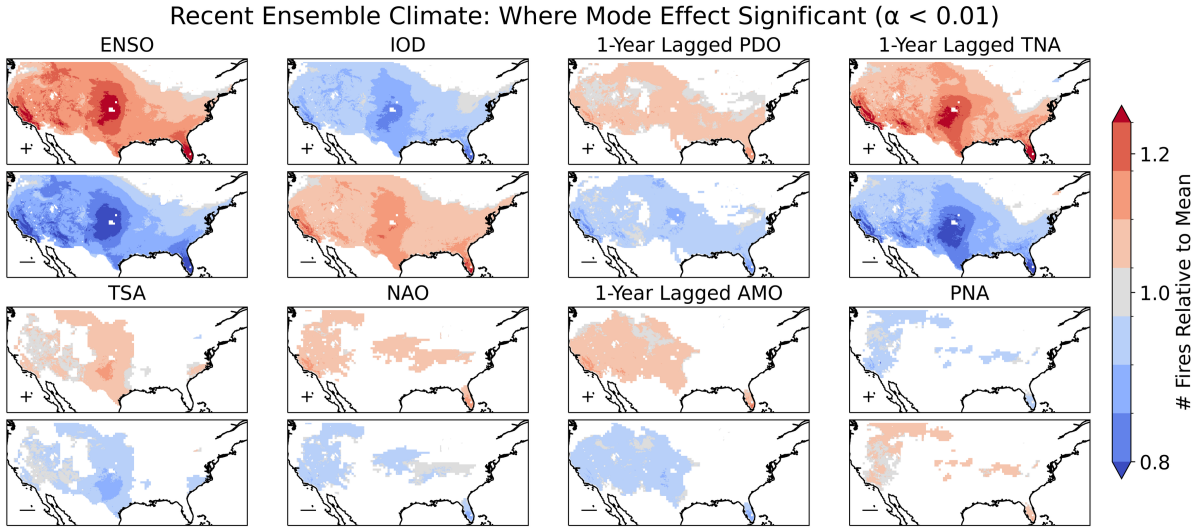

Figure 4: Maps of the effect of each climate mode on annual wildfires relative to the mean. The sign and magnitude of the relationship is given by the ratio between the annual number of wildfires in the positive (upper panels) or negative (lower panels) phase – defined as beyond plus or minus half a standard deviation from the mean respectively. The effect of each mode is shown relative to the mean annual number of wildfires – to account for any non-linearity in the effect between phases that would not be captured by linear regression. The relationship is only shown for locations where there is a significant relationship, as identified by linear regression between the index and annual number of wildfires at that location.

La Niña, the negative IOD and positive TNA+1 all show a very similar association with wildfire. The positive phase of the TNA+1 and negative phase of the IOD are associated with increased wildfire occurrences when considered alone (Figure 4). In these phases, the total number of wildfires in the contiguous US is found to increase by 14% and 12% respectively (Table 3). However, both modes are correlated to ENSO (Supplementary Section 6), and the effect of both modes decreases substantially after controlling for the phase of ENSO, from 14% to 5-8% for the positive phase of the TNA+1 and from 12% to 2-3% for the negative phase of the IOD. The biggest impact of both the negative phase of the TNA+1 and positive phase of the

IOD is on wildfire in La Niña years, where the mean number of wildfires is decreased by 12% and 9% respectively.

A multilinear regression (MLR) of annual wildfires (Figure 5) against index values of ENSO, the IOD and TNA+1 finds that ENSO is the strongest pathway controlling interannual variability for wildfires in the contiguous US. The MLR slope coefficient for ENSO has the same pattern as the association between ENSO and wildfires when not controlling for the IOD or TNA+1. The TNA+1 also has substantial influence, having an additional effect on wildfires in Mediterranean California, the southwestern US, the southern Great Plains, and southern Florida. It follows a similar pattern of effect to the single-mode association of the TNA+1 and wildfires, though the magnitude of effect is smaller compared to ENSO. The IOD has a much weaker influence on wildfires, limited to low magnitude effects in the southwestern US.

Table 3: The effect of the TNA+1 and IOD climate modes on the number of wildfires in the contiguous US in each phase of ENSO and for all years, in the recent climate time-slice of the ensemble. The sample size each percentage is based on is given in brackets.

		# Fires (3 s.f.)	TNA+1 Phase		IOD Phase	
			Positive	Negative	Positive	Negative
ENSO Phase	La Niña	44,600	+7.7% (207)	-11.9% (71)	-8.8% (23)	+3.2% (294)
	Neutral	37,700	+4.9% (145)	-6.1% (169)	-1.4% (180)	+2.2% (141)
	El Niño	32,800	+6.1% (69)	-5.2% (210)	-0.9% (273)	+3.4% (72)
All Years		37,800	+13.6% (421)	-10.1% (450)	-8.4% (476)	+11.7% (507)

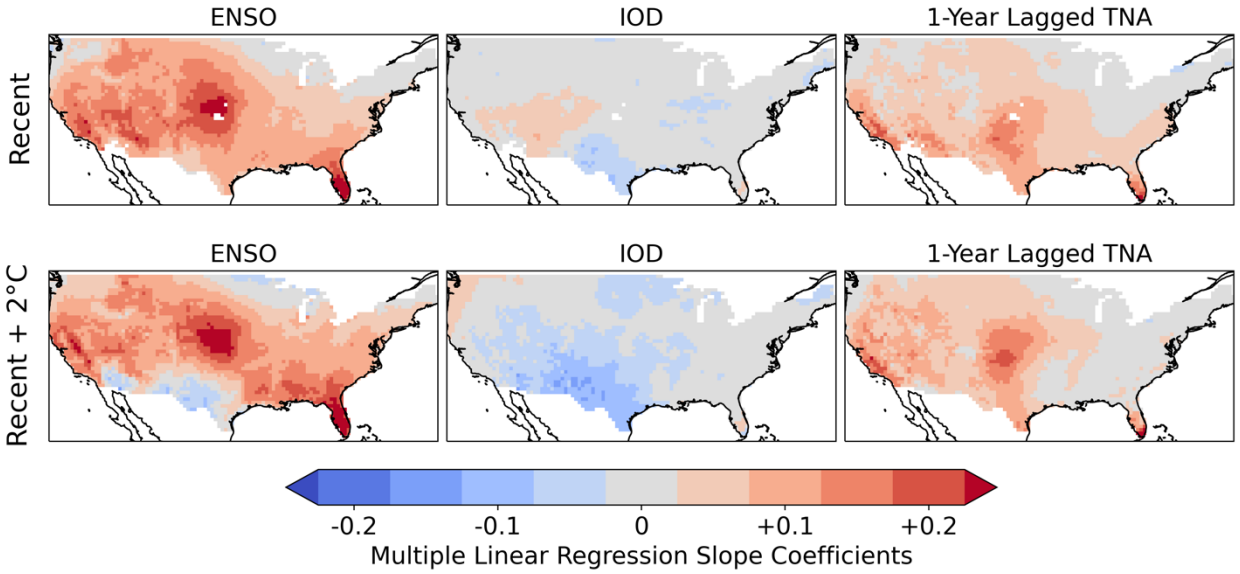

Figure 5: Multilinear regression of the annual number of wildfires relative to the mean at each grid cell against standardised values of the ENSO (SOI), IOD (DMI), and TNA+1 indices. The slope coefficients were separately calculated for each grid-cell, and are displayed for the recent and +2°C ensemble climates.

The association between ENSO and wildfire occurrences reflects the influence of ENSO on VPD and precipitation, where precipitation is also strongly linked to annual patterns in vegetation growth and fuel accumulation (Figure 6). The region associated with a strong wildfire occurrence response to ENSO in the Great Plains has a stronger VPD anomaly while in the southwestern US, the impact of ENSO on wildfire is associated with a stronger precipitation anomaly. Other modes also influence wildfires through their impacts on VPD, precipitation and GPP (Supplementary Figure 8.1).

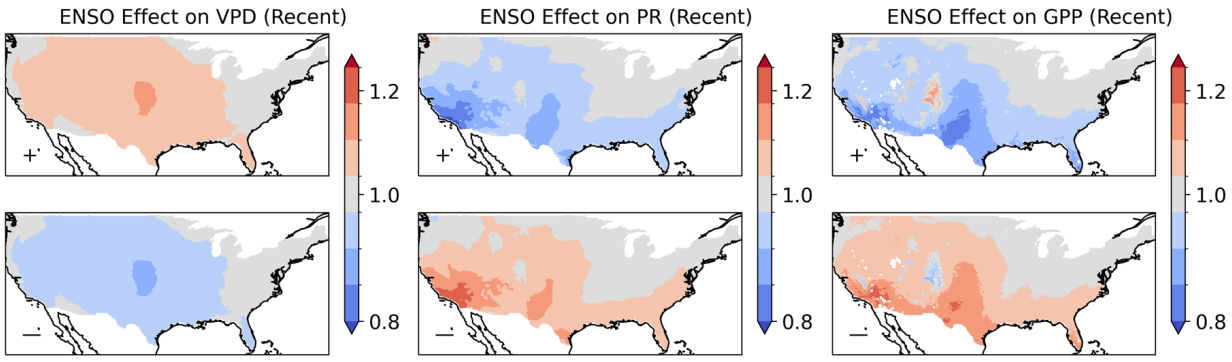

Figure 6: the relative influence of ENSO on VPD, precipitation and GPP in the recent climate for the large ensemble.

The response of the statistical distribution of annual wildfire occurrence to a climate mode varies geographically (Figure 7). The effect of ENSO on wildfires in the Great Basin, for example, produces a shift in the distribution but has limited impact on the spread. In contrast, the effect of ENSO in Southern California is to extend the spread of the distribution giving rise to an increase in the likelihood of extreme fire-years relative to the mean. There are also distinct geographic effects on wildfire distribution under ENSO, TNA+1, PNA, PDO+1 and IOD (Supplementary Section 9).

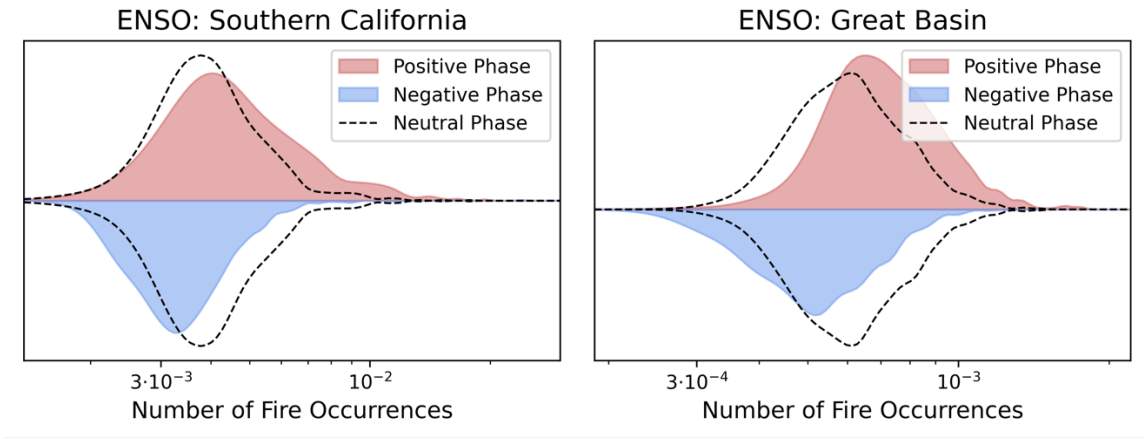

Figure 7: The frequency distribution of the modelled annual number of wildfires per km^2 across the 1600 recent climate ensemble years in the Great Basin and Southern California NIFC Geographic Area Coordination Centres (GACC) defined regions (Supplementary Figure 3.2). The distributions are plotted separately for the positive (La Niña) and negative (El Niño) phase of ENSO, with the neutral phase shown as a dashed line for comparison.

Climate modes do not have a uniform effect on meteorology, or consequent wildfire danger, throughout the year (Supplementary Section 7). ENSO has a strong impact on the length of the wildfire season (Figure 8), with increased season length in La Niña years in Mediterranean California, the Arizonan Mountains, the Great Plains and southern Florida. This contributes to the high annual numbers of wildfires in those regions (Figure 4). The effect of ENSO on the peak of the fire season is less uniform and shows an east/west divide: El Niño (La Niña) results in an earlier (later) peak to the fire season in areas to the east of the southern Great Plains, but El Niño (La Niña) results in a later (earlier) peak in the southwestern US. The effect of El Niño on the timing of the seasonal peak is stronger than that of La Niña, with La Niña increasing the frequency of wildfire occurrence in both regions and bringing the early-spring (east) and late-summer (west) fire season peaks closer together. The IOD and TNA+1 have a very similar effect

on fire seasonality to ENSO, whilst the remaining modes have limited effects on the fire seasonality (Supplementary Section 10), though the PDO+, PNA- and NAO+ phases are associated with a half-month earlier peak to the Californian fire season.

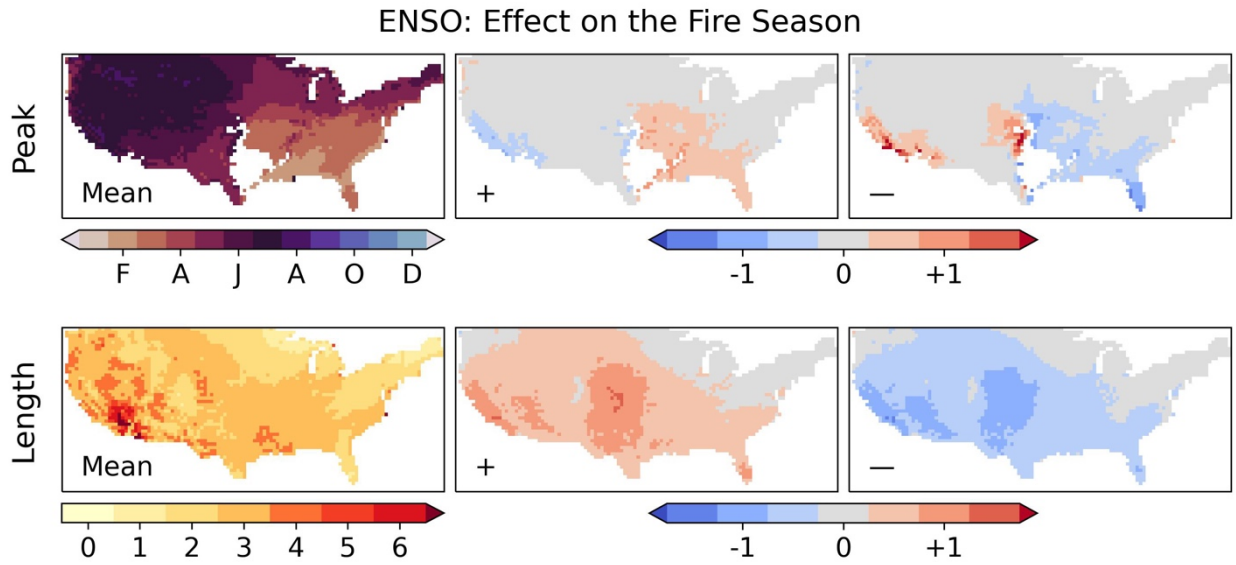

Figure 8: Top row: (left) the average seasonal phase across all locations with a seasonal concentration >0.15; (central) the average seasonal phase for all years subtracted from the average of years in the positive (La Niña) phase; (right) the average seasonal phase for all years subtracted from the average of years in the negative (El Niño) phase. Bottom row: (left) the length of the fire season in months (calculated as the number of months over the mean annual half-maximum); (central) the average season length for all years subtracted from the average of years in the positive (La Niña) phase; (right) the average season length for all years subtracted from the average of years in the negative (El Niño) phase.

4.3.3 Changes in the Effect of Global Climate Modes in a Warmer Climate

An additional +2°C increase in global mean temperature in KNMI-LENTIS results in changes to the areal extent of the significant influence of many of the climate modes on wildfire occurrences (Figure 9). There were only a few cases when the influence of a mode on wildfire changed from positive to negative, but cases where the impact of a mode changed from insignificant to significant were widespread. The AMO+1 and PNA show the greatest expansion in the area of significant effect, increasing from 38 to 68% and 16 to 56% respectively (Supplementary Section 11). Some other modes show a persistent influence in the areas they affect under recent conditions with only a slight expansion: ENSO (89 to 92%), the IOD (87 to 92%), and the TNA+1 (82 to 87%). There is also a significant expansion in the area of

significant influence on wildfire for the ENSO+1, TNA, NAO+1, AMO and AO indices. However, the TSA has no area of significant influence in the future climate, and the area of influence of the NAO shifts from the western to the central US (Supplementary Section 11).

There is a minor but statistically significant shift in the skewness of the ENSO distribution in response to warming (Supplementary Figure 5.15). However, comparing the effect on annual fires of the unaltered ENSO in the future climate, and of the future distribution mapped to percentiles in the recent climate revealed no substantial change in the effect of ENSO on wildfire occurrences due to this shift. This suggests that ENSO's projected effect on fire is mainly due to an increase in the intensity of ENSO's effect on rainfall (Figures 6 and 11) over North America, in line with consensus expectations (IPCC, 2021).

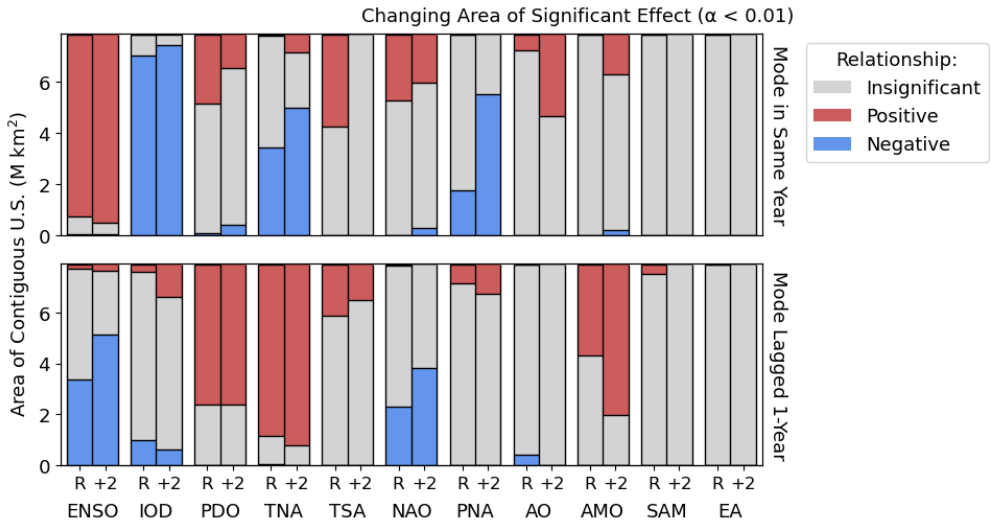

Figure 9. Difference in the significant areal influence of each climate mode in the same year and with a one-year lag between the recent ensemble (R) and the +2°C ensemble (+2). The areas are given in Supplementary Section 11. If the colour is the same in both R and +2, then the effect of the mode in that area stays the same; if the colour changes, this indicates that the effect of the mode in that area changes between the two ensemble climates.

Despite some climate modes being substantial controls on the internal variability in annual fire occurrences, the effect of – for example – La Niña in the present climate is significantly less than the effect of a further +2°C global warming (Supplementary Figure 11.10). However, in the future climate the effect of La Niña relative to the higher rate of fire activity is nonetheless projected to increase. The change in strength of the relationship between modes and the annual number of wildfires varies geographically (Figure 10). The AMO+1 and TNA+1 show the most substantial increase in the effect of their positive phase on the annual number of wildfires; both

strengthen most over the Great Plains and in the West. The positive TNA+1 and La Niña both show a weakening in their influence on annual wildfire occurrences along the southern border with Mexico, most substantially in Texas. In contrast, the negative phase of the IOD has a strengthened effect on wildfire occurrences along the southern border, strongest in Arizona and New Mexico.

The PDO+1 strengthens in its association with wildfire occurrences across its area of significant influence, with the strengthening most over the Great Plains and in California. The influence on the annual number of wildfires relative to the mean, and the area of influence of the AO and PNA (Supplementary Section 11) significantly increase, with the greatest relative increase over the Great Plains. The AMO+1, TNA+1, PNA, PDO+1, IOD, ENSO and AO modes all strengthen in their influence over the majority of the region they affected in the recent climate. As the effect of the modes in the +2°C time-slice is calculated relative to a higher mean rate of wildfire in the +2°C climate, this means the control of these global climate modes on wildfire increases even relative to the higher future interannual variability of wildfire.

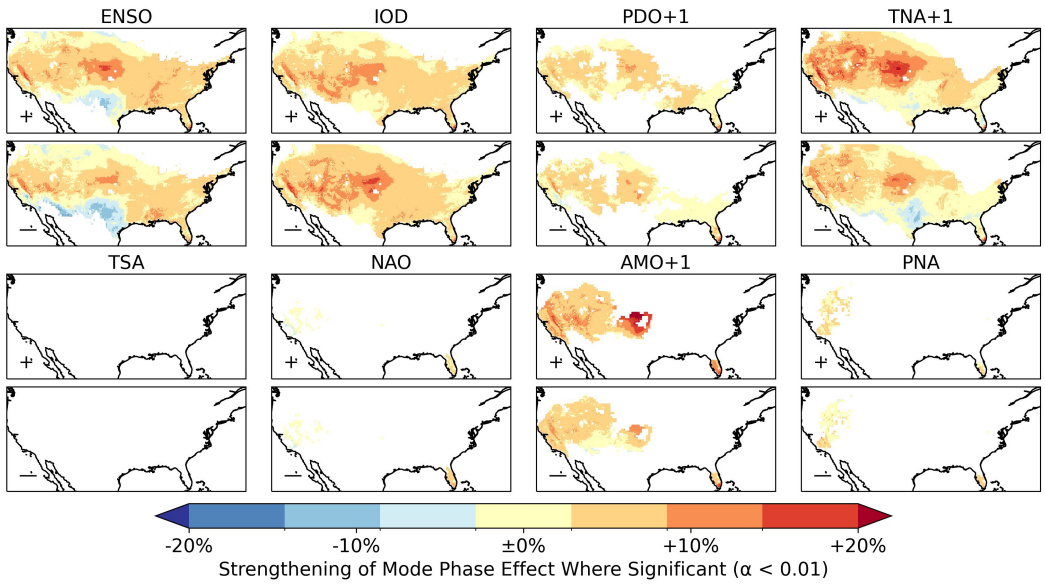

Figure 10: The strengthening or weakening of the effect of each climate mode in both phases between the recent climate and +2°C climate time-slices. Each panel shows the ratio between recent climate and the +2°C climate for the number of annual wildfires in that phase of the global climate mode relative to the mean at that location. Only regions where the effect of the mode is significant at α < 0.01 according to linear regression in both time-slices are shown.

Climate change drives a strong intensification of the relative effect of ENSO on VPD over the Great Plains (Figure 11) – corresponding to where the greatest intensification of ENSO is also modelled (Figure 10). The effect of ENSO on southwestern US precipitation is also projected to intensify with climate change, however the association with wildfire decreases in the same region. This could be explained by the diminishing effect of annual-timescale variability dryness on wildfire danger in an increasingly arid and fuel-limited environment (Abatzoglou and Williams, 2016).

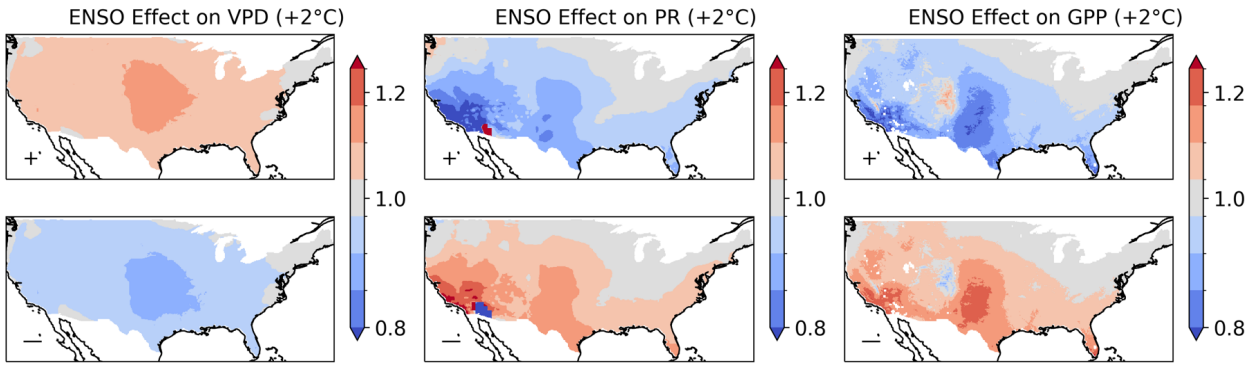

Figure 11: the relative influence of ENSO on VPD, precipitation and GPP in the +2°C climate for the large ensemble.

4.4 Discussion

Our analyses have shown that ENSO, IOD and TNA+1 are the global climate modes most associated with interannual variability in wildfire occurrence in the contiguous US. ENSO has a significant influence over 91% of the country, consistent with its use in predicting wildfire severity across the US (NIFC, 2024a,b). La Niña strongly increases annual wildfire probability over California, the interior southwestern US, the Great Plains, and southern Florida. La Niña years have been associated with increased wildfire activity in the southwestern US due to reduced precipitation (Margolis and Swetnam, 2013; Mason et al., 2017; Westerling and Swetnam, 2003), as well as in the southeastern states of Mississippi (Dixon et al., 2008) and Florida (Goodrick and Hanley, 2009). La Niña has also been associated with severe wildfires in the southern Great Plains (Lindley et al., 2014). However, we only identify a moderate effect of La Niña on wildfire occurrence for most of the southeastern US, with a highly localised effect over southern Florida. This could be explained by the strength of the effect of ENSO on precipitation (and consequent higher GPP) in the southwestern US and Florida, compared to a lesser effect over the wider southeastern US. We also identify a well-defined hotspot for the effect of La Niña on wildfire in the Great Plains, where ENSO has been linked qualitatively to wildfires (Lindley et al., 2014). VPD shows a strong response to ENSO over the Great Plains, with the increased hot, dry conditions in La Niña years therefore a likely primary contributor to the enhanced wildfire likelihood. The effect of La Niña relative to the mean wildfire rate intensifies with climate change over the Great Plains and California.

The negative IOD and positive TNA+1 show a very similar pattern of effect to La Niña when considered independently, with the TNA+1 having a greater effect. The TNA+1 and IOD are causally linked (Wang et al., 2021; Ham et al., 2013; Hameed et al., 2018; Jiang and Li, 2019) and correlated with ENSO; and the similarity of their influence on wildfire raises questions about the extent to which they are simply proxies for the phase of ENSO. Our MLR analyses show that while ENSO has the greatest influence on wildfire variability, TNA+1 also has an independent though smaller effect while the IOD has only a limited impact in the region near the US-Mexico border. The correlation of the TNA+1 and the IOD with ENSO preclude a definite attribution of the causal influence of each mode on wildfire occurrence. However, our analyses suggest that the strongest apparent pathway of influence is via ENSO and TNA+1. Although the TNA and IOD have been closely associated with burnt area at a global scale (Cardil et al., 2023), their impact of wildfires in the US has been largely ignored.

ENSO creates a moisture dipole between the northwestern and southwestern US through influencing the latitude of the jet stream (Dettinger et al., 1998; Westerling and Swetnam, 2003). It has therefore been suggested that ENSO increases wildfire activity in the northwestern US in El Niño years (Barbero et al., 2015; Johnston et al., 2017). However, there is almost no statistically significant influence in this region in our simulation of 1600 years of annual wildfire occurrences in the recent and +2°C climates, with the positive effect of El Niño on northwestern US wildfire only statistically significant over a small region. There is a possibility that this is due to an unknown bias in EC-Earth3's representation of ENSO over the region, however assessment of the mode's behaviour and effect over the US does not reveal any obvious issues (Supplementary Section 5, Döscher et al., 2022) – with the moisture dipole represented in the model. Alternatively, this could be explained by most analysis in this region having focussed on fire frequency or burnt area. El Niño has a greater effect on fire size (Heyerdahl et al., 2002; Barbero et al., 2015), a distinct property from occurrence likelihood, which could be sufficient to explain the greater rates of fire frequency for El Niño years in the tree ring record. Links between wildfire occurrence and the PDO+ (Ascoli et al., 2020; Heyerdahl et al., 2002, Norman and Taylor, 2003; Schoennagel et al., 2005) and AMO+ (Ascoli et al., 2020; and Kitzberger et al., 2007) in the northwestern US are also not significant in our analyses.

The AMO+1 is an important control on wildfire likelihood over 38% of the contiguous US under recent conditions, particularly in the West and southern Florida. The impact of the AMO on wildfires in the +2°C time-slice increases considerably in the central US and along the East Coast, with a >25% increase in annual wildfire occurrences in the Great Plains and southern Florida.; the strengthened effect of AMO+1 on US wildfire occurrence indicates that the positive relationship between this mode and wildfire also applies to higher amplitudes of the oscillation. The AMO+1 and TNA+1 show the greatest strengthening in their effect with future warming, indicating that high Atlantic SSTs in the previous year are strongly associated with interannual wildfire variability under climate warming. The AMO+ has been linked to wildfire activity in the same year (Ascoli et al., 2020; and Kitzberger et al., 2007), but our analysis shows no significant effect in the recent climate and only a minor area of influence with warming. This might seem contradictory to its multidecadal effect, but when no low-pass filtering is applied to the AMO, annual oscillations between neutral and high positive or negative values occur in its multidecadal positive or negative phases respectively (Sutton and Hodson, 2007). Atlantic SSTs in the prior year have a greater effect on US wildfire than in the same year.

The Great Plains is the region where wildfires show the most sensitivity to variation in climate modes. There is a > 25% increase in annual wildfire occurrences under recent conditions with La Niña, the positive TNA+1 and the negative IOD. Wildfire is also increased to a similar extent by the positive AMO+1 in the +2°C time-slice. The PDO+1, PNA and AO, all anticipated to change with warming (Litzow et al., 2020; Ning and Bradley, 2016; Zhang et al., 2016; Choi et al., 2010), also have a significant impact on wildfire probability in this region. The sensitivity of the Great Plains to climate variability is in part due to meteorological effects on fire weather but also reflects the importance of vegetation type. Grassland and savanna vegetation have a strong response to climate variability: higher-than-normal antecedent precipitation increases fuel production and short-term droughts cause rapid drying of grassy vegetation (Littell et al., 2009; Archibald et al., 2009). The overall abundance of the vegetation may also contribute to this sensitivity. In the interior western US, for example, temperate sierras and forested mountains have a higher sensitivity to climate variability than the surrounding desert.

The climate mode indices were derived according to standard methods. The modes of variability in climate models might differ from those in the observational record. However, all the modes considered here are represented in the recent and +2°C ensembles, and show reasonable geographic patterns in terms of the associated SST or SLP anomalies and the expected precipitation anomalies over the contiguous US. The ensemble climate modes can therefore be considered phenomenologically similar to observations, and thus to have the same causal effects on wildfire likelihood. The periodicity of multi-year oscillations cannot be assessed from the decadal time-slices. However, the transient EC-Earth3 runs from which the time-slices were sourced show the expected periodicity for each mode, including the longer periodicities of the PDO and AMO. The PDO has much higher interannual variability than the AMO, resulting in a tendency for sub-decadal oscillations within a time slice. Whilst a low-pass filtering of the PDO (and AMO) time-series might provide a better representation of decadal to multidecadal effects, both the SST and the meteorological patterns associated with these modes was correct.

Climate modes are often correlated and can modulate the effect of other climate modes. This means that the association between a single climate mode and wildfire can also embed information on other climate modes that may be more directly causally linked to wildfire activity, as shown by the analysis of the TNA, IOD and ENSO. The impact of a particular mode on wildfires can be established through consideration of the mean effect in different phases, as shown for ENSO in the southwestern US. However, there may be mechanisms that disrupt the expected patterns of climate variability associated with a particular mode. One example of this

is the impact of years with exceptional atmospheric river activity over the southwestern US which led to a reversal of the expected precipitation patterns associated with La Niña and El Niño (Luna-Niño et al., 2025).

We used commonly used metrics (Jolly et al., 2015; Abatzoglou et al., 2019) to characterise the peak timing and length of the fire season. These were defined as the month with the most fires and any months with over half the annual maximum month respectively. However, it is difficult to characterise the seasonal peak in this way when there is a similar likelihood of wildfires across most of the year and this approach also does not resolve the effect of climate modes on bimodal fire seasons, such as in the Appalachian Mountains (Lafon et al., 2005). Defining the length of the fire season relative to the average value of the highest fire month at a given location is appropriate for local comparisons but makes it difficult to compare changes across regions with very different baseline fire regimes. The similar increase in the lengthening of the fire season in the Great Plains and Mediterranean California, for example, will have different consequences given that the occurrence of wildfires is lower in the Great Plains.

We used a wildfire probability model to link climate modes to annual wildfire occurrences. The model represents the probability of wildfire events over a 0.1-hectare threshold, but does not simulate other wildfire attributes such as size or intensity. Thus, the impact of changes in climate modes on wind patterns and storm tracks that can lead to extreme wildfires are not accounted for in this study. In addition to the climate drivers of wildfire probability, we included the impact of climate-driven changes in GPP on wildfires. However, other factors that influence the likelihood of wildfire occurrence such as fuel removal, previous wildfires or lightning ignitions are not taken into account. Some studies have identified different responses to climate depending on environment – for example a difference in response to seasonal VPD in forested and non-forested ecosystems in California (Williams et al., 2019). However, such difference in response can be explained by other environmental variables – for example the key limitation of fuel production on wildfire in dry, southwestern US ecosystems. Lightning was also not accounted for in the final occurrence model, due to the poor predictability of lightning from climate variables. Furthermore, while the wildfire probability model also includes predictors related to human activity, these were held constant in our analyses. Despite these limitations, the wildfire occurrence model used has good predictive capability (Keeping et al., 2024), and is responsive to trends and variability in meteorological drivers of wildfires whilst also accounting for other human and vegetation related effects.

This paper presents strong evidence for the utility of using multiple climate modes to supplement long-range fire season forecasts, with high utility from a risk management perspective. Recent progress in seasonal fire weather forecasting (Di Giuseppe et al., 2024) means that fire weather anomalies can be predicted up to 1 month in advance globally. However, predictable modes provide additional information on the likely wildfire season – giving enough time for risk management interventions such as fuel removal and prescribed burning. Such correlations have already been found using observed data in a number of regional and local studies (Chen et al., 2011; Fernandes et al., 2011; Chen et al., 2016; Shen et al., 2019; Cardil et al., 2023). This is now supplemented in the US by modelled evidence to a considerably higher level of statistical significance.

4.5 Conclusions

Large wildfire ensembles allow the identification of high-resolution geographical patterns of the impact of climate modes on wildfire. We have identified the areal extent of the influence of different modes on wildfire for the contiguous US, their impact on the timing of the fire season, and how the relative effect on annual wildfires varies geographically under recent and future climates. ENSO, the IOD, and TNA+1 are found to be the principal climate modes associated with US wildfire variability under recent conditions, affecting 91%, 90% and 82% of the contiguous US. La Niña increases the likelihood of wildfire in the southwestern US, Great Plains and Florida. The IOD and TNA+1 have a more limited effect on US wildfire when accounting for the simultaneous effect of ENSO. Nonetheless, the TNA+1 remains a strong and widespread influence over the contiguous US in the recent and +2°C climates, and the IOD emerges as a substantial regional control in the southern US with future warming. Contrary to expectations, no significant relationship was found between El Niño and wildfire occurrences in the northwestern US. The strong association of ENSO and its related modes on annual expected fires can be explained by ENSO's strong effect on heat (VPD) and precipitation (which contributes to GPP variability). ENSO has a very strong effect on precipitation in the southwest, with a statistically significant effect on precipitation across the entire southern US. ENSO also has a broad effect on VPD in most of the US, strongest in the Great Plains.

An additional +2°C global warming strengthens the effect of some climate modes on wildfire occurrence, particularly that of the TNA+1 and AMO+1 on wildfire in the Great Plains and the West. The effect comes primarily from changes in the impact of climate modes in a warmer

climate, rather than from changes in the modes themselves. The Great Plains is the region where wildfire probability is most sensitive to climate change and variability; wildfire in the Great Plains is strongly controlled by ENSO, the IOD and TNA+1 in the recent and +2°C time-slices, and additionally by AMO+1 in the +2°C time-slice. Over the contiguous US, the number of wildfires and the areal extent of influence of the PNA, AO and PDO+1 also increase with warming. The area significantly influenced by the PNA increased from 26 to 66% and by the AO from 10 to 37%.

4.6 References

Abatzoglou JT, Williams AP (2016) Impact of anthropogenic climate change on wildfire across western US forests. PNAS 113(42):11770-11775. https://doi.org/10.1073/pnas.1607171113

Abatzoglou JT, Williams AP, Boschetti L, Zubkova M, Kolden CA (2018) Global patterns of interannual climate-fire relationships. Glob. Change Biol., 24(11):5164-5175. https://doi.org/10.1111/gcb.14405

Abatzoglou JT, Williams AP, Barbero R (2019) Global emergence of anthropogenic climate change in fire weather indices. Geophys. Res. Lett. 46(1):326-336. https://doi.org/10.1029/2018GL080959

Abram NJ, Mulvaney R, Vimeux F, Phipps SJ, Turner J, England MH (2014) Evolution of the Southern Annular Mode during the past millennium. Nat. Clim. Change 4(7):564-569. https://doi.org/10.1038/nclimate2235

Archibald S, Roy DP, van Wilgen BW, Scholes RJ (2009) What limits fire? An examination of drivers of burnt area in Southern Africa. Glob. Chang. Biol. 15(3):613-630. https://doi.org/10.1111/j.1365-2486.2008.01754.x

Ascoli D, Hacket-Pain A, LaMontagne JM, Cardil A, Conedera M, Maringer J, Motta R, Pearse IS, Vacchiano G (2020) Climate teleconnections synchronize Picea glauca masting and fire disturbance: evidence for a fire-related form of environmental pre- diction. J. Ecol. 108:1186–1198. https://doi.org/10.1111/1365-2745.13308

Ault T, Macalady A, Pederson G, Betancourt J, Schwartz M (2011) Northern hemisphere modes of variability and the timing of spring in western North America. J. Clim. 24:4003–4014. https://doi.org/10.1175/2011JCLI4069.1

Barbero R, Abatzoglou JT, Brown TJ (2015) Seasonal reversal of the influence of El Niño–Southern Oscillation on very large wildfire occurrence in the interior northwestern United States. Geophys. Res. Lett. 42:3538–3545. https://doi.org/10.1002/2015GL063428

Barnes C, Jain P, Keeping TR, Gillett N, Boucher J, et al. (2025) Disentangling the roles of natural variability and climate change in Canada's 2023 fire season. Environ. Res. Clim. 4:035013. https://doi.org/10.1088/2752-5295/adec0f

Cardil A, Rodrigues M, Ramirez J, de-Miguel S, Silva CA, Mariani M et al. (2021) Coupled effects of climate teleconnections on drought, Santa Ana winds and wildfires in southern California. Sci. Total Environ. 765:142788. https://doi.org/10.1016/j.scitotenv.2020.142788

Cardil A, Rodrigues M, Tapia M, Barbero R, Ramírez J, Stoof CR, Silva CA, Mohan M, de-Miguel S (2023) Climate teleconnections modulate global burned area. Nat Commun. 14:427. https://doi.org/10.1038/s41467-023-36052-8

Carré M, Sachs JP, Purca S, Schauer AJ, Braconnot P, Falcón RA, Julien M, Lavallée D (2014) Holocene history of ENSO variance and asymmetry in the eastern tropical Pacific. Science 345(6200):1045-1048. https://doi.org/10.1126/science.1252220

Chen Y, Randerson JT, Morton DC, DeFries RS, Collatz GJ, Kasibhatla PS, et al. (2011) Forecasting fire season severity in South America using sea surface temperature anomalies. Science, 334(6057):787-791. https://doi.org/10.1126/science.1209472

Chen Y, Morton DC, Andela N, Giglio L, Randerson JT (2016) How much global burned area can be forecast on seasonal time scales using sea surface temperatures?. Environ. Res. Lett., 11(4):045001. https://doi.org/10.1088/1748-9326/11/4/045001

Choi DH, Kug JS, Kwon WT, Jin FF, Baek HJ, Min SK (2010) Arctic Oscillation responses to greenhouse warming and role of synoptic eddy feedback. J. Geophys. Res. Atmos. 115. https://doi.org/10.1029/2010jd014160

Coburn J, Barthelmie RJ, Pryor SC (2024) Changing windstorm characteristics over the US Northeast in a single model large ensemble. Env. Res. Lett. 19(11):114045. https://doi.org/10.1088/1748-9326/ad801b

Cunningham CX, Williamson GJ, Bowman DM (2024) Increasing frequency and intensity of the most extreme wildfires on Earth. Nat. Ecol. & Evol. 8(8):1420-1425. https://doi.org/10.1038/s41559-024-02452-2

Dai A, Wigley TML (2000) Global patterns of ENSO-induced precipitation. Geophys. Res. Lett. 27(9):1283-1286. https://doi.org/10.1029/1999GL011140

Dannenberg MP, Wise EK, Janko M, Hwang T, Smith WK (2018) Atmospheric teleconnection influence on North American land surface phenology. Environ. Res. Lett. 13. https://doi.org/10.1088/1748-9326/aaa85a

Dettinger MD, Cayan DR, Diaz HF, Meko DM (1998) North–south precipitation patterns in western North America on interannual-to-decadal timescales. J. Clim. 11(12):3095-3111. https://doi.org/10.1175/1520-0442(1998)011<3095:NSPPIW>2.0.CO;2

Dixon PG, Goodrich GB, Cooke WH (2008) Using teleconnections to predict wildfires in Mississippi. Mon. Weather. Rev. 136:2804–2811. https://doi.org/10.1175/2007MWR2297.1

Döscher R, Acosta M, Alessandri A, Anthoni P, Arsouze T, Bergman T, et al. (2022). The EC-Earth3 earth system model for the coupled model intercomparison project 6. Geosci. Model. Dev. 15(7):2973–3020. https://doi.org/10.5194/gmd-15-2973-2022

Eidenshink J, Schwind B, Brewer K, Zhu ZL, Quayle B, Howard S (2007) A project for monitoring trends in burn severity. Fire Ecol. 3(1):3-21. https://doi.org/10.4996/fireecology.0301003

Enfield DB, Mestas-Nuñez AM, Mayer DA, Cid-Serrano L (1999) How ubiquitous is the dipole relationship in tropical Atlantic sea surface temperatures? J. Geophys. Res. Oceans, 104(C4):7841-7848. https://doi.org/10.1029/1998JC900109

Enfield DB, Mestas-Nunez AM, Trimble PJ (2001) The Atlantic Multidecadal Oscillation and its relationship to rainfall and river flows in the continental U.S., Geophys. Res. Lett., 28: 2077-2080.

Fan H, Yang S, Wang C, Wu Y, Zhang G (2022) Strengthening amplitude and impact of the Pacific meridional mode on ENSO in the warming climate depicted by CMIP6 models. J. Clim. 35(15):5195-5213. https://doi.org/10.1175/JCLI-D-21-0683.1

Fernandes K, Baethgen W, Bernardes S, DeFries R, DeWitt DG, Goddard L, et al. (2011) North Tropical Atlantic influence on western Amazon fire season variability. Geophys. Res. Lett. 38(12): L12701. http://dx.doi.org/10.1029/2011GL047392

Forrest M, Hetzer J, Billing M, Bowring SP, Kosczor E, Oberhagemann L, Perkins O, Warren D, Arrogante-Funes F, Thonicke K, Hickler T (2024) Understanding and simulating cropland

and non-cropland burning in Europe using the BASE (Burnt Area Simulator for Europe) model. Biogeosciences 21(23):5539-5560. https://doi.org/10.5194/bg-21-5539-2024

Freund MB, Henley BJ, Karoly DJ, McGregor HV, Abram NJ, Dommenget D (2019) Higher frequency of Central Pacific El Niño events in recent decades relative to past centuries. Nat. Geosci. 12(6):450-455. https://doi.org/10.1038/s41561-019-0353-3

Gedalof ZE, Peterson DL, Mantua NJ (2005) Atmospheric, climatic, and ecological controls on extreme wildfire years in the northwestern United States. Ecol. Appl. 15(1):154-174. https://doi.org/10.1890/03-5116

Gincheva A, Pausas JG, Torres-Vázquez MÁ, Bedia J, Vicente-Serrano SM, Abatzoglou JT, et al. (2024) The interannual variability of global burned area is mostly explained by climatic drivers. Earth's Future, 12(7):e2023EF004334. https://doi.org/10.1029/2023EF004334

Goodrick SL, Hanley DE (2009) Florida wildfire activity and atmospheric teleconnections. Int. J Wild. Fire 18:476-482. https://doi.org/10.1071/WF07034

Ham YG, Kug JS, Park JY, Jin FF (2013) Sea surface temperature in the north tropical Atlantic as a trigger for El Niño/Southern Oscillation events. Nat. Geosci. 6(2):112-116. https://doi.org/10.1038/ngeo1686

Ham YG, Choi JY, Kug JS (2017) The weakening of the ENSO–Indian Ocean Dipole (IOD) coupling strength in recent decades. Clim. Dyn. 49:249-261. https://doi.org/10.1007/s00382-016-3339-5

Hameed SN, Jin D, Thilakan V (2018) A model for super El Niños. Nat. Comm. 9(1):2528. https://doi.org/10.1038/s41467-018-04803-7

Hessl AE, McKenzie DE, Schellhaas R (2004) Drought and Pacific Decadal Oscillation linked to fire occurrence in the inland Pacific Northwest, Ecol. Appl. 14(2):425–442. https://doi.org/10.1890/03-5019

Heyerdahl EK, Brubaker LB, Agee JK (2002) Annual and decadal climate forcing of historical fire regimes in the interior Pacific Northwest, USA. Holocene 12:597–604. https://doi.org/10.1191/0959683602hl570rp

Hino M, Field CB (2023) Fire frequency and vulnerability in California. PLOS Clim. 2(2):e0000087. https://doi.org/10.1371/journal.pclm.0000087

Hoecker TJ, Parks SA, Krosby M, Dobrowski SZ (2023) Widespread exposure to altered fire regimes under 2°C warming is projected to transform conifer forests of the Western United States. Commun. Earth Environ. 4(1):295. https://doi.org/10.1038/s43247-023-00954-8

IPCC (2021) Climate Change 2021: The Physical Science Basis. Contribution of Working Group I to the Sixth Assessment Report of the Intergovernmental Panel on Climate Change [Masson-Delmotte V, Zhai P, Pirani A, Connors SL , Péan C, Berger S, et al. (eds.)] Cambridge University Press, Cambridge, United Kingdom and New York, NY, USA, https://doi.org/10.1017/9781009157896

Jiang L, Li T (2019) Relative roles of El Niño-induced extratropical and tropical forcing in generating Tropical North Atlantic (TNA) SST anomaly. Clim. Dyn. 53(7):3791-3804. https://doi.org/10.1007/s00382-019-04748-7

Johnston JD, Bailey JD, Dunn CJ (2017) Historical fire-climate relationships in contrasting interior Pacific Northwest forest types. Fire Ecol. 13:18–36. https://doi.org/10.4996/fireecology.130257453

Jolly WM, Cochrane MA, Freeborn PH, Holden ZA, Brown TJ, Williamson GJ, Bowman DM (2015) Climate-induced variations in global wildfire danger from 1979 to 2013. Nat. Commun. 6(1):7537. https://doi.org/10.1038/ncomms8537

Keeping T, Harrison SP, Prentice IC (2024) Modelling the daily probability of wildfire occurrence in the contiguous United States. Env. Res. Lett. 19(2):024036. https://doi.org/10.1088/1748-9326/ad21b0

Keeping T, Zhou D, Cai W, Shepherd C, Prentice I, Van der Wiel K, Harrison S (2025) [in review]. Present and Future Interannual Variability in Wildfire Occurrence: A Large Ensemble Application to the United States, Front. For. Glob. Chang.

Kelley DI, Prentice IC, Harrison SP, Wang H, Simard M, Fisher JB, Willis KO (2013) A comprehensive benchmarking system for evaluating global vegetation models, Biogeosciences 1: 3313–3340. https://doi.org/10.5194/bg-10-3313-2013

Kipfmueller KF, Larson ER, St. George S (2012) Does proxy uncertainty affect the relations inferred between the Pacific Decadal Oscillation and wildfire activity in the western United States?, Geophys. Res. Lett. 39:04703, https://doi.org/10.1029/2011GL050645

Kitzberger T, Brown PM, Heyerdahl EK, Swetnam TW, Veblen TT (2007) Contingent Pacific-Atlantic Ocean influence on multicentury wildfire synchrony over western North America. PNAS 104:543-548, https://doi.org/10.1073/pnas.0606078104

Kitzberger T, Swetnam TW, Veblen TT (2001) Inter-hemispheric synchrony of forest fires and the El Niño-Southern Oscillation, Glob. Ecol. Biogeogr. 10(3):315–326, https://doi.org/10.1046/j.1466-822X.2001.00234.x

Lafon CW, Hoss JA, Grissino-Mayer HD (2005) The contemporary fire regime of the central Appalachian Mountains and its relation to climate. Phys. Geogr., 26(2):126-146. https://doi.org/10.2747/0272-3646.26.2.126

Le T, Ha KJ, Bae DH, Kim SH (2020) Causal effects of Indian Ocean Dipole on El Niño–Southern Oscillation during 1950–2014 based on high-resolution models and reanalysis data. Env. Res. Lett. 15(10):1040b6. https://doi.org/10.1088/1748-9326/abb96d

Lindley TT, Murdoch GP, Guyer JL, Skwira GD, Schneider KJS, Nagle SR, Van Speybroeck KM, Smith BR, Beierle (MJ) (2014) Southern Great Plains Wildfire Outbreaks. E-J. of Sev. Storms Met. 9(2):1-43.

Littell JS, McKenzie D, Peterson DL, Westerling AL (2009) Climate and wildfire area burned in western US ecoprovinces, 1916–2003. Ecol. Appl. 19(4):1003-1021. https://doi.org/10.1890/07-1183.1

Litzow MA, Malick MJ, Bond NA, Cunningham CJ, Gosselin JL, Ward EJ (2020) Quantifying a novel climate through changes in PDO-climate and PDO-salmon relationships. Geophys. Res. Let. 47(16):e2020GL087972. https://doi.org/10.1029/2020GL087972

Lopez H, West R, Dong S, Goni G, Kirtman B, Lee SK, Atlas R (2018) Early emergence of anthropogenically forced heat waves in the western United States and Great Lakes. Nat. Clim. Change 8(5):414-420. https://doi.org/10.1038/s41558-018-0116-y

Luna-Niño R, Gershunov A, Ralph FM, Weyant A, Guirguis K, DeFlorio MJ, Cayan DR, Williams AP (2025) Heresy in ENSO teleconnections: Atmospheric Rivers as disruptors of canonical seasonal precipitation anomalies in the Southwestern US. Clim. Dyn. 63(2):115. https://doi.org/10.1007/s00382-025-07583-1

Margolis EQ, Swetnam TW (2013) Historical fire–climate relationships of upper elevation fire regimes in the south-western United States. Int. J. of Wild. Fire 22:588–598. https://doi.org/10.1071/WF12064

Martens B, Waegeman W, Dorigo WA, Verhoest NE and Miralles DG (2018) Terrestrial evaporation response to modes of climate variability. NPJ Climate and Atmospheric Science 1(1):43. https://doi.org/10.1038/s41612-018-0053-5

Mason SA, Hamlington PE, Hamlington BD, Jolly MW, Hoffman CM (2017) Effects of climate oscillations on wildland fire potential in the continental United States. Geophys. Res. Lett. 44:7002–7010. https://doi.org/10.1002/2017gl074111

Mori M, Tokinaga H, Kosaka Y, Nakamura H, Taguchi B, Tatebe H (2024) The influence of extratropical ocean on the PNA teleconnection: Role of atmosphere-ocean coupling. Geophys. Res. Lett. 51(14):e2024GL110234. https://doi.org/10.1029/2024GL110234

Muñoz-Sabater J, Dutra E, Agustí-Panareda A, Albergel C, Arduini G, Balsamo G, Boussetta S, Choulga M, Harrigan S, Hersbach H, Martens B, Miralles DG, Piles M, Rodríguez-Fernández NJ, Zsoter E, Buontempo C, Thépaut JN (2021) ERA5-Land: A state-of-the-art global reanalysis dataset for land applications. ESSD 13(9):4349-4383. https://doi.org/10.5194/essd-13-4349-2021

Muntjewerf L, Bintanja R, Reerink T, Van Der Wiel K (2023) The KNMI large ensemble time slice (KNMI–LENTIS). Geosci. Model Dev. 16(15):4581-4597. https://doi.org/10.5194/gmd-16-4581-2023

Neelin JD (2010) Climate change and climate modeling. Camb. Uni. Press.

Newman M, Alexander MA, Ault TR, Cobb KM, Deser C, Di Lorenzo E, Mantua NJ, Miller AJ, Minobe S, Nakamura H, Schneider N (2016) The Pacific decadal oscillation, revisited. J Clim. 29(12):4399-4427. https://doi.org/10.1175/JCLI-D-15-0508.1

NIFC, Predictive Services: National Interagency Fire Centre (2024) National Significant Wildfire Potential Outlook: Outlook Period – June through September 2024.

NIFC, Predictive Services: National Interagency Fire Centre (2024) National Significant Wildfire Potential Outlook: Outlook Period – December 2024 through March 2025.

Ning L, Bradley RS (2016) NAO and PNA influences on winter temperature and precipitation over the eastern United States in CMIP5 GCMs. Clim. Dyn. 46:1257-1276. https://doi.org/10.1007/s00382-015-2643-9

NOAA (2009) Climate Variability: Southern Oscillation Index. https://www.climate.gov/news-features/understanding-climate/climate-variability-southern-oscillation-index. Accessed 12 September 2025

NOAA (2025) Teleconnection Pattern Calculation Procedures. https://www.cpc.ncep.noaa.gov/products/precip/CWlink/daily_ao_index/history/method.shtml . Accessed 12 September 2025

Norman SP, Taylor AH (2003). Tropical and north Pacific teleconnections influence fire regimes in pine-dominated forests of north-eastern California, USA. J Biogeog. 30:1081–1092. https://doi.org/10.1046/j.1365-2699.2003.00889.x

NSW Environment Protection Authority (ed) (2021). NSW State of the Environment 2021. NSW Environment Protection Authority.

Pelletier F, Cardille JA, Wulder MA, White JC, Hermosilla T (2024) Revisiting the 2023 wildfire season in Canada. Sci. Rem. Sens. 10:100145. https://doi.org/10.1016/j.srs.2024.100145

Puxley BL, Martin E, Basara J, Christian JI (2024) The Wildfire Impacts of the 2017-2018 Precipitation Whiplash Event Across the Southern Great Plains. Env. Res. Lett. https://doi.org/10.1088/1748-9326/ad54da

Saji NH, Yamagata TJCR (2003) Possible impacts of Indian Ocean dipole mode events on global climate. Clim. Res. 25(2):151-169.

Schoennagel T, Veblen TT, Romme WH, Sibold JS, Cook ER (2005) ENSO and PDO variability affect drought-induced fire occurrence in Rocky Mountain subalpine forests. Ecol. Appl. 15:2000-2014. https://doi.org/10.1890/04-1579

Schubert SD, Suarez MJ, Pegion PJ, Koster RD, Bacmeister JT (2004) Causes of long-term drought in the US Great Plains. J Clim. 17(3):485-503. https://doi.org/10.1175/1520-0442(2004)017<0485:COLDIT>2.0.CO;2

Schwartz MD, Ault TR, Betancourt JL (2013) Spring onset variations and trends in the continental United States: past and regional assessment using temperature-based indices. Int. J. Clim. 33(13). https://doi.org/10.1002/joc.3625

Shen H, Tao S, Chen Y, Odman MT, Zou Y, Huang Y, et al. (2019) Global fire forecasts using both large-scale climate indices and local meteorological parameters. Glob. Biogeochem. Cycl. 33(8):1129-1145. https://doi.org/10.1029/2019GB006180

Shen X, Kretschmer M, Shepherd TG (2025) Quantifying the state-dependent causal effect of Barents–Kara Sea ice loss on the stratospheric polar vortex in a large ensemble simulation. Clim. Dyn. 63(8):1-18. https://doi.org/10.1007/s00382-025-07802-9

Short KC (2022) Spatial wildfire occurrence data for the United States, 1992-2020 [FPA_FOD_20221014]. 6th Edition. Fort Collins, CO: FSRDA. https://doi.org/10.2737/RDS-2013-0009.6

Simard AJ, Haines DA, Main WA (1985) Relations between El Nino/Southern Oscillation anomalies and wildland fire activity in the United States. Agr.For. Met. 36:93-104, https://doi.org/10.1016/0168-1923(85)90001-2 .

Stocker BD, Wang H, Smith NG, Harrison SP, Keenan TF, Sandoval D, Davis T, Prentice IC (2020) P-model v1. 0: An optimality-based light use efficiency model for simulating ecosystem gross primary production. GMD 13(3):1545-1581 https://doi.org/10.5194/gmd-13-1545-2020

Sutton RT, Hodson DL (2007) Climate response to basin-scale warming and cooling of the North Atlantic Ocean. J. Clim. 20(5):891-907. https://doi.org/10.1175/JCLI4038.1

Swain DL, Wing OE, Bates PD, Done JM, Johnson KA, Cameron DR (2020) Increased flood exposure due to climate change and population growth in the United States. Earth Fut. 8(11):.e2020EF001778. https://doi.org/10.1029/2020EF001778

Swetnam TW, Betancourt JL (1990) Fire-southern oscillation relations in the southwestern United States. Science 249:1017–1020, https://doi.org/10.1126/science.249.4972.1017

Thornton HE, Smith DM, Scaife AA, Dunstone NJ (2023) Seasonal predictability of the East Atlantic pattern in late autumn and early winter. Geophys. Res. Let. 50(1):e2022GL100712. https://doi.org/10.1029/2022GL100712

Trouet V, Taylor AH, Wahl ER, Skinner CN, Stephens SL (2010) Fire-climate interactions in the American West since 1400 CE. Geophys. Res. Lett. 37:L04702 https://doi.org/10.1029/2009GL041695

Turco M, Abatzoglou JT, Herrera S, Zhuang Y, Jerez S, Lucas DD, AghaKouchak A, Cvijanovic I (2023) Anthropogenic climate change impacts exacerbate summer forest fires in California. PNAS 120(25):e2213815120. https://doi.org/10.1073/pnas.2213815120

Van der Wiel K, Wanders N, Selten FM, Bierkens MFP (2019) Added value of large ensemble simulations for assessing extreme river discharge in a 2 C warmer world. Geophys. Res. Lett. 46(4):2093-2102. https://doi.org/10.1029/2019GL081967

Wang C, Lee SK, Enfield DB (2008) Climate response to anomalously large and small Atlantic warm pools during the summer. J. Clim. 21(11):2437-2450. https://doi.org/10.1175/2007JCLI2029.1

Wang H, Prentice IC, Keenan TF, Davis TW, Wright IJ, Cornwell WK, Evans BJ, Peng C (2017) Towards a universal model for carbon dioxide uptake by plants. Nat. Plants 3(9):734-741. https://doi.org/10.1038/s41477-017-0006-8

Wang C, Chen S, Song Z, Wang X (2021) Impacts of the Atlantic warm pool on North American precipitation and global sea surface temperature in a coupled general circulation model. Clim. Dyn. 56(3):1163-1181. https://doi.org/10.1007/s00382-020-05527-5

Westerling AL, Swetnam TW (2003) Interannual to decadal drought and wildfire in the western United States. Trans. AGU 84(49):545-555. https://doi.org/10.1029/2003EO490001

Wilks D (2016) “The stippling shows statistically significant grid points”: How research results are routinely overstated and overinterpreted, and what to do about it. Bulletin of the Am. Met. Soc. 97(12):2263-2273. https://doi.org/10.1175/BAMS-D-15-00267.1

Williams AP, Abatzoglou JT, Gershunov A, Guzman-Morales J, Bishop DA, Balch JK, et al. (2019) Observed impacts of anthropogenic climate change on wildfire in California. Earth's Fut. 7(8):892-910. https://doi.org/10.1029/2019EF001210

Zhang J, Tian W, Chipperfield MP, Xie F, Huang J (2016) Persistent shift of the Arctic polar vortex towards the Eurasian continent in recent decades. Nat. Clim. Change 6(12):1094-1099. https://doi.org/10.1038/nclimate3136

Zhou B, Cai W, Zhu Z, Wang H, Harrison SP, Prentice IC (2024) A general model for the seasonal to decadal dynamics of leaf area. bioRxiv https://doi.org/10.1101/2024.10.23.619947

4.7 Supplementary Material: Influence of climate modes on wildfire occurrence in the contiguous United States under current and future climates

The Supplementary Material is divided into eight sections. **Section 1** gives an overview of previous work linking climate modes and wildfire in the contiguous US. **Section 2** evidences the insufficiency of reanalysis data to derive climate mode/wildfire relationships. **Section 3** provides maps of the ensemble mean and spread as well as regions referred to in this study. **Section 4** provides an evaluation of the performance of the bias correction for the KNMI-LENTIS ensemble. **Section 5** provides an assessment of the representation of climate modes in the KNMI-LENTIS ensemble. **Section 6** provides additional figures showing the areal effect of individual climate models in the recent climate ensemble. **Section 7** provides the ensemble correlations between ENSO, the IOD and TNA+1 indices in the recent and +2°C climate ensembles. **Section 8** gives maps of the effect of climate modes on key predictors of wildfire occurrence. **Section 9** provides information of the effects of climate models on the probability distribution of annual wildfire numbers in different regions in the recent ensemble climate**.** **Section 10** illustrates the effect of climate modes on the wildfire seasonal length and peak timing in the recent ensemble climate. **Section 11** provides additional material on the areal extent and magnitude of the impact of climate modes in the +2°C ensemble.

The Supplementary contains the following figures and tables:

Table 1.1 Overview of previous studies of the relationships between wildfire and climate modes

Figure 2.1 The association between reanalysis (1990-2019) annual wildfires and climate modes to 0.05 FDR-corrected significance.

Figure 2.2 The association between reanalysis (1990-2019) annual wildfires and climate modes to any level of significance.

Figure 2.3 The association between observed (FPA FOD) (1992-2019) annual wildfires and climate modes to 0.05 FDR-corrected significance.

Figure 2.4 The association between observed (FPA FOD) (1992-2019) annual wildfires and climate modes to any level significance.

Figure 11.7 The geospatial effect of the IOD on the annual number of wildfire occurrences in the recent and +2°C time-slices, with the strengthening or weakening effect of the mode (relative to the mean rate of wildfire occurrence) with +2°C climate change also shown.

Figure 11.8 The geospatial effect of the ENSO on the annual number of wildfire occurrences in the recent and +2°C time-slices, with the strengthening or weakening effect of the mode (relative to the mean rate of wildfire occurrence) with +2°C climate change also shown.

Figure 11.9 The geospatial effect of the AO on the annual number of wildfire occurrences in the recent and +2°C time-slices, with the strengthening or weakening effect of the mode (relative to the mean rate of wildfire occurrence) with +2°C climate change also shown.

Figure 11.10 Comparative effect of La Niña years versus +2°C global warming on wildfire occurrence likelihood.

4.7.1 Overview of Previous Studies

Most previous studies on the association between climate modes and wildfire in the contiguous US have focussed on site-based or regional reconstructions of the wildfire record from tree ring fire-scars. These can provide analyses covering multiple decades to centuries, but necessarily only focus on a limited spatial extent. State wildfire records and remote sensing have also been used. These cover a larger and more continuous area, but cover a shorter study period where the effects of a given climate mode may be much more uncertain.

Acronyms: ENSO (El Niño Southern Oscillation), AMO (Atlantic Multidecadal Oscillation), PDO (Pacific Decadal Oscillation), SOI (Southern Oscillation Index), NAO (North Atlantic Oscillation), PDSI (Palmer Drought Severity Index), MEI (Multivariate ENSO Index), NOAA (National Oceanic and Atmospheric Administration), NCAR (National Center for Atmospheric Research), NCEP (National Centers for Environmental Prediction), PNA (Pacific/North American).

Supplementary Table 1.1: Overview of previous studies of the relationships between wildfire and climate modes for the contiguous US.

Reference	**Study Extent**	**Study Period**	**Mode Source**	**Data Source**	**Wildfire Property**
Ascoli et al. (2020)	Alaska, Yukon, Alberta, Quebec. (7, 8, 15, 7 sites)	1957–2016, 1987–2016, 1951–2016, 1989–2014	ENSO and AMO from ocean temperatures.	Correlation of *picea glauca* masting chronologies with burnt area	Burnt area
Westerling & Swetnam (2003)	Continental United States (number of trees and number of sites not stated)	1701–1978, 1916–1978	ENSO and PDO reconstructed (tree-ring) and modern (observed)	Fire scars	Fire occurrence
Hessl et al. (2004)	Central and Eastern Washington State (5 sites, 1701 trees)	1700-1990	ENSO and PDO from tree rings		
Heyerdahl et al. (2002)	Eastern Oregon and Washington States (4 sites, 3659 trees)	1687–1994	ENSO from SOI (modern) and tree rings (historical)		
Heyerdahl et al. (2008)	Interior Oregon and Washington States and Southern British Columbia Province (15 sites, 3720 trees)	1651–1900	ENSO and PDO from tree rings		
Johnston et al. (2017)	East Oregon (13 sites, 189–201 trees)	1650–1900	ENSO and PDO from published reconstructions		

			(tree rings and reanalysis meteorology)		
Kipfmueller et al. (2012)	Pacific Northwest (Oregon, Washington, Idaho, Montana, Wyoming), Central Rockies (Colorado Wyoming), Southwest (Colorado, New Mexico, Arizona) (128 sites)	1700–1900	ENSO and PDO from tree rings		
Kitzberger et al. (2007)	Sierra Madre Occidental, Arizona, Southern New Mexico, Northern New Mexico, Southern Colorado, Northern Colorado, Black Hills (South Dakota), Sierra Nevada (California), Blue Mountains (Oregon, Washington Southern British Columbia, Canada) (238 sites, 4760 trees)	1550–1924	ENSO, PDO and AMO from tree rings		
Le Goff et al. (2007)	Waswanipi (Quebec) (46 trees, 31 sites)	1720–2000	PDO, NAO, AMO from tree rings, post-reformation European weather data		
Margolis & Swetnam (2013)	Southwestern US (Utah, Colorado, Arizona, New Mexico) (n trees not stated, 16 sites)	1700-1904 (and 1905-1978 for PDSI)	ENSO, PDO and AMO from tree rings		
Moody et al. (2006)	Plumas National Forest (California) (144 trees, 4 sites)	1454–2001	ENSO and PDO from tree rings		
Norm & Taylor (2003)	Lassen National Forest (California) (112 trees, 8 sites)	1700–1849	ENSO and PDO, from pre-1900 tree rings		
Schoennagel et al. (2005)	Jasper National Park (Northern Rockies), Yellowstone National Park (Central Rockies), Rocky Mountain National Park (Southern Rockies) (1694 trees, 3 study areas)	1700– 1975	ENSO and PDO tree ring reconstructions		
Sibold & Veblen (2006)	Rocky Mountain National Park (Colorado) (6152 trees, 487 sites)	1650–1978	ENSO, PDO and AMO tree ring reconstructions		
Trouet et al. (2010)	Pacific Northwest, Northern California, Interior West, Southwest (2980 trees, 350 sites)	1441–1910, 1400–1861, 1281–1974, 1403–1859	ENSO tree ring reconstruction		
Kitzberger et al. (2001)	Southwestern United States (Arizona and New Mexico) (63 sites, 933 trees)	1914–1987	ENSO from tree rings	Fire scars and US federal	Fire occurrence

Swetnam & Betancourt (1998)	Arizona, New Mexico, Sonora (>900 trees, 63 sites)	1700–1900, 1920–1978	ENSO reconstruction (provenance unknown)	burnt area records	and burnt area
Swetnam & Betancourt (1990)	Arizona, New Mexico (n trees not stated, 28 sites)	1700–1905, 1905–1985	ENSO tree ring reconstruction		
Barbero et al. (2015)	Northwestern Ecoregions (Northern Rockies, Canadian Rockies, Middle Rockies, Idaho Batholith, Northern Basin and Range, Central Basin and Range, and Snake River Plain)	1984–2012	ENSO from reanalysis (MEI)	National/ state fire records	Very large fires
Dixon et al. (2008)	Mississippi State	1990–2006	ENSO, NAO, PNA, PDO NOAA modes		Fire occurrence and size
Simard et al. (1985)	Continental United States	1926–1978	Strong ENSO years from 9 common indicators		Fire occurrence and burnt area
Cardil et al. (2021)	Southern Coastal California Ecoregion	1953–2018	NOAA modes		Burnt area
Goodrick & Hanley (2009)	Florida State	1981–2003	PNA and NAO from NOAA		
Fauria & Johnson (2008)	Canada	1918–2005	ENSO, PDO, AO from NCAR/NOAA		
Cardil et al. (2023)	Global	1982–2018	NOAA modes	Remote sensing	Burnt area
Justino et al. (2022)	North of 40°N	2001–2020	AO and PNA from reanalysis		Fire occurrence
Mason et al. (2017)	Continental US	1979–2015	Derived from NCEP NARR	Reanalysis risk index	Fire danger

4.7.2 Viability of Reanalysis to Find Mode Effects

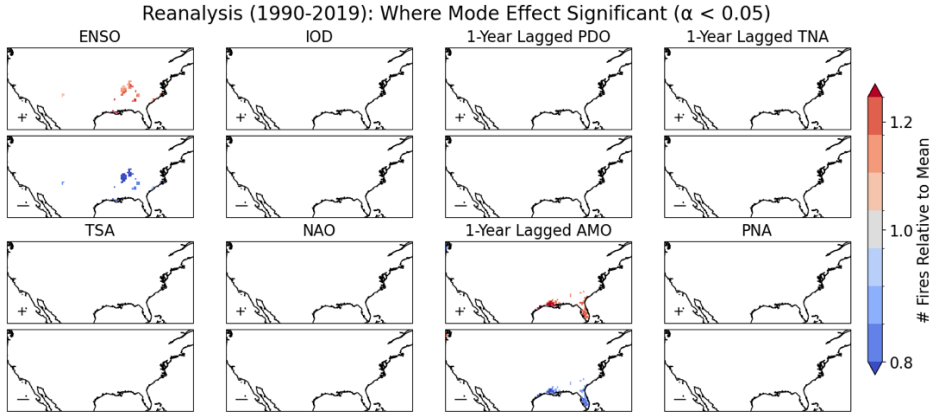

Supplementary Figure 2.1: the association between the reanalysis fire model and key climate modes where there is an FDR-corrected statistical significance level of 0.05. The sign and magnitude of the relationship is given by the ratio between the annual number of wildfires in the positive (upper panels) or negative (lower panels) phase – defined as beyond plus or minus half a standard deviation from the mean respectively. The effect of each mode is shown relative to the mean annual number of wildfires – to account for any non-linearity in the effect between phases that would not be captured by linear regression.

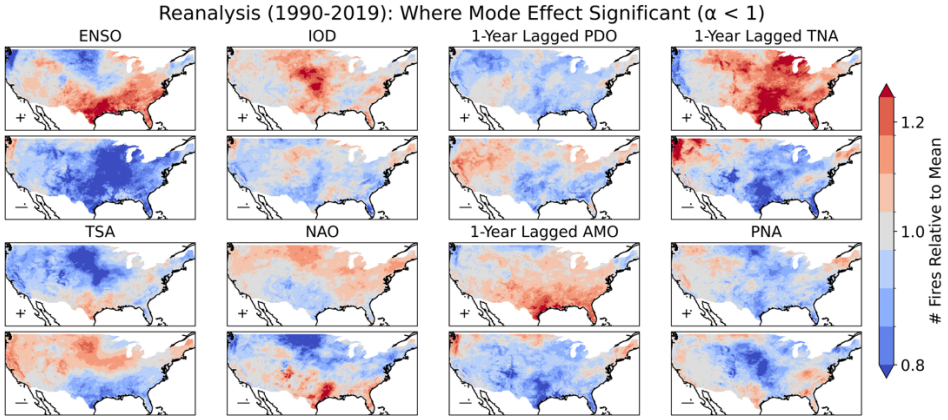

Supplementary Figure 2.2: the association between the reanalysis fire model and key climate modes with no level of statistical significance prescribed. The sign and magnitude of the relationship is given by the ratio between the annual number of wildfires in the positive (upper panels) or negative (lower panels) phase – defined as beyond plus or minus half a standard deviation from the mean respectively. The effect of each mode is shown relative to the mean annual number of wildfires – to account for any non-linearity in the effect between phases that would not be captured by linear regression.

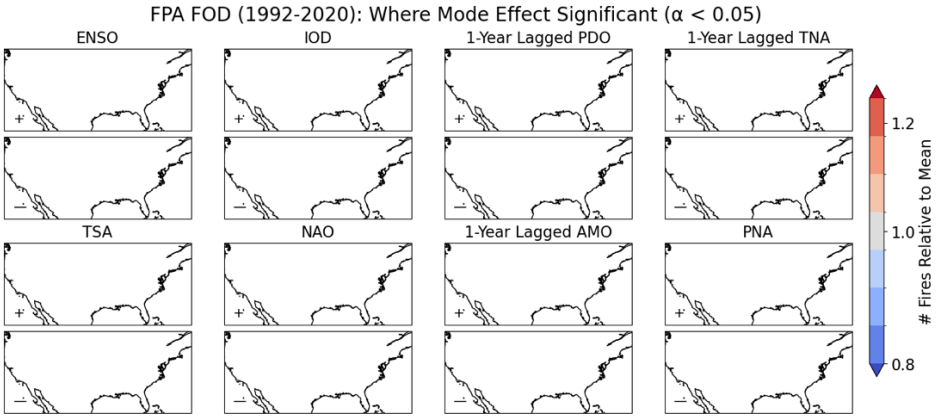

Supplementary Figure 2.3: the association between the FPA FOD fire occurrence data and key climate modes to an FDR-corrected significance of 0.05. The sign and magnitude of the relationship is given by the ratio between the annual number of wildfires in the positive (upper panels) or negative (lower panels) phase – defined as beyond plus or minus half a standard deviation from the mean respectively. The effect of each mode is shown relative to the mean annual number of wildfires – to account for any non-linearity in the effect between phases that would not be captured by linear regression. Note that the FPA FOD starts at 1992, hence the curtailed time period.

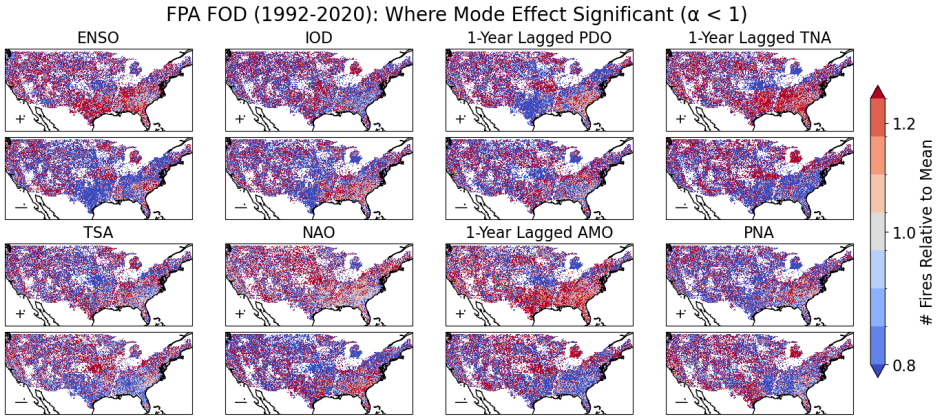

Supplementary Figure 2.4: the association between the FPA FOD fire occurrence data and key climate modes when no significance level is considered. High levels of noise and areas with insufficient data mean that a trend cannot be identified. The sign and magnitude of the relationship is given by the ratio between the annual number of wildfires in the positive (upper panels) or negative (lower panels) phase – defined as beyond plus or minus half a standard deviation from the mean respectively. The effect of each mode is shown relative to the mean annual number of wildfires – to account for any non-linearity in the effect between phases that would not be captured by linear regression. Note that the FPA FOD starts at 1992, hence the curtailed time period.

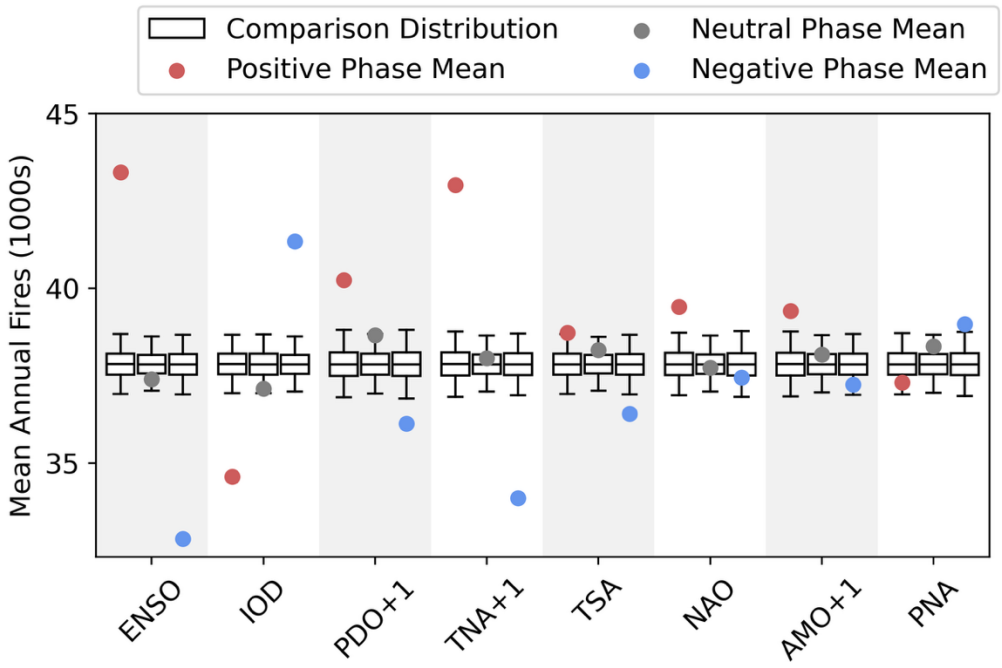

Supplementary Figure 2.5: The distribution of the modelled annual number of wildfires for the recent climate ensemble under different mode phases compared to the distribution of all years, per Shen et al. (2025). The dots show the actual mean value of modelled annual fires. The boxplots show the distribution of the mean number of annual fires, drawn from the distribution of years but with the same sample size as the number of years in that phase in the reanalysis period – repeated 10,000 times. The outer limits of the boxplots represent the 2.5th and 97.5th percentiles, and the three internal lines correspond to the 25th, 50th and 75th percentiles of the bootstrapped distribution.

4.7.3 Context on Regions and Climate Change Signal

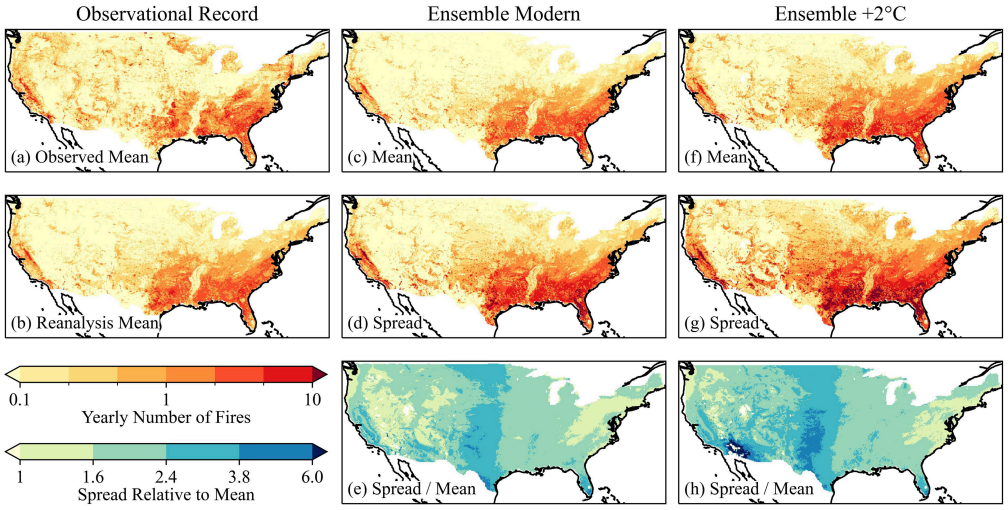

Supplementary Figure 3.1: Reproduced from Keeping et al. (2025). Modelled and observed patterns in the annual number of wildfires greater than 0.1 hectares, with both the mean and 1st-99th percentile spread shown. The plots show (a) the observed annual mean of the wildfire occurrence record for 1992–2020; (b) the modelled reanalysis mean for 1990–2019; (c) the modelled ensemble mean for the modern (2000–2009 climate); (d) the modelled ensemble spread for the modern; (e) the ratio of model spread and mean for the ensemble modern; (f) the +2°C ensemble mean (2000–2009 climate plus 2°C of warming); (g) the +2°C ensemble spread; and (h) the ratio of model spread and mean for the +2°C ensemble. Note that the FPA FOD starts at 1992, hence the slightly curtailed time period.

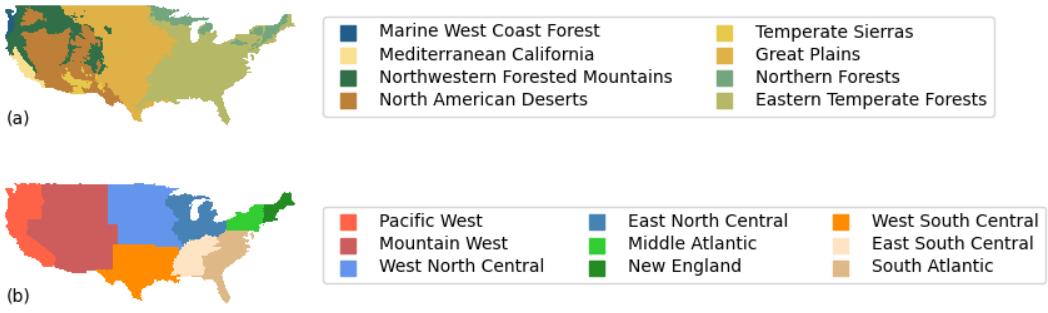

Supplementary Figure 3.2: an overview of (a) the ecoregions and (b) the National Interagency Fire Center Geographic Area Coordination Center (NIFC GACC) regions referred to in this study.

4.7.4 Bias Correction Performance

*Supplementary Table 4.1: KNMI-LENTIS bias correction performance statistics in comparison to ERA5 data for input into fire occurrence model. Based on correlation of top four moments for data aggregated monthly at 2π * ensemble resolution. The variables are mean daily surface windspeed (sfcwind); daytime mean vapour pressure deficit (vpd); diurnal temperature range (dtr); precipitation (pr); prior 5-day precipitation (pr_5d); prior 50-day GPP (GPP_50d); prior year GPP (GPP_1yr).*

R^2	sfcwind	vpd	dtr	snc	pr	pr_5d	GPP_50d	GPP_1yr
Mean	0.922	0.987	0.983	0.994	0.985	0.985	0.881	0.773
Variance	0.567	0.812	0.684	0.409	0.726	0.771	<0	<0
Skewness	0.073	<0	0.741	0.098	0.110	0.307	<0	0.531
Kurtosis	0.020	<0	0.052	<0	<0	<0	<0	0.266

4.7.5 Global Climate Mode Representation in KNMI-LENTIS

Supplementary Figures 5.1-5.11 show that the Sea Level Pressure (SLP) and Sea Surface Temperature (SST) phenomena (specified in each figure caption) associated with each global climate mode are all adequately represented in the KNMI-LENTIS ensemble. The Atlantic Multidecadal Oscillation (AMO) shows the characteristic AMO+ warm pool in the northern Atlantic, with the correct region of highest anomaly off the Greenland coast. The Tropical South Atlantic (TSA) shows the characteristic TSA+ warm sea surface temperatures below West Africa, spreading in effect to the Caribbean Sea. The Tropical North Atlantic (TSA) shows the expected TNA+ warm band in the northern tropics, with cool effects towards the equator and in the extratropical west Atlantic. The Southern Annular Mode (SAM) shows the expected low pressure system over Antarctica associated with the SAM+. The Pacific/North American (PNA) oscillations strongly shows the expected PNA+ low in the northeastern Pacific; but does not show clearly the expected western US high and eastern US low – though the associated arctic high in the PNA+ is present. The Pacific Decadal Oscillation (PDO) shows the expected cool sea surface temperature jet off the west coast of Japan, and the pooling of warmer water against West North America. The North Atlantic Oscillation (NAO) shows the expected sea surface temperature quadrupole with warmer sea surface temperatures of the eastern US and in Northern Europe, and cooler sea surface temperatures off Greenland and West Africa. The Indian Ocean Dipole (IOD) shows the expected gradient of cool to warm sea surface temperatures from the west to east Indian Ocean in the negative mode. El Niño Southern Oscillation (ENSO) shows the expected warm jet along the equator in El Niño (SOI-) with cooler sea surface temperature pools north and south of it in the west and central Pacific. The East Atlantic (EA) oscillation shows the northern pressure low and southern pressure high in the Atlantic associated with the EA+. The Arctic Oscillation (AO) shows the expected low pressure system over the Arctic associated with the AO+.

The effect of each global climate mode (Supplementary Figure 5.12) on precipitation patterns over the contiguous US in the recent climate ensemble is consistent with expectations. For ENSO, wetter conditions are expected during La Niña in the northwestern and inland East US, and during El Niño in the southern latitudes of the US (Ropelewski and Halpert, 1987). These features are all well represented in the ensemble. For the IOD, precipitation conditions are expected to be highly correlated to ENSO, with limited independent influence (Hu et al., 2023). This is matched in the ensemble, with the IOD showing highly similar patterns to ENSO but

with a lesser overall magnitude of effect. For the PDO, southwestern precipitation is associated with a strong increase in the positive phase (Dai, 2013), in other regions the effect is limited for the annually averaged index (Kumar et al., 2013). This is well represented in the ensemble. For the TNA, the association with precipitation, like the IOD, is confounded by its close association with ENSO (Kushnir et al., 2010). The association with ENSO is matched in the ensemble, with the precipitation pattern a weakened version of that observed under ENSO. The TSA is not association with US precipitation. In the ensemble it has a minor negative effect in the central US. For the NAO, higher winter precipitation can result from a positive phase in the eastern US (Ning and Bradley, 2014), but this effect is dominated by ENSO (Tang et al., 2023; Ning and Bradley, 2014) whilst in the southwestern US conditions are wetter in the negative phase including when controlling for ENSO (Tang et al., 2023). In the ensemble this southwestern effect is well-represented, whilst the eastern effect is not, this can be explained by the dominant effect of ENSO on precipitation in the region. For the AMO, a decrease on contiguous US precipitation is associated with the positive phase, though this effect is patchy over the region (Hu et al., 2011). No clear effect is apparent in the ensemble data, possible due to the index signal not being smoothed over a decadal timescale. For the PNA, the positive phase is associated with elevated rainfall in the great Plains and East coast and reduced rainfall in the northwestern US (Leathers et al., 1991). In the ensemble, the East coast and Great Plains effects are seen, but there is an additional stronger effect in the southwestern US as well as no effect in the northwest; this can be explained by correlation (Soulard et al., 2019) between the positive PNA and El Niño. For the AO, high precipitation totals are expected over the central US (Hu and Feng, 2010). This effect is well represented in the ensemble, but an additional effect is present in the southwestern US; this can be explained by correlation (Simpkins, 2021) between the AO and NAO. The EA is not associated with an effect on US meteorology, but has been linked to a modulation of the NAO (Rodrigo, 2021). The ensemble shows limited diverging effect on precipitation between its phases. The SAM is not associated with a direct impact on US meteorology. The ensemble shows a minor positive effect for the central US. Overall, the major effects on precipitation are well-represented in the ensemble, although confounding effects from correlation and modulating-effects between modes can render the signal hard to attribute.

The transient, continuous runs of the two multidecadal modes both show clear decadal or longer time-period oscillations (Supplementary Figures 5.13-5.14). The amplitude of multidecadal oscillations in the AMO is comparable to the amplitude of sub-decadal oscillations, meaning

that a clear multidecadal signal emerges in the annual index values considered in this study. On the other hand, the sub-decadal timescale oscillations in the PDO are significantly greater than the multidecadal oscillations, meaning that a multidecadal effect does not emerge and sub-decadal oscillations dominate as the key effect in this study.

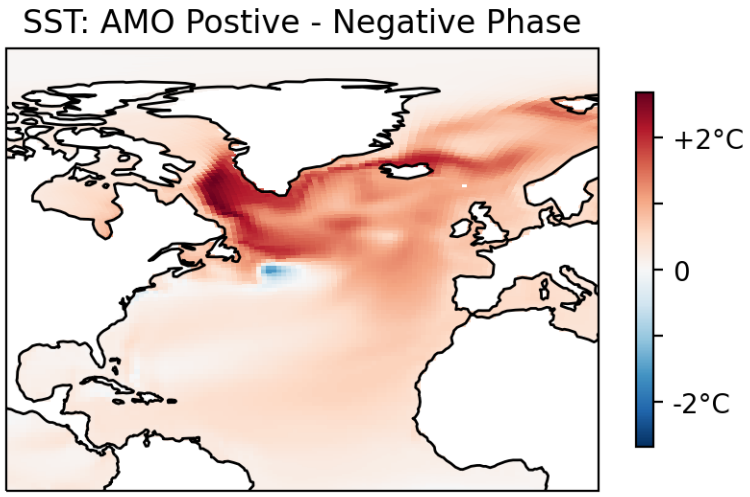

Supplementary Figure 5.1: The sea surface temperature pattern of the Atlantic Multidecadal Oscillation (AMO) in the recent climate ensemble, showing the characteristic AMO+ warm pool in the northern Atlantic, with the correct region of highest anomaly off the Greenland coast.

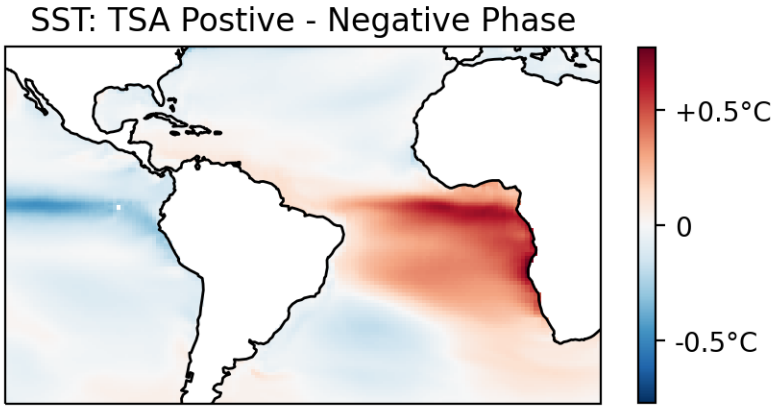

Supplementary Figure 5.2: The sea surface temperature pattern of the Tropical South Atlantic (TSA) in the recent climate ensemble, showing the characteristic TSA+ warm sea surface temperatures below West Africa, spreading in effect to the Caribbean Sea.

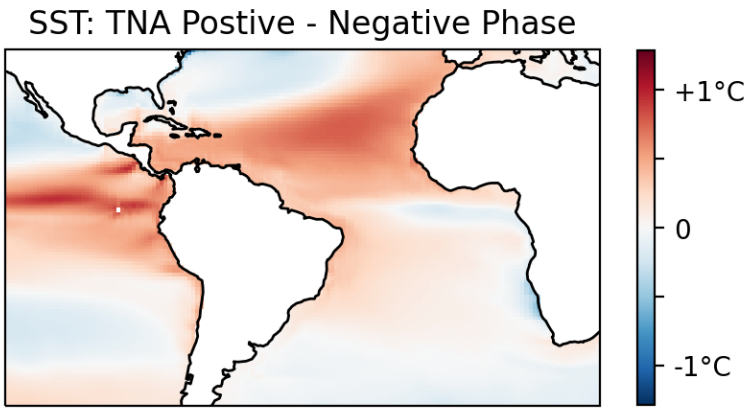

Supplementary Figure 5.3: The sea surface temperature pattern of the Tropical North Atlantic (TNA) in the recent climate ensemble, the TNA+ warm band in the northern tropics, with cool effects towards the equator and in the extratropical west Atlantic.

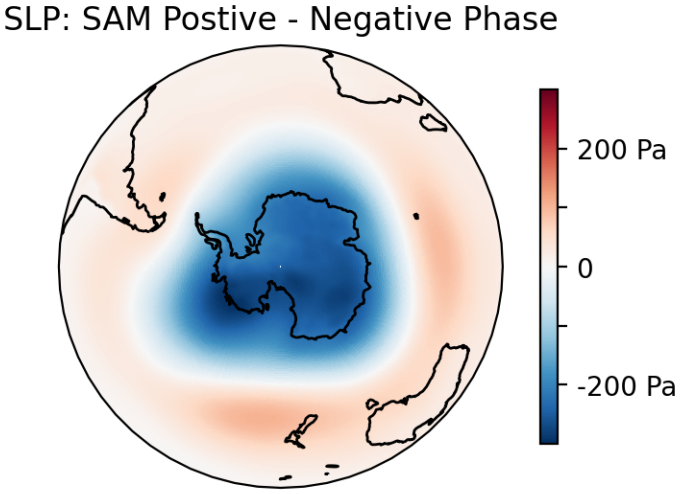

Supplementary Figure 5.4: The sea-level pressure pattern of the Southern Annular Mode (SAM) in the recent climate ensemble, showing the expected low pressure system over Antarctica associated with the SAM+.

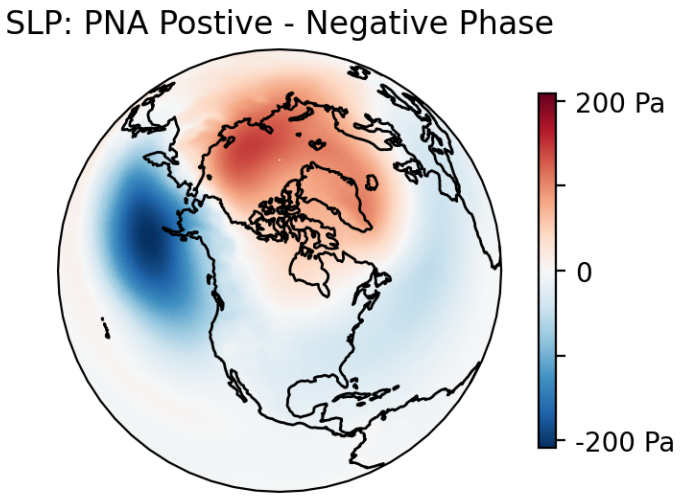

Supplementary Figure 5.5: The sea-level pressure pattern of the Pacific/North America (PNA) in the recent climate ensemble, showing strongly the expected PNA+ low in the northeastern Pacific. Does not show clearly the expected western US high and eastern US low, though the associated arctic high in the PNA+ is present.

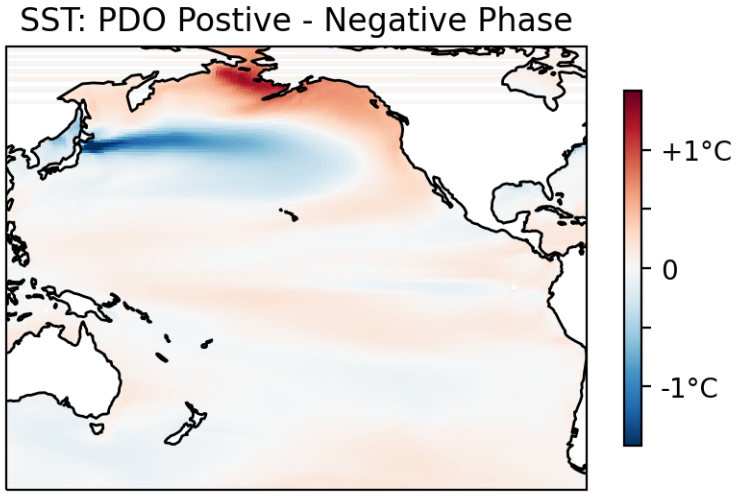

Supplementary Figure 5.6: The sea surface temperature pattern of the Pacific Decadal Oscillation (PDO) in the recent climate ensemble, showing the expected cool sea surface temperature jet off the west coast of Japan, and the pooling of warmer water against West North America.

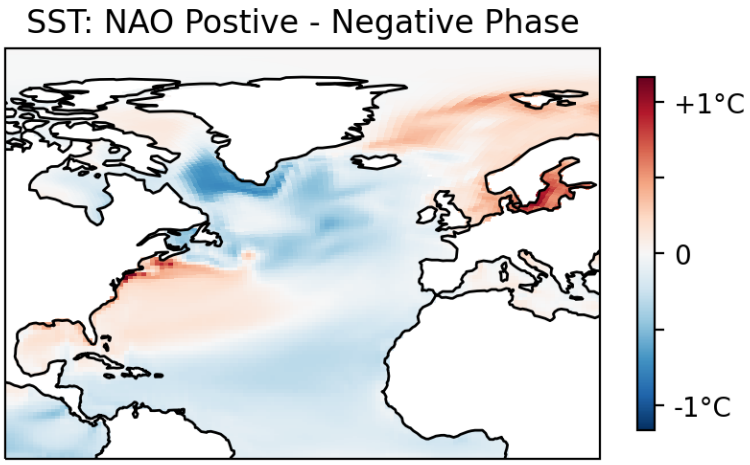

Supplementary Figure 5.7: The sea surface temperature pattern of the North Atlantic Oscillation (NAO) in the recent climate ensemble, showing the expected sea surface temperature quadrupole with warmer sea surface temperatures of the eastern US and in Northern Europe, and cooler sea surface temperatures off Greenland and West Africa.

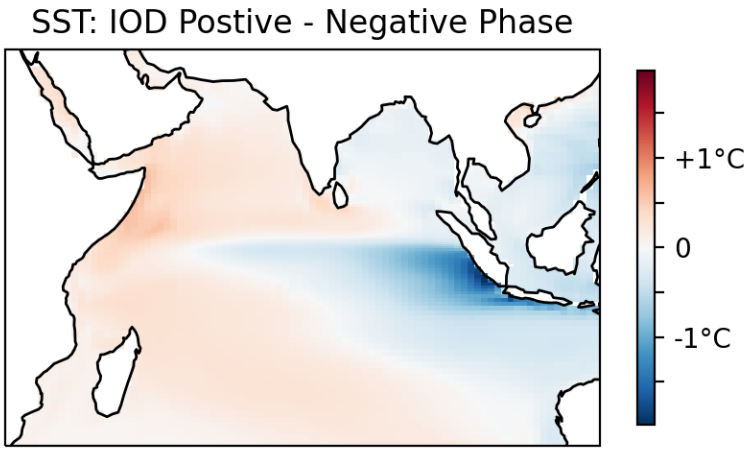

Supplementary Figure 5.8: The sea surface temperature pattern of the Indian Ocean Dipole (IOD) in the recent climate ensemble, showing the expected gradient of cool to warm sea surface temperatures from the west to east Indian Ocean in the negative mode.

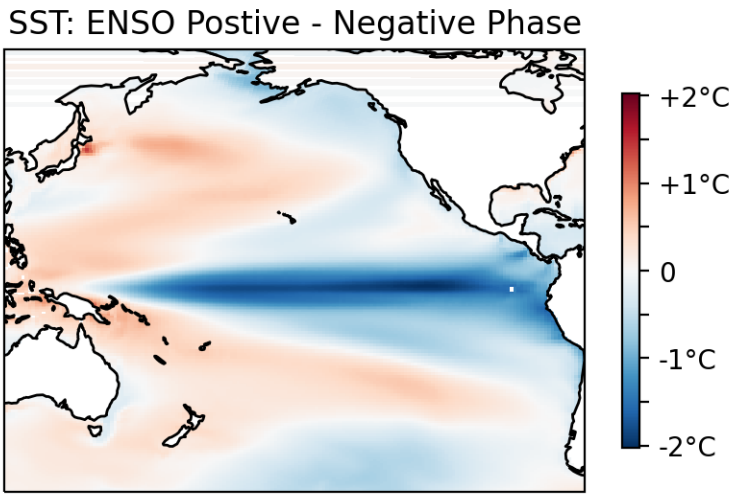

Supplementary Figure 5.9: The sea surface temperature pattern of El Niño Southern Oscillation (ENSO) in the recent climate ensemble, this shows the expected warm jet along the equator in El Niño (SOI-) with cooler sea surface temperature pools north and south of it in the west and central Pacific.

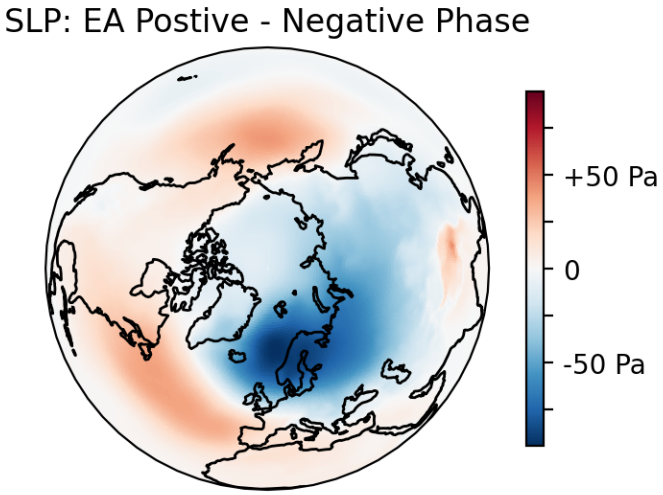

Supplementary Figure 5.10: The sea-level pressure pattern of the East Atlantic (EA) in the recent climate ensemble, showing a northern pressure low and southern pressure high in the Atlantic associated with the EA+.

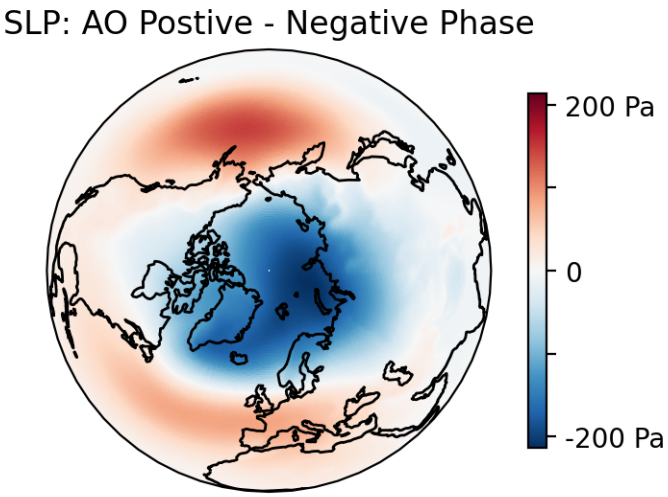

Supplementary Figure 5.11: The sea-level pressure pattern of the Arctic Oscillation (AO) in the recent climate ensemble, showing the expected low pressure system over the Arctic associated with the AO+.

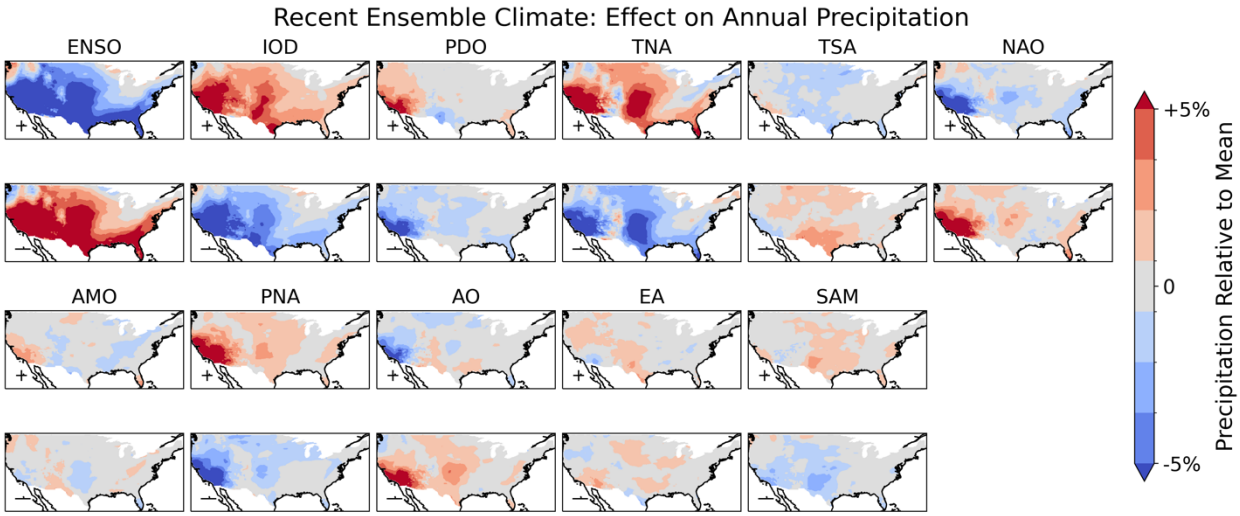

Supplementary Figure 5.12: The effect of the phase of each climate mode (greater or lesser than half of a standard deviation from zero) on annual precipitation totals relative to the mean rate.

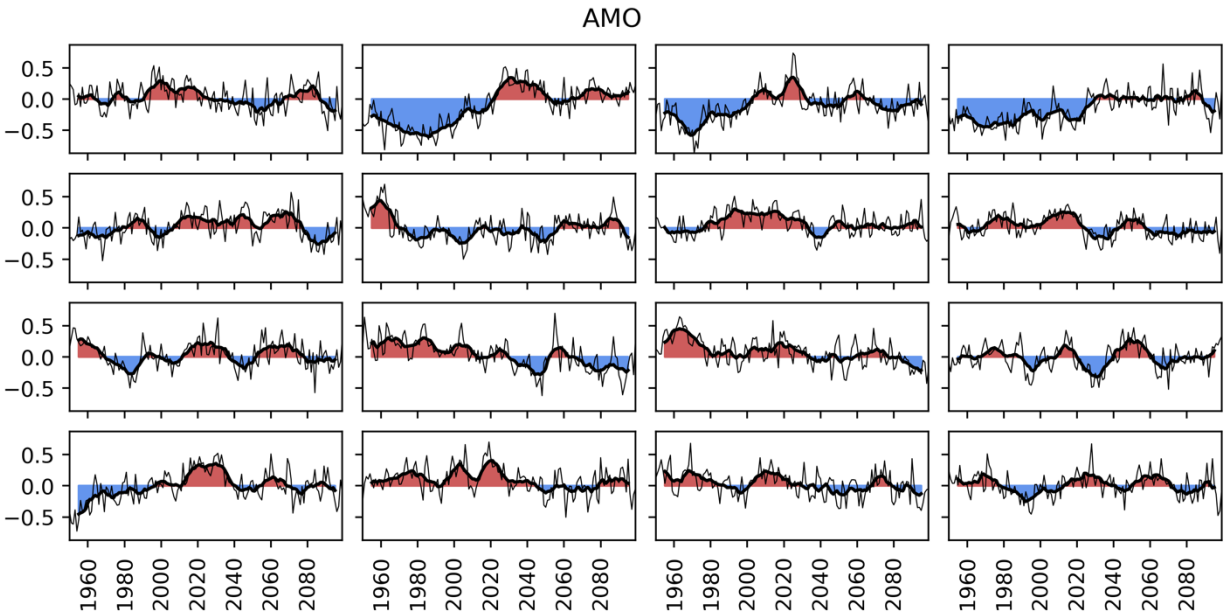

Supplementary Figure 5.13: The 16 transient runs of the AMO index from which the 160 ensemble members for each time-slice are derived. The thin line shows the annual timeseries and the thicker, under-filled line shows the decadally smoothed, centered average.

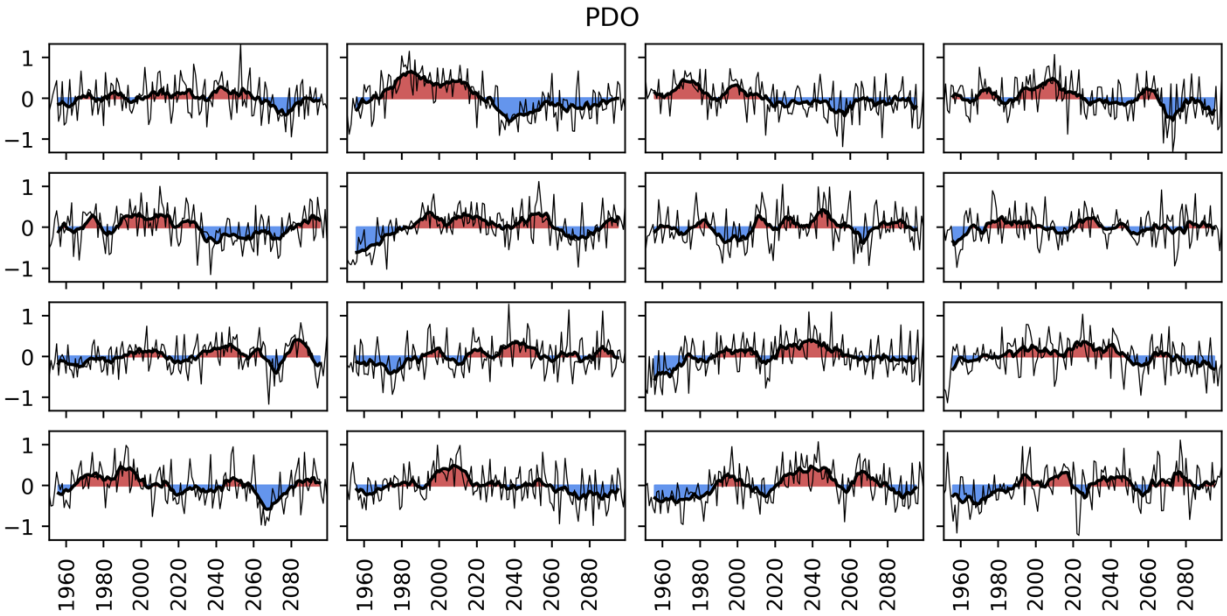

Supplementary Figure 5.14: The 16 transient runs of the PDO index from which the 160 ensemble members for each time-slice are derived. The thin line shows the annual timeseries and the thicker, under-filled line shows the decadally smoothed, centered average.

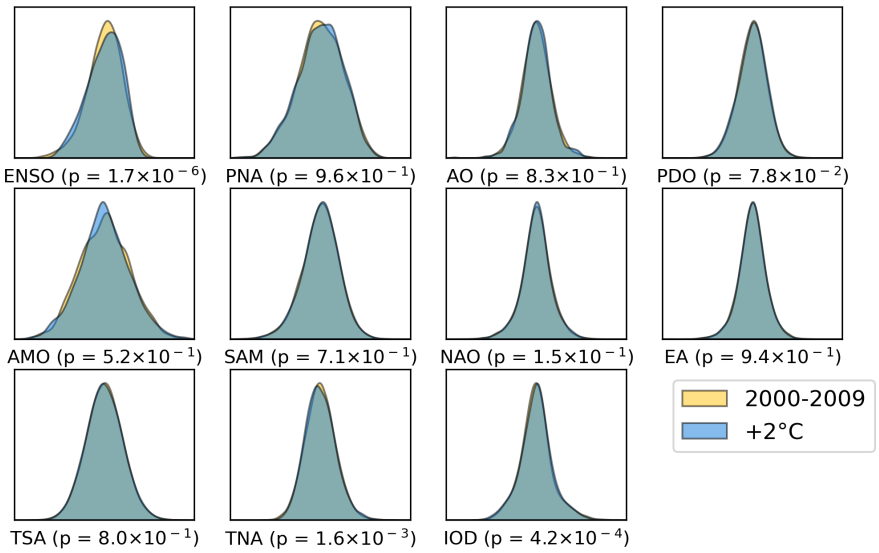

Supplementary Figure 5.15: Distributions, with K-S test p-values for difference in distribution in both periods. There are small but statistically significant shifts in the ENSO, IOD and TNA distributions.

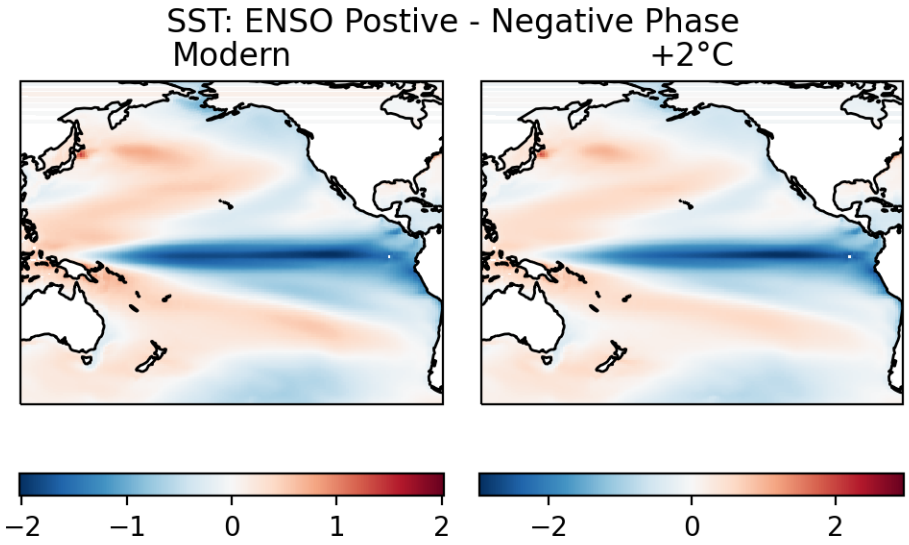

Supplementary Figure 5.16: The sea surface temperature pattern of El Niño Southern Oscillation (ENSO) in the recent (left) and future (right) time slice of the climate ensemble.

4.7.6 Correlations Between ENSO, IOD and TNA+1

The El Niño Southern Oscillation (ENSO) is correlated with the Indian Ocean Dipole (IOD) and Tropical North Atlantic (TNA) in the ensemble. The below scatter plots given an overview of that relationship in the ensemble recent and +2°C climates, the TNA+1 is correlated to ENSO, whilst the IOD is more strongly anti-correlated. Both modes become more strongly correlated with future warming.

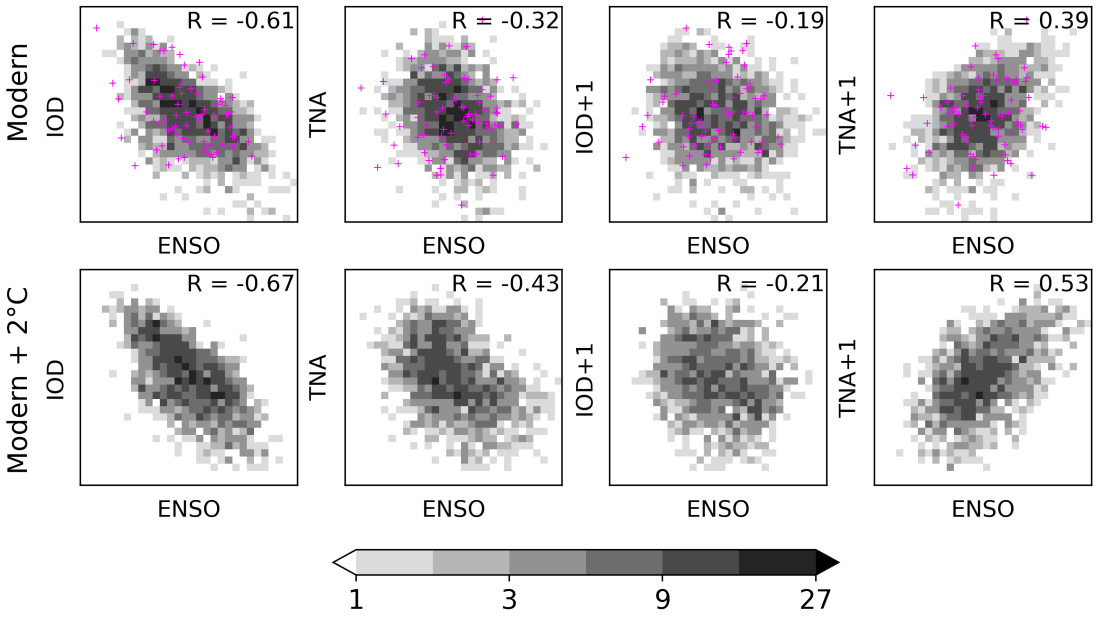

Supplementary Figure 6.1: Scatterplots showing relationship between ENSO, IOD and TNA. Each datapoint is one annual value. Reanalysis data overlaid with crosses.

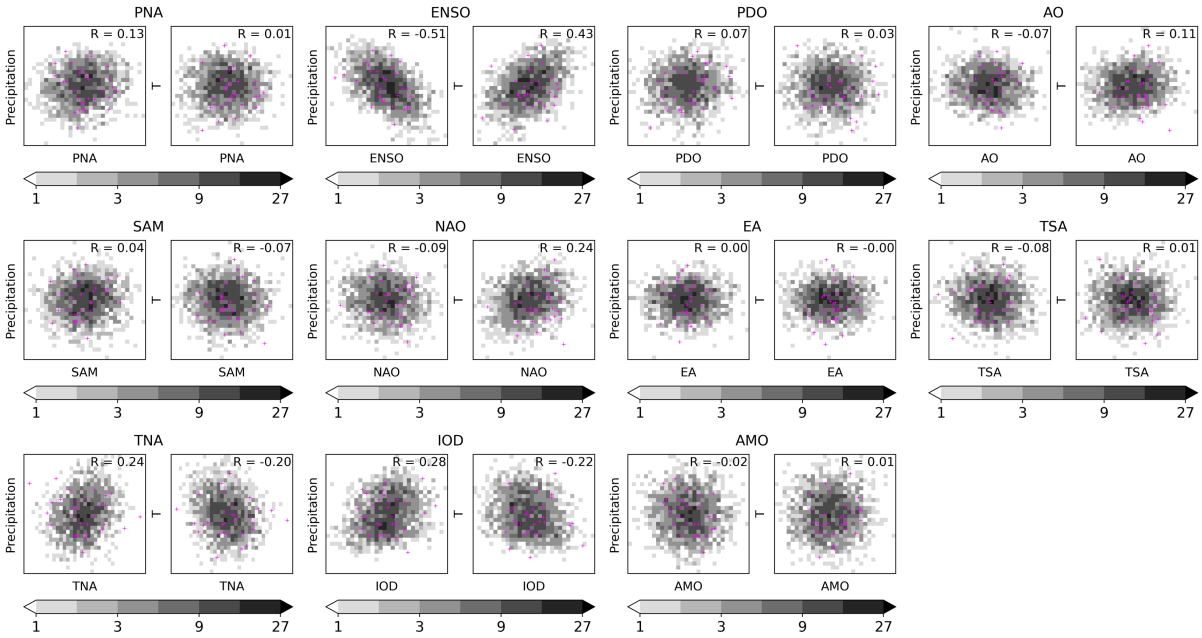

Supplementary Figure 6.2: Scatterplots of annual temperature and precipitation averaged over CONUS against climate mode values for the ensemble 2000-2009 climate. Each datapoint is one annual value. Reanalysis values are overlayed as crosses for the period 1990-2019.

4.7.7 **Areal Effect of Climate Modes in Recent Climate**

This section shows (Supplementary Figure 7.1) the area of positive, negative and insignificant effect of each mode to a much high threshold of significance – finding that La Niña, the negative Indian Ocean Dipole (IOD), and positive 1-year lagged Tropical North Atlantic all persist as strongly associated with wildfire occurrence. The areal effect of each mode is also broken down by meteorological season (Supplementary Figure 7.2), with modes having the greatest area of significant effect on relative change in wildfire occurrence during summer (June to August, JJA) except for the Pacific Decadal Oscillation (December to February, DJF) and Tropical South Atlantic oscillation (March to May, MAM). Maps showing the area and magnitude of the effect for each mode not shown in the main text (Figure 4) are presented in Supplementary Figure 7.3, the major effects are the Pacific Decadal Oscillation, Tropical North Atlantic, and 1-year lagged El Niño Southern Oscillation.

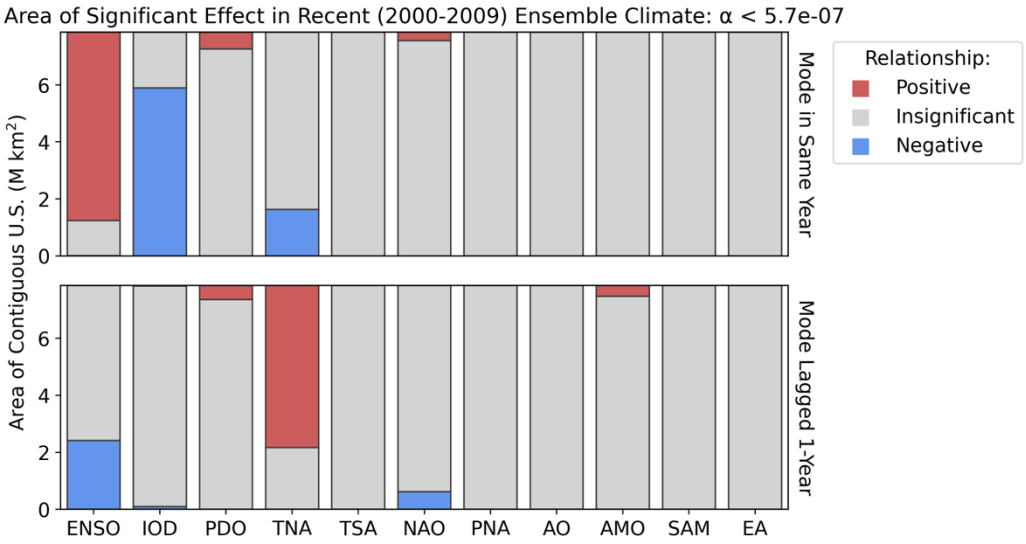

Supplementary Figure 7.1: The area of significant effect for each climate mode over the contiguous US, to an extremely strict FDR-corrected significance threshold of 5.7 x 10^{-7} (equivalent to 5-sigma)

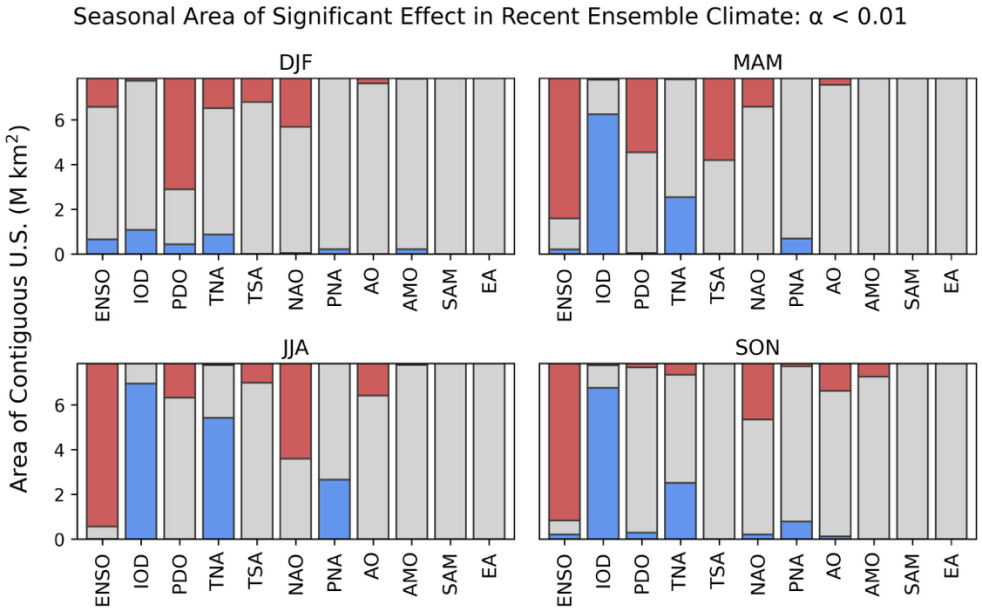

Supplementary Figure 7.2: The seasonal (DJF, MAM, JJA, SON) areas of significant effect for each climate mode over the contiguous US. Significance was determined by the p-value of the linear regression between the climate mode's index value and the seasonal number of fires in each 0.1° grid-cell, to an FDR-corrected significance threshold of 0.01. The slope of the regression determined the sign of the relationship between annual fires and the index.

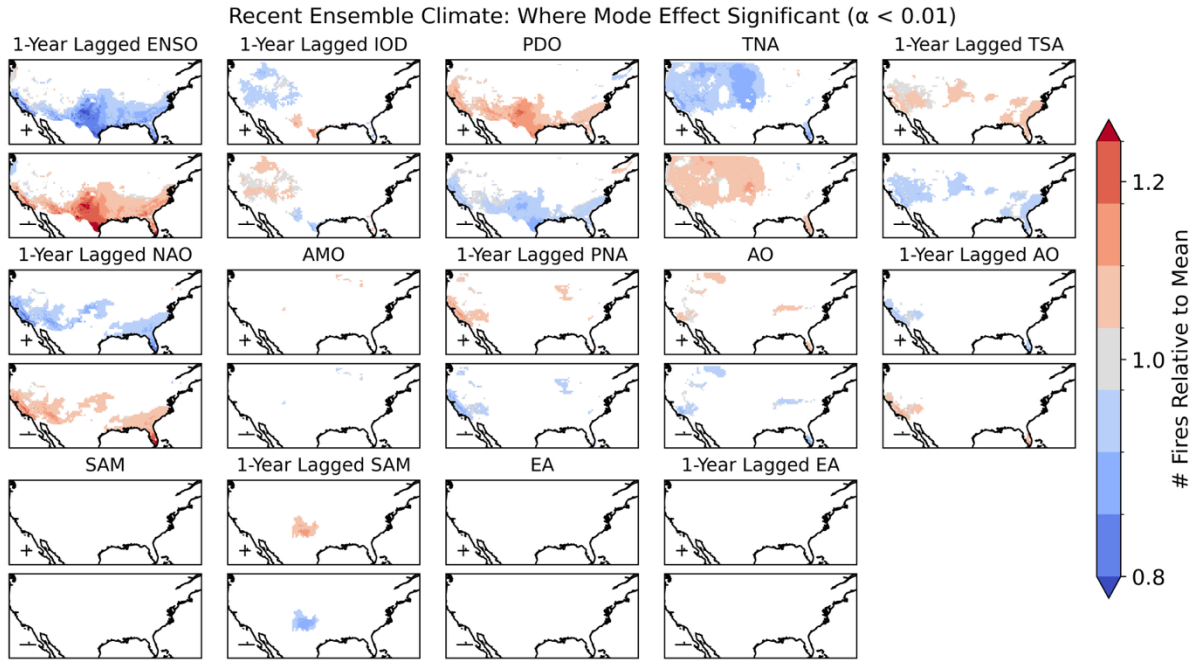

Supplementary Figure 7.3: For all modes not shown in figure 4, showing locations for which linear regression determined a significant relationship between the annual number of fires and the climate mode's index; the ratio between the annual number of fires in the positive and negative phases of each mode relative to the mean annual number of fires.

4.7.8 Effect of Climate Modes on Wildfire Drivers

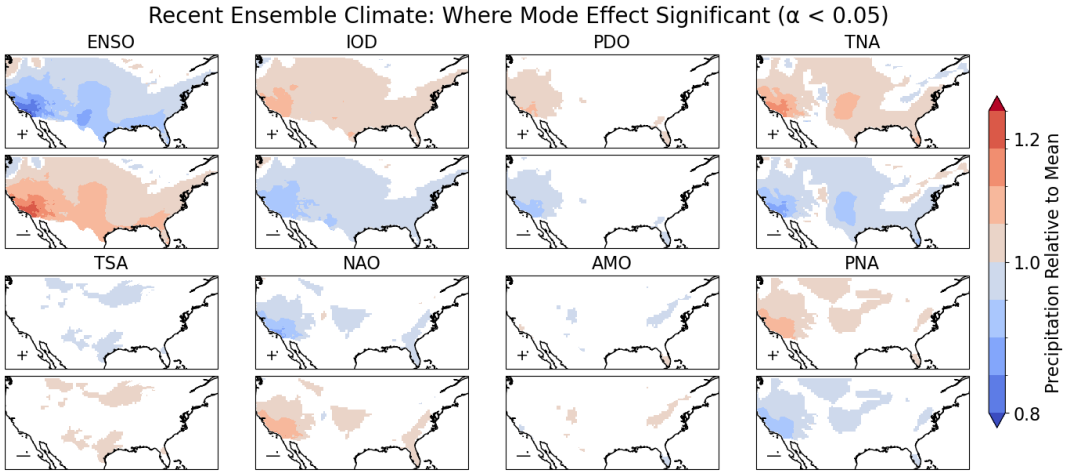

Supplementary Figure 8.1: the relative influence of climate modes on annual precipitation in the recent climate for the large ensemble.

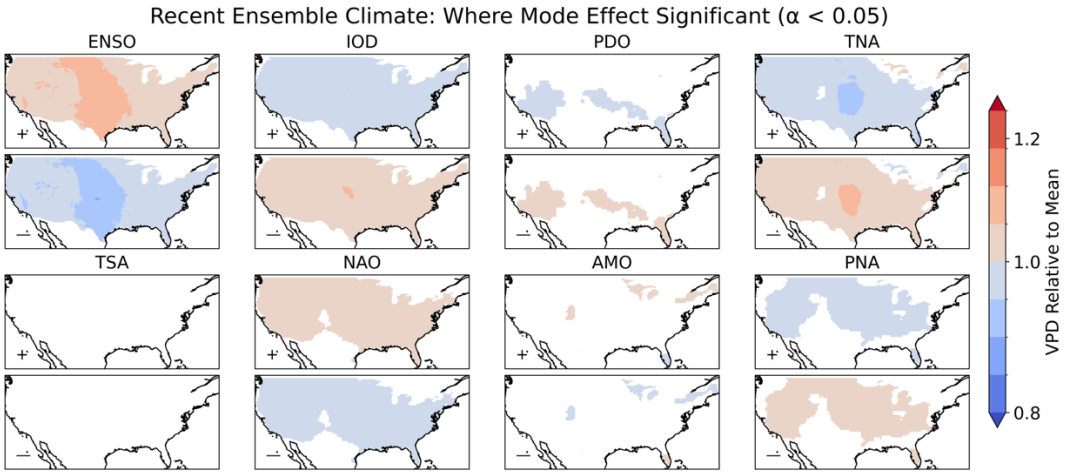

Supplementary Figure 8.2: the relative influence of climate modes on annual VPD in the recent climate for the large ensemble.

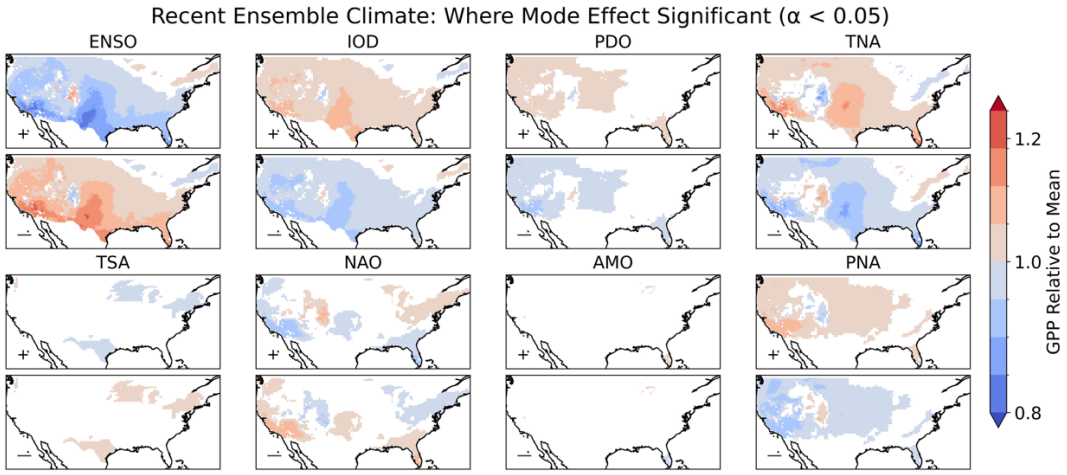

Supplementary Figure 8.3: the relative influence of climate modes on annual GPP in the recent climate for the large ensemble.

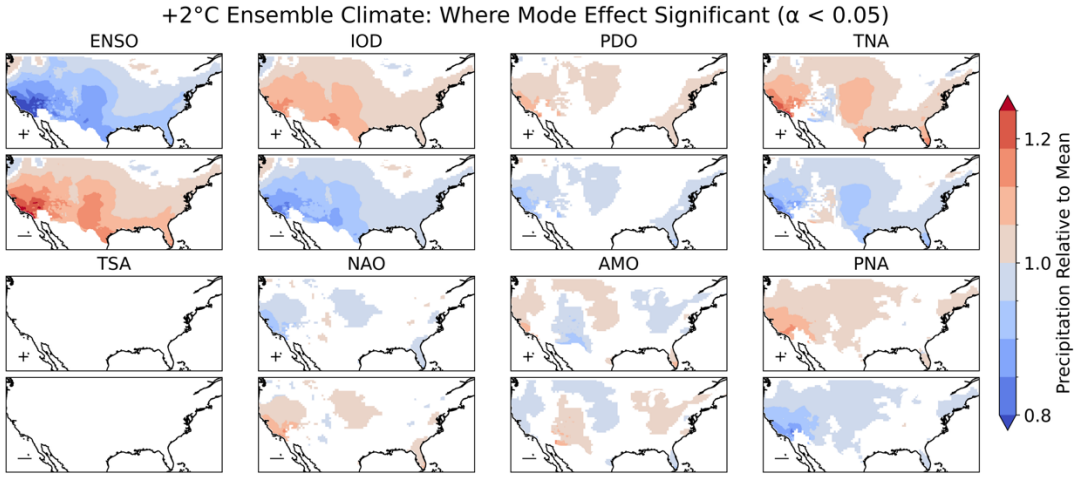

Supplementary Figure 8.4: the relative influence of climate modes on annual precipitation in the +2°C climate for the large ensemble.

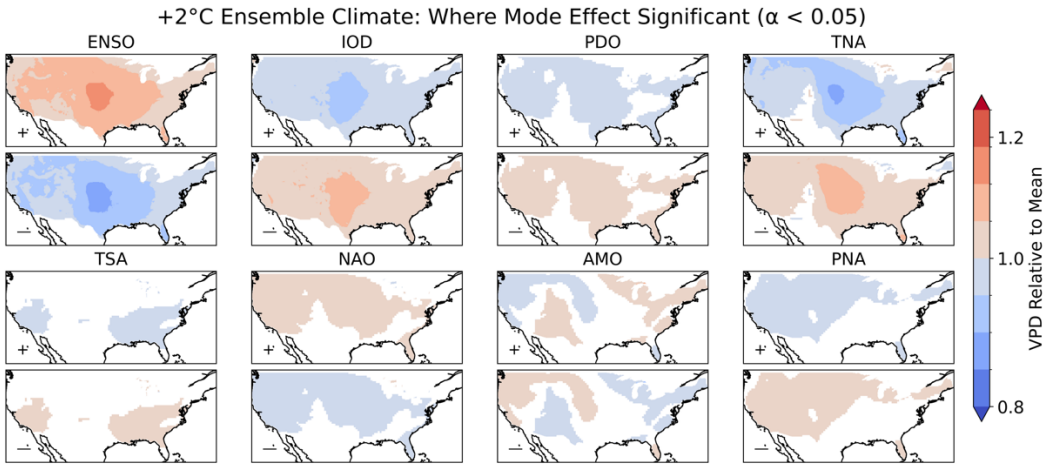

Supplementary Figure 8.5: the relative influence of climate modes on annual VPD in the +2°C climate for the large ensemble.

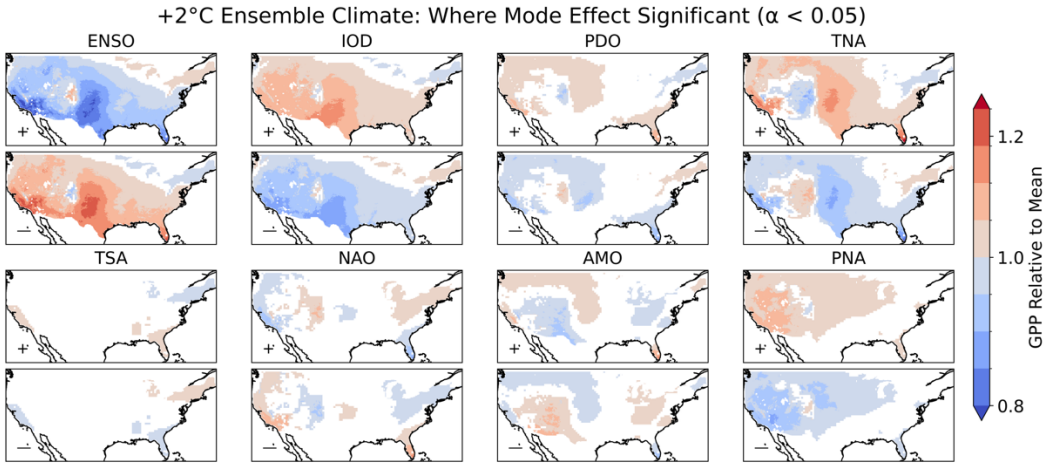

Supplementary Figure 8.6: the relative influence of climate modes on annual GPP in the +2°C climate for the large ensemble.

4.7.9 Regional probability distribution functions of Annual Wildfires Given Climate Mode Phase

This section shows the difference in the positive and negative phase distributions for all wildfire administrative fire regions in the US (Geographic Area Coordination Centres) – for the AMO+1, TSA, TNA+1, PNA, PDO+1, NAO, IOD, and ENSO. In some regions, the mode's effect is to spread the distribution further in the wildfire prone phase, such as in Southern California or the Southwest, whilst in others the mode's effect is solely on the distribution centre, such as in Northern California or the Great Basin. The strongest effects on the distribution are that of ENSO, the TNA+1 and IOD, whilst the AMO+1, PDO+1, and PNA also have significant regional effects. Western regions show a greater response in the distribution than ecoregions, although this could be partially explained by their small extent.

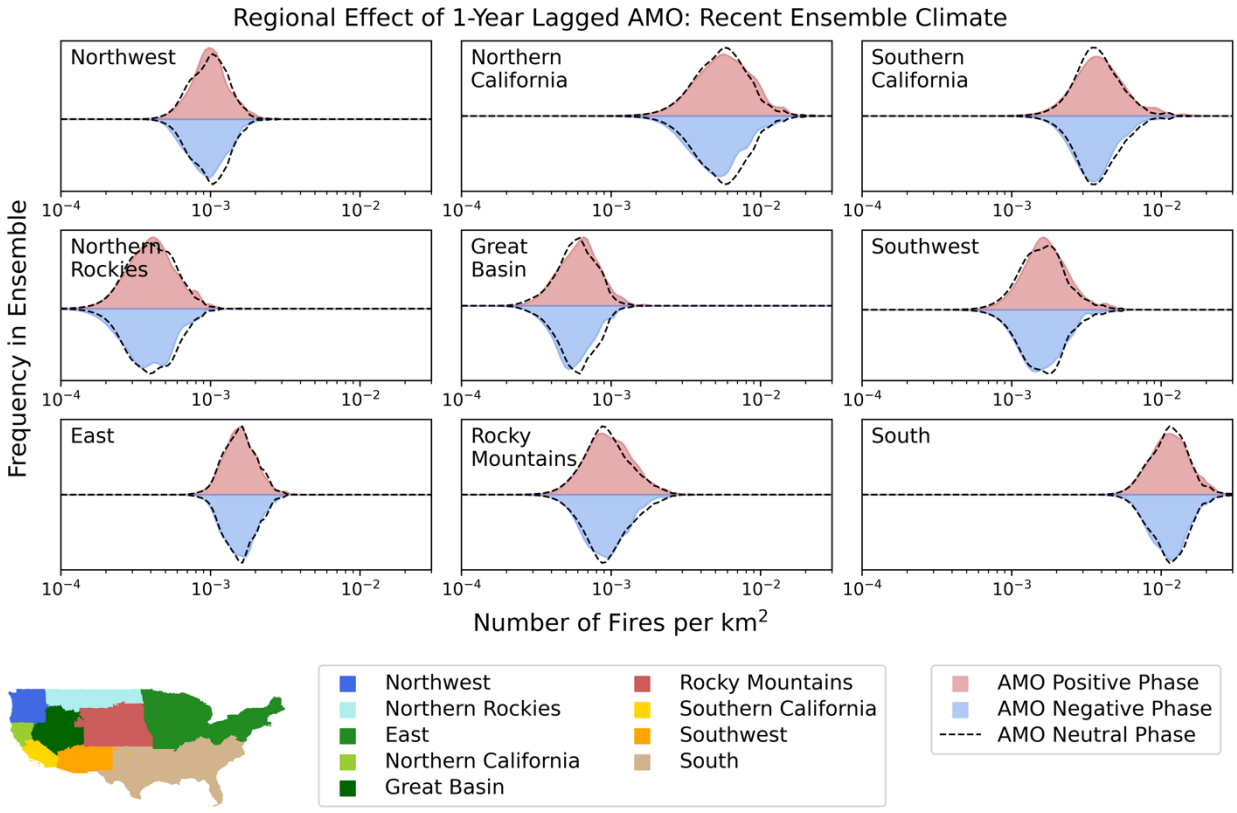

Supplementary Figure 9.1: the effect of Atlantic Multidecadal Oscillation (AMO) on US wildfire distributions regionally.

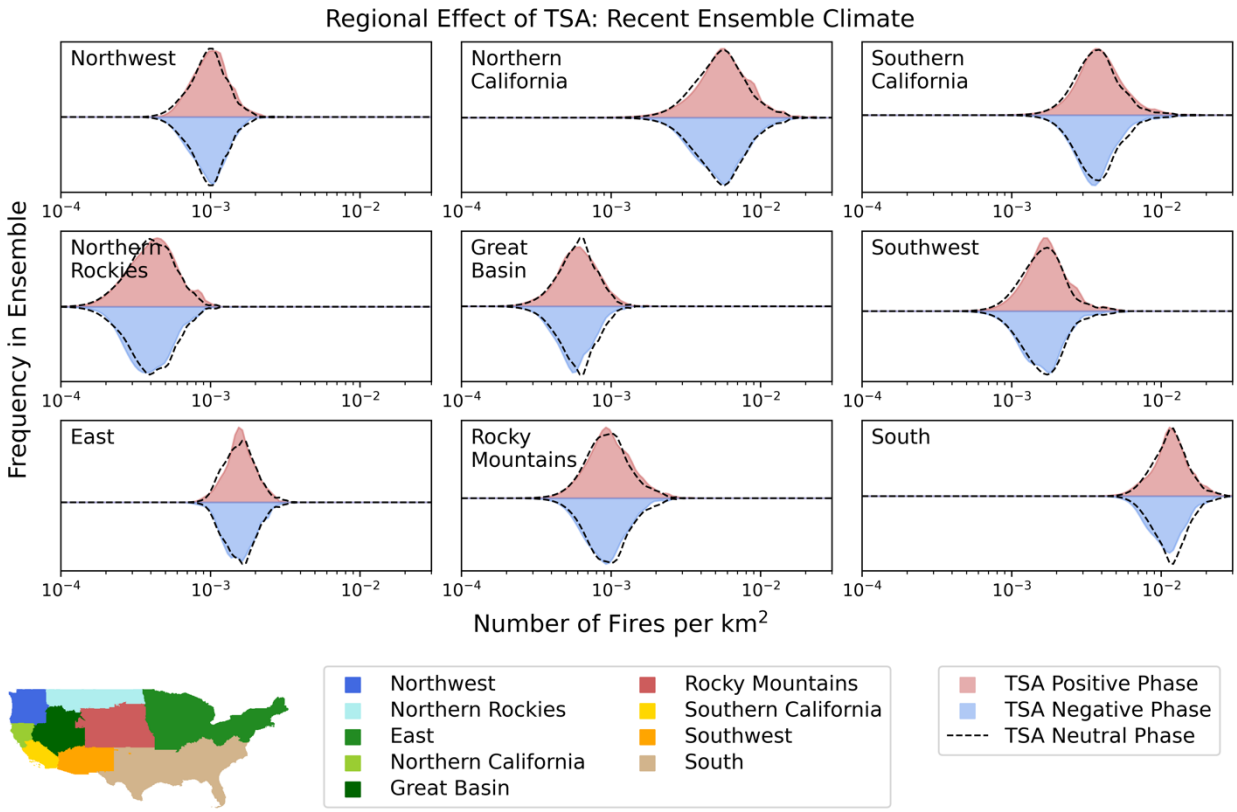

Supplementary Figure 9.2: the effect of Tropical South Atlantic (TSA) on US wildfire distributions regionally.

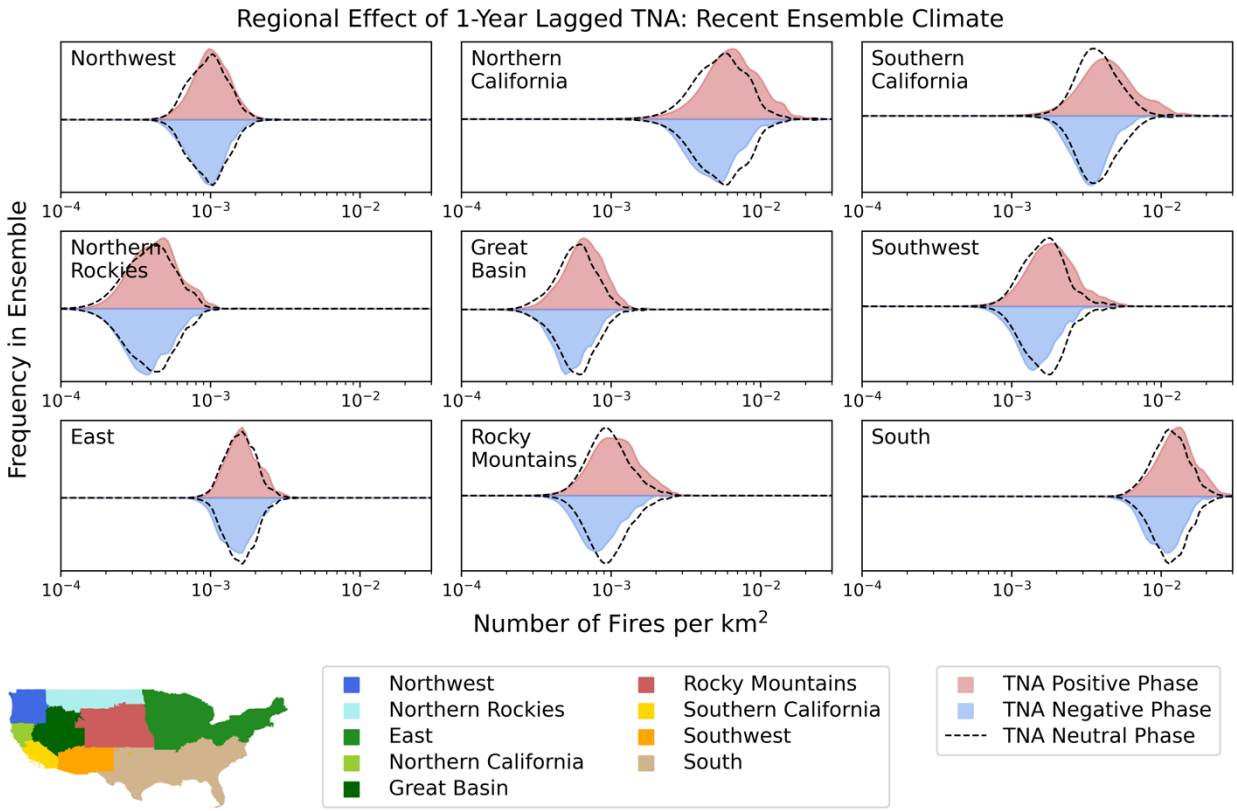

Supplementary Figure 9.3: the effect of 1-year lagged Tropical North Atlantic (TNA+1) on US wildfire distributions regionally.

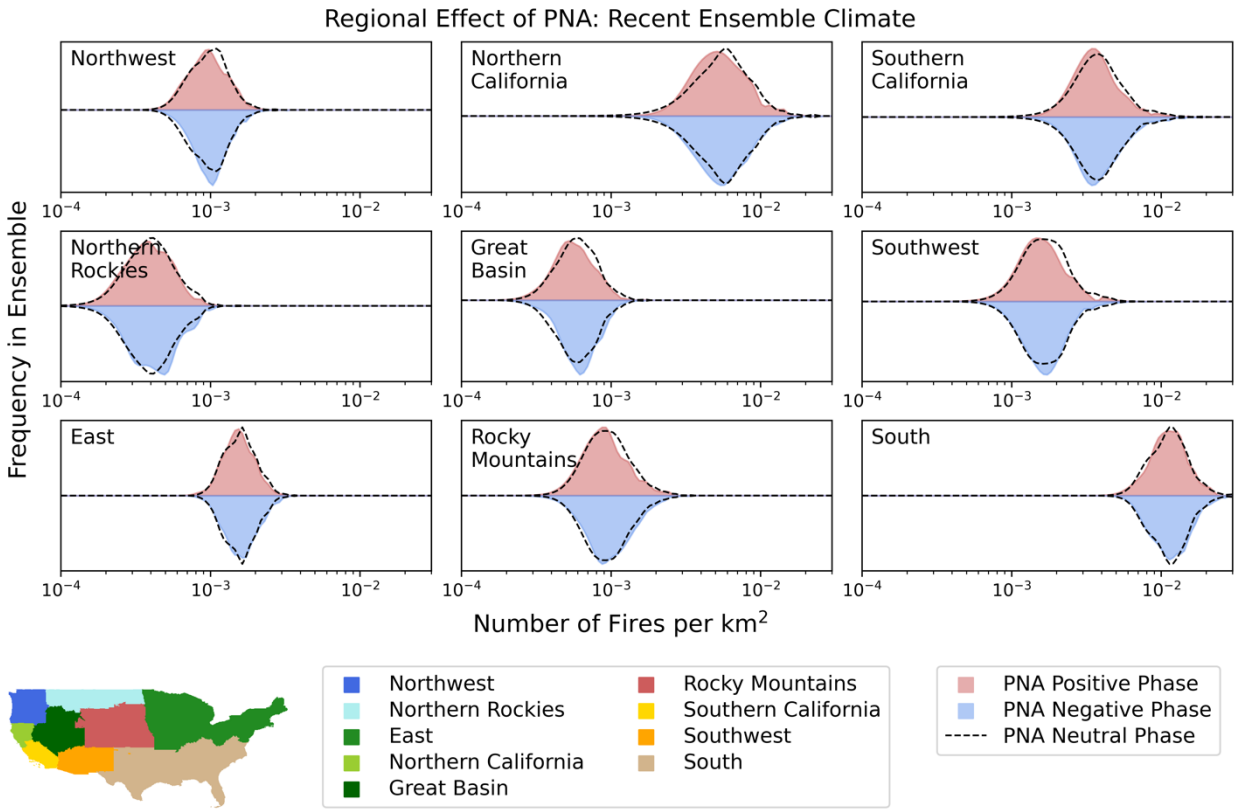

Supplementary Figure 9.4: the effect of Pacific/North American (PNA) on US wildfire distributions regionally.

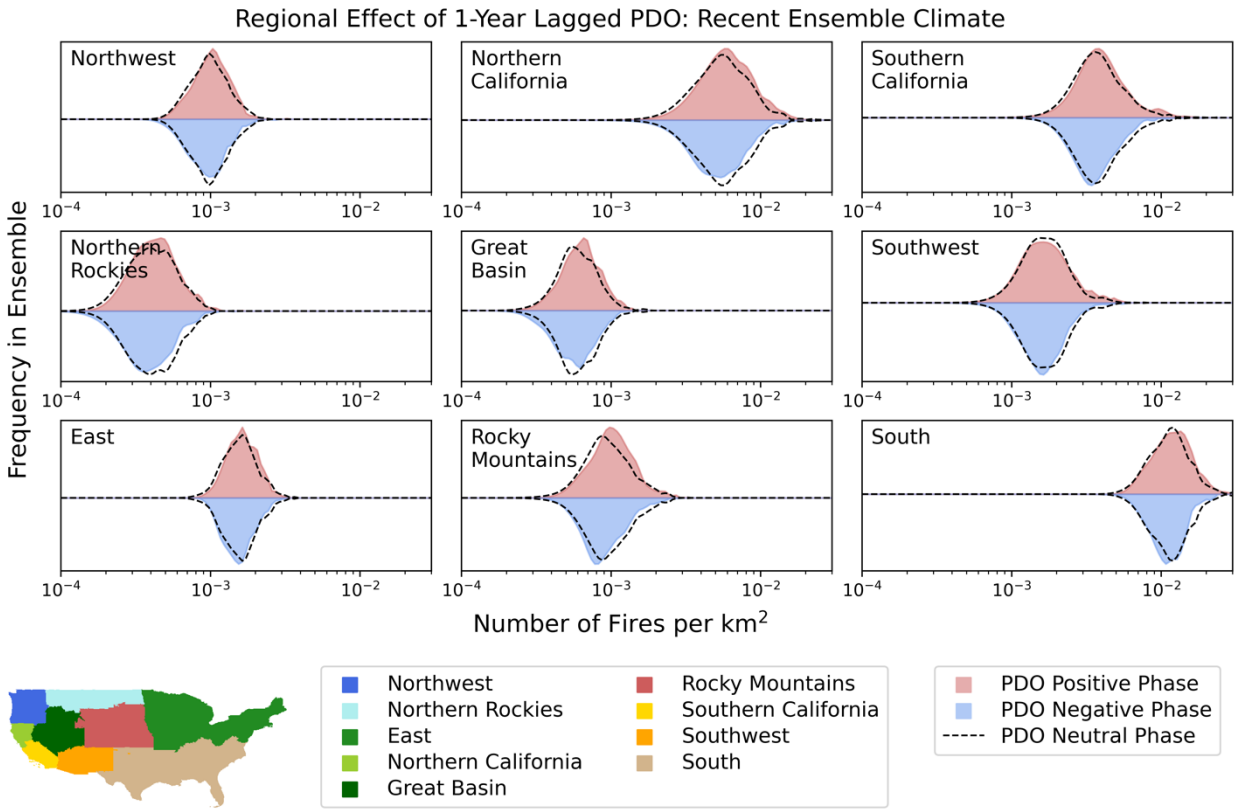

Supplementary Figure 9.5: the effect of 1-year lagged Pacific Decadal Oscillation (PDO+1) on US wildfire distributions regionally.

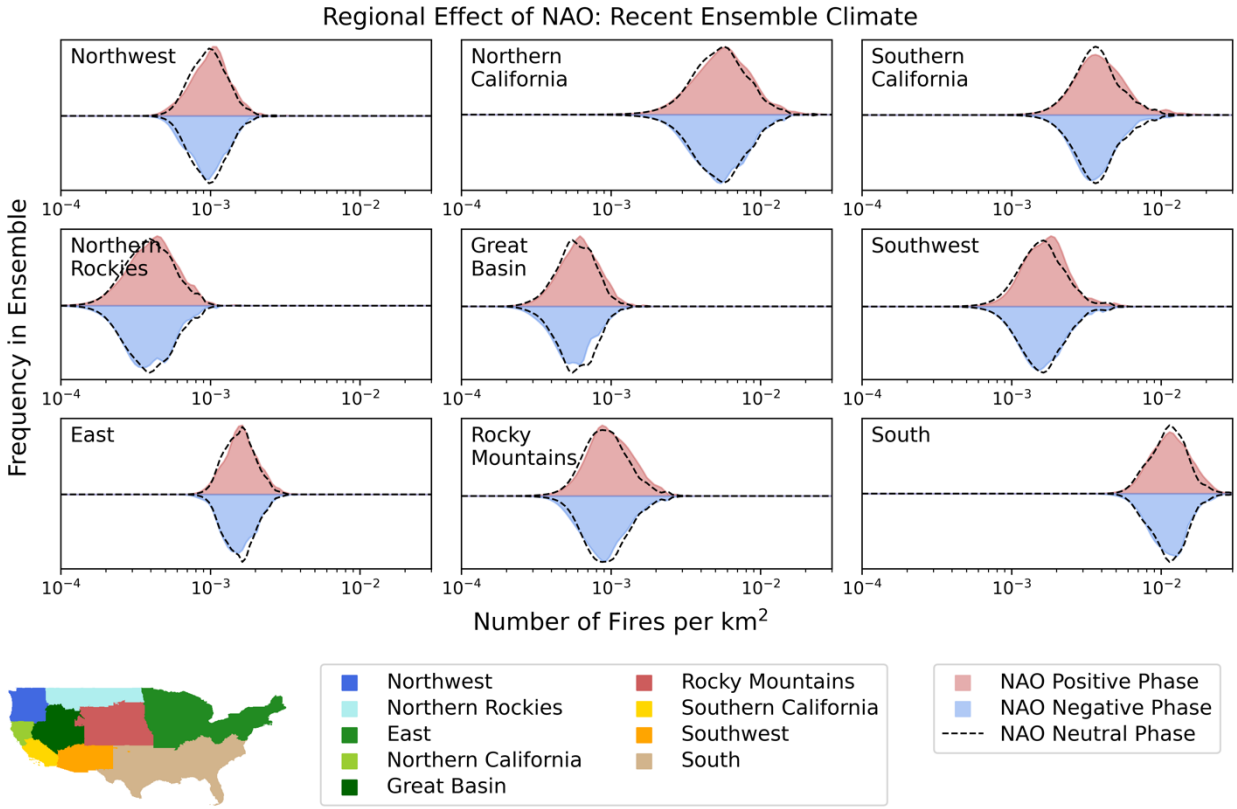

Supplementary Figure 9.6: the effect of North Atlantic Oscillation (NAO) on US wildfire distributions regionally.

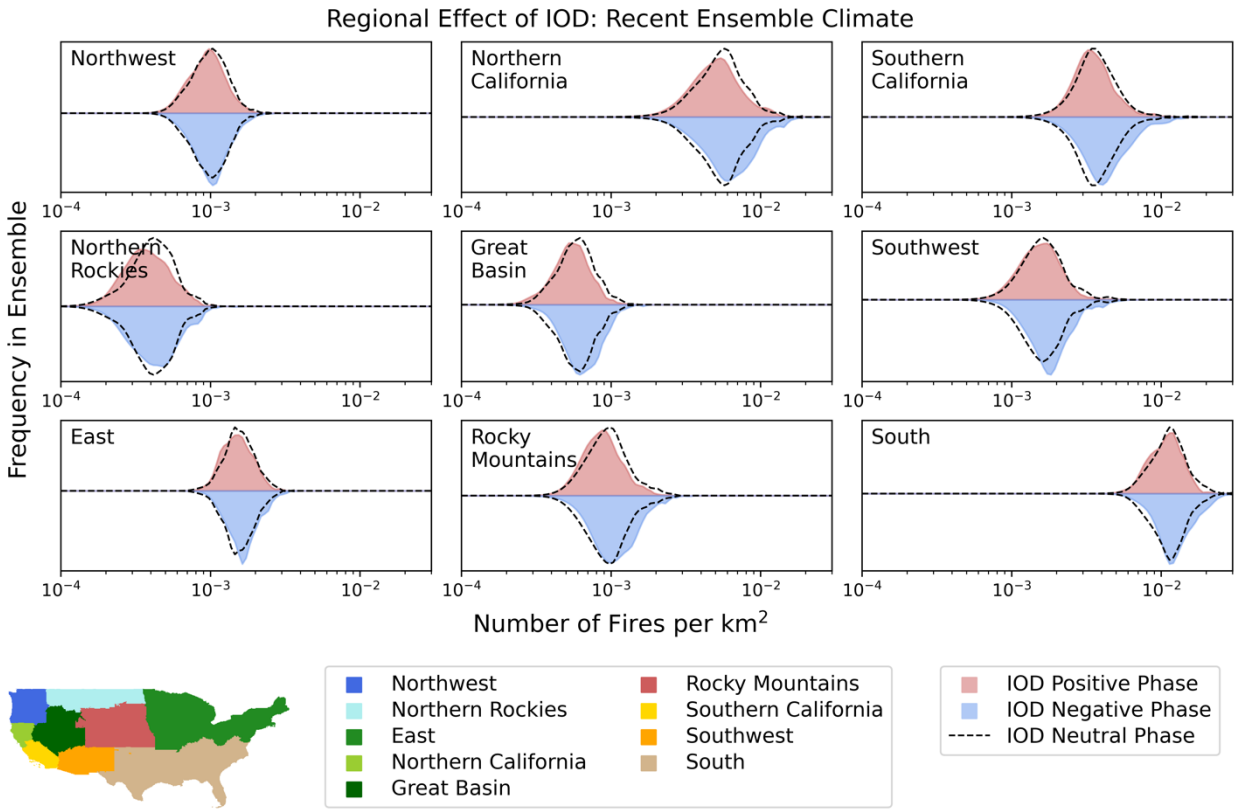

Supplementary Figure 9.7: the effect of Indian Ocean Dipole (IOD) on US wildfire distributions regionally.

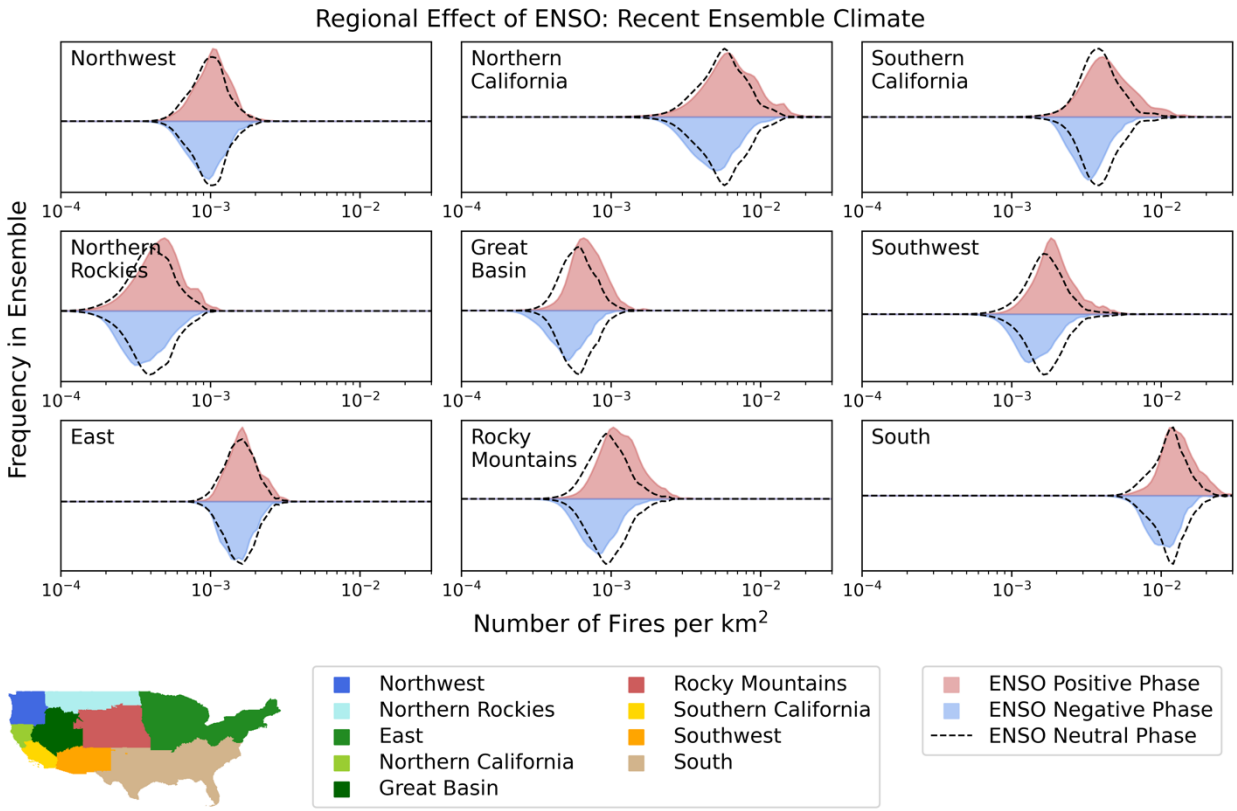

Supplementary Figure 9.8: the effect of El Niño Southern Oscillation (ENSO) on US wildfire distributions regionally.

4.7.10 Wildfire Season Length and Peak Timing Given Climate Mode Phase

El Niño shows a strong effect on the seasonal timing, resulting in an earlier fire season peak east of the Great Plains and a later fire season peak west of the Great Plains and in the southwestern US. The reverse of this effect is apparent in La Niña years, but is not as strong in its difference from the mean. This El Niño like effect on the fire season is also apparent in the negative 1-year lagged Tropical North Atlantic (TNA+1), the positive Indian Ocean Dipole (IOD), and the negative 1-year lagged Pacific Decadal Oscillation (PDO+1) in order of decreasing strength. The negative Pacific/North American and positive North Atlantic Oscillation are also associated with a half-month earlier peak in the Californian fire season. The effect on the length of the fire season corresponds to the areas where the modes are most associated with an increase in the number of wildfires (Figure 4). This signal is strongest for the increasing effect under La Niña in the southwestern US, the Great Plains, and southern Florida, an effect also visible in the IOD and TNA+1.

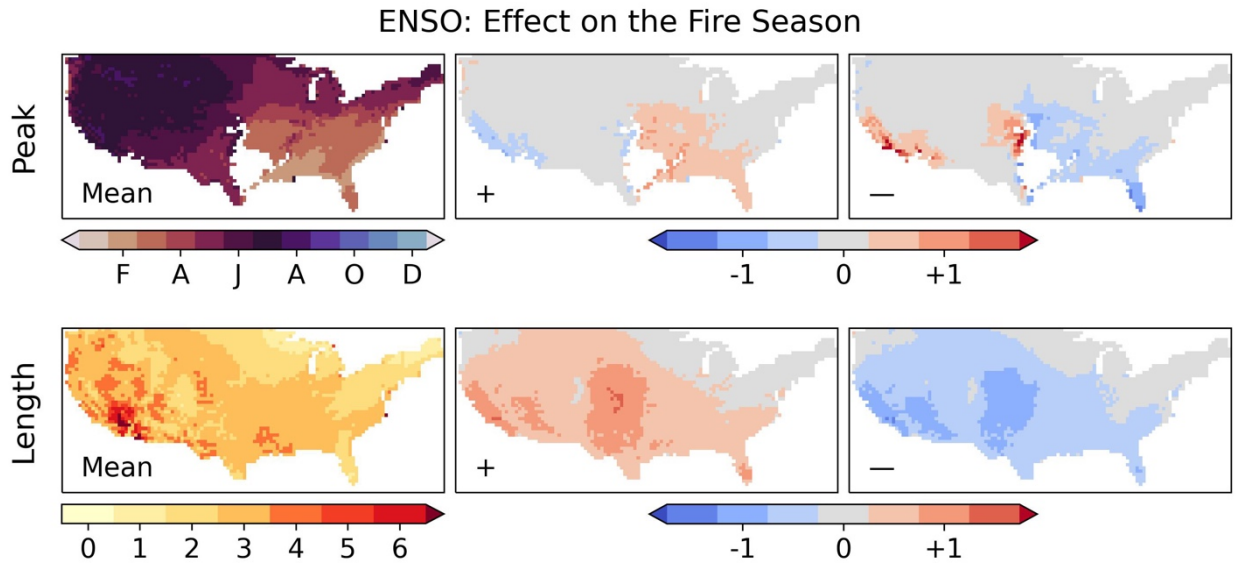

Supplementary Figure 10.1: top row; the average seasonal phase across all locations with sufficiently high seasonal concentration (over 0.15), and the effect of the phase of El Niño Southern Oscillation (ENSO) on the timing of the seasonal peak in months. Bottom row; the length of the fire season in months (calculated as the number of months over the mean annual half-maximum) and the effect of the phase of ENSO on the season length in months.

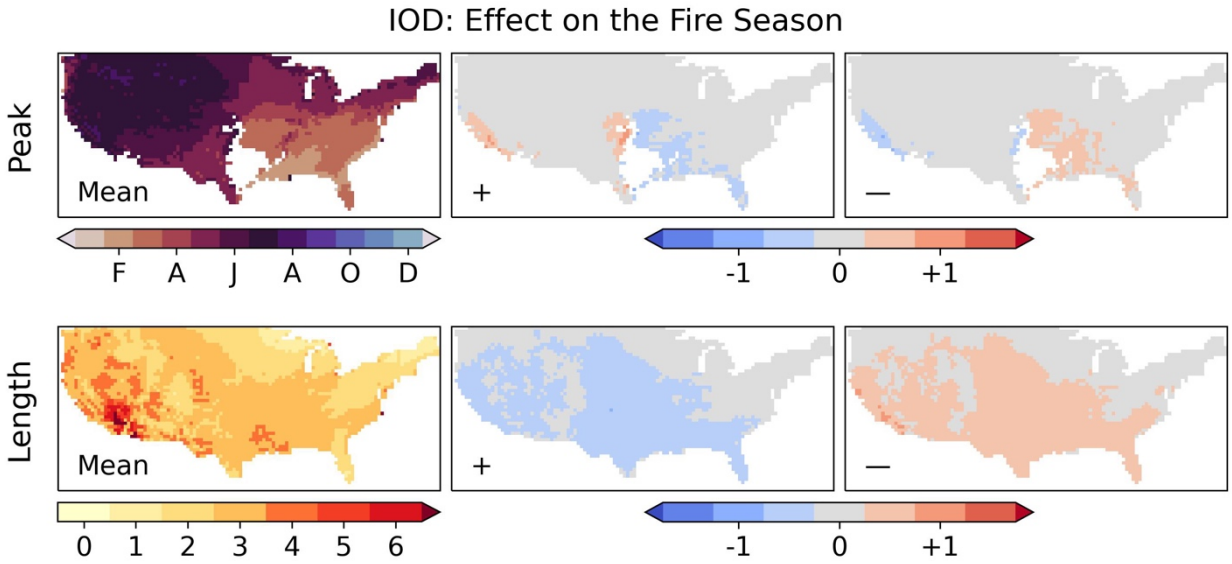

Supplementary Figure 10.2: top row; the average seasonal phase across all locations with sufficiently high seasonal concentration (over 0.15), and the effect of the phase of the Indian Ocean Dipole (IOD) on the timing of the seasonal peak in months. Bottom row; the length of the fire season in months (calculated as the number of months over the mean annual half-maximum) and the effect of the phase of IOD on the season length in months.

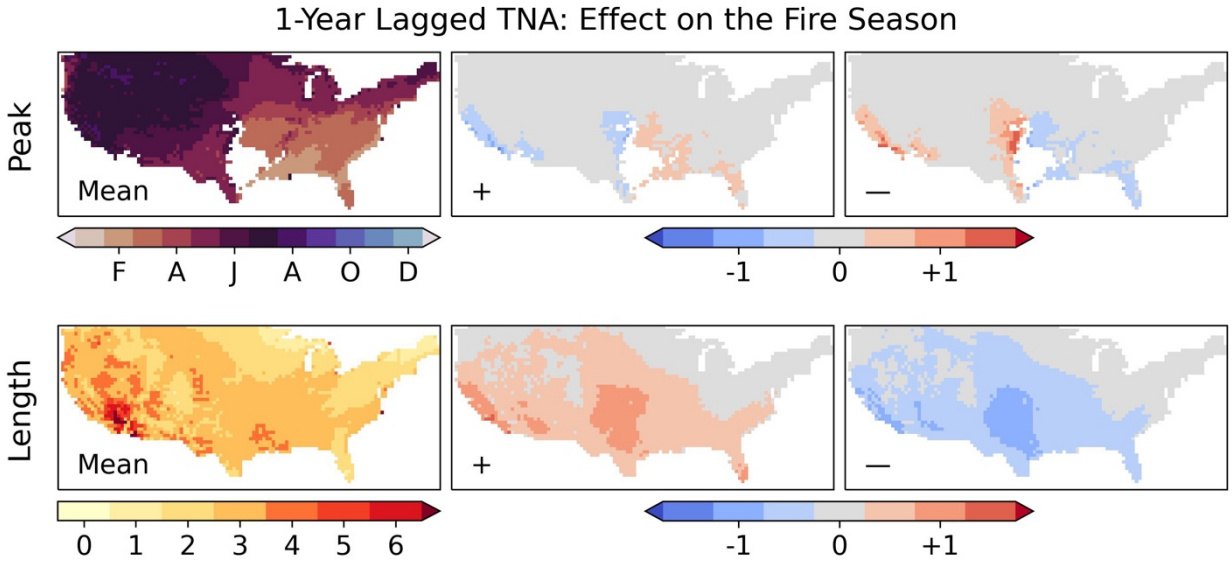

Supplementary Figure 10.3: top row; the average seasonal phase across all locations with sufficiently high seasonal concentration (over 0.15), and the effect of the phase of the 1-year lagged Tropical North Atlantic (TNA+1) on the timing of the seasonal peak in months. Bottom row; the length of the fire season in months (calculated as the number of months over the mean annual half-maximum) and the effect of the phase of TNA+1 on the season length in months.

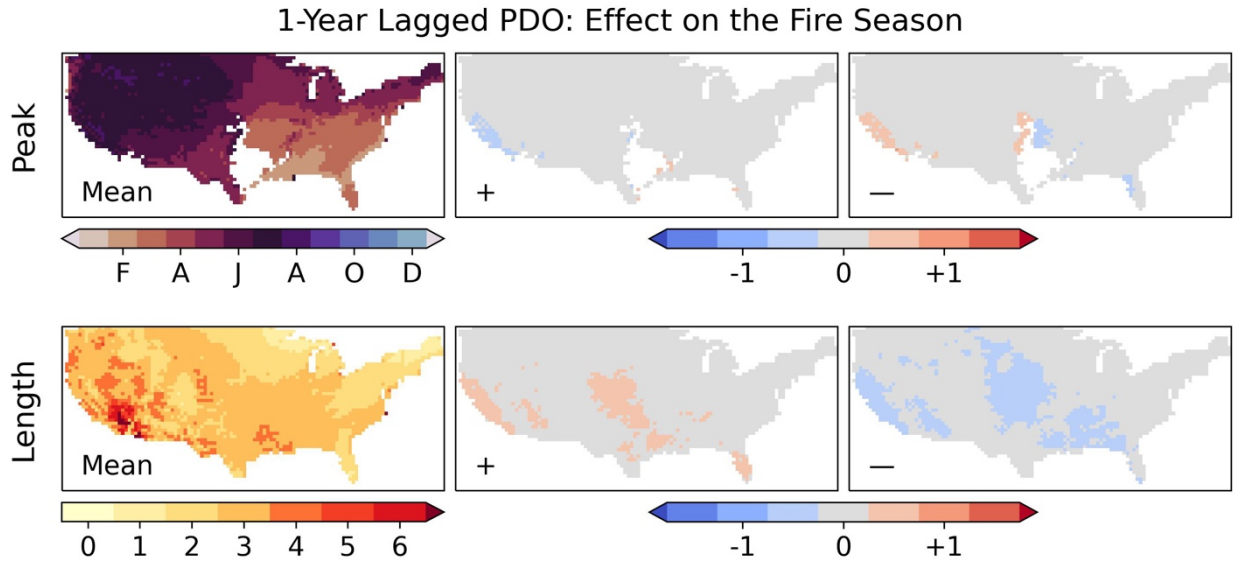

Supplementary Figure 10.4: top row; the average seasonal phase across all locations with sufficiently high seasonal concentration (over 0.15), and the effect of the phase of the 1-year lagged Pacific Decadal Oscillation (PDO+1) on the timing of the seasonal peak in months. Bottom row; the length of the fire season in months (calculated as the number of months over the mean annual half-maximum) and the effect of the phase of PDO+1 on the season length in months.

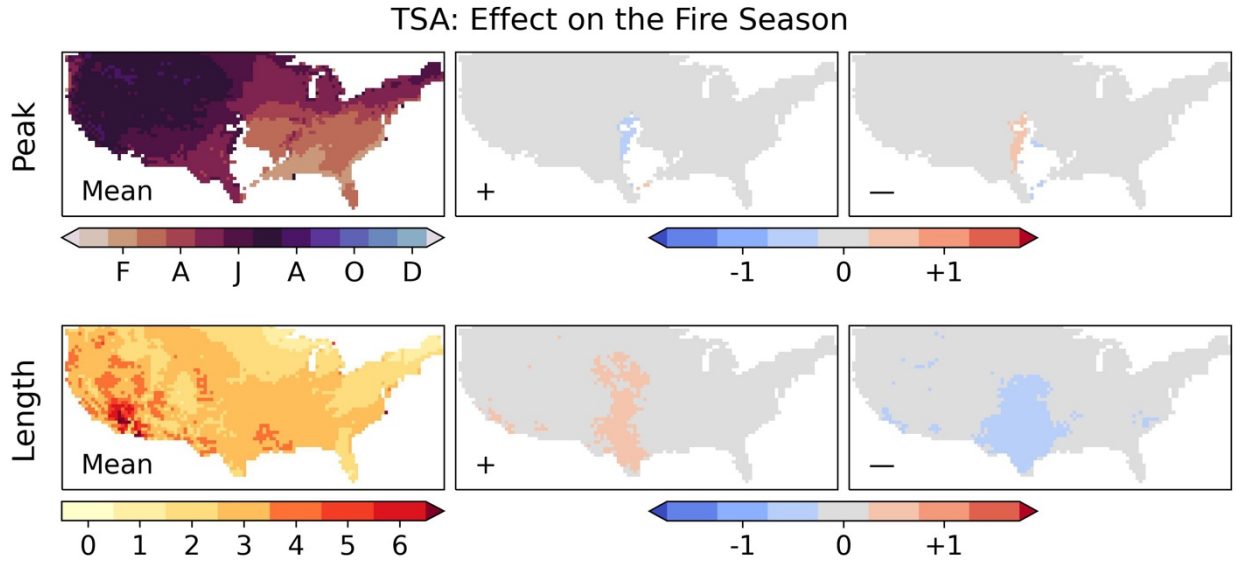

Supplementary Figure 10.5: top row; the average seasonal phase across all locations with sufficiently high seasonal concentration (over 0.15), and the effect of the phase of the Tropical South Atlantic (TSA) on the timing of the seasonal peak in months. Bottom row; the length of the fire season in months (calculated as the number of months over the mean annual half-maximum) and the effect of the phase of TSA on the season length in months.

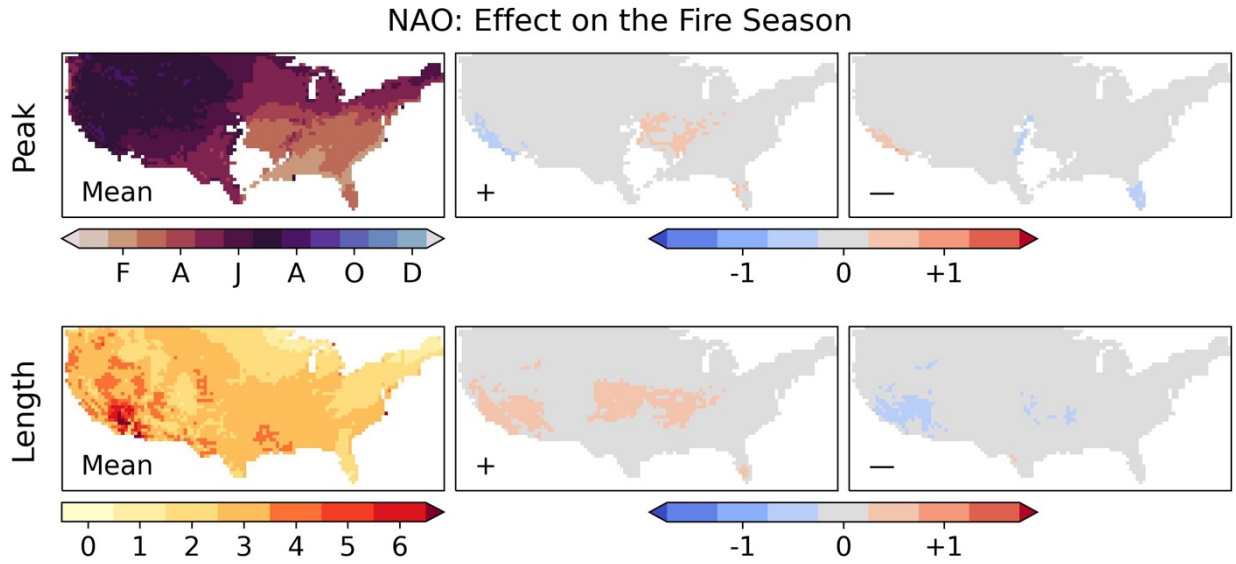

Supplementary Figure 10.6: top row; the average seasonal phase across all locations with sufficiently high seasonal concentration (over 0.15), and the effect of the phase of the North Atlantic Oscillation (NAO) on the timing of the seasonal peak in months. Bottom row; the length of the fire season in months (calculated as the number of months over the mean annual half-maximum) and the effect of the phase of NAO on the season length in months.

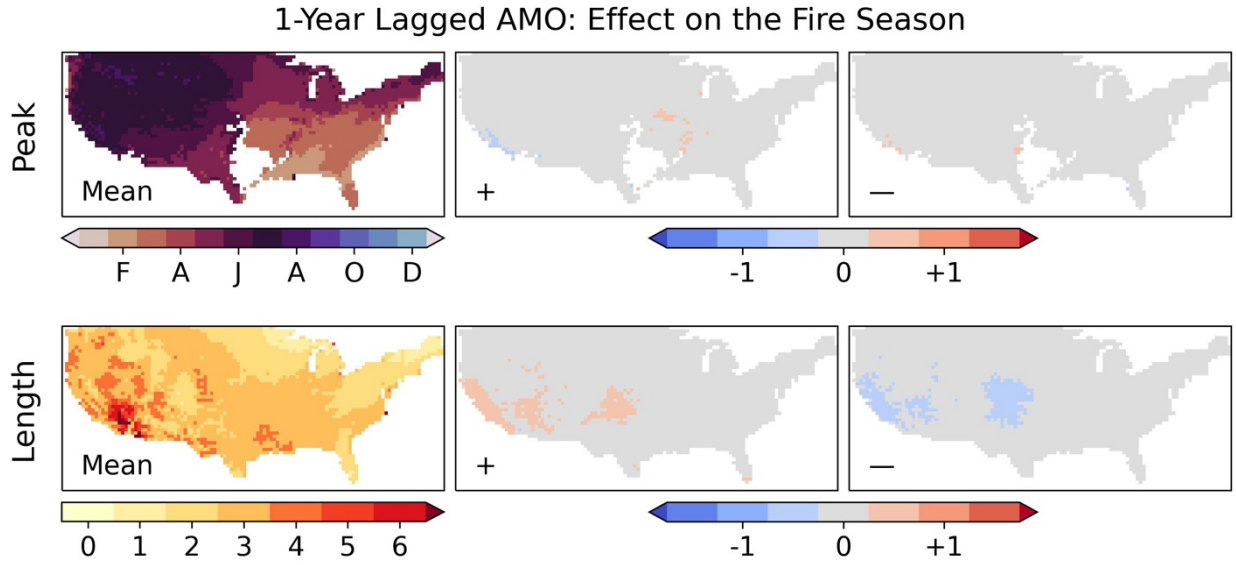

Supplementary Figure 10.7: top row; the average seasonal phase across all locations with sufficiently high seasonal concentration (over 0.15), and the effect of the phase of the 1-year lagged Atlantic Multidecadal Oscillation (AMO+1) on the timing of the seasonal peak in months. Bottom row; the length of the fire season in months (calculated as the number of months over the mean annual half-maximum) and the effect of the phase of AMO+1 on the season length in months.

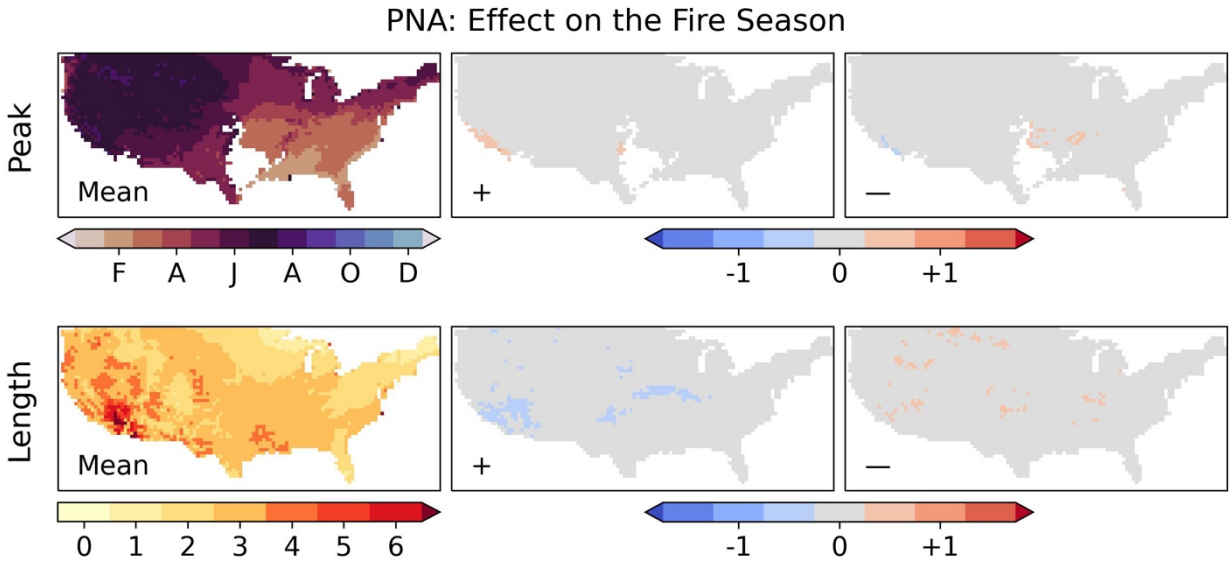

Supplementary Figure 10.8: top row; the average seasonal phase across all locations with sufficiently high seasonal concentration (over 0.15), and the effect of the phase of the Pacific/North American (PNA) on the timing of the seasonal peak in months. Bottom row; the length of the fire season in months (calculated as the number of months over the mean annual half-maximum) and the effect of the phase of PNA on the season length in months.

4.7.11 Effect of Future Climate Change on Wildfire's Relationship with Global Climate Modes

Supplementary Table 11.1 gives the numerical values corresponding the Figure 9 in the main text, showing the change in the areal effect of modes from the recent to +2°C climates.

Maps are then shown for the relative change in the number of wildfires for the recent and +2°C ensemble climates where the effect is significant to $p<0.001$; the strengthening of the effect in the regions where the relationships is significant in both climates (as shown in Figure 10) is also shown for context. In addition to the strengthening effects described in Section 3.3 of the main text, these maps show significant changes in the patterns of influence of some modes. The 1-year lagged Atlantic Multidecadal Oscillation (AMO+1) shows a very strong increase in its area and strength of effect on wildfire occurrence, covering much of the eastern US in the +2°C scenario. The Pacific/North American (PNA) and Arctic Oscillation (AO) also increase significantly in their area of effect, covering much of the central US in the +2°C climate; whilst the Tropical South Atlantic (TSA) declines to having almost no influential area.

Supplementary Table 11.1: Percentage of contiguous US area significantly affected by each mode in the +2°C period. Three asterisks indicate a changed area over 30%, two asterisks indicate a changed area over 10%, one asterisk indicates a changed area over 5%.

		Was Insignificant			Was Positive			Was Neg		
		N/A	+	-	N/A	+	-	N/A	+	
Same Year	ENSO	3.6	5.0	0.2	2.0	88.9	0.0	0.1	0.0	0.
	IOD	3.6	0.4	*5.8	0.0	0.1	0.0	1.0	0.0	89
	PDO	57.9	2.4	3.1	**17.7	16.4	1.3	0.7	0.0	0.
	TNA	19.5	*8.8	**25.5	0.1	0.6	0.0	*6.3	0.0	39
	TSA	47.5	0.0	0.0	***52.2	0.0	0.0	0.3	0.0	0.
	NAO	53.7	*7.8	4.4	**14.7	19.4	0.0	0.0	0.0	0.
	PNA	30.0	0.1	***43.6	0.0	0.0	0.0	2.6	0.0	23
	AO	61.5	**28.8	0.0	1.9	7.8	0.0	0.0	0.0	0.
	AMO	79.8	**17.1	3.1	0.0	0.0	0.0	0.0	0.0	0.
	SAM	100.0	0.0	0.0	0.0	0.0	0.0	0.0	0.0	0.
	EA	100.0	0.0	0.0	0.0	0.0	0.0	0.0	0.0	0.
Lagged	ENSO	22.6	2.4	**29.0	0.3	1.0	0.8	*8.5	0.0	35

	IOD	62.8	**12.4	*7.5	0.1	3.7	0.0	**12.5	0.4	0.
	PDO	20.9	*5.8	0.0	*7.0	66.3	0.0	0.0	0.0	0.
	TNA	8.5	*5.5	0.0	1.0	84.7	0.0	0.3	0.0	0.
	TSA	66.3	*6.7	0.0	**13.9	13.1	0.0	0.0	0.0	0.
	NAO	44.6	0.0	**22.7	0.2	0.0	0.0	*5.1	0.0	27
	PNA	79.5	**10.6	0.0	4.2	5.7	0.0	0.0	0.0	0.
	AO	97.3	0.0	0.0	0.0	0.0	0.0	2.7	0.0	0.
	AMO	18.0	***34.5	0.0	*5.8	41.5	0.0	0.1	0.0	0.
	SAM	95.1	0.0	0.0	4.9	0.0	0.0	0.0	0.0	0.
	EA	100.0	0.0	0.0	0.0	0.0	0.0	0.0	0.0	0.

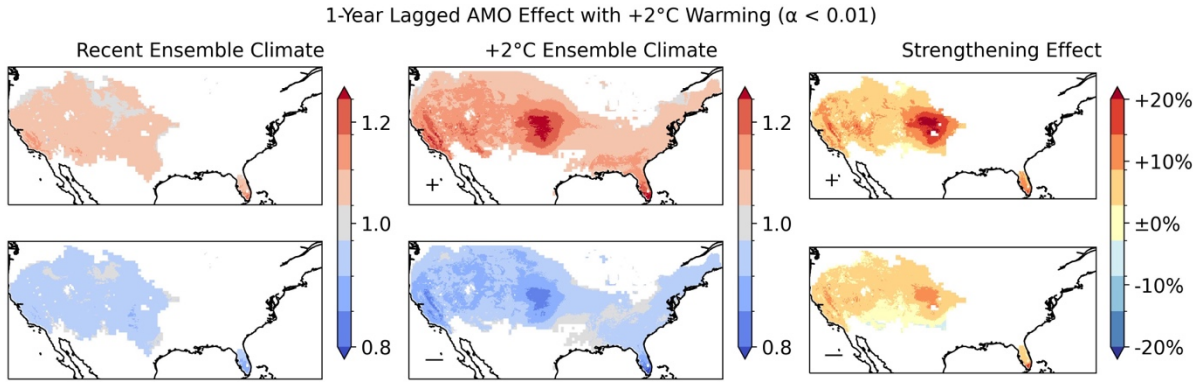

Supplementary Figure 11.1: A comparison of the significant areas of effect of the 1-year lagged Atlantic Multidecadal Oscillation (AMO+1) in the recent and +2°C time periods, with the ratio of the overlapping significant areas of effect shown in the right-hand column.

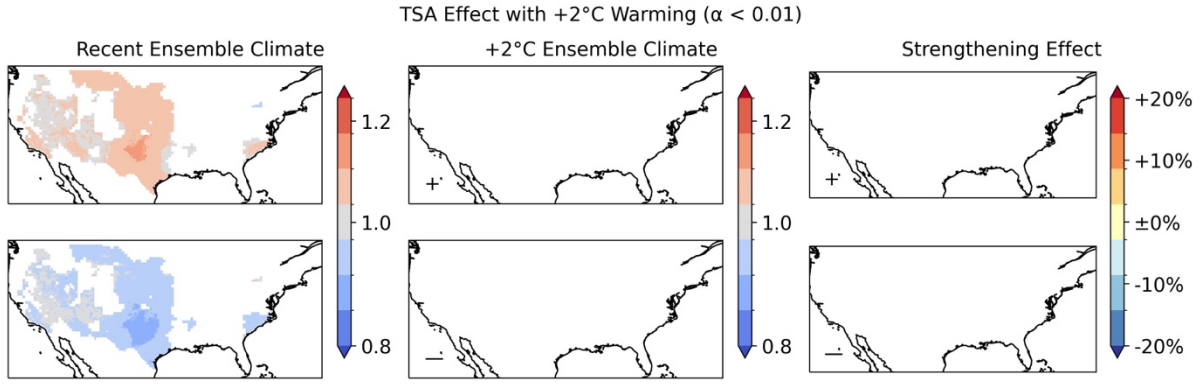

Supplementary Figure 11.2: A comparison of the significant areas of effect of the Tropical South Atlantic (TSA) in the recent and +2°C time periods, with the ratio of the overlapping significant areas of effect shown in the right-hand column.

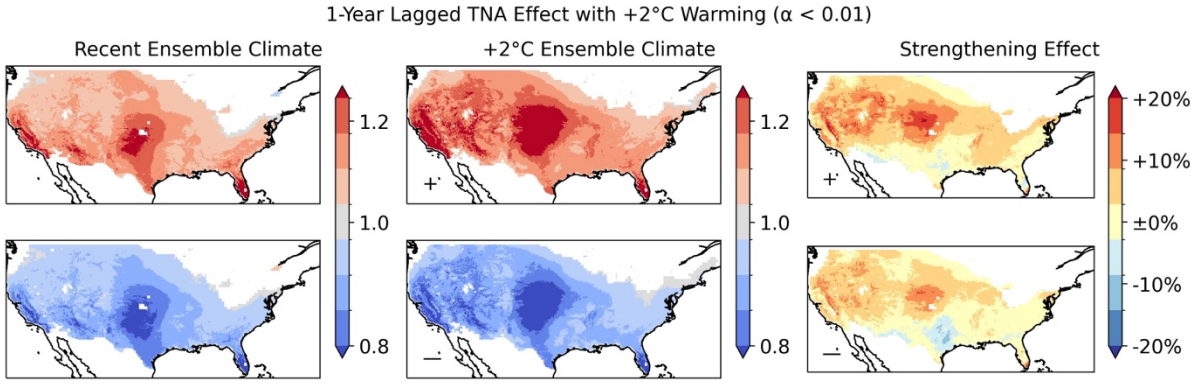

Supplementary Figure 11.3: A comparison of the significant areas of effect of the 1-year lagged Tropical North Atlantic (TNA+1) in the recent and +2°C time periods, with the ratio of the overlapping significant areas of effect shown in the right-hand column.

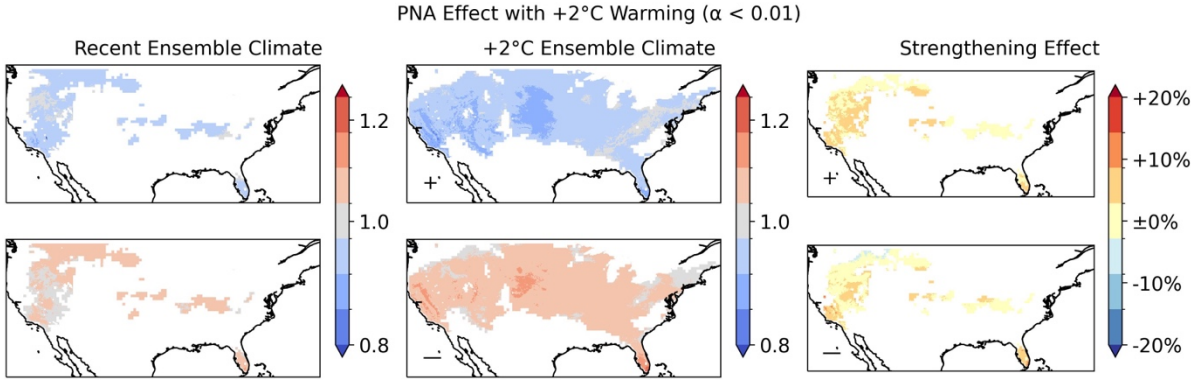

Supplementary Figure 11.4: A comparison of the significant areas of effect of the Pacific/North American (PNA) in the recent and +2°C time periods, with the ratio of the overlapping significant areas of effect shown in the right-hand column.

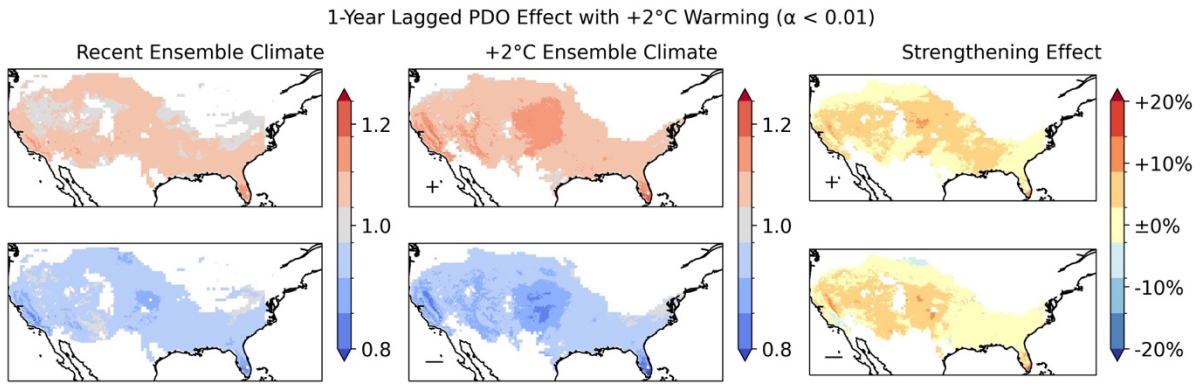

Supplementary Figure 11.5: A comparison of the significant areas of effect of the 1-year lagged Pacific Decadal Oscillation (PDO+1) in the recent and +2°C time periods, with the ratio of the overlapping significant areas of effect shown in the right-hand column.

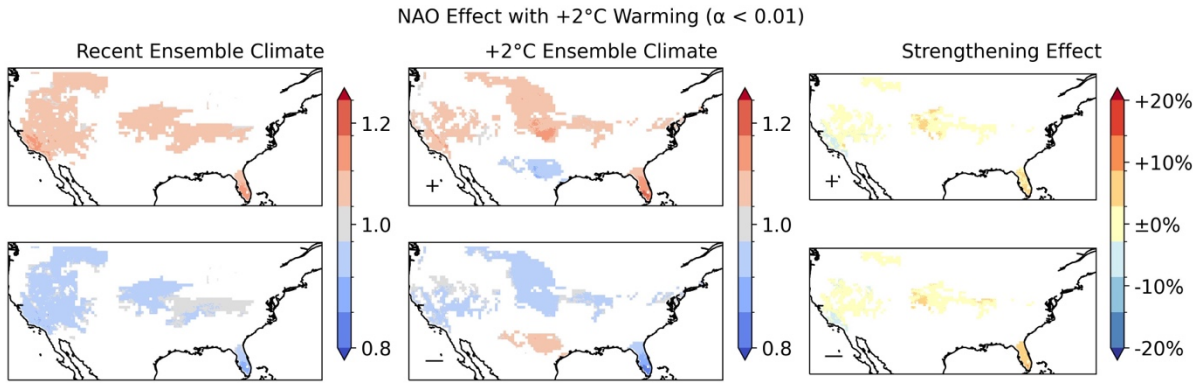

Supplementary Figure 11.6: A comparison of the significant areas of effect of the North Atlantic Oscillation (NAO) in the recent and +2°C time periods, with the ratio of the overlapping significant areas of effect shown in the right-hand column.

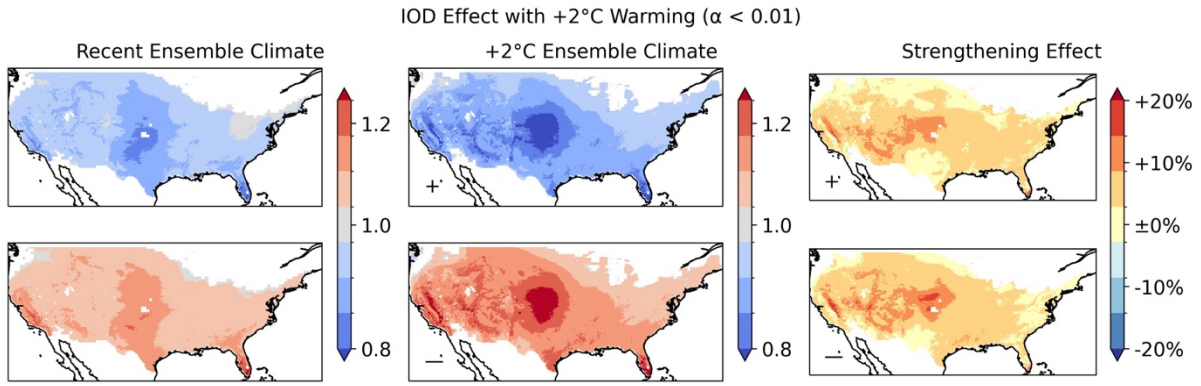

Supplementary Figure 11.7: A comparison of the significant areas of effect of the Indian Ocean Dipole (IOD) in the recent and +2°C time periods, with the ratio of the overlapping significant areas of effect shown in the right-hand column.

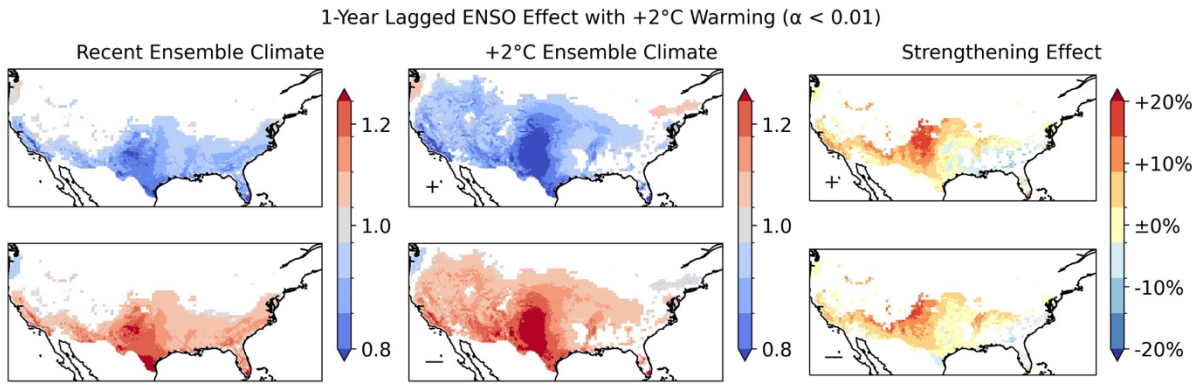

Supplementary Figure 11.8: A comparison of the significant areas of effect of El Niño Southern Oscillation (ENSO) in the recent and +2°C time periods, with the ratio of the overlapping significant areas of effect shown in the right-hand column.

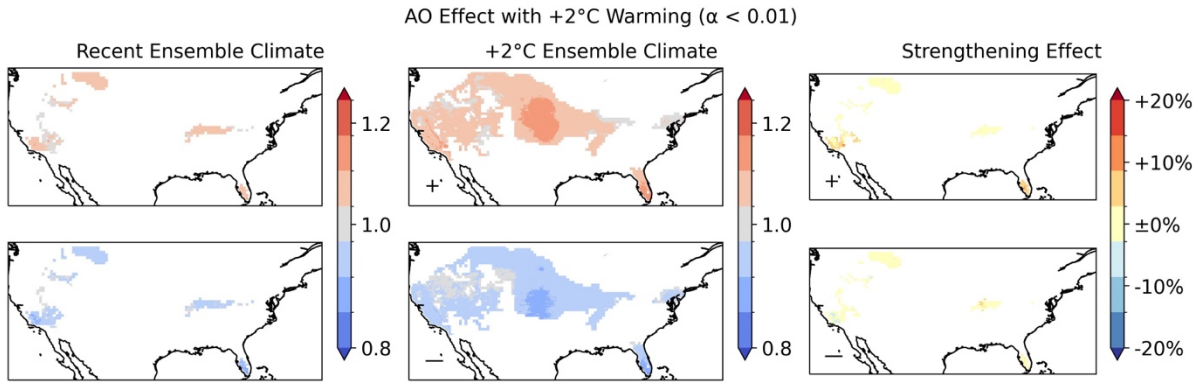

Supplementary Figure 11.9: A comparison of the significant areas of effect of the Arctic Oscillation (AO) in the recent and +2°C time periods, with the ratio of the overlapping significant areas of effect shown in the right-hand column.

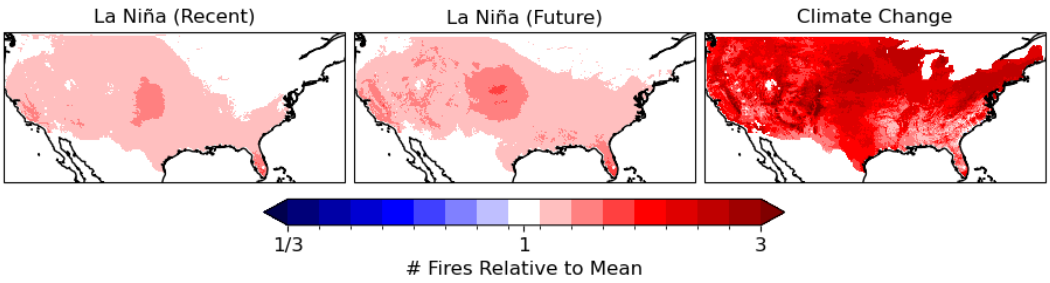

Supplementary Figure 11.10: The magnitude of internal variability in annual fire occurrences due to a climate mode state (La Niña) relative to the mean number of fires in the recent and +2°C warmer climates in comparison to the difference between the recent and future climates. Left: the difference between the average annual number of wildfires in La Niña years and across all years in the recent (2000-2009) climate. Centre: the difference between the average annual number of wildfires in La Niña years and across all years in the +2°C warmer climate. Right: the difference between the average annual number of wildfires across all years in the recent (2000-2009) and future (+2°C warmer) climates.

4.7.12 Supplementary References

Ascoli D, Hacket-Pain A, LaMontagne JM, Cardil A, Conedera M, Maringer J, Motta R, Pearse IS, Vacchiano G (2020) Climate teleconnections synchronize Picea glauca masting and fire disturbance: evidence for a fire-related form of environmental pre- diction. J. Ecol. 108:1186–1198. https://doi.org/10.1111/1365-2745.13308

Ault T, Macalady A, Pederson G, Betancourt J, Schwartz M (2011) Northern hemisphere modes of variability and the timing of spring in western North America. J. Clim. 24:4003–4014. https://doi.org/10.1175/2011JCLI4069.1

Barbero R, Abatzoglou JT, Brown TJ (2015) Seasonal reversal of the influence of El Niño–Southern Oscillation on very large wildfire occurrence in the interior northwestern United States. Geophys. Res. Lett. 42:3538–3545. https://doi.org/10.1002/2015GL063428

Cardil A, Rodrigues M, Tapia M, Barbero R, Ramírez J, Stoof CR, Silva CA, Mohan M, de-Miguel S (2023) Climate teleconnections modulate global burned area. Nat Commun. 14:427. https://doi.org/10.1038/s41467-023-36052-8

Cardil A, Rodrigues M, Ramirez J, de-Miguel S, Silva CA, Mariani M, Ascoli D (2021) Coupled effects of climate teleconnections on drought, Santa Ana winds and wildfires in southern California, Sci. Tot. Env. 765:142788. https://doi.org/10.1016/j.scitotenv.2020.142788

Dai A (2013) The influence of the inter-decadal Pacific oscillation on US precipitation during 1923–2010. Clim. Dyn. 41(3):633-646. https://doi.org/10.1007/s00382-012-1446-5

Dannenberg MP, Wise EK, Janko M, Hwang T, Smith WK (2018) Atmospheric teleconnection influence on North American land surface phenology. Environ. Res. Lett. 13. https://doi.org/10.1088/1748-9326/aaa85a

Dixon PG, Goodrich GB, Cooke WH (2008) Using teleconnections to predict wildfires in Mississippi. Mon. Weather. Rev. 136:2804–2811. https://doi.org/10.1175/2007MWR2297.1

Fauria M, Johnson EA (2008) Climate and wildfires in the North American boreal forest. Philos Trans R Soc Lond B Biol Sci. 363:2317-29. https://doi.org/10.1098/rstb.2007.2202

Goodrick SL, Hanley DE (2009) Florida wildfire activity and atmospheric teleconnections. Int. J Wild. Fire 18:476-482. https://doi.org/10.1071/WF07034

Hessl AE, McKenzie DE, Schellhaas R (2004) Drought and Pacific Decadal Oscillation linked to fire occurrence in the inland Pacific Northwest, Ecol. Appl. 14(2):425–442. https://doi.org/10.1890/03-5019

Heyerdahl EK, Brubaker LB, Agee JK (2002) Annual and decadal climate forcing of historical fire regimes in the interior Pacific Northwest, USA. Holocene 12:597–604. https://doi.org/10.1191/0959683602hl570rp

Heyerdahl EK, McKenzie D, Daniels LD, Hessl AE, Littell JS, Mantua NJ (2008) Climate drivers of regionally synchronous fires in the inland northwest (1651–1900). Int. J. Wildland Fire, 17(1):40–49. https://doi.org/10.1071/WF07024

Hu Q, Feng S (2010) Influence of the Arctic oscillation on central United States summer rainfall. J. Geophy. Res. Atmos, 115(D1). https://doi.org/10.1029/2009JD011805

Hu Q, Feng S, Oglesby RJ (2011) Variations in North American summer precipitation driven by the Atlantic multidecadal oscillation. J. Clim. 24(21):5555-5570. https://doi.org/10.1175/2011JCLI4060.1

Hu ZZ, Kumar A, Jha B, Chen M, Wang W (2023) The tropical Indian Ocean matters for US winter precipitation variability and predictability. Env. Res. Lett. 18(7):074033. https://doi.org/10.1088/1748-9326/ace06e

Johnston JD, Bailey JD, Dunn CJ (2017) Historical fire-climate relationships in contrasting interior Pacific Northwest forest types. Fire Ecol. 13:18–36. https://doi.org/10.4996/fireecology.130257453

Justino F, Bromwich DH, Schumacher V. (2022) Arctic Oscillation and Pacific-North American pattern dominated-modulation of fire danger and wildfire occurrence. NPJ Clim. Atmos. Sci. 5:52. https://doi.org/10.1038/s41612-022-00274-2

Kipfmueller KF, Larson ER, St. George S (2012) Does proxy uncertainty affect the relations inferred between the Pacific Decadal Oscillation and wildfire activity in the western United States?, Geophys. Res. Lett. 39:04703, https://doi.org/10.1029/2011GL050645

Kitzberger T, Brown PM, Heyerdahl EK, Swetnam TW, Veblen TT (2007) Contingent Pacific-Atlantic Ocean influence on multicentury wildfire synchrony over western North America. PNAS 104:543-548, https://doi.org/10.1073/pnas.0606078104

Kitzberger T, Swetnam TW, Veblen TT (2001) Inter-hemispheric synchrony of forest fires and the El Niño-Southern Oscillation, Glob. Ecol. Biogeogr. 10(3):315–326, https://doi.org/10.1046/j.1466-822X.2001.00234.x

Kumar A, Wang H, Wang W, Xue Y, Hu ZZ (2013). Does knowing the oceanic PDO phase help predict the atmospheric anomalies in subsequent months?. J. Clim. 26(4):1268-1285. https://doi.org/10.1175/JCLI-D-12-00057.1

Kushnir Y, Seager R, Ting M, Naik N, Nakamura J (2010) Mechanisms of tropical Atlantic SST influence on North American precipitation variability. J. Clim. 23(21):5610-5628. https://doi.org/10.1175/2010JCLI3172.1

Le Goff H, Flannigan MD, Bergeron Y, Girardin MP (2007) Historical fire regime shifts related to climate teleconnections in the Waswanipi area, central Quebec, Canada. Int. J. Wild. Fire 16:607-618. https://doi.org/10.1071/WF06151

Leathers DJ, Yarnal B, Palecki MA (1991) The Pacific/North American teleconnection pattern and United States climate. Part I: Regional temperature and precipitation associations. J. Clim. 4(5):517-528. https://doi.org/10.1175/1520-0442(1991)004<0517:TPATPA>2.0.CO;2

Mason SJ, Goddard L (2001) Probabilistic precipitation anomalies associated with ENSO. Bull. A. Met. Soc. 82(4):619-638. https://doi.org/10.1175/1520-0477(2001)082<0619:PPAAWE>2.3.CO;2

Margolis EQ, Swetnam TW (2013) Historical fire–climate relationships of upper elevation fire regimes in the south-western United States. Int. J. of Wild. Fire 22:588–598. https://doi.org/10.1071/WF12064

Mason SA, Hamlington PE, Hamlington BD, Jolly MW, Hoffman CM (2017) Effects of climate oscillations on wildland fire potential in the continental United States. Geophys. Res. Lett. 44:7002–7010. https://doi.org/10.1002/2017gl074111

Moody TJ, Fites-Kaufman J, Stephens SL (2006) Fire history and climate influences from forests in the Northern Sierra Nevada, USA. Fire Ecol 2:115–141. https://doi.org/10.4996/fireecology.0201115

Ning L, Bradley RS (2014) Winter precipitation variability and corresponding teleconnections over the northeastern United States. J. Geo. Res. Atmos. 119(13):7931-7945. https://doi.org/10.1002/2014JD021591

Norman SP, Taylor AH (2003). Tropical and north Pacific teleconnections influence fire regimes in pine-dominated forests of north-eastern California, USA. J Biogeog. 30:1081–1092. https://doi.org/10.1046/j.1365-2699.2003.00889.x

Rodrigo FS (2021) Exploring combined influences of seasonal East Atlantic (EA) and North Atlantic Oscillation (NAO) on the temperature-precipitation relationship in the Iberian Peninsula. Geosci. 11(5):211. https://doi.org/10.3390/geosciences11050211

Ropelewski CF, Halpert MS (1987) Global and regional scale precipitation patterns associated with the El Niño/Southern Oscillation. Mon. Weath. Rev. 115(8):1606-1626. https://doi.org/10.1175/1520-0493(1987)115<1606:GARSPP>2.0.CO;2

Schoennagel T, Veblen TT, Romme WH, Sibold JS, Cook ER (2005) ENSO and PDO variability affect drought-induced fire occurrence in Rocky Mountain subalpine forests. Ecol. Appl. 15:2000-2014. https://doi.org/10.1890/04-1579

Sibold JS, Veblen TT (2006) Relationships of subalpine forest fires in the Colorado Front Range with interannual and multidecadal-scale climatic variation, J. Biogeogr., 33(5):833–842. https://doi.org/10.1111/j.1365-2699.2006.01456.x

Simard AJ, Haines DA, Main WA (1985) Relations between El Nino/Southern Oscillation anomalies and wildland fire activity in the United States. Agr.For. Met. 36:93-104, https://doi.org/10.1016/0168-1923(85)90001-2

Simpkins G (2021). Breaking down the NAO–AO connection. Nat. Rev. Earth Env. 2(2):88-88. https://doi.org/10.1038/s43017-021-00139-x

Soulard N, Lin H, Yu B (2019) The changing relationship between ENSO and its extratropical response patterns. Sci. Rep. 9(1):6507. https://doi.org/10.1038/s41598-019-42922-3

Swetnam TW, Betancourt JL (1998) Mesoscale disturbance and ecological response to decadal climatic variability in the American Southwest. J. Clim. 11:3128–3147. https://doi.org/10.1175/1520-0442(1998)011<3128:MDAERT>2.0.CO;2

Swetnam TW, Betancourt JL (1990) Fire-southern oscillation relations in the southwestern United States. Science 249:1017–1020, https://doi.org/10.1126/science.249.4972.1017

Tang X, Li J, Zhang Y, Li Y, Zhao S (2023) Synergistic effect of El Niño and negative phase of North Atlantic Oscillation on winter precipitation in the southeastern United States. J. Clim. 36(6):1767-1791. https://doi.org/10.1175/JCLI-D-22-0293.1

Trouet V, Taylor AH, Wahl ER, Skinner CN, Stephens SL (2010) Fire-climate interactions in the American West since 1400 CE. Geophys. Res. Lett. 37:L04702 https://doi.org/10.1029/2009GL041695

Westerling AL, Swetnam TW (2003) Interannual to decadal drought and wildfire in the western United States. Trans. AGU 84(49):545-555. https://doi.org/10.1029/2003EO490001

Discussion and Conclusions

In this thesis, I have presented a new model to predict the likelihood of wildfire occurrence. I then ran that model using outputs from a large ensemble (LE) climate model to investigate the interannual variability of wildfire occurrences in both the recent climate and a climate subject to a further +2°C global warming. Finally, I used this LE to assess the association of wildfire occurrence activity with global climate modes in the contiguous US, and the effect of future climate change on these relationships. The approach taken to address these questions included some key innovations, including (1) the use of an LE instead of a single climate model run to quantify uncertainties stemming from intrinsic internal climate variability, (2) the focus on climate modes as potential precursors of fire occurrence, and (3) the approach to variable and variable-domain selection.

5.1 Overview of Key Innovations

5.1.1 Driving Wildfire Model with an LE

5.1.1.1 Characterising Interannual Variability

Weather conditions and vegetation properties are key controls on the wildfire regime, with annual patterns in atmospheric moisture demand (VPD) and vegetation growth (GPP) able to predict distinct wildfire regimes (Harrison et al., 2025b). Seasonal weather – and its effect on plant productivity – is stochastic, meaning that an individual seasonal realisation of the weather is one of many possible outcomes in a particular climate. Interannual variability in weather conditions can therefore be directly linked to the strong variability between fire years at federal (USA) or national (EU) scales (San-Miguel-Ayanz et al., 2024; Finco et al., 2012). This variability in annual wildfire can lead to difficulty in assessing likely fire year severities which systems could experience. Most wildfire modelling efforts have used a single realisation of the climate and therefore of climate-driven vegetation properties (e.g. Hantson et al., 2020; Li et al., 2024; Sullivan et al., 2022; Burton et al., 2024). This can give a realistic overview of what actually happened but is a very small sample of the possible conditions that could occur, whether a reanalysis of observed weather or a climate model run is used to run the fire model. A single realisation is thus insufficient to predict the distribution of possible outcomes in the near-term using the current climate, or in the future using climate projections. The application of the wildfire occurrence model with a large climate ensemble (Chapter 3) is a key tool for characterising the distribution of possible wildfire year outcomes.

The distribution of fire weather has been assessed using LE methods (Squire et al., 2021), but such studies do not consider the effect of the vegetation response to climate variability. The spread of average fire year outcomes has also been assessed by applying a wildfire model to different projected rates of climate change (Sullivan et al., 2022). However, as climate variability is not well-characterised by a single model run, this places an upper and lower bound on average annual wildfire conditions given emissions pathway uncertainty and does not relate to the spread in a given projected climate. Epistemic uncertainty on the distribution of possible wildfire outcomes has also been tested, for example, by using the uncertainty on model parameters (Sullivan et al., 2022) or on the best weighting of multiple deterministic wildfire predictions (Burton et al., 2024). Such methods are useful best estimates given model limitations, but again do not allow for the full extent of interannual variability in modelled wildfire to be assessed.

In this thesis, I apply input data derived from a bias-corrected and downscaled 160-member large ensemble (Chapter 3) to the wildfire occurrence model (Chapter 2) for the recent (2000-2009) and future (a further +2°C) climates. This provides a distribution of potential fire years that can be used to assess expected annual wildfire occurrence to different return periods, and how those occurrence levels respond to future climate change. Using an LE to characterise a climate-related impact is standard in other research areas such as flooding (Cloke et al., 2012; Van der Wiel et al., 2019), extreme heat (McHugh et al., 2023), and storms (Yoshida et al., 2017). LE applications are especially valuable when accounting for climate change, as the distribution at a given global mean surface temperature is not well sampled by realised weather before it is changed by further warming. Furthermore, with a much larger sample size the determinants of high activity fire years can be established to a higher level of statistical significance. A leave-one-out application of the LE shows that variability in annual GPP is of emerging importance in determining fire year variability as the climate changes, and that variability in VPD is the predominant control on the severity of extreme fire years (Chapter 3). It also allows a better characterisation of the wildfire regime from a preparedness and operational perspective. For example, the 1-in-100-year wildfire season length is an important statistic to ensure that there are sufficient resources for a long fire season. This cannot be determined from a single climate realisation, as the number of years with sufficiently similar climate conditions is much less than 100.

5.1.1.2 Defining the Effect of Global Climate Modes

Climate modes are oscillating regional patterns in the coupled ocean-atmospheric system, such as the Atlantic Multidecadal Oscillation (AMO) or El Niño Southern Oscillation (ENSO). The phases of these climate modes persist for seasonal to multidecadal time periods and condition the likelihood of different seasonal weather outcomes (Wang and Schimel, 2003; Kenyon and Hegerl, 2008). The effect of climate modes on weather in turn affects wildfire, for example through the effect of altered precipitation patterns on fuel accumulation or of temperature extremes on fuel moisture (Shen et al., 2019). Many climate modes exhibit identifiable precursors, such as through anomalies in sea surface temperatures, pressure and wind shear (Chang et al., 2007; Zhang et al., 2014). This enables climate modes to be predicted months in advance and thus provides a method to predict wildfire in the coming season.

Applying a wildfire model to a large ensemble time-slice has the advantage of delivering a large dataset in an approximately static climate, allowing the association of global climate modes with wildfire to be rigorously determined (Chapter 4). The LE method finds the continuously varying geographic pattern of the association between a climate mode and wildfire occurrences, giving both the magnitude and significance level of the relationship. Previous work on the association between climate modes and wildfire (Chapter 4, Supplementary Table 1.1) has focussed on statistical significance. This does not directly map onto the magnitude of a climate mode's effect, which is the more important variable from a risk management perspective. Whilst the LE has been applied in this thesis to find the effect on annual wildfire occurrences, the method is also applicable to other wildfire models for variables such as fire size or intensity.

Climate mode-wildfire associations have previously been examined using remote sensing data from recent decades, regional wildfire records, and multi-century tree-ring analysis. The LE approach I have presented (Chapter 4) addresses limitations in each of these methodologies. Remotely sensed wildfire records start at approximately 1980, so are limited by the short time-period of the observational record. Longer timescale climate modes have undergone few oscillations in this period which, in conjunction with the noisiness of wildfire data, means that relationships cannot be resolved to a high level of confidence in most regions (Cardil et al., 2023), even whilst not accounting for the false discovery rate accounted for in this thesis. Multi-decadal national and regional wildfire records have also been used (Cardil et al., 2021; Dixon et al., 2008; Fauria and Johnson, 2007), but the records are also often too short to resolve

relationships between wildfire and longer timescale modes. Additionally, fire activity data is often aggregated over large areas, which may obscure geographic differences in the effect of climate modes. Multi-century tree-ring analysis (Kitzberger et al., 2007; Le Goff et al., 2007; Sibold and Veblen, 2006) can address the timescale issue but only informs on a specific site. Results from this method have therefore not been scaled to large regions and cannot identify continuous geographic patterns in a mode's effect. Very recent progress in machine learning reconstructed burnt area (Guo et al., 2025) has provided wildfire data from 1900, which could be used with verification from short-period satellite or spatially discontinuous tree-ring based analyses.

5.1.2 Overcoming Issues in Wildfire Occurrence Modelling

5.1.2.1 Flexible Variable Selection

Wildfire likelihood is conditioned by multiple effects, or 'drivers'. These include topographic effects – such as terrain ruggedness and elevation, meteorological controls on fuel moisture and fire dynamics – such as evaporative demand, precipitation and wind, human influence on the landscape – through ignitions, fire suppression and land-use, and the effect of vegetation – due to fuel loads and plant flammability (Chapter 1, Jones et al., 2022). Whilst the number of effects that influence wildfire are confined to controls on ignitions, heat-release and spread, there are many variables that have been used to represent these underlying factors. One example would be the use of either precipitation, or atmospheric humidity or temperature related effects to model fuel drying (Haas et al., 2024). Furthermore, once a physically sound variable has been chosen, it can be parameterised based on multiple different statistics and time periods. There are therefore a very high number of potential predictors, making variable selection a key problem for wildfire model development. As ignition sources are random and variation in fuel composition and moisture cannot be exactly known, a probabilistic modelling approach is necessary (Taylor et al., 2013). This makes the robust selection of predictors with a strong physical basis especially important.

The major factors included in wildfire models are natural ignitions, human ignitions, live and dead vegetation amounts, plant flammability traits, fuel moisture, wind, topography, and human suppression of fires (Chapter 1, Rabin et al., 2017; Haas et al., 2024). An illustrative example of the poor consensus on which effects to include is the number of variables that have been used in wildfire models to characterise the amount and continuity of vegetation. These include gross primary production (GPP), the fraction of absorbed photosynthetically active radiation, the leaf

area index, vegetation optical depth, net primary production, and solar-induced fluorescence (Bistinas et al., 2014; Forkel et al., 2017; Kuhn-Régnier et al., 2021; Haas et al., 2022; Di Giuseppe, 2023; Forrest et al., 2024). Similarly, temperature, specific humidity, relative humidity, vapour pressure deficit (VPD), dry days, and soil moisture have been used to quantify the effect of atmospheric moisture demand (Krawchuk et al., 2009; Kuhn-Régnier et al., 2021; Haas et al., 2022; Son et al., 2024). Even given the selection of a specific variable, numerous statistics of that variable can be viable predictors. For example, VPD is used to describe the fuel drying response to variations in temperature and humidity (Williams et al., 2019), however the minimum, maximum, daytime mean, 24-hour mean, and various multi-day means have all been shown to be useful predictors of wildfire (Chapter 2, Balch et al., 2022; Haas et al., 2022). The effect of vegetation is also predictive at multiple different antecedent timescales – recent plant growth decreases wildfire likelihood, whilst long-term growth increases the likelihood (Chapter 2, Kuhn-Régnier et al., 2021; Haas et al., 2022). This reflects the fact that long-term growth increases fuel availability whereas recent growth can only occur when plant-available moisture is high, meaning that the fuel is likely too wet to burn.

The optimal set of predictors also varies with scale. For example, at a spatial resolution of approximately 25 km, vegetation abundance (annual GPP) is a key predictor of burnt area but reduces fire intensity (Haas et al., 2022). This control on burnt area is partially because GPP is strongly controlled by the fraction of photosynthesising (and thus burnable) land-cover in that grid-cell. However, at a 30m resolution, vegetation abundance (annual NDVI) is predictive of the high intensity, high mortality wildfires (Parks et al., 2018) that occur in high fuel load environments (Chapter 1). Timescale can also alter a variable's effect, meaning the optimal predictors depend on a wildfire model's temporal resolution, which vary from sub-daily (Li et al., 2024) to annual (Krawchuk et al., 2009) timesteps. For example, at daily timescales high VPD increases wildfire likelihood but over long timescales limits plant growth and reduces wildfire viability (Grossiord et al., 2020).

A number of different methods have been used to select predictors. Haas et al. (2022) use a backwards selection algorithm, eliminating predictors from a generalised linear model (GLM) that do not meet a t-value (significance) greater than 4.5 and variance inflation factor less than 5. This prioritises the selection of highly statistically significant relationships, increasing the likely applicability of the model to out of sample scenarios. However, backwards variable selection is not computationally feasible for large candidate variable sets. Backwards

elimination can also result in the selection of a local rather than global optimum, where an initially eliminated variable could have resulted in a better performing model had a covariate been removed instead (Chowdhury and Turin, 2020). The significance level at which variables are eliminated is also an arbitrary decision compared to methods that optimise for overall model performance. Mukunga et al. (2023) also use a backwards selection algorithm, eliminating predictors from a random forest if they do not meet a variance inflation condition of less than 10. This method targets the greatest span of variables that can be used without introducing multicollinearity and thus emphasises capturing the effects present in the training data most completely. This method shares the backwards elimination issues of Haas et al. (2022) and does not optimise for model performance or predictor significance. Forrest et al. (2024) apply a process of "informed trial and error" in which different variables for key effects such as fire weather or fuel availability are substituted for and evaluated by the model's explained deviance. This is a constrained approach, balancing expert knowledge of wildfire drivers and predictive power. It is not computationally scalable to large sets of candidate predictors and does not test variable combinations that the expert has not considered.

The method I have presented (Chapter 2) uses a variable selection algorithm that tests to see if removing an existing variable improves model performance before calculating the optimal new variable to add. This addresses a number of issues raised by other variable selection methods. Using an automated variable selection algorithm allows for consideration of a much larger pool of candidate variables. The inclusion of a step testing for an improvement by replacing any existing variable is a measure against selection of a local optimum. This is an issue for forwards (backwards) variable selection methods, as the greatest initial improvement from selecting (eliminating) a variable at that step does not relate to that variable being in the set of predictors that maximises model performance (Chowdhury and Turin, 2020). Furthermore, this method optimises for the best overall combination of candidate variables by optimising for model likelihood, as opposed to assessing the significance of individual variables.

Another key advantage of the variable selection algorithm presented in Chapter 1 is that the selection procedure was repeated across multiple training datasets – to assess the consistency of selected variables and select the sets of predictors that perform best. Key driving effects included rural population density, long-term and recent plant productivity, and plant cover type. The combination of diurnal temperature range, night-time VPD, snow-cover and recent precipitation were found to be the most important meteorological predictors. I extended this

work (in Haas et al., 2024) by forcing the selection of each candidate variable in a reduced pool of potential variables and then finding the remaining selected variables across 100 training datasets. This application allows for how well a predictor combines with other key effects to be assessed. For example, if daily insolation is a predictor then shorter antecedence GPP is selected more frequently, or if temperature is a predictor then relative humidity often replaces VPD.

5.1.2.2 Optimisation of Predictor Domains in Linear Wildfire Models

A specific variable may only have an effect on the likelihood of wildfire occurrence in a particular part of its total range, or it may have a positive effect in one part and a negative effect in another. For example, precipitation decreases the immediate likelihood of wildfire but has a much greater effect up to approximately 10 mm d^{-1}, i.e. under conditions that vary from completely dry to moderately moist fuel conditions. There can also be 'humped' relationships between predictors and wildfire. The intermediate productivity hypothesis (Pausas and Ribeiro, 2013) is an example of this. Increasing GPP is associated with an increase in wildfire activity due to higher fuel availability up to an intermediate value of GPP, before further increases of GPP above this value lead to a decrease in wildfire activity as the environment becomes too moist for wildfire. A similar effect is apparent for population density, where wildfire occurrences increase up to an intermediate value, beyond which occurrences decrease (Chapter 1). Thresholds beyond which a variable's effect saturates or changes sign are not accounted for in many statistical wildfire models, including Krawchuk et al. (2009), Haas et al. (2022), Fan et al. (2023), Forrest et al. (2024). This approach is justified for some effects, as monotonic modelled relationships are able to predict emergent unimodal patterns. Linear responses to primary production and moisture predictors combine to produce the humped relationship along the productivity gradient (Bistinas et al., 2014). However, this cannot be assumed to be true for all emergent patterns and does not account for the fact that only some parts of the range of a predictor may cause a significant change in wildfire likelihood.

In this thesis, the domain optimisation method (Chapter 2) iteratively tests clipping each predictor variable's domain (meaning the range of possible values of an independent variable) by raising or decreasing the domain's lower or upper bound respectively. If no initial improvement in model likelihood is found, increasing reductions in the predictors' domains are tested. This algorithm thus identifies the sections of each variable's domain driving the most significant change in wildfire likelihood, eliminating sections of the domain at points beyond which it has no significant additional effect. Some existing wildfire models and fire weather

indices prescribe a heuristic threshold at which this occurs (e.g. Knorr et al., 2014; Van Wagner, 1987). On the other hand, the method I have presented flexibly calculates the optimal cut-off threshold given the training data and other predictors. The precipitation candidate variable varies from 0 to 450 mm d^{-1}, but after optimisation its effective domain is reduced to 0 to 13 mm d^{-1}. This selection captures the saturating effect of rainfall on vegetation flammability and increases the model's predictive power by driving a stronger effect in that critical part of the domain. The upper bound of annual average GPP was clipped at approximately 140 μg C m^{-2} s^{-1} (from 230 μg C m^{-2} s^{-1}), and the effect of population density was cut-off at approximately 7 persons km^{-2} (pre-clipped at 25 persons km^{-2} from 56,000 persons km^{-2}). This reflects the humped response of wildfire likelihood to these variables (Chapter 1, Figure 3). Another key feature of the domain optimisation algorithm is that each step tests for the overall improvement to the model given the other variables included and their domains. Thus, the method optimises for the best combined set of variable domains.

5.2 Summary of Key Findings

In addition to the methodological contributions made (Section 5.1.2), this thesis has also yielded useful findings. The wildfire occurrence model (Chapter 2) identified the key drivers of wildfire occurrence greater than 0.1 ha size in the contiguous USA. The most important human driver was the population density gradient in sparsely habited areas. Annual-multiannual plant growth and recent plant growth were always found to be important, although the degree of antecedence of each varied. Plant cover type was also commonly selected: shrubland and crop cover reduced wildfire occurrence likelihood, and forest and grassland increased wildfire likelihood. The key meteorological effects were controls on atmospheric moisture demand, recent precipitation and snow cover. The most selected combination of atmospheric moisture controls was night-time VPD and diurnal temperature range. These are non-standard wildfire model predictors but relate to widely used variables such as daily average VPD or relative humidity. An explanation for the process captured here is the combined effect of a pre-dawn fine fuel moisture level that is then acted upon by heating during the day.

The LE identified three key areas in which interannual variability has a particularly large effect on annual wildfire outcomes (Chapter 3). These are the small, but nonetheless highly wildfire prone, regions of southern Florida and Mediterranean California, and the much larger Great Plains. Chapter 3 also provided support for the idea for the emergence of a climate change driven fuel limitation on wildfire regimes in the western USA (Abatzoglou et al., 2021) and

identified an increase in the importance of long- and short-term drying effects on fire-year variability in the historically humid southeastern USA.

Chapter 4 extended existing research on the role of climate modes on wildfire activity in the contiguous USA (Kitzberger et al., 2007; Barbero et al., 2015; Mason et al., 2017). The identification of the additional significant effect of the lagged Tropical North Atlantic (TNA+1) climate mode to the relationship between North American wildfire and ENSO is important because seasonal prediction of wildfires generally focuses only on ENSO (NIFC, 2025). The identification of a greater synchronicity of the East and West USA fire season peaks in more wildfire prone La Niña years has implications for resource sharing between regional wildfire management organisations. Finally, these analyses provided projections of the effects of future climate change on these modes and shows that these could indeed be very different. There is, for example, a strong increase in the effects of the TNA+1 and AMO+1 on annual wildfire in the Great Plains and western USA in the future projections, as well as an increase in the area where the Pacific/North American, Arctic Oscillation and Pacific Decadal Oscillation climate modes, which have only a limited impact in the modern climate, are projected to have a significant effect under a further 2°C global warming.

5.2.1 Contributions to Better Defining Risk

The probability distribution output of the LE (Chapter 3) is useful from a risk preparedness perspective. A deterministic picture of wildfire danger predicts the mean outcome, and is not useful for predicting rare, high impact events because of the climate's internal stochasticity. Simulating the distribution of possible outcomes, and how that distribution is expected to change, allows risk managers to prepare for unseen events, using knowledge of their probability to balance the impact of an extreme year and the necessary resource expenditure to mitigate that impact. This distribution also provides information on the likelihood of wildfire events that have happened. This is critical context for investigation of catastrophic wildfire seasons (e.g. NHRA, 2023; CIFFC, 2024) that then informs policy on emergency preparedness. When used in the context of a future climate, the resulting present and future distributions can be used to find the change in severity for a fire year of a given rarity, or to find the change in likelihood for a pre-defined high impact year. A hazard distribution is essential for catastrophe risk modelling since different hazard intensities have different impacts on exposed people or property (Mitchell-Wallace et al., 2017). Likely annual wildfire occurrence is not the most appropriate hazard intensity metric to model risk to property, for which fire-line intensity, flame

length and the likelihood of large fires are better metrics (Wibbenmeyer and Robertson, 2022; Salis et al., 2013, Thompson et al., 2015). Nonetheless, it is a useful metric as days with many wildfire outbreaks require higher resource expenditure for wildfire to be contained at the landscape scale.

Predictable climate modes (Chapter 4) offer scope for seasonal to multiannual wildfire forecasting. Recent progress in seasonal fire weather forecasting (Di Giuseppe et al., 2024) means that fire weather anomalies can be predicted up to a minimum horizon of one month globally. But this timeframe is not long enough for risk management activities such as mechanical fuel removal, prescribed burning and assessing emergency response systems, which must be implemented months in advance. The strong effect of climate modes on likely annual wildfire occurrences, means that climate mode precursors could be used to provide a longer-term probabilistic prediction of the likely fire season severity. This capability is likely of growing importance, as both extreme wildfire incidence and the association between climate modes and wildfire activity have been found to increase with future climate change (Cunningham et al., 2024; Chapter 4).

5.3 Research Limitations and Future Work

5.3.1 Limitations of SMILEs

In this thesis I have focused on the aleatoric uncertainty arising from a single model initial condition perturbed large ensemble (SMILE) – KNMI LENTIS (Muntjewerf et al., 2023). At regional scales, internal climate variability significantly outweighs the effect of different models' representation of the weather distribution in the present climate, but differences between models become the dominant source of uncertainty in future projections (Lehner et al., 2020; von Trentini et al., 2020). The future projection of annual wildfire occurrences in Chapters 3 and 4 should therefore be interpreted as the shift in the distribution of possible fire years under this specific GCM – presenting a significant caveat on using this work to project future changes in USA fire regime. However, Chapters 3 and 4 are primarily focussed on identifying patterns of variability in wildfire internal to the present and future climates, and understanding the drivers of that internal variability. A SMILE is appropriate for exploring these questions, as it enables a focus solely on stochastic variability in weather between years, without the confounding effect of differences in physics schemes.

It would be beneficial to look at additional SMILEs derived from other GCMs, to understand the uncertainty on the spread of the wildfire distribution that comes from differences between climate models. Although, the primary source of uncertainty in future projections is the emissions scenario, use of multiple SMILEs would help to characterise the uncertainty due to both internal variability and model structural uncertainty in future fire occurrence. Use of multiple SMILEs could also decrease uncertainty about the association between climate modes and wildfire, as the representation of climate modes varies between climate models (Maher et al., 2024).

5.3.2 Limitations of the Statistical Model

The wildfire occurrence model (Chapter 2) used in this thesis employed a GLM framework. Good model performance was achieved through careful variable selection (Section 5.1.2.1), the limitation of each predictor's effect to its most predictive subdomain (Section 5.1.2.2), and a rescaling of the model output to address the underestimation of wildfire extremes in GLMs (Forrest et al., 2024). The parsimonious GLM modelling framework was chosen to prioritise the selection of highly likely and interpretable drivers, by constraining selected variables to those with strong, linear effects on the log-odds of daily wildfire probability. The domain-optimisation and power-law rescaling adaptations both introduce two additional degrees of freedom into the predictor relationships and the model link function respectively. These adaptations are both highly constrained. The predictors constrained to be linear within the selected domain and static otherwise, and the rescaling of the link function constrained to a monotonic function. Through these constraints, the model focusses on the main effects driving wildfire likelihood at the continental scale.

This rigidity comes with predictive limitations. First, the model assumes a spatially consistent response to fundamental driving relationships, which could impact model performance in environments in which predictors have a non-standard effect. This is unlikely to be an issue for predictors relating to physical processes, where emergent patterns in wildfire activity can be derived from linear causal effects (Bistinas et al., 2014). However, to account for the effect of certain processes on wildfire likelihood – mostly from people and vegetation traits – indirect variables that affect multiple causal processes (Section 1.2, Table 1) are often the only available predictors. Such effects can have varying effects on wildfire depending on fire ecology, for example the differing effect of landscape fragmentation on burnt area in fire-adapted and non-adapted ecosystems (Harrison et al., 2025a).

Second, by enforcing linear relationships within a single subdomain of each predictor, secondary nonlinear effects may not be accounted for. The precipitation subdomain was limited to 0-13 mm d^{-1}, ensuring the strong dampening effect of low precipitation totals on wildfire likelihood are captured. However, for example, a stronger precipitation effect from 0-1 mm d^{-1} or weaker but significant effect from 13-20 mm d^{-1} would not be captured in the linear model. Such effects would be fit by less constrained statistical methods, such as generalised additive models or spline-based models, as well as by all commonly used ML modelling techniques.

Third, predictors were selected before domain optimisation, as simultaneously solving both optimisation problems would have dramatically increased the necessary compute. This introduces a bias towards variables with a strong overall effect, which could mean that abrupt or non-monotonic variable effects are not accounted for. The development of a bespoke variable selection method on the basis of predictor subdomain effects is a clear avenue for future work, and could offer a more complete exploration of the important drivers of wildfire. Nonetheless, model evaluation (Chapter 2) and the substantial truncations in precipitation and population density from the domain optimisation algorithm show good predictive and feature selection capability.

Many machine learning methods, including random forests, gradient boosted machines, and neural networks, can account for discontinuous effects in driving variables and have been highly successful in predicting present patterns in wildfire (Forkel et al., 2017; Jain et al., 2020; McNorton et al., 2024; Son et al., 2024). Unlike the GLM method used in this thesis, the outputs of these ML models are not constrained to a linear functional form, and are therefore able to closely match nonlinear effects and variable interactions that affect wildfire likelihood and behaviour – generally achieving higher classification accuracy compared to linear statistical models. ML methods also address the three limitations discussed above. There is no constraint on variable effects remaining constant along environmental gradients, meaning that potential spatially varying predictor effects can be accounted for; there is also no restriction on nonlinear predictor effects; and specific variable features are selected directly, instead of a subsequent domain optimisation process. From a wildfire forecasting – or present to near-term risk modelling – perspective, the application of ML techniques to the key variable associations identified in Chapter 2, as well as emergent associations in Chapters 3 and 4, could be highly useful.

Machine learning methods are not used in the wildfire occurrence model presented in this thesis. The adapted-GLM method is a highly constrained statistical framework specifically targeted at identifying strong, linear, single-variable relationships that relate to generalisable causal effects across diverse environments. In contrast to modelling methods with many more degrees of freedom, this limits the risk of overfitting the model to the data and ensures a conservative extrapolation into a future climate – which may include environmental conditions poorly sampled in currently available observational data. Due to the continuing evolution of advanced predictive modelling techniques, there is no widely accepted, formal distinction between statistical and ML methods. One distinction between the two modelling 'cultures' is on the basis of whether an initial model form is assumed – data modelling – or generated by the modelling process – algorithmic modelling (Breiman, 2001). By this dichotomy, the model presented in this thesis is constrained but algorithmic, as the predictors, their critical driving domains, and the ultimate functional form of the link function are all optimised for automatically. Another way of distinguishing modelling methods, is the degree to which constraints are imposed on the functional form of the model. The adapted GLM framework presented here is less constrained than a simple GLM due to the predictor domain optimisation and link function rescaling. It is, however, significantly more constrained than some statistical methods – such as generalised additive models or multiplicative adaptive regression splines – and all machine learning models. The choice not to use these other methods was taken due to an emphasis on the inference of strong predictor effects with broad applicability, over pure predictive power of in-sample training data.

5.3.3 Increasing Operational Utility

As the potential for rapid fire spread and intensity are often already well characterised by fire weather indices, a model only predicting occurrence likelihood already provides significant additional utility from an operational perspective and has therefore been targeted by forecasters such as ECMWF (McNorton et al., 2024). However, the threshold fire size used here (0.1 ha) is arbitrary, and was chosen to maximise the amount of training data whilst filtering out very noisy small fire data. The occurrence modelling method could therefore also be applied to larger, and likely more hazardous, wildfire events. In addition, the variable selection and domain optimisation components of the modelling method are directly applicable to predicting other wildfire properties such as fire size, burnt area, intensity, severity and emissions.

The occurrence model (Chapter 2) was developed for the contiguous USA due to the availability of high-quality wildfire data in the region. There are a uniquely high number of good quality wildfire hazard models for the USA, so application of this model to other regions would likely be more fruitful from a risk perspective. As the key predictors identified in the contiguous USA are globally available and are trained on environments that span a wide range of extratropical fire regimes (Harrison et al., 2025b; Chapter 1), there is scope for the model to be applied to other regions without being retrained on local data. The extent to which such an application would capture wildfire likelihood patterns in a new region as well as for the contiguous USA would have to be carefully assessed. However, a comparative analysis between a retrained and unaltered model could also provide insight into the similarities and differences in the drivers of wildfire occurrence between regions (Bistinas et al., 2013).

5.3.4 Improvement of Fire-Enabled DGVMs

The wildfire occurrence model could also be used to improve existing global wildfire models. The variety of controls accounted for go significantly beyond the simple occurrence modules in FireMIP Dynamic Global Vegetation Models (DGVMs) (Rabin et al., 2017), which account for the viability of wildfire based on fuel moisture and availability and can include a lightning and population density driven ignition sub-module. GlobFIRM (Thonicke et al., 2001) and SIMFIRE-BLAZE (Knorr et al., 2014) do not allow for multiple wildfire occurrences per grid-cell per day, and MC-FIRE (Conklin et al., 2016) does not account for ignitions or fuel availability when simulating wildfire occurrences. By incorporating key processes missing from these models, model performance issues could be addressed – for example the underestimation of African burnt area due to the single fire limitation in GlobFIRM (Li et al., 2024). Other global wildfire models have an ignitions sub-module (Lehsten et al., 2009; Li et al., 2013; Melton and Arora, 2016; Mangeon et al., 2016) but the replacement of these modules with an integrated small fire occurrence module would be a means to increase predictive power and present a falsifiable output at the occurrence stage of the wildfire model.

The ensemble running of the variable selection algorithm over a large set of 47 candidate predictors (Chapter 2) is useful from a model development perspective, and can be used as a comprehensive assessment of key predictor effects over the region (Haas et al., 2024). An expansion of this work over a larger set of predictors to test for further improvement in model performance with new effects would be useful for future model development. This might be particularly useful in terms of socioecological predictors, allowing us to assess economic,

demographic and behavioural variables. This is a key line of research for the continued development of new wildfire models that fully integrate the intentional and unintentional anthropogenic influence on fire (Shuman et al., 2022; Perkins et al., 2023). Another line of investigation could be to more closely examine the effect of different variable antecedences. Antecedent conditions have been found to be important predictors of wildfire in some studies (Kuhn-Régnier et al., 2021, Richardson et al., 2022). A limited range of antecedences of GPP, VPD and precipitation were examined in Chapter 2. This range could be expanded. It would also be useful to investigate whether other fire drivers have antecedent states that should be taken into consideration.

5.4 Overall Conclusions

I have presented a wildfire occurrence model that addresses previous limitations of statistical wildfire models through a flexible variable selection algorithm, optimisation for the driving domain of each variable, and power law rescaling of the GLM output. The method is generalisable to other regions, different spatial and temporal scales, and other wildfire properties such as intensity or size. I used this method to identify the drivers of daily wildfire likelihood in the contiguous USA, and showed the importance of (1) including antecedent GPP in both recent months and over annual or longer timescales, (2) diurnal temperature range as a predictor, and (3) population density is most predictive of wildfire likelihood if only at relatively low values (< 7 persons km^{-2}).

The LE application of the wildfire occurrence model showed that climate change increased the average expected annual number of wildfires over almost the entire contiguous USA but increased the variability between fire years even more. This interannual variability in the fire regime was primarily controlled by daily timescale fuel curing (VPD) and annual timescale fuel productivity (annual GPP). With future climate change, the limitation of fuel productivity on annual wildfires became more influential, especially in the western USA, whilst curing processes (both daily drying and longer-term drought effects) emerged as key regional drivers in the southeastern USA. The LE application is useful in characterising the uncertainty associated with inherent stochasticity to realised weather conditions and has particular benefits from a risk management perspective.

The LE ensemble was used to examine the associations between wildfire and climate modes. The strongest climate mode influencing annual wildfire in the USA are ENSO and the TNA+1;

these modes combine in effect over the Great Plains, Mediterranean California and southern Florida. The AMO+1 also emerged as a strong influence on wildfire likelihood with future climate change. Climate modes can also significantly influence the timing of the wildfire season: in El Niño years, for example, the southeastern USA spring fire season peak is earlier in the year and in the southwestern USA the summer fire season peak is later.

5.5 References

Abatzoglou JT, Battisti DS, Williams AP, Hansen WD, Harvey BJ, et al. (2021) Projected increases in western US forest fire despite growing fuel constraints. Commun. Earth Environ. 2(1), 227. https://doi.org/10.1038/s43247-021-00299-0

Balch JK, Abatzoglou JT, Joseph MB, Koontz MJ, Mahood AL, et al. (2022) Warming weakens the night-time barrier to global fire. Nature 602, 442-448. https://doi.org/10.1038/s41586-021-04325-1

Barbero R, Abatzoglou JT, Brown TJ (2015) Seasonal reversal of the influence of El Niño-Southern Oscillation on very large wildfire occurrence in the interior northwestern United States. Geophys. Res. Lett. 42 3538–3545. https://doi.org/10.1002/2015GL063428

Bistinas I, Oom D, Sá AC, Harrison SP, Prentice IC, et al. (2013). Relationships between human population density and burned area at continental and global scales. PLoS One 8(12) e81188. https://doi.org/10.1371/journal.pone.0081188

Bistinas I, Harrison SP, Prentice IC, Pereira JMC (2014) Causal relationships versus emergent patterns in the global controls of fire frequency. Biogeosci. 11(18) 5087-5101. https://doi.org/10.5194/bg-11-5087-2014

Breiman L (2001) Statistical modeling: The two cultures (with comments and a rejoinder by the author). Stat. Sci. 16(3):199-231.

Burton C, Lampe S, Kelley DI, Thiery W, Hantson S, et al. (2024) Global burned area increasingly explained by climate change. Nat. Clim. Chang. 14, 1186-1192. https://doi.org/10.1038/s41558-024-02140-w

Cardil A, Rodrigues M, Ramirez J, de-Miguel S, Silva CA, et al. (2021) Coupled effects of climate teleconnections on drought, Santa Ana winds and wildfires in southern California. Sci. Total Environ. 765, 142788. https://doi.org/10.1016/j.scitotenv.2020.142788

Cardil A, Rodrigues M, Tapia M, Barbero R, Ramírez J, et al. (2023) Climate teleconnections modulate global burned area. Nat. Commun. 14, 427. https://doi.org/10.1038/s41467-023-36052-8

Chang P, Zhang L, Saravanan R, Vimont DJ, Chiang JC, et al. (2007) Pacific meridional mode and El Niño–Southern oscillation. Geophys. Res. Lett., 34(16). https://doi.org/10.1029/2007GL030302

Chowdhury MZI, Turin TC (2020) Variable selection strategies and its importance in clinical prediction modelling. Fam. Med. Commun. Health 8(1) e000262. https://doi.org/10.1136/fmch-2019-000262

CIFFC (2024) Canada Report 2023 Fire Season. https://www.ciffc.ca/sites/default/files/2024-03/CIFFC_2023CanadaReport_FINAL.pdf (accessed 28/06/2025)

Cloke HL, Wetterhall F, He Y, Freer JE, Pappenberger F (2013) Modelling climate impact on floods with ensemble climate projections. Q. J. R. Meteorol. Soc. 139(671), 282-297. https://doi.org/10.1002/qj.1998

Conklin DR, Lenihan JM, Bachelet D, Neilson RP, Kim JB (2016) MCFire Model Technical Description. USDA, Forest Service. https://doi.org/10.2737/PNW-GTR-926

Cunningham CX, Williamson GJ, Bowman DM (2024) Increasing frequency and intensity of the most extreme wildfires on Earth. Nat. Ecol. Evol. 8(8), 1420-1425. https://doi.org/10.1038/s41559-024-02452-2

Di Giuseppe F (2023) Accounting for fuel in fire danger forecasts: the fire occurrence probability index (FOPI). Environ. Res. Lett. 18, 064029. https://doi.org/10.1088/1748-9326/acd2ee

Di Giuseppe F, Vitolo C, Barnard C, Libertá G, Maciel P, et al. (2024) Global seasonal prediction of fire danger. Sci. Data 11(1), 128. https://doi.org/10.1038/s41597-024-02948-3

Dixon PG, Goodrich GB, Cooke WH (2008) Using teleconnections to predict wildfires in Mississippi. Mon. Weather Rev. 136(7) 2804-2811. https://doi.org/10.1175/2007MWR2297.1

ECMWF (2023) Annual Report 2023. Available at: https://www.ecmwf.int/sites/default/files/elibrary/062024/81569-annual-report-2023.pdf (Accessed 30/5/2025)

Fan H, Yang X, Zhao C, Yang Y, Shen Z (2023) Spatiotemporal variation characteristics of global fires and their emissions. Atmos. Chem. Phys., 23(13), 7781-7798. https:/doi.org/10.5194/acp-23-7781-2023

Fauria M, Johnson E (2008) Climate and wildfires in the North American boreal forest. Phil. Trans. R. Soc. B 363, 2315-2327. https://doi.org/10.1098/rstb.2007.2202

Finco M, Quayle B, Zhang Y, Lecker J, Megown KA, et al. (2012) Monitoring trends and burn severity (MTBS): Monitoring wildfire activity for the past quarter century using Landsat data. In: Morin RS, Liknes GC (2012) Moving from status to trends: Forest Inventory and Analysis (FIA) symposium. USDA, 222-228.

Forkel M, Dorigo W, Lasslop G, Teubner I, Chuvieco E, et al. (2017) A data-driven approach to identify controls on global fire activity from satellite and climate observations (SOFIA V1). Geosci. Model Dev. 10(12), 4443-4476. https://doi.org/10.5194/gmd-10-4443-2017

Forrest M, Hetzer J, Billing M, Bowring SPK, Kosczor E, et al. (2024) Understanding and simulating cropland and non-cropland burning in Europe using the BASE (Burnt Area Simulator for Europe) model. Biogeosciences 21(23), 5539-5560. https://doi.org/10.5194/bg-21-5539-2024

Guo Z, Li W, Ciais P, Sitch S, van der Werf GR, et al. (2025) Reconstructed global monthly burned area maps from 1901 to 2020. Earth Syst. Sci. Data [preprint]. https://doi.org/10.5194/essd-2024-556

Grossiord C, Buckley TN, Cernusak LA, Novick KA, Poulter B, et al. (2020) Plant responses to rising vapor pressure deficit. New Phyt. 226(6), 1550-1566. https://doi.org/10.1111/nph.16485

Haas O, Prentice IC, Harrison SP (2022) Global environmental controls on wildfire burnt area, size, and intensity. Environ. Res. Lett. 17, 065004. https://doi.org/10.1088/1748-9326/ac6a69

Haas O, Keeping T, Gomez-Dans J, Prentice IC, Harrison SP (2024) The global drivers of wildfire. Front. Environ. Sci. 12, 1438262. https://doi.org/10.3389/fenvs.2024.1438262

Hantson S, Kelley DI, Arneth A, Harrison SP, Archibald S, et al. (2020) Quantitative assessment of fire and vegetation properties in simulations with fire-enabled vegetation models from the Fire Model Intercomparison Project. Geosci. Model Dev. 13(7), 3299-3318. https://doi.org/10.5194/gmd-13-3299-2020

Harrison SP, Haas O, Bartlein PJ, Sweeney L, Zhang G (2025a) Climate, Vegetation, People: Disentangling the Controls of Fire at Different Timescales. Phil. Trans. R. Soc. B 380(1924). https://doi.org/10.1098/rstb.2023.0464

Harrison SP, Shen Y, Haas O, Sandoval DC, Sapkota D, et al. (2025b) An eco-evolutionary approach to defining wildfire regimes. Comm. Earth Environ. [in review]

Jain P, Coogan SC, Subramanian SG, Crowley M, Taylor S, et al. (2020) A review of machine learning applications in wildfire science and management. Environ. Rev. 28(4):478-505. https://doi.org/10.1139/er-2020-0019

Jones MW, Abatzoglou JT, Veraverbeke S, Andela N, Lasslop G, et al. (2022) Global and Regional Trends and Drivers of Fire Under Climate Change. Rev. Geophys. 60(3). https://doi.org/10.1029/2020RG000726

Kenyon J, Hegerl GC (2008) Influence of modes of climate variability on global temperature extremes. J. Clim., 21(15), 3872-3889. https://doi.org/10.1175/2008JCLI2125.1

Kitzberger T, Brown PM, Heyerdahl EK, Swetnam TW, Veblen TT (2007) Contingent Pacific–Atlantic Ocean influence on multicentury wildfire synchrony over western North America. PNAS, 104(2) 543-548. https://doi.org/10.1073/pnas.0606078104

Knorr W, Kaminski T, Arneth A, Weber U (2014) Impact of human population density on fire frequency at the global scale. Biogeosciences 11(4), 1085-1102. https://doi.org/10.5194/bg-11-1085-2014

Krawchuk MA, Moritz MA, Parisien M, Van Dorn J, Hayhoe K (2009) Global Pyrogeography: the Current and Future Distribution of Wildfire. PLoS ONE 4(4), e5102. https://doi.org/10.1371/journal.pone.0005102

Kuhn-Régnier A, Voulgarakis A, Nowack P, Forkel M, Prentice IC, et al. (2021) The importance of antecedent vegetation and drought conditions as global drivers of burnt area. Biogeosciences 18(12), 3861-3879. https://doi.org/10.5194/bg-18-3861-2021

Le Goff H, Flannigan MD, Bergeron Y, Girardin MP (2007) Historical fire regime shifts related to climate teleconnections in the Waswanipi area, central Quebec, Canada. Int. J. Wildland Fire 16(5), 607. https://doi.org/10.1071/WF06151

Lehner F, Deser C, Maher N, Marotzke J, Fischer EM, et al. (2020) Partitioning climate projection uncertainty with multiple large ensembles and CMIP5/6. Earth Syst. Dynam. 11(2), 491-508. https://doi.org/10.5194/esd-11-491-2020

Lehsten V, Tansey K, Balzter H, Thonicke K, Spessa A, et al. (2009) Estimating Carbon Emissions from African Wildfires. Biogeosciences 6(3), 349-360. https://doi.org/10.5194/bg-6-349-2009

Li F, Levis S, Ward DS (2013) Quantifying the Role of Fire in the Earth System – Part 1: Improved Global Fire Modeling in the Community Earth System Model (CESM1). Biogeosciences 10(4), 2293-2314. https://doi.org/10.5194/bg-10-2293-2013

Li F, Song X, Harrison SP, Marlon JR, Lin Z, et al. (2024) Evaluation of global fire simulations in CMIP6 Earth system models. Geosci. Model Dev. 17(23), 8751-8771. https://doi.org/10.5194/gmd-17-8751-2024

Maher N, Phillips AS, Deser C, Wills RCJ, Lehner F, et al. (2024) The updated Multi-Model Large Ensemble Archive and the Climate Variability Diagnostics Package: New tools for the study of climate variability and change. EGU [preprint]. https://doi.org/10.5194/egusphere-2024-3684

Mangeon S, Voulgarakis A, Gilham R, Harper A, Sitch S, et al. (2016) INFERNO: A fire and emissions scheme for the UK Met Office's Unified Model. Geosci. Model Dev., 9(8), 2685-2700. https://doi.org/10.5194/gmd-9-2685-2016

Mason SA, Hamlington PE, Hamlington BD, Jolly MW, Hoffman CM (2017) Effects of climate oscillations on wildland fire potential in the continental United States. Geophys. Res. Lett. 44 7002-7010. https://doi.org/10.1002/2017gl074111

McHugh CE, Delworth TL, Cooke W, Jia L (2023) Using Large Ensembles to Examine Historical and Projected Changes in Record-Breaking Summertime Temperatures Over the Contiguous United States. Earth's Fut. 11(12). https://doi.org/10.1029/2023EF003954

McNorton JR, Di Giuseppe F, Pinnington E, Chantry M, Barnard C (2024) A Global Probability-Of-Fire (PoF) Forecast. Geophys. Res. Lett. 51(12). https://doi.org/10.1029/2023GL107929

Melton JR, Arora VK (2016) Competition Between Plant Functional Types in the Canadian Terrestrial Ecosystem Model (CTEM) v. 2.0. Geosci. Model Dev. 9(1), 323-361. https://doi.org/10.5194/gmd-9-323-2016

Mitchell-Wallace K, Jones M, Hillier J, Foote M (2017) Natural catastrophe risk management and modelling: A practitioner's guide. Wiley.

Mukunga T, Forkel M, Forrest M, Zotta R, Pande N, et al. (2023) Effect of Socioeconomic Variables in Predicting Global Fire Ignition Occurrence. Fire 6(5), 197. https://doi.org/10.3390/fire6050197

Muntjewerf L, Bintanja R, Reerink T, van der Wiel K (2023) The KNMI Large Ensemble Time Slice (KNMI–LENTIS). Geosci. Model Dev. 16(15), 4581-4597. https://doi.org/10.5194/gmd-16-4581-2023

NHRA (2023) Understanding the Black Summer bushfires through research: a summary of key findings from the Bushfire and Natural Hazards CRC, report, available at www.naturalhazards.com.au/black-summer (accessed 28/06/2025)

NIFC (2025) Monthly Seasonal Outlook. https://www.nifc.gov/nicc-files/predictive/outlooks/monthly_seasonal_outlook.pdf (accessed 28/06/2025)

Parks SA, Holsinger LM, Panunto MH, Jolly WM, Dobrowski SZ, et al. (2018) High-severity fire: evaluating its key drivers and mapping its probability across western US forests. Environ. Res. Lett. 13, 044037. https://doi.org/10.1088/1748-9326/aab791

Pausas JG, Ribeiro E (2013) The global fire–productivity relationship. Glob. Ecol. Biogeog., 22(6), 728-736. https://doi.org/10.1111/geb.12043

Perkins O, Kasoar M, Voulgarakis A, Smith C, Mistry J, et al. (2024) A global behavioural model of human fire use and management: WHAM! v1. 0. Geosci. Model Dev., 17(9), 3993-4016. https://doi.org/10.5194/gmd-17-3993-2024

Rabin SS, Melton JR, Lasslop G, Bachelet D, Forrest M, et al. (2017) The Fire Modeling Intercomparison Project (FireMIP), phase 1: experimental and analytical protocols with detailed model descriptions. Geosci. Model Dev. 10(3), 1175-1197. https://doi.org/10.5194/gmd-10-1175-2017

Richardson D, Black AS, Irving D, Matear RJ, Monselesan DP, et al. (2022) Global increase in wildfire potential from compound fire weather and drought. NPJ Clim. Atmos. Sci., 5(1), 23. https://doi.org/10.1038/s41612-022-00248-4

San-Miguel-Ayanz J, Durrant T, Boca R, Maianti P, Libertá G, et al. (2024) Forest Fires in Europe, Middle East and North Africa 2023. Publ. Off. EU. https://doi.org/10.2760/8027062

Salis M, Ager AA, Arca B, Finney MA, Bacciu V, et al. (2012) Assessing exposure of human and ecological values to wildfire in Sardinia, Italy. Int. J. Wildland Fire, 22(4), 549-565. https://doi.org/10.1071/WF11060

Shen H, Tao S, Chen Y, Odman MT, Zou Y, et al. (2019) Global fire forecasts using both large-scale climate indices and local meteorological parameters. Glob. Biogeochem. Cycl., 33(8), 1129-1145. https://doi.org/10.1029/2019GB006180

Shuman JK, Balch JK, Barnes RT, Higuera PE, Roos CI, et al. (2022) Reimagine fire science for the anthropocene. PNAS nexus, 1(3). https://doi.org/10.1093/pnasnexus/pgac115

Sibold JS, Veblen TT (2006) Relationships of subalpine forest fires in the Colorado Front Range with interannual and multidecadal-scale climatic variation. J. Biogeog. 33(5) 833-842. https://doi.org/10.1111/j.1365-2699.2006.01456.x

Son R, Stacke T, Gayler V, Nabel JEMS, Schnur R, et al. (2024) Integration of a Deep-Learning-Based Fire Model Into a Global Land Surface Model. J. Adv. Model Earth Syst. 16(1). https://doi.org/10.1029/2023MS003710

Squire DT, Richardson D, Risbey JS, Black AS, Kitsios V, et al. (2021) Likelihood of unprecedented drought and fire weather during Australia's 2019 megafires. npj Clim. Atmos. Sci. 4, 64. https://doi.org/10.1038/s41612-021-00220-8

Sullivan A, Baker E, Kurvits T, Popescu A, Paulson AK, et al. (2022) Spreading like Wildfire: The Rising Threat of Extraordinary Landscape Fires. UNEP.

Taylor SW, Woolford DG, Dean CB, Martell DL (2013) Wildfire prediction to inform fire management: statistical science challenges. Stat. Sci. 28(4) 586-615. http://dx.doi.org/10.1214/13-STS451

Thompson MP, Haas JR, Gilbertson-Day JW, Scott JH, Langowski P, et al. (2015) Development and application of a geospatial wildfire exposure and risk calculation tool. Environ. Model. Softw. 63, 61-72. https://doi.org/10.1016/j.envsoft.2014.09.018

Thonicke K, Venevsky S, Sitch S, Cramer W (2001) The role of fire disturbance for global vegetation dynamics: coupling fire into a Dynamic Global Vegetation Model. Glob. Ecol. Biogeog., 10(6), 661-677. https://doi.org/10.1046/j.1466-822X.2001.00175.x

van der Wiel K, Wanders N, Selten FM, Bierkens MFP (2019) Added Value of Large Ensemble Simulations for Assessing Extreme River Discharge in a 2 °C Warmer World. Geophys. Res. Lett. 46(4), 2093-2102. https://doi.org/10.1029/2019GL081967

Van Wagner C (1987). Development and structure of the Canadian forest fire weather index system. Canadian Forestry Service, Forestry Technical Report 35.

von Trentini F, Aalbers EE, Fischer EM, Ludwig R (2020) Comparing interannual variability in three regional single-model initial-condition large ensembles (SMILEs) over Europe. Earth Syst. Dynam. 11(4), 1013-1031. https://doi.org/10.5194/esd-11-1013-2020

Wang G, Schimel D (2003) Climate change, climate modes, and climate impacts. Ann. Rev. Environ. Res., 28(1), 1-28. https://doi.org/10.1146/annurev.energy.28.050302.105444

Wibbenmeyer M, Robertson M (2022) The distributional incidence of wildfire hazard in the western United States. Environ. Res. Lett. 17, 064031. https://doi.org/10.1088/1748-9326/ac60d7

Williams AP, Abatzoglou JT, Gershunov A, Guzman-Morales J, Bishop DA, et al. (2019) Observed Impacts of Anthropogenic Climate Change on Wildfire in California. Earth's Future 7(8), 892-910. https://doi.org/10.1029/2019EF001210

Yoshida K, Sugi M, Mizuta R, Murakami H, Ishii M (2017) Future Changes in Tropical Cyclone Activity in High-Resolution Large-Ensemble Simulations. Geophys. Res. Lett. 44(19), 9910-9917. https://doi.org/10.1002/2017GL075058

Zhang H, Clement A, Di Nezio P (2014) The South Pacific meridional mode: A mechanism for ENSO-like variability. J. Clim., 27(2), 769-783. https://doi.org/10.1175/JCLI-D-13-00082.1

Appendix

This appendix contains an additional paper, which includes an extension of the work presented in Chapter 2.

frontiers | Frontiers in Environmental Science

TYPE Review
PUBLISHED 06 September 2024
DOI 10.3389/fenvs.2024.1438262

OPEN ACCESS

EDITED BY
Chenghao Wang,
University of Oklahoma, United States

REVIEWED BY
Huilin Huang,
Pacific Northwest National Laboratory (DOE), United States
Subhajit Bandopadhyay,
University of Southampton, United Kingdom

*CORRESPONDENCE
Sandy P. Harrison,
s.p.harrison@reading.ac.uk

RECEIVED 25 May 2024
ACCEPTED 22 August 2024
PUBLISHED 06 September 2024

CITATION
Haas O, Keeping T, Gomez-Dans J, Prentice IC and Harrison SP (2024) The global drivers of wildfire.
Front. Environ. Sci. 12:1438262.
doi: 10.3389/fenvs.2024.1438262

The global drivers of wildfire

Olivia Haas[1,2], Theodore Keeping[1,2], José Gomez-Dans[2,3,4], I. Colin Prentice[2,5] and Sandy P. Harrison[1,2]*

[1]Geography and Environmental Science, University of Reading, Reading, United Kingdom, [2]Leverhulme Centre for Wildfires, Environment and Society, Imperial College London, London, United Kingdom, [3]Department of Geography, King's College London, London, United Kingdom, [4]NERC National Centre for Earth Observation (NCEO), Reading, United Kingdom, [5]Georgina Mace Centre for the Living Planet, Department of Life Sciences, Imperial College London, Silwood Park Campus, London, United Kingdom

Changes in wildfire regimes are of growing concern and raise issues about how well we can model risks in a changing climate. Process-based coupled fire-vegetation models, used to project future wildfire regimes, capture many aspects of wildfire regimes poorly. However, there is now a wealth of information from empirical studies on the climate, vegetation, topography and human activity controls on wildfire regimes. The measures used to quantify these controls vary among studies, but certain variables consistently emerge as the most important: gross primary production as a measure of fuel availability, vegetation cover as a measure of fuel continuity, and atmospheric humidity as a measure of fuel drying. Contrary to popular perception, ignitions are generally not a limiting factor for wildfires. In this review, we describe how empirical fire models implement wildfire processes, synthesise current understanding of the controls on wildfire extent and severity, and suggest ways in which fire modelling could be improved.

KEYWORDS

wildfire regimes, drivers of wildfire, empirical modelling, fuel availability, fuel continuity, fuel drying, wildfire modelling

Highlights

- Empirical analyses of the controls on wildfires consistently identify vegetation properties associated with fuel availability and continuity and climate factors associated with fuel drying as the most important influences on wildfire extent and severity.
- Ignitions, whether anthropogenic or natural, are generally not limiting.
- Fire size, burnt area and fire intensity are influenced by different factors; current relationships between these aspects of wildfire could become decoupled in an altered climate.
- Some hypotheses embedded in 'process-based' fire-vegetation models are inconsistent with empirical evidence, implying a need for a re-design.

Introduction

Wildfires are unplanned fires that occur in natural ecosystems, although the ignition source can be natural (most often lightning) or anthropogenic. Wildfires occur on all vegetated continents. Current remotely-sensed based estimates suggest that something of the order of 2.6% ± 0.3% (GFED4: Giglio et al., 2013) to 5.9% ± 0.5% (GFED5: Chen et al., 2023) of the global vegetated area burns each year. Wildfires have been the most important cause of disturbance in natural ecosystems for millions of years (Scott, 2000; Scott and

Glasspool, 2006; Harrison et al., 2010) and indeed are fundamental to the maintenance of many ecosystems and floras (Pausas and Keeley, 2009; Pausas et al., 2017; Harrison et al., 2021; Pausas and Keeley, 2023). The fire regime, the long-term characteristics of wildfires in specific environments (Lavorel et al., 2007; Archibald et al., 2018) as expressed in terms of fire size, intensity, extent or frequency, shapes ecosystem properties and plant reproductive traits. Some ecosystems rely on frequent wildfires for the establishment of dominant plant-types, whilst others can only support infrequent burning (Archibald et al., 2013; Archibald et al., 2018; Harrison et al., 2021; Foster et al., 2018; Simpson et al., 2021).

At a global scale, burnt area has declined in recent decades (Andela et al., 2017; Forkel et al., 2019; Jones et al., 2022; Zubkova et al., 2023). This decline is driven by changes in the tropical savannas of northern Africa and grasslands in Asia, and to a lesser extent by changes in southern Africa and Europe (Zubkova et al., 2023); other regions of the world have shown no significant trends in the past two decades. Nevertheless, recent years have been marked by extreme wildfire seasons, characterised by increased frequency, seasonality, size, intensity or severity of wildfires, in several regions, including Europe (Carnicer et al., 2022; Grünig et al., 2023), Siberia (Kharuk et al., 2022; Ponomarev et al., 2023) and the western United States (Singleton et al., 2019; Mueller et al., 2020; Jones et al., 2022; Wasserman and Mueller, 2023). These extreme wildfires have been widely attributed to anthropogenic climate change (Abatzoglou et al., 2019; Kirchmeier-Young et al., 2019; Williams et al., 2019; Bowman et al., 2020; Abram et al., 2021; van Oldenborgh et al., 2021). Model projections suggest that burnt area will increase by 13%–15% by 2030 and by 20%–40% by 2050 (UNEP, 2022). The focus on future changes in burnt area may be misleading, however, since some studies show that changes in other aspects of the fire regime, such as intensity, may be decoupled from changes in burnt area under altered climate states (Haas et al., 2023; Haas et al., 2024).

Wildfire regimes are controlled by factors related to climate, vegetation, landscape characteristics and human activities (Bowman et al., 2009; Harrison et al., 2010; Bowman et al., 2011). Many of these controls are incorporated in some way in global fire-enabled vegetation models (Rabin et al., 2017) or are implicit in empirically based global fire models. Nevertheless, while these models can predict the broad global patterns of burnt area, they struggle to reproduce fire season length or the interannual variability of wildfires (Hantson et al., 2020). It is unclear how well they reproduce other aspects of wildfire regimes, such as fire intensity, since this has not been a focus of model evaluation. Even though the current generation of fire-enabled vegetation models reproduce modern global patterns of burnt area, there are significant differences between them in even the sign of historic trends in burnt area reflecting differences in the sensitivity to individual forcings (Teckentrup et al., 2019) and an incomplete or inaccurate description of key processes associated with vegetation properties and anthropogenic influences on wildfire (Forkel et al., 2019). There have been many empirical studies analysing the controls on wildfires at a global scale, many conducted since the initial development of the current generation of fire-enabled vegetation models (Forkel et al., 2019) and these could provide a basis for improving model representations of key processes. This effort would require an assessment of the robustness of the findings across studies, and diagnosis of the underlying mechanisms.

The aim of this perspective is to identify key variables needed to model different aspects of wildfire regimes and how these could be incorporated in a global modelling framework. We first review how empirical (data-based) fire models treat key controls on fire processes. We then review global studies of different fire properties to assess whether there is a consensus about the importance of specific drivers of burnt area, occurrence, fire size and fire intensity. Finally, we suggest ways in which current understanding of these empirical relationships could be used to improve models and thus our ability to predict changes in fire regimes under future climate change.

Wildfire modelling: The state-of-the-art

Wildfires are simulated in dynamic global vegetation models (DGVMs) and land-surface models (LSMs) through specific modules (Hantson et al., 2016; Jones et al., 2022). There are two basic types: process-based (see e.g., CTM: Arora and Boer, 2005; Melton and Arora, 2016; SPITFIRE: Thonicke et al., 2010; CLM-Li: Li et al., 2012; Li et al., 2013) and empirical (see e.g., GLOBFIRM: Thonicke et al., 2001; Kloster et al., 2010; SIMFIRE-BLAZE: Knorr et al., 2014; INFERNO: Mangeon et al., 2016) modules. Process-based models simulate the behaviour of individual wildfires using theoretical equations for ignitions and fire spread, alongside parameterisations based on laboratory or field experiments, and typically produce estimates of burnt area by scaling up to the grid-cell level (generally $0.5^{\circ} \times 0.5^{\circ}$ or coarser). Although much of the focus of fire modelling has been on burnt area and carbon emission, some process-based models explicitly simulate the number and size of individual fires. Empirical models do not try to simulate individual wildfires but simulate the emergent properties of the fire generally using statistical relationships between assumed drivers and fire properties (usually burnt area) across a grid. Comparisons of process-based and empirical models made in the context of the Fire Modelling Intercomparison Project (FireMIP: Hantson et al., 2016; Rabin et al., 2017) have shown that empirical models perform at least as well as process-based models in simulating global patterns of burnt area under modern conditions (Hantson et al., 2020). Both empirical and process-based fire models are incorporated in LSM components of the climate models used in the sixth phase of the Coupled Model Intercomparison Project (CMIP6), and show comparable performance in simulating modern burnt area and emissions (Li et al., 2024).

Although all the FireMIP models can reproduce the spatial patterns in burnt area under modern conditions reasonably well, they tend to overestimate the length of the fire season and do not capture the interannual variability in wildfires (Hantson et al., 2020). Perhaps more importantly, the models disagreed on the sign and magnitude of the trend in global burnt area over the 20th century (Teckentrup et al., 2019; Jones et al., 2022). Furthermore, although the models captured the emergent observed relationships between burnt area and various climate factors influencing wildfires, they

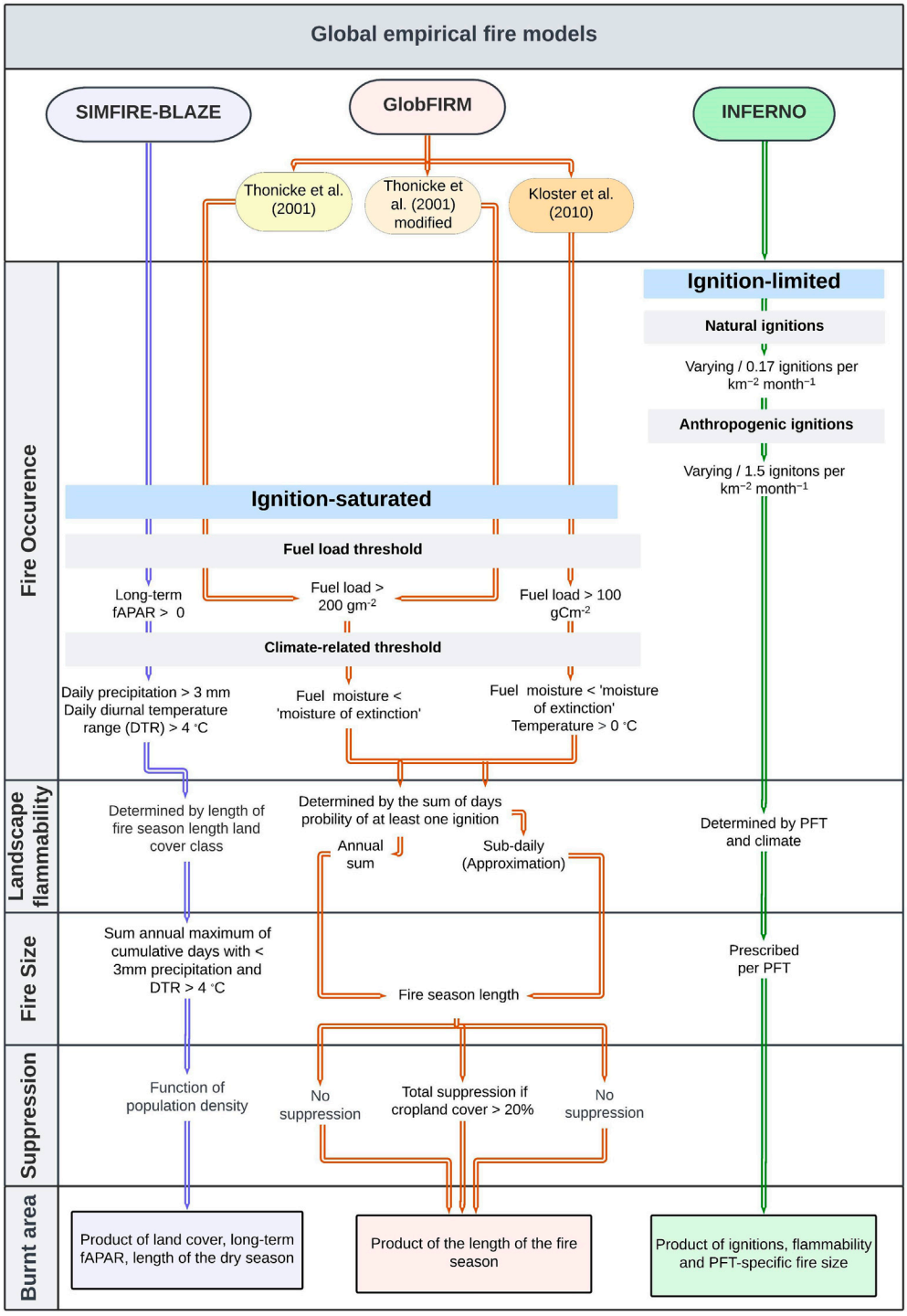

FIGURE 1
Flow diagram showing how processes related to the simulation of burnt area are treated in empirical models from FireMIP.

failed to capture the observed relationships with other drivers (Forkel et al., 2019; Teckentrup et al., 2019). These analyses imply that the incorporation of process understanding in both empirical and process-based models is incomplete.

This incompleteness is illustrated by differences in the three empirically based models (Figure 1; Supplementary Table 1) that have been used in FireMIP: GLOBFIRM (Thonicke et al., 2001; Kloster et al., 2010), SIMFIRE-BLAZE (Knorr et al., 2014) and INFERNO (Mangeon et al., 2016). Fire occurrence is determined by ignitions in INFERNO, where the number of natural and anthropogenic ignitions is prescribed. However, ignitions are not considered to be limiting in GLOBFIRE and SIMFIRE-BLAZE and occurrence is therefore entirely determined by fuel load and climate conditions. SIMFIRE-BLAZE uses a threshold of climatological

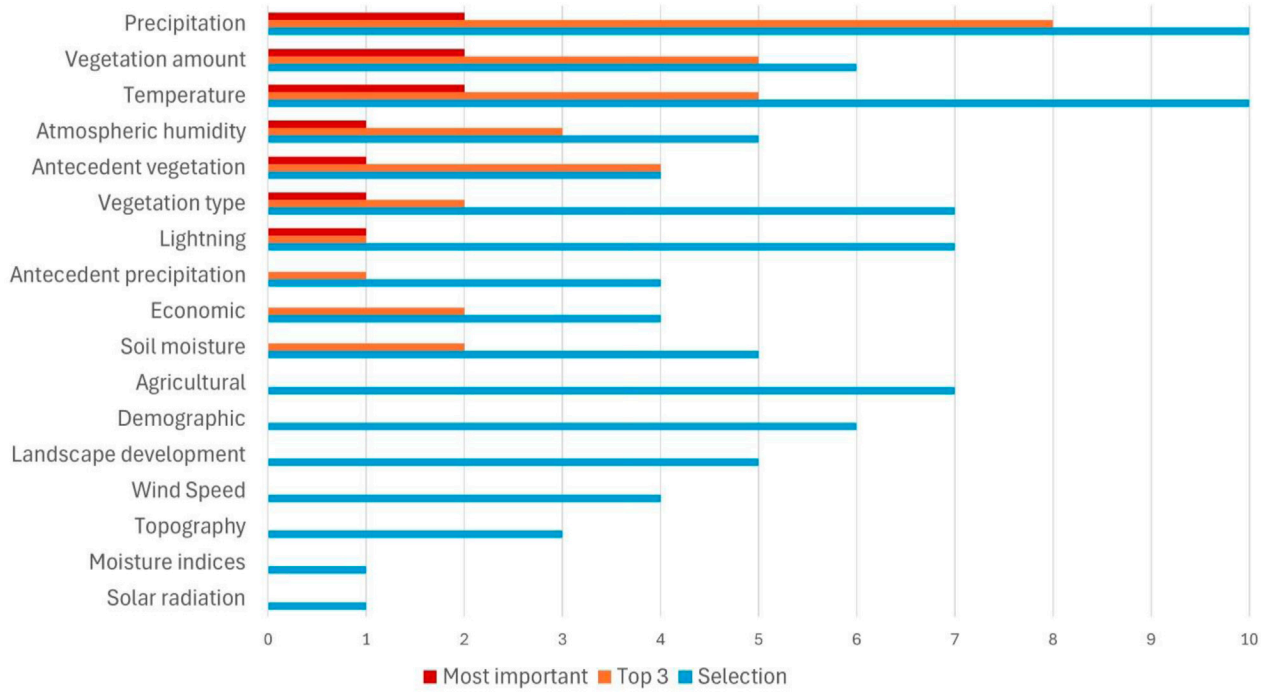

FIGURE 2
Summary of variables selected and considered important for predictions of burnt area in global empirical analyses. The individual bars show the number of studies which included the variable as a predictor (blue), the number of times the variable was selected as the most important driver of burnt area (red) and the number of times the variable was in the top three predictors (pink).

values of the fraction of absorbed photosynthetically active radiation (fAPAR) as an index of fuel load, whereas the variants of GLOBFIRM use thresholds of fuel load explicitly to determine fire occurrence. SIMFIRE-BLAZE also uses thresholds for daily precipitation and diurnal temperature range to determine fire occurrence, while GLOBFIRM only allows fire to occur when fuel moisture content is less than the moisture of extinction. The Kloster et al. (2010) variant of GLOBFIRM also imposes a daily minimum temperature threshold on occurrence. All three models consider landscape flammability, determined by plant functional type (PFT) in INFERNO, by the length of the fire season and landcover class in SIMFIRE-BLAZE and by the total number of days with a probability of fire ignition greater than one in GLOBFIRM. Fire size is also determined differently by the three models: by climate conditions in SIMFIRE-BLAZE, fire season length in GLOBFIRM and by PFT in INFERNO. The standard version of GLOBFIRM does not account for fire suppression, but the other models take account of this either through population density (SIMFIRE-BLAZE, the Kloster et al. (2010) version of GLOBFIRM and INFERNO) or through cropland area (the modified version of GLOBFIRM in Thonicke et al., 2001). The final estimate of burnt area is the product of land cover, longterm fAPAR and the length of the dry season in SIMFIRE-BLAZE, whereas it is determined by the number of ignitions, flammability and PFT-specific fire size in INFERNO, and determined by the length of the fire season in GLOBFIRM. These differences in the processes considered and in the final simulation of burnt area between the empirical models clearly highlight the uncertainties in understanding of the empirical controls on fire.

Empirical studies of the controls on burnt area

A review of the literature identified 10 empirical global studies that examined the controls on wildfires, using either machine-learning or more traditional regression-based approaches, and ranked them according to their relative importance in determining burnt area (Supplementary Table 2). Although these studies used different analytical approaches, and included different numbers of explanatory variables, they all provide an assessment of which variables are significant and a quantitative ranking of the importance of these variables (see Supplementary Table 3), allowing at least a qualitative comparison of the consistency of the results. Several other studies looked at the influence of specific controls (e.g., Knorr et al., 2014; Lasslop et al., 2015; Krawchuk and Moritz, 2011) or have derived predictions based on optimizing multiple controls without prioritizing them (e.g., Boer et al., 2021); or examined controls on interannual variability rather than burnt area (e.g., Abatzoglou et al., 2018). These studies do not provide a ranking of the importance and are therefore not considered here.

The initial selection of variables reflects hypotheses about the mechanisms involved in wildfire occurrence and spread. It is therefore not surprising that variables related to climate (often some measure of precipitation and temperature) are selected in most studies (Figure 2). More surprisingly, the relative importance of these variables does not reflect the frequency with which they are included in analyses. In particular, atmospheric humidity is consistently shown to be an important variable although it is included in analyses only half as frequently as temperature and

precipitation. Field studies indicate that atmospheric humidity is a strong control on both live and dead fuel moisture (Dickman et al., 2023) and this probably explains its emergence as an important variable. However, in a modelling context, fuel moisture is more often represented by soil moisture (only indirectly related to humidity) or some kind of moisture index - both of which are shown to be relatively unimportant in these empirical analyses. Variables related to fuel availability, such as the current vegetation amount and vegetation type, are included equally frequently in these global analyses. The current amount of vegetation has a different influence on burnt area from the amount during antecedent periods (Kuhn-Régnier et al., 2021) and thus these two variables should be considered separately. Variables related to the instantaneous amount of vegetation, which impacts both fuel availability and fuel continuity, emerge as more diagnostic than vegetation type. When considering both instantaneous and antecedent conditions, vegetation amount emerges as the single most important control on burnt area, being the most important predictor in a third of the studies (Figure 2). This suggests that models that explicitly consider fuel loads or measures such as fAPAR that are closely related to vegetation production are more likely to capture the processes involved in modulating burnt area than models that rely on PFT-specific parameterisations. A number of variables related to ignitions (lightning, demographic measures) or to fire spread (wind speed, topography) are routinely included in these empirical analyses, but turn out to be less important determinants of burnt area at a global scale. This helps to explain why models that assume that ignitions are saturated perform as well as those that explicitly try to estimate the frequency of natural and human ignitions. Factors relating to landscape fragmentation (e.g., measures of agricultural activity or landscape development) are also less important than climate and vegetation factors in determining burnt area. Landscape fragmentation has an impact on limiting fire spread, but this impact is complex and depends on the nature of the fragmentation and the vegetation type (Armenteras et al., 2017; Harrison et al., 2021; Rosan et al., 2022; Harrison et al., 2024). Current measures of and assumptions about the role of fragmentation, both in empirical and process-based models, are likely over-simplified. More generally, no variable representative of human activity and its impact emerges as a strong control on burnt area. This highlights that the current ways in which we represent this impact in global models are most likely inadequate and unable to capture the desired human effects.

Even in the broad categories related to climate and vegetation, there are differences in the specific metrics employed in different empirical studies. Precipitation, for example, can be represented by average monthly values, total precipitation within the typical burn period or a specific season, or precipitation during an antecedent period of varying length. However, these different choices frequently relate to different processes: average monthly data is largely a measure of the immediate impact of precipitation on fuel moisture whereas antecedent precipitation is more likely to be related to the control of aridity on vegetation growth and fuel accumulation. Both the instantaneous and antecedent measures of precipitation emerge as important controls of burnt area, and they have been shown to have different (and contrasting) effects (Kuhn-Régnier et al., 2021). This poses problems in empirical analyses since the inclusion of more than one predictor variable to represent a key process means that the influence of both may be down-weighted. There is no ideal solution to this problem since there are still uncertainties about which specific processes need to be considered and which predictive variables would best represent these processes. One approach that has been used is systematic variable selection, in which a large number of individual variables are tested for their contribution in a large number of models constructed by systematically including or excluding individual variables (e.g., Tracy et al., 2018; Keeping et al., 2024).

Systematic variable selection analyses provide support for the importance of climate, vegetation and human parameters in driving fire occurrence. Figure 3 shows the frequency of variable selection, using a forward-backward selection algorithm (Keeping et al., 2024), for the prediction of fires >0.25 acres for the contiguous United States in a 12-variable model, given the selection of one initial variable, in a suite of 1,000 variable selection runs (see Supplementary Figure 1 for full matrix). Diurnal temperature range is consistently chosen in all of the runs, even when other temperature variables are selected as the initial variable. Similarly, 5-day precipitation, snow cover, antecedent GPP and rural population density are consistently selected as important in more than 90% of the selection runs. This analysis confirms the importance of the factors that emerge as important controls on fire in global analyses - including factors influencing fuel load (such a vegetation cover or GPP), fuel drying (such as relative humidity, precipitation), and fire spread (such as population density or crop cover). However, some factors that have been used as predictors of fire occurrence in regional empirical studies, such as minimum temperature or the presence of powerlines, are never selected in this analysis. This shows that some factors that might be thought of as influencing fire occurrence have no additional predictive power in the model and are thus not important at a global scale.

Few studies have examined the global controls on fire properties other than burnt area. Three studies were identified that explicitly looked at the environmental controls of fire occurrence (Shmuel and Heifetz, 2022; 2023; Mukunga et al., 2023; Zhang et al., 2023) and four that examined the global controls of fire size (Hantson et al., 2015; Shmuel and Heifetz, 2022; Haas et al., 2022; Zhang et al., 2023). Despite the limited number of studies, factors relating to human activity were shown to have a less significant effect on fire occurrence than authors expected (Zhang et al., 2023; Shmuel and Heifetz, 2022) although gross domestic product (GDP) did emerge as a significant control (Mukunga et al., 2023). Cropland fraction was shown to increase ignitions in one study (Mukunga et al., 2023); this contradicts the assumption that croplands have a consistent, suppressing effect on wildfire activity as registered by fire size and burnt area. Wind speed was also shown to have a negative effect on fire occurrence above a threshold of 3–4 m/s-1 (Shmuel and Heifetz, 2023). Fire size follows a power-law (Randerson et al., 2012), and Hantson et al. (2015) used this assumption to investigate the drivers of fire size. They showed that there is a negative linear relationship between cropland cover and fire size but the relationship with population density was humped, with fire size peaking at intermediate levels of population density. Similar assumptions underpin the study of Andela et al. (2017), which suggests that agricultural expansion has been a key driver of the reduction in fire size (and the number of fires and global total burnt area) in recent decades. Zhang et al. (2023) also showed the dominant role of

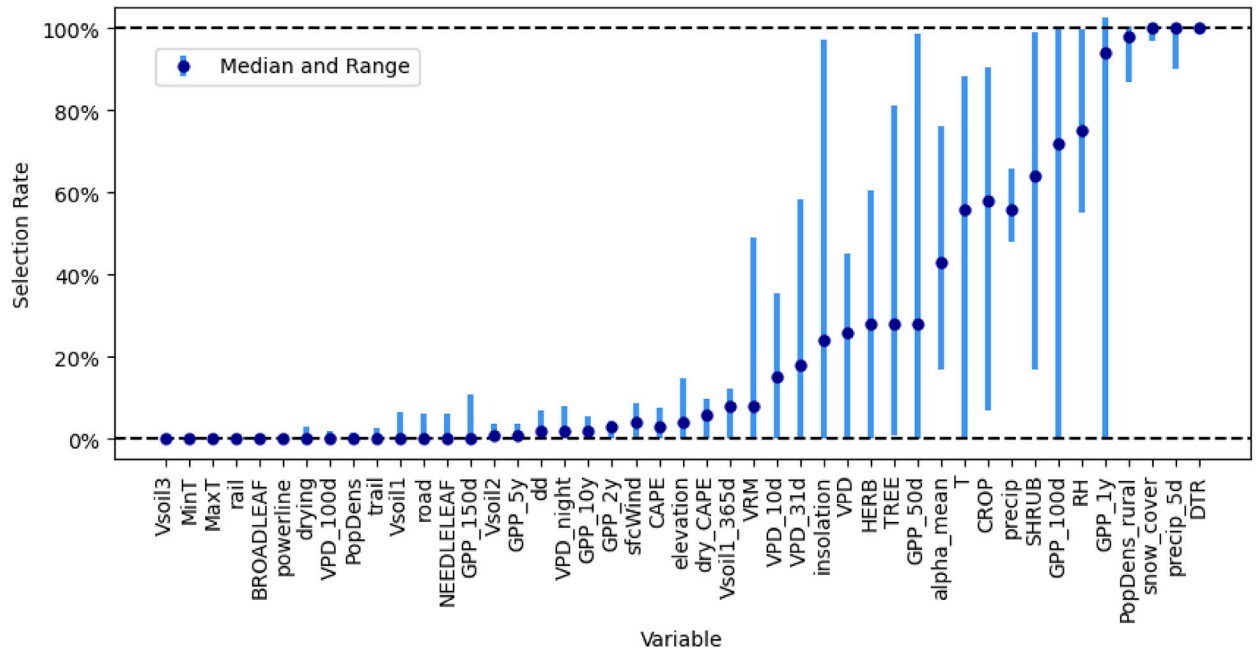

FIGURE 3
Outcome of systematic variable selection, showing the initial variable included in the model and the median and range of the number of times it was selected. The variables are: Vsoil3 – daily soil water volume in second layer (28–100 cm) (m^3/m^3), MinT–minimum daily temperature (°C), MaxT–maximum daily temperature (°C), rail–total length of rail lines per km^2 (km/km^2), BROADLEAF–the fraction of broadleaf plants (%), powerline–total length of powerlines per km^2 (km/km^2), drying–cumulated vapour pressure deficit in prior dry spell (Pa days), VPD_100d–mean vapour pressure deficit over prior 100 days (Pa), PopDens–population density ($people/km^2$), trail–total length of walking trails per km^2 (km/km^2), road–total length of roads per km^2 (km/km^2), Vsoil1 – daily soil water volume in top layer (0–7 cm) (m^3/m^3), NEEDLELEAF–the fraction of needleleaf plants (%), GPP_150d–Gross Primary Production in prior 150 days (μ $gC/m^2/s$), Vsoil2 – daily soil water volume in second layer (7–28 cm) (m^3/m^3), GPP_5y–Gross Primary Production in prior 5 years (μ $gC/m^2/s$), dd–prior dry days (<0.1 mm precipitation) (days), VPD_night–mean vapour pressure deficit in night-time (Pa), GPP_10y–Gross Primary Production in prior 10 years (μ $gC/m^2/s$), GPP_2y–Gross Primary Production in prior 2 years (μ $gC/m^2/s$), sfcWind–surface windspeed (m/s), CAPE–convective atmospheric potential energy (J/kg), elevation–elevation (m, dry_CAPE–convective atmospheric potential energy if day is dry (J/kg), Vsoil1_365d–soil water volume in top layer (0–7 cm) averaged over prior 365 days (m^3/m^3), VRM–vector roughness metric (unitless), VPD_10d–mean vapour pressure deficit over prior 10 days (Pa), VPD_31d–mean vapour pressure deficit over prior 31 days (Pa), solar_insolation–downwelling shortwave solar radiation ($J/m^2/s$), VPD–daily mean vapour pressure deficit (Pa), HERB–the fraction of herbaceous plants (%), TREE–the fraction of forest (%), GPP_50d–Gross Primary Production in prior 50 days (μ $gC/m^2/s$), alpha_mean–the average annual ratio of actual to potential evapotranspiration (kg/kg), T–daily mean temperature (°C), CROP–the fraction of cropland (%), precip–daily precipitation (kg), SHRUB–the fraction of shrubland (%), GPP_100d–Gross Primary Production in prior 100 days (μ $gC/m^2/s$), RH–relative humidity (%), GPP_1y–Gross Primary Production in prior 1 year (μ $gC/m^2/s$), popDens_rural–population density clipped at 25 people per km^2 ($people/km^2$), snow_cover–snow cover fraction (%), precip_5d–precipitation in prior 5 days (kg), DTR–diurnal temperature range (°C).

human activity in decreasing global BA through suppressing fire size rather than fire numbers as well as a limited effect of climate and vegetation in driving fire size (Zhang et al., 2023). This finding is in line with work showing that road density and cropland cover have a strong limiting effect on fire size, but that vegetation predictors had a less significant effect (Haas et al., 2022). These various studies make it clear that human activities influence different fire properties in different ways and that factors that increase ignitions may have the opposite impact on overall burnt area or fire intensity.

Some previous studies have focused on the relationship between different aspects of fire regimes (e.g., size, frequency, intensity) and grouped distinct clusters of these properties into fire regimes (e.g., Archibald et al., 2013; Pereira et al., 2022; Fan et al., 2023; Pias et al., 2023; Garcia et al., 2022; Yang et al., 2023). Luo et al. (2017) proposed that there is a humped relationship between fire frequency and fire intensity, with the highest-intensity fires occurring at intermediate levels of fire occurrence. This finding presumably reflects the fact that frequent fires fragment the landscape (Laurent et al., 2019) and reduce fuel load and fuel continuity (Archibald et al., 2013; Luo et al., 2017), whereas environments characterised by low fire frequency may have high fuel loads but must inevitably be too wet to burn.

Only one study (Haas et al., 2022) has separately examined the role of individual predictors on different aspects of the fire regime, comparing the drivers of burnt area, fire size and fire intensity. Starting from a common set of 16 predictors, that study showed that some variables were important for one property but either had no influence or had the opposite effect on the others. For example, both annual GPP and the seasonality of dry days have a positive effect on burnt area, but no influence on fire size and reduce fire intensity (Figure 4). Overall, whereas burnt area is primarily driven by factors influencing fuel availability and fuel dryness and is reduced by landscape fragmentation, fire size is increased by factors promoting fire spread such as wind speed but is also reduced by landscape fragmentation. Fire intensity is primarily driven by tree cover; the strong positive relationship with road density probably reflects deforestation fires. These results are broadly compatible with the emergent relationships between different fire properties shown in

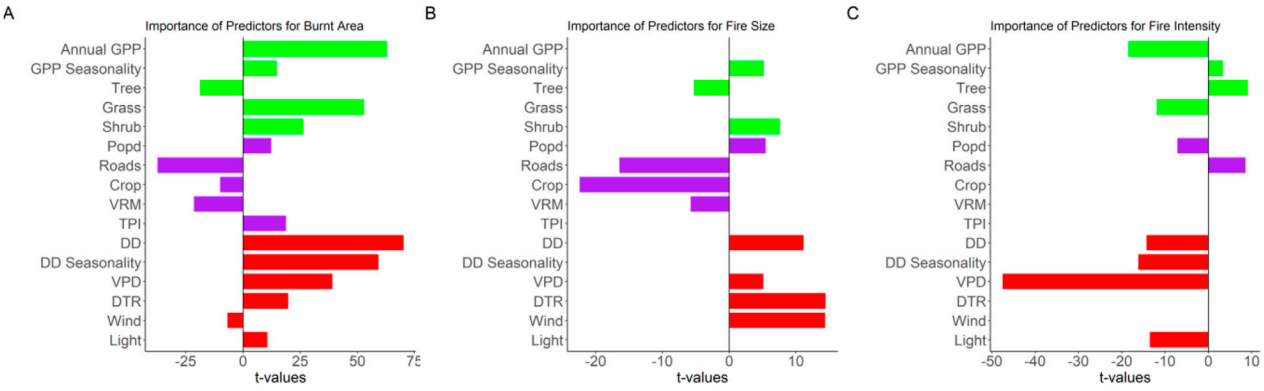

FIGURE 4
Empirical analysis of the relative importance (as measured by t-values) of individual predictors for **(A)** burnt area, **(B)** fire size and **(C)** fire intensity. Green represents variables related to vegetation properties, red represents variables related to climate, and purple represents natural and anthropogenic variables related to landscape fragmentation. GPP, gross primary production; Popd, population densitiy; VRM, vector ruggedness measure: TPI, topographic position index; DD, dry days; VPD, vapour pressure deficit; DTR, diurnal temperature range; Wind, windspeed; Light, Lightning; tree, grass, shrub, crop are the fractional cover of each land type. Redrawn from Haas et al., (2022).

previous studies. However, they have strong implications for process-based fire modelling since they imply that changes in fire properties could be decoupled under changed climates (Haas et al., 2023; Haas et al., 2024) and so the processes underlying burnt area, fire size and fire intensity need to be distinguished.

Lessons for fire science and modelling

Consistent patterns are emerging from empirical analyses that are leading to an improved understanding of wildfire regimes and their environmental controls. These provide a basis for improving the treatment of wildfire in a modelling context. Here, we summarise the lessons learnt from these empirical analyses about what factors are important and suggest ways in which these lessons could be incorporated into process-based models.

GPP consistently emerges as the most important control on wildfires. Both total GPP and the seasonality of GPP have a positive impact on burnt area. The influence of seasonality is consistent with studies that show that antecedent GPP has an opposite effect from the GPP during the wildfire season (Forkel et al., 2017; Kuhn-Régnier et al., 2021): high GPP in the period before the fire season means that fuel loads are high, whereas high GPP at the time of a fire could only be sustained if climate conditions were favourable, i.e., the fuel is likely too wet to burn. Studies that have included measures of antecedent conditions have generally found them to be important controls on wildfires. This is also consistent with the negative impact of GPP on fire intensity. These various measures of GPP appear to be reasonably good surrogates for fuel loads. Given the limited field information available globally about fuel loads (see e.g., Pettinari and Chuvieco, 2016; McNorton and Di Giuseppe, 2024), this suggests that GPP (or net primary production, NPP) can usefully serve as a surrogate in a modelling context. However, this means that it is important to ensure that the vegetation component of process-based wildfire models simulate GPP (or NPP) accurately to ensure an accurate simulation of wildfire regimes (Forkel et al., 2019).

Vegetation cover emerges from the empirical analyses as an important influence on wildfire, particularly the relative abundance of trees versus herbaceous plants. The nature of the vegetation cover is a crucial factor in influencing fuel continuity and fire spread. Globally, grass-dominated landscapes tend to lower fire intensity but produce more burnt area. However, empirical analyses that include PFTs as predictors do not show that they have an influence on wildfire properties. Many fire models have PFT-specific parameterisations, but this arises largely because of inheriting the PFT concept from the dynamic vegetation models used to provide vegetation characteristics (Cranko Page et al., 2024). Since this multiplies the number of, often poorly specified, parameters needed, simplifying the linkages between vegetation properties and wildfire processes would be useful. There are studies suggesting that individual species are fire-promoting but, at the scale of global modelling, it seems more likely that the traits which promote fire spread, such as the presence of volatile oils or ladder-fuel structure (Blauw et al., 2017; Popović et al., 2021; Rodman et al., 2021; Chen et al., 2023a; Chen et al., 2023b), should be explicitly represented in fire-enabled vegetation models.

The empirical analyses show that climatic variables that influence atmospheric humidity, and hence fuel drying, such as vapour pressure deficit (VPD) or the diurnal temperature range consistently emerge as an important control on wildfires. Precipitation, as such, is likely chiefly influential in so far as it is a surrogate for the more direct influence of atmospheric humidity on fuel drying. In studies that include precipitation and some measure of atmospheric dryness, precipitation may also be a reflection of direct fuel wetting. Soil moisture has been widely used in a modelling context to account for fuel dryness, but empirical studies which have tested this, or used aridity indices, indicate that these are not good predictors. In the absence of explicit simulation of the fuel bed and fuel moisture, models could replace soil moisture with parameterisations based on climatic factors such as VPD, which are more closely aligned to the process of fuel drying.

Empirical analyses indicate that ignitions are not a limiting factor for wildfire occurrence at a global scale. Lightning is

important for ignitions in many ecosystems. Lightning initiates ca 90% of wildfires in Siberia (Ivanov and Ivanova, 2010) and the majority of fires in Alaska (Kasischke et al., 2010) and northern Canada (Coogan et al., 2020). Changes in the incidence of lightning have been associated with increases in wildfires in these regions during the historical and recent past (e.g., Vachula et al., 2022; Veraverbeke et al., 2017). Nevertheless, even in these regions, climate and vegetation factors that influence fuel load and fuel drying play an important part in determining the occurrence of wildfires. Given this, models that prescribe anthropogenic and lightning ignitions, such as the empirical model INFERNO (Mangeon et al., 2016) and virtually all process-based models (Rabin et al., 2017), are likely focusing on the wrong process. As the differences in the prescribed relationships used by different models show (Teckentrup et al., 2019), the relationships are also poorly constrained. Most models use population density to encapsulate both anthropogenic ignitions and (direct and indirect) suppression (Rabin et al., 2017; Li et al., 2024), but this conflates two distinct processes which are influenced by different factors. Remote-sensed fire products are now available at much higher resolution, and this means that they now capture small fires, many of which are explicitly set for agricultural purposes such as preparing fields or removing waste (Millington et al., 2022). The use of total population density as a measure of anthropogenic ignitions for both wildfires and agricultural fires, ignores both differences between these two types of fire and the complexity of the cultural uses of fire.

Empirical analyses do not support the hypotheses about human impacts on wildfire currently embedded in process-based models. The peaked relationship between burnt area and population density used in many models (Rabin et al., 2017; Li et al., 2024) is an emergent property of the system and not a causal mechanism (Bistinas et al., 2014). Including other factors reflecting human transformation of the landscape, such as road density for example, transforms the relationship between burnt area and population density from negative (Bistinas et al., 2014) to positive (Haas et al., 2022). There have been attempts to provide a more nuanced picture of human impacts, through the inclusion of economic measures such as GDP (e.g., Mukunga et al., 2023), but while these factors may influence the number of ignitions they rarely turn out to be important predictors of other properties such as burnt area and do not improve the predictions of wildfire regimes. Cultural differences in human influence on fire (Pyne, 2014; Huffman, 2013; Millington et al., 2022) need to be expressed in a way that takes account of the intent and practice of deliberate and managed burning. Separate treatments of wildfires and agricultural fires are required in a modelling context, since their controls are very different.

Fragmentation is important in limiting fire spread, and this is reflected in the importance of factors such as crop cover and population density, which are indirect measures of fragmentation of the landscape, in the empirical analyses. However, a more nuanced approach to measuring fragmentation is needed if this is to be implemented in a modelling context. There is a growing understanding that the impacts of fragmentation differ between ecosystems (Armenteras et al., 2017; Harrison et al., 2021; Rosan et al., 2022; Harrison et al., 2024), and that this can be broadly explained in terms of the degree to which an ecosystem is adapted to frequent fires or not. However, more systematic analyses are required before these insights can be properly incorporated into models.

Empirical analyses of the controls on wildfire need to be more explicit about which processes are hypothesised to be controlled by specific variables. This will ensure that the variables tested are not redundant and/or acting on two different aspects of the wildfire regime. It would also be useful to adopt more systematic approaches to the evaluation of the inclusion/exclusion of specific variables and their contributions. Nevertheless, although there are gaps in our understanding of the controls on wildfires, especially related to the role of humans and the influence of landscape fragmentation, empirical analyses at the global scale already provide insights that could be used to improve process representations in process-based fire-vegetation models. The most obvious improvements are to use variables more closely aligned to the processes of generating fuel loads and of fuel drying. Separating the treatment of different aspects of the fire regime, most particularly by simulating fire intensity separately from fire size and overall burnt area, would also be a useful improvement. While the existing empirical models themselves can be useful in projecting the response of wildfires to future climate change (e.g., Haas et al., 2024), improved process-based models will be necessary in the long run to be able to examine feedbacks from fire to the climate system.

Author contributions

OH: Conceptualization, Investigation, Writing–review and editing. TK: Conceptualization, Investigation, Writing–review and editing. JG-D: Conceptualization, Investigation, Writing–review and editing. IP: Conceptualization, Investigation, Writing–review and editing. SH: Conceptualization, Formal Analysis, Investigation, Writing–original draft, Writing–review and editing.

Funding

The author(s) declare that financial support was received for the research, authorship, and/or publication of this article. OH, TK, ICP and SPH acknowledge support from the LEMONTREE (Land Ecosystem Models based On New Theory, obseRvations and ExperimEnts) project, funded through the generosity of Eric and Wendy Schmidt by recommendation of the Schmidt Futures programme. The grant number for the Lemontree funding is: Grant number 355.

Acknowledgments

This paper is a contribution to the work of the Vegetation-Fire giraffe team of the Leverhulme Centre for Wildfires, Environment and Society (https://centreforwildfires.org/). We thank members of the giraffe team for discussions during the development of this work.

Conflict of interest

The authors declare that the research was conducted in the absence of any commercial or financial relationships that could be construed as a potential conflict of interest.

Publisher's note

All claims expressed in this article are solely those of the authors and do not necessarily represent those of their affiliated organizations, or those of the publisher, the editors and the reviewers. Any product that may be evaluated in this article, or claim that may be made by its manufacturer, is not guaranteed or endorsed by the publisher.

Supplementary material

The Supplementary Material for this article can be found online at: https://www.frontiersin.org/articles/10.3389/fenvs.2024.1438262/full#supplementary-material

References

Abatzoglou, J. T., Williams, A. P., and Barbero, R. (2019). Global emergence of anthropogenic climate change in fire weather indices. *Geophys. Res. Lett.* 46, 326–336. doi:10.1029/2018gl080959

Abatzoglou, J. T., Williams, A. P., Boschetti, L., Zubkova, M., and Kolden, C. A. (2018). Global patterns of interannual climate–fire relationships. *Glob. Change Biol.* 24, 5164–5175. doi:10.1111/gcb.14405

Abram, N. J., Henley, B. J., Sen Gupta, A., Lippmann, T. J. R., Clarke, H., Dowdy, A. J., et al. (2021). Connections of climate change and variability to large and extreme forest fires in southeast Australia. *Commun. Earth Environ.* 2 (8), 8. doi:10.1038/s43247-020-00065-8

Andela, N., Morton, D. C., Giglio, L., Chen, Y., van der Werf, G. R., Kasibhatla, P. S., et al. (2017). A human-driven decline in global burned area. *Science* 356, 1356–1362. doi:10.1126/science.aal4108

Archibald, S., Lehmann, C. E. R., Belcher, C. M., Bond, W. J., Bradstock, R. A., Daniau, A.-L., et al. (2018). Biological and geophysical feedbacks with fire in the Earth system. *Env. Res. Lett.* 13, 033003. doi:10.1088/1748-9326/aa9ead

Archibald, S., Lehmann, C. E. R., Gómez-Dans, J. L., and Bradstock, R. A. (2013). Defining pyromes and global syndromes of fire regimes. *Proc. Natl. Acad. Sci. U. S. A.* 110, 6442–6447. doi:10.1073/pnas.1211466110

Armenteras, D., Barreto, J. S., Tabor, K., Molowny-Horas, R., and Retana, J. (2017). Changing patterns of fire occurrence in proximity to forest edges, roads and rivers between NW Amazonian countries. *Biogeosci.* 14, 2755–2765. doi:10.5194/bg-14-2755-2017

Arora, V. K., and Boer, G. (2005). Fire as an interactive component of dynamic vegetation models. *J. Geophys. Res.* 110, G02008. doi:10.1029/2005JG000042

Bistinas, I., Harrison, S. P., Prentice, I. C., and Pereira, J. M. C. (2014). Causal relationships versus emergent patterns in the global controls of fire frequency. *Biogeosci* 11, 5087–5101. doi:10.5194/bg-11-5087-2014

Blauw, L. G., van Logtestijn, R. S. P., Broekman, R., Aerts, R., and Cornelissen, J. H. C. (2017). Tree species identity in high-latitude forests determines fire spread through fuel ladders from branches to soil and vice versa. *For. Ecol. Manage.* 400, 475–484. doi:10.1016/j.foreco.2017.06.023

Boer, M. M., De Dios, V. R., Stefaniak, E. Z., and Bradstock, R. A. (2021). A hydroclimatic model for the distribution of fire on Earth. *Environ. Res. Comm.* 3, 035001. doi:10.1088/2515-7620/abec1f

Bowman, D. M., Balch, J., Artaxo, P., Bond, W. J., Cochrane, M. A., D'Antonio, C. M., et al. (2011). The human dimension of fire regimes on Earth. *J. Biogeog.* 38, 2223–2236. doi:10.1111/j.1365-2699.2011.02595.x

Bowman, D. M. J. S., Balch, J. K., Artaxo, P., Bond, W. J., Cochrane, M. A., D'Antonia, C. M., et al. (2009). Fire in the earth system. *Science* 324, 481–484. doi:10.1126/science.1163886

Bowman, D. M. J. S., Kolden, C. A., Abatzoglou, J. T., Johnston, F. H., van der Werf, G. R., and Flannigan, M. (2020). Vegetation fires in the anthropocene. *Nat. Rev. Earth Environ.* 1, 500–515. doi:10.1038/s43017-020-0085-3

Carnicer, J., Alegria, A., Giannakopoulos, C., Di Giuseppe, F., Karali, A., Koutsias, N., et al. (2022). Global warming is shifting the relationships between fire weather and realized fire-induced CO_2 emissions in Europe. *Sci. Rep.* 12, 10365. doi:10.1038/s41598-022-14480-8

Chen, F., Si, L., Zhao, F., and Wang, M. (2023a). Volatile oil in *Pinus yunnanensis* potentially contributes to extreme fire behavior. *Fire* 6, 113. doi:10.3390/fire6030113

Chen, Y., Hall, J., van Wees, D., Andela, N., Hantson, S., Giglio, L., et al. (2023b). Multi-decadal trends and variability in burned area from the fifth version of the Global Fire Emissions Database (GFED5). *Earth Syst. Sci. Data* 15, 5227–5259. doi:10.5194/essd-15-5227-2023

Coogan, S. C. P., Cai, X., Jain, P., and Flannigan, M. D. (2020). Seasonality and trends in human- and lightning-caused wildfires ≥2 ha in Canada, 1959–2018. *Int. J. Wildland Fire* 29, 473–485. doi:10.1071/WF19129

Cranko Page, J., Abramowitz, G., De Kauwe, M. G., and Pitman, A. J. (2024). Are plant functional types fit for purpose? *Geophys. Res. Lett.* 51, e2023GL104962. doi:10.1029/2023GL104962

Dickman, L. T., Jonko, A. K., Linn, R. R., Altintas, I., Atchley, A. L., Bär, A., et al. (2023). Integrating plant physiology into simulation of fire behavior and effects. *New Phytol.* 238, 952–970. doi:10.1111/nph.18770

Fan, H., Yang, X., Zhao, C., Yang, Y., and Shen, Z. (2023). Spatiotemporal variation characteristics of global fires and their emissions. *Atmos. Chem. Phys.* 23, 7781–7798. doi:10.5194/acp-23-7781-2023

Forkel, M., Dorigo, W., Lasslop, G., Chuvieco, E., Hantson, S., Heil, A., et al. (2019). Recent global and regional trends in burned area and their compensating environmental controls. *Environ. Res. Comm.* 1, 051005. doi:10.1088/2515-7620/ab25d2

Forkel, M., Dorigo, W., Lasslop, G., Teubner, I., Chuvieco, E., and Thonicke, K. (2017). A data-driven approach to identify controls on global fire activity from satellite and climate observations (SOFIA V1). *Geosci. Model Dev.* 10, 4443–4476. doi:10.5194/gmd-10-4443-2017

Foster, C. N., Barton, P. S., MacGregor, C. I., Catford, J. A., Blanchard, W., and Lindenmayer, D. B. (2018). Effects of fire regime on plant species richness and composition differ among forest, woodland and heath vegetation. *Appl. Veg. Sci.* 21, 132–143. doi:10.1111/avsc.12345

García, M., Pettinari, M. L., Chuvieco, E., Salas, J., Mouillot, F., Chen, W., et al. (2022). Characterizing global fire regimes from satellite-derived products. *Forests* 13, 699. doi:10.3390/f13050699

Giglio, L., Randerson, J. T., and van der Werf, G. R. (2013). Analysis of daily, monthly, and annual burned area using the fourth-generation global fire emissions database (GFED4). *J. Geophys. Res. Biogeosci.* 118, 317–328. doi:10.1002/jgrg.20042

Grünig, M., Seidl, R., and Senf, C. (2023). Increasing aridity causes larger and more severe forest fires across Europe. *Glob. Change Biol.* 29, 1648–1659. doi:10.1111/gcb.16547

Haas, O., Prentice, I., and Harrison, S. (2024). Global wildfires on a changing planet. *In revision, Nat. Commun.*

Haas, O., Prentice, I. C., and Harrison, S. P. (2022). Global environmental controls on wildfire burnt area, size and intensity. *Environ. Res. Lett.* 17, 065004. doi:10.1088/1748-9326/ac6a69

Haas, O., Prentice, I. C., and Harrison, S. P. (2023). Examining the response of wildfire properties to climate and atmospheric CO_2 change at the Last Glacial Maximum. *Biogeosci* 20, 3981–3995. doi:10.5194/bg-20-3981-2023

Hantson, S., Arneth, A., Harrison, S. P., Kelley, D. I., Prentice, I. C., Rabin, S. S., et al. (2016). The status and challenge of global fire modelling. *Biogeosci* 13, 3359–3375. doi:10.5194/bg-13-3359-2016

Hantson, S., Kelley, D. I., Arneth, A., Harrison, S. P., Archibald, S., Bachelet, D., et al. (2020). Quantitative assessment of fire and vegetation properties in simulations with fire-enabled vegetation models from the Fire Model Intercomparison Project. *Geosci. Model Dev.* 13, 3299–3318. doi:10.5194/gmd-13-3299-2020

Hantson, S., Pueyo, S., and Chuvieco, E. (2015). Global fire size distribution is driven by human impact and climate. *Glob. Ecol. Biogeogr.* 24, 77–86. doi:10.1111/geb.12246

Harrison, S. P., Marlon, J., and Bartlein, P. J. (2010). "Fire in the earth system," in *Changing climates, earth Systems and society. International year of planet earth, climate change theme*. Editor J. Dodson (Legacy: Springer-Verlag), 21–48.

Harrison, S. P., Prentice, I. C., Bloomfield, K., Dong, N., Forkel, M., Forrest, M., et al. (2021). Understanding and modelling wildfire regimes: an ecological perspective. *Environ. Res. Lett.* 16, 125008. doi:10.1088/1748-9326/ac39be

Harrison, S. P., Haas, O., Bartlein, P. J., Sweeney, L., and Zhang, G. (in press 2024). Climate, vegetation, people: disentangling the controls of fire at different timescales. *Philos. Trans. R. Soc. B.*

Huffman, M. R. (2013). The many elements of traditional fire knowledge: synthesis, classification, and aids to cross-cultural problem solving in fire dependent systems around the world. *Ecol. Soc.* 18, 3. doi:10.5751/es-05843-180403

Ivanov, V. A., and Ivanova, G. A. (2010). *Wildfires from lightning in forests of Siberia*. Novosibirsk: Nauka.

Jones, M. W., Abatzoglou, J. T., Veraverbeke, S., Andela, N., Lasslop, G., Forkel, M., et al. (2022). Global and regional trends and drivers of fire under climate change. *Rev. Geophys.* 60, e2020RG000726. doi:10.1029/2020rg000726

Kasischke, E. S., Verbyla, D. L., Rupp, T. S., McGuire, A. D., Murphy, K. A., Jandt, R., et al. (2010). Alaska's changing fire regime — implications for the vulnerability of its boreal forestsThis article is one of a selection of papers from the Dynamics of Change in Alaska's Boreal Forests: resilience and Vulnerability in Response to Climate Warming. *Can. J. For. Res.* 40, 1313–1324. doi:10.1139/X10-098

Keeping, T., Harrison, S. P., and Prentice, I. C. (2024). Modelling the daily probability of wildfire occurrence in the contiguous United States. *Environ. Res. Lett.* 19, 024036. doi:10.1088/1748-9326/ad21b0

Kharuk, V. I., Dvinskaya, M. L., Im, S. T., Golyukov, A. S., and Smith, K. T. (2022). Wildfires in the siberian arctic. *Fire* 5, 106. doi:10.3390/fire5040106

Kirchmeier-Young, M. C., Gillett, N. P., Zwiers, F. W., Cannon, A. J., and Anslow, F. S. (2019). Attribution of the influence of human-induced climate change on an extreme fire season. *Earth's Future* 7, 2–10. doi:10.1029/2018EF001050

Kloster, S., Mahowald, N. M., Randerson, J. T., Thornton, P. E., Hoffman, F. M., Levis, S., et al. (2010). Fire dynamics during the 20th century simulated by the community land model. *Biogeosci* 7, 1877–1902. doi:10.5194/bg-7-1877-2010

Knorr, W., Kaminski, T., Arneth, A., and Weber, U. (2014). Impact of human population density on fire frequency at the global scale. *Biogeosci.* 11, 1085–1102. doi:10.5194/bg-11-1085-2014

Krawchuk, M. A., and Moritz, M. A. (2011). Constraints on global fire activity vary across a resource gradient. *Ecology* 92, 121–132. doi:10.1890/09-1843.1

Kuhn-Régnier, A., Voulgarakis, A., Nowack, P., Forkel, M., Prentice, I. C., and Harrison, S. P. (2021). The importance of antecedent vegetation and drought conditions as global drivers of burnt area. *Biogeosci* 18, 3861–3879. doi:10.5194/bg-18-3861-2021

Lasslop, G., Hantson, S., and Kloster, S. (2015). Influence of wind speed on the global variability of burned fraction: a global fire model's perspective. *Int. J. Wildland Fire* 24, 989–1000. doi:10.1071/wf15052

Laurent, P., Mouillot, F., Moreno, M. V., Yue, C., and Ciais, P. (2019). Varying relationships between fire radiative power and fire size at a global scale. *Biogeosci* 16, 275–288. doi:10.5194/bg-16-275-2019

Lavorel, S., Flannigan, M. D., Lambin, E. F., and Scholes, M. C. (2007). Vulnerability of land systems to fire: interactions among humans, climate, the atmosphere, and ecosystems. *Mitig. Adapt. Strateg. Glob. Change* 12, 33–53. doi:10.1007/s11027-006-9046-5

Li, F., Levis, S., and Ward, D. S. (2013). Quantifying the role of fire in the earth system – Part 1: improved global fire modeling in the community earth system model (CESM1). *Biogeosci* 10, 2293–2314. doi:10.5194/bg-10-2293-2013

Li, F., Song, X., Harrison, S. P., Marlon, J. R., Lin, Z., Leung, L. R., et al. (2024). Evaluation of global fire simulations in CMIP6 Earth system models. *Geosci. Model Dev*. doi:10.5194/gmd-2024-85

Li, F., Zeng, X. D., and Levis, S. (2012). A process-based fire parameterization of intermediate complexity in a Dynamic Global Vegetation Model. *Biogeosci* 9, 2761–2780. doi:10.5194/bg-9-2761-2012

Luo, R., Hui, D., Miao, N., Liang, C., and Wells, N. (2017). Global relationship of fire occurrence and fire intensity: a test of intermediate fire occurrence-intensity hypothesis. *J. Geophys. Res. Biogeosci.* 122, 1123–1136. doi:10.1002/2016jg003722

Mangeon, S., Voulgarakis, A., Gilham, R., Harper, A., Sitch, S., and Folberth, G. (2016). INFERNO: a fire and emissions scheme for the UK Met Office's Unified Model. *Geosci. Model Dev.* 9, 2685–2700. doi:10.5194/gmd-9-2685-2016

McNorton, J. R., and Di Giuseppe, F. (2024). A global fuel characteristic model and dataset for wildfire prediction. *Biogeosci* 21, 279–300. doi:10.5194/bg-21-279-2024

Melton, J. R., and Arora, V. K. (2016). Competition between plant functional types in the Canadian Terrestrial Ecosystem Model (CTEM) v. 2.0. *Geosci. Model Dev.* 9, 323–361. doi:10.5194/gmd-9-323-2016

Millington, J. D., Perkins, O., and Smith, C. (2022). Human fire use and management: a global database of Anthropogenic fire impacts for modelling. *Fire* 5, 87. doi:10.3390/fire5040087

Mueller, S. E., Thode, A. E., Margolis, E. Q., Yocom, L. L., Young, J. D., and Iniguez, J. M. (2020). Climate relationships with increasing wildfire in the southwestern US from 1984 to 2015. *For. Ecol. Manage.* 460, 117861. doi:10.1016/j.foreco.2019.117861

Mukunga, T., Forkel, M., Forrest, M., Zotta, R. M., Pande, N., Schlaffer, S., et al. (2023). Effect of socioeconomic variables in predicting global fire ignition occurrence. *Fire* 6, 197. doi:10.3390/fire6050197

Pais, C., Gonzalez-Olabarria, J. R., Elimbi Moudio, P., Garcia-Gonzalo, J., González, M. C., and Shen, Z. J. M. (2023). Global scale coupling of pyromes and fire regimes. *Comm. Earth & Environ.* 4, 267. doi:10.1038/s43247-023-00881-8

Pausas, J. G., and Keeley, J. E. (2009). A burning story: the role of fire in the history of life. *BioSci* 59, 593–601. doi:10.1525/bio.2009.59.7.10

Pausas, J. G., and Keeley, J. E. (2023). Evolutionary fire ecology: an historical account and future directions. *BioSci.* 73, 602–608. doi:10.1093/biosci/biad059

Pausas, J. G., Keeley, J. E., and Schwilk, D. W. (2017). Flammability as an ecological and evolutionary driver. *J. Ecol.* 105, 289–297. doi:10.1111/1365-2745.12691

Pereira, J. M., Oom, D., Silva, P. C., and Benali, A. (2022). Wild, tamed, and domesticated: three fire macroregimes for global pyrogeography in the Anthropocene. *Ecol. Applic.* 32, e2588. doi:10.1002/eap.2588

Pettinari, M. L., and Chuvieco, E. (2016). Generation of a global fuel data set using the Fuel Characteristic Classification System. *Biogeosci* 13, 2061–2076. doi:10.5194/bg-13-2061-2016

Ponomarev, E. I., Zabrodin, A. N., Shvetsov, E. G., and Ponomareva, T. V. (2023). Wildfire intensity and fire emissions in Siberia. *Fire* 6, 246. doi:10.3390/fire6070246

Popović, Z., Bojović, S., Marković, M., and Cerdà, A. (2021). Tree species flammability based on plant traits: a synthesis. *STOTEN* 800, 149625. doi:10.1016/j.scitotenv.2021.149625

Pyne, S. J. (2014). *World fire: the culture of fire on earth*. Seattle, Washington, United States: University of Washington Press.

Rabin, S., Melton, J. R., Laslop, G., Bachelet, D., Forrest, M., Hantson, S., et al. (2017). The Fire Modeling Intercomparison Project (FireMIP), phase 1: experimental and analytical protocols with detailed model descriptions. *Geosci. Model Dev.* 10, 1175–1197. doi:10.5194/gmd-10-1175-2017

Randerson, J., Chen, Y., van der Werf, G. R., Rogers, B., and Morton, D. (2012). Global burned area and biomass burning emissions from small fires. *J. Geophys. Res.-Biogeo.* 117, G04012. doi:10.1029/2012JG002128

Rodman, K. C., Veblen, T. T., Andrus, R. A., Enright, N. J., Fontaine, J. B., Gonzalez, A. D., et al. (2021). A trait-based approach to assessing resistance and resilience to wildfire in two iconic North American conifers. *J. Ecol.* 109, 313–326. doi:10.1111/1365-2745.13480

Rosan, T. M., Sitch, S., Mercado, L. M., Heinrich, V., Friedlingstein, P., and Aragão, L. E. O. C. (2022). Fragmentation-driven divergent trends in burned area in Amazonia and Cerrado. *Front. For. Glob. Change* 5. doi:10.3389/ffgc.2022.801408

Scott, A. C. (2000). The Pre-Quaternary history of fire. *Palaeogeogr. Palaeoclimatol. Palaeoecol.* 164, 281–329. doi:10.1016/s0031-0182(00)00192-9

Scott, A. C., and Glasspool, I. J. (2006). The diversification of Paleozoic fire systems and fluctuations in atmospheric oxygen concentration. *Proc. Natl. Acad. Sci. U. S. A.* 103, 10861–10865. doi:10.1073/pnas.0604090103

Shmuel, A., and Heifetz, E. (2022). Global wildfire susceptibility mapping based on machine learning models. *Forests* 13, 1050. doi:10.3390/f13071050

Shmuel, A., and Heifetz, E. (2023). Empirical evidence of reduced wildfire ignition risk in the presence of strong winds. *Fire* 6, 338. doi:10.3390/fire6090338

Simpson, K. J., Jardine, E. C., Archibald, S., Forrestel, E. J., Lehmann, C. E. R., Thomas, G. H., et al. (2021). Resprouting grasses are associated with less frequent fire than seeders. *New Phytol.* 230, 832–844. doi:10.1111/nph.17069

Singleton, M. P., Thode, A. E., Sanchez Meador, A. J., and Iniguez, J. M. (2019). Increasing trends in high-severity fire in the southwestern USA from 1984 to 2015. *For. Ecol. Manage.* 433, 709–719. doi:10.1016/j.foreco.2018.11.039

Teckentrup, L., Harrison, S. P., Hantson, S., Heil, A., Melton, J. R., Forrest, M., et al. (2019). Response of simulated burned area to historical changes in environmental and anthropogenic factors: a comparison of seven fire models. *Biogeosci* 16, 3883–3910. doi:10.5194/bg-16-3883-2019

Thonicke, K., Spessa, A., Prentice, I. C., Harrison, S. P., Dong, L., and Carmona-Moreno, C. (2010). The influence of vegetation, fire spread and fire behaviour on biomass burning and trace gas emissions: results from a process-based model. *Biogeosci* 7, 1991–2011. doi:10.5194/bg-7-1991-2010

Thonicke, K., Venevsky, S., Sitch, S., and Cramer, W. (2001). The role of fire disturbance for global vegetation dynamics: coupling fire into a dynamic global vegetation model. *Glob. Ecol. Biogeog.* 10, 661–677. doi:10.1046/j.1466-822x.2001.00175.x

Tracy, J. L., Trabucco, A., Lawing, M., Giermakowski, J. T., Tchakerian, M., Drus, G. M., et al. (2018). Random subset feature selection for ecological niche models of wildfire activity in Western North America. *Ecol. Model.* 383, 52–68. doi:10.1016/j.ecolmodel.2018.05.019

United Nations Environment Programme (UNEP) (2022). *Spreading like wildfire – the rising threat of extraordinary landscape fires*. Nairobi: A UNEP Rapid Response Assessment.

Vachula, R. S., Liang, J., Sae-Lim, J., and Xie, H. (2022). Ignition frequency and climate controlled Alaskan tundra fires during the Common Era. *Quat. Sci. Rev.* 280, 107418. doi:10.1016/j.quascirev.2022.107418

van Oldenborgh, G. J., Krikken, F., Lewis, S., Leach, N. J., Lehner, F., Saunders, K. R., et al. (2021). Attribution of the Australian bushfire risk to anthropogenic climate change. *Nat. Hazards Earth Syst. Sci.* 21, 941–960. doi:10.5194/nhess-21-941-2021

Veraverbeke, S., Rogers, B., Goulden, M., Jandt, R., Miller, C., Wiggins, E., et al. (2017). Lightning as a major driver of recent large fire years in North American boreal forests. Nature *Clim. Change*. *Nat. Clim. Chang.* 7, 529–534. doi:10.1038/nclimate3329

Wasserman, T. N., and Mueller, S. E. (2023). Climate influences on future fire severity: a synthesis of climate-fire interactions and impacts on fire regimes, high-severity fire, and forests in the western United States. *Fire Ecol.* 19, 43. doi:10.1186/s42408-023-00200-8

Williams, A. P., Abatzoglou, J. T., Gershunov, A., Guzman-Morales, J., Bishop, D. A., Balch, J. K., et al. (2019). Observed impacts of anthropogenic climate change on wildfire in California. *Earth's Future* 7, 892–910. doi:10.1029/2019EF001210

Yang, X., Zhao, C., Zhao, W., Fan, H., and Yang, Y. (2023). Characterization of global fire activity and its spatiotemporal patterns for different land cover types from 2001 to 2020. *Environ. Res.* 227, 115746. doi:10.1016/j.envres.2023.115746

Zhang, Y., Mao, J., Ricciuto, D. M., Jin, M., Yu, Y., Shi, X., et al. (2023). Global fire modelling and control attributions based on the ensemble machine learning and satellite observations. *Sci. Remote Sens.* 7, 100088. doi:10.1016/j.srs.2023.100088

Zubkova, M., Humber, M. L., and Giglio, L. (2023). Is global burned area declining due to cropland expansion? How much do we know based on remotely sensed data? *Int. J. Remote Sens.* 44, 1132–1150. doi:10.1080/01431161.2023.2174389